

Evaluating the effects of HIV-1 infection on haematopoietic stem cell colony formation

Submitted in fulfilment of the requirements for the degree:

MSc Medical Immunology

Candice Lee Herd

Submitted 14/06/2019

Supervisor: Professor M.S. Pepper

Co-supervisor: Dr. C.Durandt

Declaration of Authenticity

I hereby declare the work herein contained to be my own, original work, and that any contributors are appropriately acknowledged. Furthermore, I declare that all source material is cited appropriately, and to my knowledge, neither I nor any declared contributors are aware of any plagiarism in the following work.

Contributor	Contribution
Prof M.S. Pepper (Supervisor)	Experiment design and project direction Proofreading and corrections
Dr C. Durandt (Co-supervisor)	Experiment design and project direction Proofreading and corrections
Mrs J. Mellet (PhD student)	Experiment design and execution
Miss C.L. Herd (MSc student)	Experiment design and execution Dissertation and manuscript preparation

I hereby submit the following title as my own work, and that all contributors (if any) are listed in the above table.

Title of work:

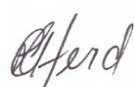
Evaluating the effects of HIV-1 infection on haematopoietic stem cell colony formation

(MSc Dissertation)

Date: 28/03/2019

Name: Candice Lee Herd

Signature:



Acknowledgements

I would like to thank my supervisor, Professor Michael S. Pepper, for the opportunity to learn and grow as a scientist and as a person. It has and continues to be my privilege. I would also like to thank my co-supervisor, Dr Chrisna Durandt, for her patience, assistance, and endless hours in the lab.

I would like to thank my funding bodies, the National Research Foundation (NRF), the Polyomyelitis Research Foundation (PRF), and the Institute for Cellular and Molecular Medicine (ICMM) for financial support during my MSc.

To the staff and obstetricians at Netcare Femina Women's Hospital (2016-2019) who allowed us to consent their patients and collected umbilical cord and blood for us, you were instrumental to the work described in this dissertation. To the expectant mothers and their families who gave us the opportunity to perform this research. To the staff at the Alberts Cellular Therapy centre (2018-2019), and the patients and their families who gave consent for leukapheresis products to be released for research purposes. Thank you all!

To Travers and my colleagues in the Enchanted Grotto, past and present. Words cannot describe the journey. Each of you is a jewel. Your inspiration and support carried me when I couldn't tell the direction of the tide. Thank you, Juanita, Carina, Candice (Cpt), Catherine, Cheryl, Elize, Mqondisi, Aurona, and Simone.

My watch has ended.

Dedication

In memory of my Father, who always encouraged my wild academic aspirations, and to my Mother for her continued love and support during them.

Table of Contents

Declaration of Authenticity.....	i
Acknowledgements.....	ii
Dedication.....	ii
Table of Contents.....	iii
Table of Figures.....	xii
Table of Tables.....	xxvi
List of Abbreviations.....	xxx
Chapter 1 Introduction, aims, and objectives.....	1
1.1 Introduction.....	1
1.2 Aim and Objectives.....	4
1.2.1 Aim.....	4
1.2.2 Objectives.....	4
1.3 References.....	5
Chapter 2 Literature review.....	8
2.1 Stem cells.....	8
2.1.1 Introduction to stem cells.....	8
2.1.1.1 Definition.....	8
2.1.1.2 Cradle to grave.....	8
2.1.1.3 The stem cell niche.....	10
2.1.2 Types of stem cells.....	11
2.1.2.1 Embryonic stem cells.....	11
2.1.2.2 Adult stem cells.....	11
2.1.2.2.1 Haematopoietic stem cells.....	11
2.1.2.2.2 Mesenchymal stem cells.....	11
2.1.2.2.3 Other adult stem cells.....	12
2.1.2.3 Induced pluripotent stem cells.....	12
2.1.3 Stem cells in regenerative medicine.....	12
2.2 Haematopoietic stem cells.....	13
2.2.1 Biology and function.....	13
2.2.1.1 Purpose.....	13
2.2.2 Haematopoietic stem/progenitor cell therapy.....	13
2.2.2.1 Haematopoietic system reconstitution – a clinical first.....	13
2.2.2.2 Haematopoietic stem/progenitor cell transplant.....	14
2.2.2.2.1 Background.....	14
2.2.2.2.2 Sources of haematopoietic stem/progenitor cells for haematopoietic stem/progenitor cell transplant.....	14
2.2.2.2.3 Haematopoietic stem/progenitor cell dose in haematopoietic stem/progenitor cell transplant.....	15
2.2.2.3 Haematopoietic stem/progenitor cells in gene therapy.....	16

2.2.3	Phenotype and heterogeneity	16
2.2.4	Haematopoiesis	19
2.2.4.1	Stem cell maintenance – the bone marrow niche	19
2.2.4.1.1	Cellular profile of the bone marrow niche.....	19
2.2.4.1.2	Cytokine profile of the bone marrow niche.....	20
2.2.4.2	Haematopoiesis – dynamic reconstitution.....	21
2.2.4.2.1	Haematopoiesis – a symphony of cytokines.....	22
2.2.4.2.2	Colony-forming unit assays.....	25
2.3	Human immunodeficiency virus and haematopoiesis.....	26
2.3.1	Human immunodeficiency virus – a global view	26
2.3.1.1	Background	26
2.3.1.2	Replication and persistence	26
2.3.1.2.1	Replication	26
2.3.1.2.2	Persistence.....	29
2.3.2	Towards a cure: human immunodeficiency virus gene therapy	30
2.3.3	Human immunodeficiency virus and haematopoietic stem/progenitor cells...31	
2.3.3.1	Haematopoietic stem/progenitor cell susceptibility to human immunodeficiency virus.....	31
2.3.3.1.1	Human immunodeficiency virus-associated haematological abnormalities.....	32
2.3.3.1.2	Conflicting literature	33
2.4	Summary	41
2.5	References.....	42
Chapter 3	Human immunodeficiency virus detection, quantitation, and infectivity	55
3.1	Introduction.....	55
3.1.1	Viral genome detection	56
3.1.1.1	Background	56
3.1.1.1.1	Nucleic acid polymerisation.....	56
3.1.1.2	Detecting human immunodeficiency virus nucleic acids	57
3.1.2	Viral protein detection.....	57
3.1.2.1	Background	57
3.1.2.2	Detecting viral proteins	58
3.1.3	Indirect detection	58
3.2	Ethical and safety considerations.....	59
3.2.1	Ethical approval.....	59
3.2.2	Safety considerations.....	59
3.3	Donor testing.....	60
3.3.1	Principles.....	60
3.3.2	Test and quality control	60
3.3.2.1	Sample preparation	60
3.3.2.2	Quality control steps	61
3.4	P24 Enzyme-linked immunosorbent assay	62
3.4.1	Introduction	62

3.4.2	Principles.....	62
3.4.3	Methods.....	63
3.4.3.1.1	Enzyme-linked immunosorbent assay protocol.....	63
3.4.3.1.2	Standard curve preparation.....	65
3.4.4	Data processing.....	66
3.5	Nucleic acid detection.....	67
3.5.1	Introduction.....	67
3.5.1.1	Background.....	67
3.5.1.2	Amplicon analysis.....	68
3.5.2	Primer design.....	69
3.5.2.1	Important factors in primer design.....	69
3.5.2.1.1	Melting temperatures.....	70
3.5.2.1.2	Secondary structures.....	70
3.5.2.2	In silico primer design.....	71
3.5.2.3	Primer design output.....	75
3.5.3	Primer validation.....	77
3.5.3.1	Introduction.....	77
3.5.3.2	Primer synthesis.....	77
3.5.3.3	Sample material preparation.....	77
3.5.3.4	DNA extraction and quantification.....	78
3.5.3.4.1	QIAamp DNA micro kit reagent preparation.....	78
3.5.3.4.2	DNA extraction procedure.....	78
3.5.3.4.3	Nucleic acid quantification by NanoDrop®.....	79
3.5.3.5	Polymerase chain reaction.....	80
3.5.3.5.1	Reaction preparation.....	80
3.5.3.5.2	Thermocycling specifications.....	81
3.5.3.6	Agarose gel electrophoresis.....	81
3.5.3.6.1	Gel preparation.....	81
3.5.3.6.2	Sample preparation for gel loading.....	82
3.5.3.6.3	Electrophoresis.....	82
3.5.3.6.4	Visualisation and interpretation of gel images.....	83
3.5.4	Limit of detection determination.....	85
3.5.4.1	Rationale.....	85
3.5.4.2	Method.....	85
3.5.4.2.1	Sample material preparation.....	85
3.5.4.2.2	DNA extraction.....	86
3.5.4.2.3	Limit of detection polymerase chain reaction.....	88
3.5.4.2.4	Agarose gel electrophoresis.....	89
3.5.4.3	Results and interpretation.....	89
3.6	GHOST green fluorescent protein assay.....	91
3.6.1	Introduction.....	91
3.6.2	Cell culture and maintenance.....	92

3.6.2.1	GHOST cell thawing	92
3.6.2.2	GHOST passaging	93
3.6.2.2.1	Enzymatic dissociation	93
3.6.2.2.2	Non-enzymatic dissociation	93
3.6.2.3	GHOST cell cryopreservation	94
3.6.3	Flow cytometry	94
3.6.3.1	Introduction	94
3.6.3.2	Instruments	95
3.6.3.2.1	Instruments and configurations	95
3.6.3.2.2	Protocols	98
3.6.3.3	Enumeration	98
3.6.3.3.1	General sample preparation	98
3.6.3.3.2	General enumeration	99
3.6.3.4	Post-sort purity	101
3.6.3.5	GHOST cell gating strategies	101
3.6.3.5.1	Sample preparation	101
3.6.3.5.2	Gating strategy	102
3.6.3.6	GHOST cell sorting	103
3.6.3.6.1	Purpose	103
3.6.3.6.2	Sample preparation	104
3.6.3.6.3	Gating strategy	105
3.6.4	GHOST green fluorescent protein assay setup and optimisation	106
3.6.4.1	GHOST cell CD4 expression	106
3.6.4.1.1	Introduction	106
3.6.4.2	GHOST cell phenotype	106
3.6.4.2.1	Sample preparation for phenotype	106
3.6.4.2.2	Results and outcome	107
3.6.4.3	CD4 messenger RNA expression	109
3.6.4.3.1	RNA extraction	111
3.6.4.3.2	Reverse transcription	113
3.6.4.3.3	CD4 messenger RNA detection polymerase chain reaction	114
3.6.4.3.4	CD4 polymerase chain reaction amplicon analysis	116
3.6.4.3.5	Results and interpretation	116
3.6.4.4	Effect of dissociation and detection method on CD4 phenotype	118
3.6.4.4.1	Dissociation method investigation - rationale	118
3.6.4.4.2	Detection method investigation – rationale	118
3.6.4.4.3	Fluorochrome comparison and CD4-recovery over time	120
3.6.4.5	Validation of CD4 expression on CD4 ^{high} GHOST cells	123
3.6.4.5.1	Effect of dissociation method on CD4 ^{high} GHOST cell CD4	123
3.6.4.5.2	CD4 recovery in culture on sorted CD4 ^{high} GHOST cells	125
3.6.5	GHOST green fluorescent protein assay optimisation	126
3.6.5.1	Introduction	126
3.6.5.2	Dissection of variables	127

3.6.5.2.1	Replicates and pooling.....	127
3.6.5.2.2	Polybrene® concentrations.....	127
3.6.5.2.3	Cell counts and seeding density.....	127
3.6.6	GHOST green fluorescent protein assay – method.....	131
3.6.6.1	Preparation of CD4 ^{high} GHOST cells for infection.....	133
3.6.6.2	Day 1 count and infection.....	133
3.6.6.2.1	Day 1 count.....	133
3.6.6.2.2	Infection.....	134
3.6.6.3	Green fluorescent protein detection.....	136
3.6.7	Results, calculations, and statistical considerations.....	137
3.6.7.1	Flow cytometry.....	137
3.6.7.2	Statistical considerations.....	137
3.7	Summary.....	143
3.8	References.....	144
Chapter 4	Human immunodeficiency virus production.....	148
4.1	Introduction.....	148
4.1.1	Virus used for experimental purposes.....	149
4.1.1.1	Primary human immunodeficiency virus-1C isolates.....	149
4.1.1.2	Human immunodeficiency virus-1B molecular clones.....	150
4.2	Ethical considerations.....	152
4.3	Molecular clone production.....	152
4.3.1	Overview.....	152
4.3.2	Transformation.....	153
4.3.2.1	Introduction.....	153
4.3.2.2	Medium preparation.....	153
4.3.2.3	Method.....	154
4.3.2.4	Transformant selection and culture.....	155
4.3.2.4.1	Selecting transformants.....	155
4.3.2.4.2	Transformant culture.....	156
4.3.2.4.3	Transformed Stbl2™ cryopreservation.....	156
4.3.3	Plasmid DNA extraction.....	157
4.3.3.1	NucleoSpin® Plasmid Miniprep plasmid DNA extraction.....	157
4.3.3.1.1	Reagent preparation.....	157
4.3.3.1.2	NucleoSpin® plasmid DNA extraction procedure.....	157
4.3.3.2	NucleoBond® Xtra Maxi EF plasmid DNA extraction.....	159
4.3.3.2.1	Reagent preparation.....	159
4.3.3.2.2	NucleoBond® plasmid DNA extraction procedure.....	160
4.3.4	Transfection.....	162
4.3.4.1	Background.....	162
4.3.4.2	HEK293T cell culture and maintenance.....	163
4.3.4.2.1	HEK293T cell culture and passaging.....	163
4.3.4.2.2	HEK293T cell enumeration by flow cytometry.....	164

4.3.4.3	Transfection - method	165
4.3.4.3.1	HEK293T cells	165
4.3.4.3.2	Preparation of transfection reactions.....	166
4.3.4.3.3	Transfection of HEK293T cells.....	166
4.3.5	Human immunodeficiency virus-1B molecular clone harvest.....	167
4.3.6	Molecular clone production optimisation	167
4.3.6.1	Number of harvests	167
4.3.6.2	Virus-encoding plasmid integrity and infectious yield	168
4.3.6.2.1	Agarose gel electrophoresis.....	168
4.3.6.2.2	Results and interpretation	169
4.4	Propagation of HIV in peripheral blood mononuclear cells.....	172
4.4.1	Cell stocks.....	172
4.4.1.1	Peripheral blood mononuclear cell isolation from peripheral blood.....	172
4.4.1.2	Peripheral blood mononuclear cell enumeration by flow cytometry.....	173
4.4.1.2.1	Sample preparation	174
4.4.1.2.2	Gating strategy.....	174
4.4.1.3	Peripheral blood mononuclear cell cryopreservation.....	175
4.4.2	Propagation of human immunodeficiency virus in peripheral blood mononuclear cells.....	176
4.4.2.1	Overview.....	176
4.4.2.2	Human immunodeficiency virus propagation in peripheral blood mononuclear cells – method	176
4.4.2.2.1	Peripheral blood mononuclear cell thawing.....	177
4.4.2.2.2	Peripheral blood mononuclear cell activation.....	177
4.4.2.2.3	Infection	179
4.4.2.2.4	Feeds	179
4.4.2.2.5	Cell-free supernatant and infected peripheral blood mononuclear cell harvest	180
4.4.2.2.6	Control medium for experiments	181
4.4.3	Primary virus propagation optimisation	181
4.4.3.1	Harvest cycles	182
4.4.3.2	Feeding cycles.....	183
4.4.3.2.1	Feed 1 co-culture split.....	183
4.4.3.2.2	Upscaling virus production	184
4.4.3.3	Peripheral blood mononuclear cell-propagated virus loses virulence over time	186
4.5	Summary of virus produced	187
4.6	References.....	188
Chapter 5	Haematopoietic stem/progenitor cell isolation and purification.....	191
5.1	Introduction.....	191
5.2	Ethical considerations	193
5.2.1	Sample collection.....	193

5.2.2	Human immunodeficiency virus testing	194
5.3	Sample processing.....	194
5.3.1	Umbilical cord blood processing.....	194
5.3.1.1	Sample collection and storage	194
5.3.1.2	Isolation of umbilical cord blood-derived mononuclear cells containing haematopoietic stem/progenitor cells	194
5.3.2	Leukapheresis processing	195
5.3.2.1	Sample receipt and storage.....	195
5.3.2.2	Leukapheresis thawing and processing.....	196
5.3.2.2.1	Leukapheresis thawing	196
5.3.2.2.2	Thawed leukapheresis processing	196
5.4	Haematopoietic stem/progenitor cell enumeration	198
5.4.1	Flow cytometer and configuration	198
5.4.2	Sample preparation for enumeration.....	199
5.4.2.1	Umbilical cord blood-derived samples.....	199
5.4.2.2	Leukapheresis product-derived samples.....	199
5.4.3	Gating strategy.....	200
5.5	Optimisation of leukapheresis processing	202
5.5.1	Working temperature	202
5.5.1.1	Method	202
5.5.1.2	Results and outcome	203
5.5.2	Post-thaw resuspension medium	204
5.5.2.1	Method	204
5.5.2.2	Results and outcome	205
5.5.3	Dead cell removal	206
5.5.3.1	Density-gradient centrifugation	206
5.5.3.2	Slow centrifugation.....	207
5.5.3.3	Results and outcome	207
5.6	CD34 ⁺ haematopoietic stem/progenitor isolation.....	210
5.6.1	Magnetic-activated cell sorting	210
5.6.1.1	Introduction	210
5.6.1.2	Method	211
5.6.1.2.1	Magnetic labelling.....	212
5.6.1.2.2	Column-based magnetic separation	212
5.6.1.2.3	Eluting labelled cells.....	212
5.6.1.3	Purity and yield evaluation	213
5.6.1.3.1	Purity.....	213
5.6.1.3.2	Yield.....	214
5.6.2	Fluorescence-activated cell sorting	215
5.6.2.1	Instrument configuration	215
5.6.2.2	Sample preparation and gating strategies	217

5.6.2.2.1	Haematopoietic stem/progenitor cell sorts from umbilical cord blood-derived mononuclear cells	217
5.6.2.2.2	Haematopoietic stem/progenitor cell sorts from leukapheresis.....	219
5.7	Summary	221
5.8	References.....	222
Chapter 6	Haematopoietic stem/progenitor cell colony-forming unit assays and human immunodeficiency virus infection	224
6.1	Introduction.....	224
6.2	Colony-forming unit assay set up and optimisation	226
6.2.1	Background	226
6.2.2	Method optimisation	227
6.2.2.1	Colony-forming unit assay method framework	227
6.2.2.2	Cell seeding density	227
6.2.2.3	Post-sort distribution.....	228
6.2.2.4	Grid-scoring and counting conventions	228
6.2.2.4.1	Grid-scoring.....	228
6.2.2.4.2	Colony counting conventions.....	229
6.2.2.5	Establishing the colony-forming unit atlas	231
6.2.2.5.1	Colony recognition	231
6.2.2.5.2	Counting tools.....	233
6.3	CD34 ⁺ haematopoietic stem/progenitor cell colony-forming unit assays.....	237
6.3.1	Rationale	237
6.3.2	Method	238
6.3.2.1	Sample preparation	238
6.3.2.3	Data capture and processing.....	240
6.3.2.3.1	Data capture.....	240
6.3.2.3.2	Data processing.....	240
6.3.2.3.3	Statistical analysis	241
6.3.3	Results and outcome	241
6.3.3.1	Variance within sorted populations	241
6.3.3.2	Variance between haematopoietic stem/progenitor cell populations....	246
6.3.3.3	Outcome	249
6.4	Effect of human immunodeficiency virus infection on haematopoietic stem/progenitor cell colony formation	250
6.4.1	Introduction	250
6.4.2	Optimisation of haematopoietic stem/progenitor cell infection strategy	251
6.4.2.1	Experimental design	251
6.4.2.2	Infection.....	252
6.4.2.3	DNA extraction	253
6.4.2.4	Human immunodeficiency virus detection polymerase chain reaction ..	256
6.4.2.5	Outcome	257
6.4.3	Methods and outcomes	257

6.4.3.1	CD34 ⁺ haematopoietic stem/progenitor cell isolation.....	257
6.4.3.2	Haematopoietic stem/progenitor cell infection.....	258
6.4.3.3	Colony-forming unit assay and polymerase chain reaction.....	260
6.4.3.3.1	Colony-forming assay.....	260
6.4.3.3.2	Polymerase chain reaction.....	262
6.4.4	Limitations.....	265
6.5	References.....	266
Chapter 7	Concluding remarks	269
7.1	Conclusions and limitations	269
7.2	Future work.....	271
Appendix I	BSL2+ Operations and Safety Manual	I
Appendix II	Ethics approval documentation	LI

Table of Figures

Figure 2.1: Classical model of haematopoiesis, compiled and adapted from literature^{5, 55, 97}. The model depicts unidirectional differentiation of an HSC into terminally differentiated haematopoietic cells following asymmetric, self-renewing cell division through a series of progenitors (HPCs). Cell surface phenotypes are indicated in blue; the dotted grey line indicates trans-differentiation, where sufficient stimulus allows the CLP or CMP to overcome lineage restriction to produce cells of the other lineage. The different markers supposed to be expressed by the true, self-renewing HSC are CD34, CD133, CD90, and CD117, which are under discussion in literature. The consensus is that all HSPCs are negative for lineage-specific (Lin)-markers until well-committed to a particular lineage. The common lymphoid progenitor (CLP) and common myeloid progenitor (CMP) are distinguished from more primitive HSPCs by expression of CD38, and only after differentiation do lineage markers become expressed.18

Figure 2.2: The bone marrow niche shown in windows of increasing resolution, used with permission from the corresponding author¹⁰⁰. The primary residential organ of HSCs is the bone marrow, but they may also home to the liver and spleen (A). The bone marrow niche consists of the endosteal and perivascular niches (B), which function to maintain HSC quiescence and retain HSPCs in the bone marrow niche (C) through the maintenance of critical cytokine gradients (D).....20

Figure 2.3: Major haematopoietic cytokines and their roles in haematopoiesis, adapted for reuse^{5, 120}. Cytokines are indicated in purple next to the differentiation path they promote^{97, 104}. Colonies produced in CFU assays of myeloid lineages are shown in green¹⁰. FLT3-L and IL-7 facilitate the differentiation of HSPCs into lymphoid cells (natural killer cells, and T- and B-lymphocytes) through the CLP. Myeloid differentiation is initiated in HSPCs by IL-3, GM-CSF, and SCF stimulation, forming the CMP. The CMP forms multilineage colonies consisting of granulocytes, erythrocytes, macrophages, and megakaryocytes (CFU-GEMM). The CMP can differentiate into the granulocyte-macrophage (GM) progenitor with GM-CSF stimulation, which form granulocyte-macrophage colonies (CFU-GM), or the megakaryocyte-erythrocyte (ME) progenitor with SCF, IL-3, and GM-CSF stimulation. GM progenitors stimulated with GM-

CSF, IL-6, IL-3, and SCF can also produce single-lineage macrophage (CFU-M) or granulocyte (CFU-G) colonies when additionally stimulated with M-CSF and G-CSF, respectively. ME progenitors form either erythroid colonies in burst-forming units (BFU-E) or CFUs (together called B/CFU-E), or megakaryocyte colonies (CFU-Mk) when stimulated with EPO or TPO, respectively.....24

Figure 2.4: The HIV genome with three distinct reading frames. HIV proteins are indicated as encoded in colour-coded genes, with links indicating the trans-frame protein-coding regions. Figure used with permission¹³⁵27

Figure 2.5: Representation of the HIV life cycle, designed by 5W Infographic and reused with permission¹³⁶. HIV-1 binding to target cell receptors CD4 and CCR5/CXCR4 begins the cycle of replication consisting of reverse transcription of the viral genome to proviral DNA which is integrated into the host cell genome. Transcription and translation of the proviral genome results in the assembly and release of newly-packaged virions by budding from the host cell membrane.....29

Figure 3.1: An HIV virus particle, adapted from literature^{1, 2, 10}, indicating the size range of HIV particles, and the location of various viral proteins and nucleic acids which can be used to detect HIV.55

Figure 3.2: Schematic representation of the Lenti-X™ Rapid Titre p24 ELISA kit; image available from the Lenti-X™ Rapid Titre p24 ELISA kit user manual.....63

Figure 3.3: Typical sample layout in an 8-well strip of Lenti-X™ Rapid Titre p24 ELISA kits. ..64

Figure 3.4: p24 Standard curve generated using the Lenti-X™ Rapid Titre p24 ELISA kit (lot number KCL05161; plate lot number P1094). The equation of the line of best fit (dotted line) used to estimate p24 concentrations relative to the standard curve is shown on the graph.66

Figure 3.5: A schematic representation of the principles of PCR, used with permission²⁹. Cycles of denaturing DNA templates followed by primer annealing and polymerisation (elongation) of target DNA regions selected by primers is shown.68

Figure 3.6: PCR amplicon analysis by agarose gel electrophoresis. The direction of DNA migration is from the negative terminal to the positive terminal, as a result of the applied electric current. Over time, colorimetric tracking (blue band near positive terminal) indicates that the DNA amplicons have migrated through the length of the gel and will likely be resolved. Visualisation by UV light shows DNA amplicons stained by fluorescent dyes on the gel not visible with the naked eye.69

Figure 3.7: Examples of primer secondary structures, generated using the IDT OligoAnalyzer online tool. (A) Hairpin structure which does not result in elongation but prevents primer from binding to target. (B) Hairpin structure with a 3'-overhang which will result in elongation. (C) Homodimer between primers of the same sequence with a 3'-overhang which could result in elongation. (D) Heterodimer between two primers in a primer pair with a 3'-overhang which will result in elongation.71

Figure 3.8: Example output of NCBI primer analysis (Primer-BLAST) using the full-length consensus sequence for HIV-1C generated in CLC Main Workbench for a primer pair designed to amplify a portion of the HIV-1C *Env* gene. (A) Specificity of primers to target relative to the Refseq mRNA database, and the location of the amplicon resulting from PCR using these primers is shown. (B) Primer details returned in the same primer analysis report, indicating the amplicon (product) length, and T_M , GC-content, and self-complementarity values of the primer pair. The values for self- and self-3'-complementarity correspond to the propensity for self-complementation. Lower values (≤ 3) are therefore preferred.73

Figure 3.9: OligoAnalyzer and OligoCalc primer analysis tool outputs for the forward primer indicated in Figure 3.8B, as a supplement to Primer-BLAST analysis. Within-primer potential secondary structures best illustrated by the OligoAnalyzer tool (A), ranked from most likely to least likely. Potential self-annealing (B) and primer specifics (C) calculated by OligoCalc show similar results to both Primer-Blast and OligoAnalyzer outputs.74

Figure 3.10: Thermocycling conditions and their respective descriptions applied during PCR reactions.81

Figure 3.11: HIV LTR-*gag* and V3 primer validation and annealing temperature optimisation. (H) The FastRuler™ LR loaded in lane 1 for each gel, indicating known fragment sizes of 1500,

850, 400, 200, 50 bp. (A-G) Lanes 2-9 for each gel show PCR products generated using annealing temperatures 54 (lane 2), 55.5 (lane 3), 57 (lane 4), 58.5 (lane 5), 60 (lane 6), 61.5 (lane 7), 63 (lane 8), and 64.5°C (lane 9) respectively. DNA extracted from GHOST cells exposed to the following HIV-1 isolates: Yu2 (A), 89.6 (B), NL4-3 (C), SW7 (D), and CM9 (E) was amplified using isolate-specific primers against the LTR-*gag* region of the HIV proviral genome. DNA extracted from GHOST cells exposed to only primary HIV-1C isolates SW7 (F) and CM9 (G) was amplified using isolate-specific primers against the V3-encoding region of the HIV proviral genome.....83

Figure 3.12: Limit of detection PCR gel images. Grey boxes in each image indicate where amplification of the LTR-*gag* region was observed. (A) Limit of detection PCR reactions for HIV-1B isolates. FastRuler™ MR ladder (D) was loaded in lanes 1 and 21, and the L32 positive amplification control for HIV negative DNA was loaded in lane 2. Lanes 3-7 were loaded with 0.1%, 1%, 5%, 10%, 20% Yu2-infected GHOST cell LTR-*gag* PCR product respectively, and lane 8 with the HIV unexposed GHOST cell LTR-*gag* PCR product. The same pattern was repeated for 89.6-infected GHOST cell LTR-*gag* PCR products (lanes 9-14) and NL4-3-infected GHOST cell LTR-*gag* PCR products (lanes 15-19). HIV-unexposed PCR products for the LTR-*gag* amplification was loaded in lane 20 as the negative control. (B & C) Limit of detection PCR reactions for HIV-1C isolates SW7 (B) and CM9 (C). Lanes 1 and 10 were loaded with FastRuler™ MR, lane 2 was loaded with the no template control for each primer pair, and lane 3 was loaded with the L32 positive amplification control performed on HIV-unexposed GHOST cell DNA. Lanes 4-9 were loaded with the respective isolate-specific LTR-*gag* PCR products containing 0.1%, 1%, 5%, 10%, 20%, and no HIV-infected cell DNA respectively.....90

Figure 3.13: FACSAria™ laser/detector configuration used for GHOST cell phenotype and sorting experiments. (A) The blue laser excites fluorochromes at 488 nm and was used to detect FITC and GFP on B, and SSC on C. (B) The yellow/green laser excites fluorochromes at 561 nm and was used to detect PC7 on A and 7-AAD on B. (C) The violet laser excites fluorochromes at 407 nm and was used to detect BV605 on D. (D) The red laser excites fluorochromes at 633 nm and was used to detect APC on C.97

Figure 3.14: Enumeration of GHOST cells using Flow-Count™ fluorospheres. (A) 10 022 intact, viable GHOST cells are selected in the region GHOST cells. (B) 7085 Flow-Count™ beads are detected in the Cal region.....100

Figure 3.15: Gating strategy routinely used for GHOST cell enumeration, CD4 phenotype, and GFP expression. (A) A FS Lin versus 7-AAD two-parameter plot with Flow-Count™ beads excluded was used to select viable cells, which stain negative for 7-AAD and are indicated in the VIABLE region. (B) A two-parameter FS Lin versus SSC Log plot gated on the “VIABLE” region to identify viable, intact cell GHOST cells (GHOST cells region). (C) A two-parameter plot of Flow-Count versus time, with the number of beads captured indicated in the Cal region. (D & E) Two-parameter FS Lin versus CD4-APC plots gated on “GHOST cells” were used to enumerate CD4⁺ GHOST cells. (D) GHOST cells stained with CD4-APC iso, used to set the “CD4+” region. (E) GHOST cells stained with CD4-APC. (F) A two-parameter FS Lin versus GFP plot of HIV-unexposed GHOST cells which do not express GFP. (G) The same two-parameter plot as in F showing HIV-exposed GHOST cells expressing GFP.103

Figure 3.16: Flow cytometry and gating strategies used for GHOST cell sorts. (A) A two-parameter FS Lin versus 7-AAD was used to select viable (7-AAD negative) GHOST cells, captured in the “VIABLE” region. (B) A two-parameter FS Lin versus SSC plot gated on viable GHOST cells (“VIABLE” region) was used to capture intact GHOST cells. (C) A two-parameter FS Lin versus GFP plot gated on “GHOST cells” was used to sort GFP⁻ GHOST cells (“GFP-“ region) from HIV-unexposed GHOST cells. (D) The same two-parameter FS Lin versus GFP plot without the “GFP-“ gate was used to sort GFP⁺ GHOST cells (“GFP+”) from HIV-exposed GHOST cells. (E) A two-parameter FS Lin versus CD4-APC plot gated on “GHOST cells” was used to sort CD4^{high} low-passage GHOST cells. (F) Representative post-sort purity achieved after sorting CD4^{high} GHOST cells.....105

Figure 3.17: GHOST cell phenotype analysis using CCR5-PC7, CXCR4-BV605, and CD4-FITC. (A) A representative two-parameter plot of CXCR4-BV605 versus CCR5-PC7 of GHOST cells stained with the isotype combination used to set the four quadrants indicated on the plot. (B) Same plot as A, representing data obtained for GHOST cells stained with CXCR4-BV605 and CCR5-PC7. Sub-populations of GHOST cells with different co-receptor expression profiles are shown. (C) A representative two-parameter plot of SSC Log versus CD4-FITC for the isotype

tube (unstained for CD4-FITC) used to set the “CD4+” region. (D) Same plot as C for GHOST cells stained with CD4. GHOST cells expressing CD4 should have appeared in the “CD4+” region.109

Figure 3.18: Sequential gating strategy used to sort CD4^{high} and CD4^{low} GHOST cells for mRNA evaluation. (A) Viability of GHOST cells negative for 7-AAD captured in the “Viable” region on a FS Lin versus 7-AAD two-parameter plot. (B) Viable, intact GHOST cells were selected in the region “GHOST cells” on a two-parameter FS Lin versus SSC Log plot. (C) The pre-sort CD4 population shown on a two-parameter SSC Log versus CD4-APC plot. The regions “CD4 low” (pink) and “CD4 high” (purple) were sorted. (D) Post-sort purity for CD4^{low} GHOST cells is shown on the same plot as in C. (E) The same two-parameter plot as in C shows the post-sort purity of CD4^{high} GHOST cells.111

Figure 3.19: Gel image of CD4 cDNA PCR to assess the CD4-expressing construct in GHOST cells. (A) Lanes 1 and 11 were loaded with FastRuler™ LR DNA ladder shown in B for amplicon size estimation. Lanes 2 and 3 were loaded with the NTC_{PCR} and L32 PCR positive controls respectively. Lanes 4 and 5 were loaded with the NTC_{RT} and NRC reverse transcription controls respectively. Lanes 6-10 contained CD4 PCR products for TZM-bl (lane 6), PBMC (lane7), Ghost CD4^{high} (lane 8), Ghost CD4^{low} (lane 9), and HEK293T (lane 10) cells.116

Figure 3.20: *In silico* CD4 mRNA transcript prediction explaining the presence of the 186 bp amplicon observed in HEK293T and PBMC mRNA pools assayed by RT-PCR.117

Figure 3.21: The discrepancy in CD4 detection between unsorted GHOST cells stained with CD4-FITC and CD4-APC. (A) Two-parameter FS Lin versus CD4-FITC plot unstained for CD4-FITC, used to set the “CD4-FITC+” region. (B) The same plot as A, using cells stained with CD4-FITC. (C) Two-parameter FS Lin versus CD4-APC plot unstained for CD4-APC used to set the “CD4-APC+” region. (D) The same plot as C, using cells stained with CD4-APC and the “CD4-APC+” region set on the unstained control. (E) The same plot as D, with the “CD4-APC+” region set on the division between the two populations of CD4-APC expression, as the “CD4-FITC+” region divides the two populations. The difference between D and E illustrates the need for an isotype control for CD4-APC, in order to correctly resolve the CD4⁺ population from the CD4⁻ population.119

Figure 3.22: CD4 recovery on five biological replicates (BR) of GHOST cells post-trypsinisation, detected using CD4-APC.122

Figure 3.23: CD4 recovery on five biological replicates (BR) of GHOST cells post-trypsinisation, detected using CD4-FITC.122

Figure 3.24: Effect of dissociation method on CD4 detection of sorted CD4^{high} GHOST cells. (A) A two-parameter FS Lin versus CD4-APC plot used to set the “CD4+” region on non-enzymatically dissociated CD4^{high} GHOST cells stained with CD4-APC iso. (B) The same two-parameter plot as in A, for non-enzymatically dissociated CD4^{high} GHOST cells stained with CD4-APC. (C) A two-parameter FS Lin versus CD4-APC plot used to set the “CD4+” region on enzymatically dissociated CD4^{high} GHOST cells stained with CD4-APC iso. (D) The same two-parameter plot as in C, for enzymatically dissociated CD4^{high} GHOST cells stained with CD4-APC.124

Figure 3.25: GHOST cell growth curves for GFP assay optimisation showing average cell counts of triplicate wells for two stocks (A and B) of GHOST cells assayed at three time points. ...131

Figure 3.26: Functional titration of HIV on GHOST cells by limiting dilution, based on GFP expression in HIV-infected GHOST cells. (A) Functional titration of HIV by exposing a known number of GHOST cells to known dilutions of virus (dilution 1 being the least dilute and dilution 4 being the most dilute. HIV-infected cells are detected by the expression of GFP (green cells), detectable 48 hr post-infection. (B) Transcription of the HIV-2 LTR-driven GFP transgene in GHOST cells, activated by the binding of Tat from infecting HIV-1 to the HIV-2 LTR, resulting in the expression of GFP in HIV-infected cells.132

Figure 3.27: GHOST GFP assay plate layout. Dilutions of HIV to be added to each well are indicated in the wells. Empty wells contained 1 mL PBS. R1-3 represent technical replicates.133

Figure 3.28: Illustration of the preparation of dilution series employed for the GHOST GFP assay. Blue values indicate volumes used for HIV-1C primary HIV-1 isolate titrations, and green values indicate volumes used for HIV-1B molecular clone titrations. Dilution series were prepared by adding medium to each tube (2-6) as indicated, then adding the starting volume

of HIV to tube 1, and transferring the volumes of HIV indicated from tube 1 to tube 5 (illustrated by the dilution series tube transfer diagram). Polybrene® was added to a concentration of 20 µg/mL, and the volumes of each dilution (last row) were dispensed into the corresponding wells illustrated in Figure 3.27.136

Figure 4.1: Outlines of strategies for the production of primary virus (propagation in PBMCs, pink) and molecular clones (molecular clone production, purple). Functional titration of virus produced by both strategies is described in 3.6.6 *GHOST GFP assay Method*.149

Figure 4.2: Sequential gating strategy for HEK293T cell enumeration. (A) A two-parameter FS Lin versus SSC Log plot was used to identify intact HEK293T cells (“HEK293T cell” region). A “NOT BEADS” Boolean gate was applied to this plot to exclude Flow-Count™ beads from HEK293T cells in the region “HEK293T cells”. (B) Viable HEK293T cells were captured in the “VIABLE” region on a two-parameter FS Lin versus 7-AAD plot. (C) A two-parameter Flow-Count versus TIME plot was used to enumerate the Flow-Count™ beads analysed (“Ca” region).....165

Figure 4.3: Representation of the migration of three plasmid forms of p89.6 to illustrate the migration of the three forms of plasmid DNA. Ladders are not shown as the largest band on available ladders was smaller than p89.6, at 10 000 bp.170

Figure 4.4: Gel image and DNA ladders used for electrophoretic analysis of plasmids from different stocks for comparative purposes. (A) Lanes 1 and 15 were loaded with FastRuler™ HR DNA ladder, and lanes 2 and 14 were loaded with FastRuler™ MR DNA ladder. Lanes 3-5 were loaded with pNL4-3 preparations in the order (left to right) depicted in Table 4.7. Lanes 6-8 were loaded with pYu2 preparations in the same order, and lanes 9-11 contain p89.6 DNA. Lane 12 was loaded with pUC19 DNA. (B) FastRuler™ HR DNA ladder band sizes, loaded in lanes 1 and 15 of (A). (C) FastRuler™ MR DNA ladder band sizes, loaded in lanes 2 and 14 of (A).....171

Figure 4.5: Sequential gating strategy used to phenotype and enumerate PBMC stocks for HIV propagation. (A) A two-parameter FS Lin versus SSC Log plot was used to identify intact PBMCs, captured in the “PBMCs” region, gated on the Boolean gate “NOT BEADS” to exclude Flow-Count™ beads from cell analyses. (B) Viable PBMCs were identified using a two-

parameter SSC Log versus 7-AAD plot gated on PBMCs based on negative staining for 7-AAD, indicated by the “VIABLE” region. (C) Viable PBMCs expressing the panleukocyte marker CD45 (leukocytes) were identified using a two-parameter SSC Log versus CD45-KO plot gated on viable PBMCs. Leukocytes identified by expression of CD45 were captured in the “Leukocytes” region, which were then used to identify monocytes and T-cells from the remaining leukocytes. (D) A two-parameter plot showing SSC Log versus CD4-FITC (gated on “Leukocytes”) was used to distinguish monocytes (CD45⁺CD4^{dim}, moderate to high SSC; red population) and CD4⁺ T-cells (CD45⁺CD4⁺, moderate SSC; purple population). (E) Flow-Count™ bead events were captured in the “Cal” region for enumeration purposes.....175

Figure 4.6: In-house modified strategy for HIV propagation in PHA-P/IL-2-stimulated PBMCs.176

Figure 4.7: Hypothetical illustration of HIV quasispecies formation during HIV propagation. Different coloured virions in each flask represent different populations of HIV which abide in each flask due to mutation resulting from reverse transcription. Each vertical flask series represents a step in HIV production, namely initial infection, feed 1, and feed 2. Grey dotted arrows represent points of pooling, before each feed and before harvesting.185

Figure 5.1: Haematopoiesis and the expression of HSPC surface markers^{3, 4, 6, 11}. The self-renewing HSC divides asymmetrically to produce a self-renewing HSC and HPC, which will differentiate as directed by cytokine signalling. The heterogenous CD34⁺ HSPC population is outlined by the blue dotted line.192

Figure 5.2: Histopaque density-gradient centrifugation facilitates separation of MNCs from granulocytes, erythrocytes, and platelets.195

Figure 5.3: Effect of staining medium on isotype control staining (Stem-Kit) during leukapheresis-derived HSPC enumeration. Stemkit iso staining of AP181122-01 cells stained in RPMI (A) versus AP181122-01 cells stained in TP₄ buffer (B).....197

Figure 5.4: ISHAGE-derived gating strategy applied to the enumeration of CD34⁺ HSPCs derived from both UCB and leukapheresis products. Plots represent UCB-MNCs. (A) Viable cells were selected based on negative 7-AAD staining. (B) Viable leukocytes were selected on

CD45 expression (“Leukocytes”) in the two-parameter SSC Lin versus CD45-FITC plot gated on the “Viable” region. (C and D) The “CD34+ HSPCs” region was confirmed in random samples using the Stem-Kit isotype control (C), using a SSC Lin versus CD34-PE two-parameter plot. (D) Viable leukocytes expressing CD34 (CD34+ HSPCs) were captured in the “CD34+ HSPC” region. (E) Flow-Count™ beads were identified in the “Cal” region and used to calculate absolute cell numbers.201

Figure 5.5: Effect of working temperature on post-thaw viability of leukapheresis-derived cells. (A) Viability of cells (AP181010) processed and resuspended on ice contrasted with (B) the viability of cells (AP180823) processed and resuspended using pre-cooled (4°C) solutions.204

Figure 5.6: Effect of post-thaw resuspension buffer on post-thaw viability. (A) Viability of cells resuspended in RPMI. (B) Viability of cells resuspended in TP₄ buffer.206

Figure 5.7: Post-centrifugation density gradient of leukapheresis-derived cells in RPMI loaded on histopaque.207

Figure 5.8: Effect of dead cell removal technique on viability and CD34-recovery. (A) The viability of cells subjected to density-gradient centrifugation on histopaque was compared to (B) the viability of cells subjected to slow centrifugation. (C) The SSC Lin profiles compared to CD45 expression is indicated for post-histopaque, and (D) post-slow centrifugation. (E) The percentage of CD34⁺ HSPCs after dead cell removal by layering on histopaque was compared to (F) slow centrifugation.....209

Figure 5.9: Principles of direct selection by MACS.211

Figure 5.10: Post-thaw (A; C; E) and post-MACS (B; D; F) comparison in terms of viability, leukocyte proportion, and CD34+ HSPC enrichment. (A) The viability of AP180823 post-processing is contrasted with (B) the viability post-MACS indicated by negative staining for 7-AAD. (C) The proportion of leukocytes post-processing compared to (D) post-MACS is indicated by positive staining for CD45. (E) The proportion of CD34+ HSPCs post-processing is compared to (F) the enriched proportion of CD34+ HSPCs post-MACS.....214

Figure 5.11: FACS Aria Fusion laser/detector configuration for HSPC sorting experiments. (A) The blue laser excited fluorochromes at 488 nm and was used to detect SSC on C and FITC on B. (B) The violet laser excites fluorochromes at 407 nm and was used to detect Zombie Violet™ on F. (C) The yellow/green laser excites fluorochromes at 561 nm and was used to detect 7-AAD on B, PC7 on A, and PE on E. (D) The red laser excites fluorochromes at 633 nm and was used to detect APC-Cy7 on A, and APC on C.216

Figure 5.12: Sequential gating strategy for sorting HSPC sub-populations from UCB-MNCs, and resulting post-sort purity of the CD34⁺Lin⁻ HSPC population. (A) Dead cells were excluded by positive staining for 7-AAD. (B) Viable leukocytes expressing low levels of CD45 were selected in the CD45 dim region. (C) Viable, CD45 dim cells already expressing lineage-specific markers were excluded in the Lin⁻ region. (D) The co-expression of CD34 and CD38 on viable, CD45^{dim}Lin⁻ HSPCs is shown, where CD38⁻, CD38^{dim}, and CD38⁺ populations also expressing CD34 are indicated. Post-sort purity of the viable, CD45^{dim}CD34⁺Lin⁻ sorted population (E and F), indicating 100% purity of the sorted population. (E) The viable, CD45^{dim}Lin⁻ population post-sort purity (pre-sort population shown in C). (F) The viable, CD45^{dim}Lin⁻CD34⁺ population post-sort purity (pre-sort population indicated by CD34⁺ populations in D).219

Figure 5.13: Sequential gating strategy for sorting CD34⁺ HSPCs from CD34-enriched populations. Cell debris was excluded by selecting intact cells (A), which were sorted for viability by negative staining for 7-AAD (B). Live cells expressing CD34 are encompassed in the region CD34⁺ (C), and viable, CD34⁺ sorted cells are indicated in the region Sorted CD34⁺ cells.221

Figure 6.1: Schematic representation of haematopoiesis (adapted from literature⁹⁻¹¹), showing HSC and HSPC phenotype markers (blue), CFUs (green), and colony images relevant to CFU assays. Colony images were obtained from the CFU assay resource “The Human Colony Forming Cell (CFC) Assay Using Methylcellulose-based Media” protocol (R&D Systems) available at <https://www.rndsystems.com/resources/protocols/human-colony-forming-cell-cfc-assay-using-methylcellulose-based-media>.225

Figure 6.2: Counting grid scored onto the bottom of each well of 24-well plates, showing the grid block positions used for colony counting.229

Figure 6.3: Single/multiple colony designation from the CFU atlas for colony counting standardisation. Images above were adapted from the STEMCELL Technologies technical manual (version 4.2.0) for human CFU assays using Methocult¹³, and the STEMVision automated colony counter technical manual. Circles indicate how colonies were counted. (A) Overlapping CFU-GM (blue circle) and B/CFU-E (red circle) were counted as separate colonies. (B) Well-resolved colonies, with a CFU-GEMM encircled in blue and B/CFU-E in red. The granulocyte/macrophage “halo” in the CFU-GEMM is noteworthy as it distinguishes the CFU-GEMM from the B/CFU-E. (C) Two nodes of a single CFU-GM colony are encircled in yellow, indicating that two overlapping nodes of the same colony type in the same plane are counted as one colony. (D) The difference between CFU-M (green circle) and CFU-GM (blue circle) is shown, with good resolution between the colonies. (E) Multiple lobes of a single CFU-GEMM are encircled in orange, distinguishable from a B/CFU-E by the granulocyte/macrophage halo. (F) A single large BFU-E with multiple lobes (and no granulocyte/macrophage halo) is shown in contrast to a single small BFU-E (G), which show the resolution which can be used to count erythroid colonies as a single colony.....230

Figure 6.4: Picture atlas for haematopoietic colony recognition with key points for easy identification of colonies characterised (Table 6.1). (A) Characteristics of CFU-GEMM colonies. (B) Characteristics of B/CFU-E colonies. (C) Characteristics of CFU-G colonies. (D) Characteristics of CFU-M colonies. (E) Characteristics of CFU-GM colonies. Colony images were obtained from the CFU assay resource “The Human Colony Forming Cell (CFC) Assay Using Methylcellulose-based Media” protocol (R&D Systems) available from <https://www.rndsystems.com/resources/protocols/human-colony-forming-cell-cfc-assay-using-methylcellulose-based-media>.....232

Figure 6.5: Schematic representation of clonal expansion and differentiation of HSPCs into terminally differentiated cells and the expression of key cell surface markers over time. The blue block indicates the range of phenotypes selected for CFU assays performed in this study.238

Figure 6.6: Typical HSPC population sort plate layout. The sorted population phenotypes are shown in each well. Unlabelled wells contained 1 mL PBS or PBS supplemented with 2% pen/strep.240

Figure 6.7: Average number of colonies counted for each sorted HSPC population, per biological replicate. Error bars represent the standard deviation of technical repeats. GEMM indicates CFU-GEMM (granulocyte, erythrocyte, megakaryocyte, macrophage) colonies, GM indicates CFU-GM (granulocyte-macrophage) colonies, G indicates CFU-G (granulocyte) colonies, M indicates CFU-M (macrophage) colonies, E indicates B/CFU-E (erythroid) colonies, and Mk indicate CFU-Mk (megakaryocyte) colonies. (A) CD34⁺ HSPC colonies; (B) CD34⁺Lin⁻ HSPC colonies; (C) CD34⁺Lin⁻CD38⁺ HSPCs colonies; (D) CD34⁺Lin⁻CD38^{dim} HSPC colonies; (E) CD34⁺Lin⁻CD38⁻ HSPC colonies.....246

Figure 6.8: Colony variance between HSPC populations, and distribution of colony types for each sorted HSPC population, displayed in a box-and-whisker plot. The data represents five biological replicates. The lowest and highest values are indicated by the whiskers, and the mean number of colonies is indicated by the line bisecting each box. Significance tested by two-way ANOVA with Tukey correction for multiplicity is indicated by asterisks; * $p \leq 0.05$, ** $p \leq 0.01$, *** $p \leq 0.001$, **** $p < 0.0001$248

Figure 6.9: Compiled gel image of HIV detected in CYT⁺ and CYT⁻ UCB-derived CD34⁺ sorted HSPCs at MOI3 and MOI10, 24 hr post-infection. (A) Lane 1 was loaded with the FastRuler™ LR DNA ladder (shown in B). Lanes 2 and 4 were loaded with NTC for the L32 (lane 2) and LTR (lane 4) primer pairs. Lane 3 was loaded with the PCR products amplified using the L32 primer pair and HIV- CYT- MOI10 DNA as the positive reaction control. To show LTR primer specificity, a positive control (CM9-infected PBMC DNA, lane 5) and negative control (HIV-unexposed PB-01 DNA, lane 6) were loaded. Lanes 7-10 were loaded with the PCR products for MOI3 CYT⁺, MOI3 CYT⁻, MOI10 CYT⁺, and MOI10 CYT⁻ respectively, amplified using LTR primer pair. Lanes 11-14 were loaded with the PCR products for HIV- MOI3 CYT⁺, HIV- MOI3 CYT⁻, HIV- MOI10 CYT⁺, and HIV- MOI10 CYT⁻ respectively, amplified using the LTR primer pair. The grey block indicates where amplification was observed.257

Figure 6.10: Plate layout for CD34⁺ HSPC exposure to three infection conditions, towards evaluating the effects of HIV infection on HSPC colony formation. CFS refers to HIV CFS-exposed cells, control refers to cells mock-infected in RPMI, and CM refers to cells mock-infected with conditioned medium. CYT⁺ indicates cells incubated overnight with cytokines, and CYT⁻ indicates cells incubated overnight without cytokines.259

Figure 6.11: Plate layout for CFU assay of pilot experiment, seeded 24 hr post-infection. HIV CFS refers to HIV CFS-exposed cells, control refers to cells mock-infected in RPMI, and CM refers to cells mock-infected with conditioned medium. CYT+ indicates cells incubated overnight with cytokines, and CYT- indicates cells incubated overnight without cytokines. Empty wells contained 1 mL PBS (2% pen/strep).....261

Table of Tables

Table 2.1: Classes of stem cell potency explained.....	9
Table 2.2: Summary of literature regarding HIV infection of HSPCs. Where HIV derived from patients was used but not evaluated for subtype, the country in which patients were recruited is stated if known.	35
Table 3.1: GeneXpert in-built QC steps, what they control for, and the reasons for failure, measured with each test run.	61
Table 3.2: An example of results obtained during setup of a standard curve for the Lenti-X™ Rapid Titre p24 ELISA (kit lot number KCL05161; plate lot number P1094).	65
Table 3.3: Primer pairs and sequences for detecting HIV nucleic acids. Primers highlighted in grey indicate primers taken from or adapted from literature.	76
Table 3.4: Concentrations, protein purity (A_{260}/A_{280} ratio), and salt purity (A_{260}/A_{230} ratio) of HIV-exposed GHOST DNA extracted for HIV-1 primer validations.	80
Table 3.5: Cell ratios for each set of HIV-infected (GFP+) sorted GHOST cells to HIV unexposed GHOST cells for DNA extraction.....	86
Table 3.6: Concentrations, protein purity (A_{260}/A_{280} ratio), and salt purity (A_{260}/A_{230} ratio) of GHOST cell DNA extracted to determine the limit of detection of the in-house PCR protocol.	87
Table 3.7: Gallios™ laser and filter configurations including fluorescent detection channels (FL) used to detect emission spectra of laser-excited fluorochromes.	96
Table 3.8: RNA concentrations, protein purity (A_{260}/A_{280}), and salt purity (A_{260}/A_{230}) for RNA extracted from PBMCs, TZM-bl cells, GHOST cells sorted for low- and high-CD4 expression, and HEK293T cells.	112
Table 3.9: Reverse transcription reactions set-up using the SensiFAST cDNA reverse transcription kit.....	114

Table 3.10: PCR reactions set up for CD4 mRNA detection.....	115
Table 3.11: Biological replicate (BR) designation of different GHOST cell stocks for the CD4 recovery and fluorochrome detection experiment.	120
Table 3.12: CD4 recovery (indicated as %) post-trypsinisation of CD4 ^{high} GHOST cells.	126
Table 3.13: GHOST cell proliferation assayed in triplicate at three time points for two stocks of GHOST cells.....	130
Table 3.14: Calculations used to obtain Day 1 absolute counts of HIV-unexposed GHOST cells. GHOST count, number of beads, and calibration factor were obtained as described in 3.6.3.5 <i>GHOST cell gating strategies</i> (Figure 3.15). Absolute counts were calculated according to Equation 3.1 as described in 3.6.3.3.2 <i>General enumeration</i>	139
Table 3.15: Breakdown of calculations performed on Day 3 to obtain IU/mL (derived from Equation 3.2) from functional titration in the GHOST GFP assay.....	140
Table 3.16: Example of an IU/mL calculation with real data obtained for the GHOST GFP assay of HIV-1C primary isolate SW7_010818. The green block indicates the mean day 1 cell count used in further calculations, pink blocks indicate the three closest IU/mL values used to calculate the average, and blue blocks indicate values excluded from further calculations.	141
Table 4.1: Details of HIV-1C primary isolates produced in PBMCs.....	150
Table 4.2: Details of HIV-1B molecular clones produced in this study.....	151
Table 4.3: NucleoSpin® plasmid DNA extraction concentrations, protein purity (A_{260}/A_{280} ratio), and salt purity (A_{260}/A_{230} ratio).	159
Table 4.4: NucleoSpin® plasmid DNA extraction concentrations, protein purity (A_{260}/A_{280} ratio), and salt purity (A_{260}/A_{230} ratio).	162
Table 4.5: Transfection reaction setup for T75 and T150 flasks of HEK293T cells.	166

Table 4.6: Functional titrations of three consecutive HIV CFS harvests from HIV-1B molecular clones produced by HEK293T transfection. Non-infectious titres are shown in purple.	168
Table 4.7: Plasmid DNA preparations used to evaluate plasmid DNA integrity.....	169
Table 4.8: Gallios™ laser and filter configuration used for PBMC phenotyping, showing the relevant antibodies or stains and the respective detection channels.....	173
Table 4.9: A summary of the schedule of events for the propagation of R5-, R5X4-, and X4-tropic HIV-1C primary isolates. Details of the number of PBMCs required to initiate propagation experiments and for the various feed cycles are included.	178
Table 4.10: p24 ELISA results comparing day 10 and day 14 HIV CFS harvests for CM1.	182
Table 4.11: Functional titres for successive productions of HIV-1C primary isolates CM9 and SW7 showing a gradual decrease in infectivity over time. Non-infectious harvests (IU/mL ≤ 10 ⁴) are shown in purple.....	186
Table 4.12: Representative HIV-1B and HIV-1C HIV CFS stocks and their functional titres generated by the GHOST GFP assay.	187
Table 5.1. Summary of Gallios flow cytometer laser and filter configuration, channel designations and fluorochromes (used in this series of experiments).....	198
Table 5.2: Percent viabilities for leukapheresis products processed with different post-thaw resuspension media.	205
Table 5.3: Percentage viability, and leukocyte and CD34+ HSPC proportions post-thaw compared to dead cell removal strategies.	208
Table 5.4: Paired post-processing and post-MACS viability and purity results for UCB-MNCs and leukapheresis-derived cells.....	213
Table 6.1: Haematopoietic colony classification criteria and categories.	231

Table 6.2: Per-well counting sheet laminated for recording colonies of a single well while counting. Colonies of each type were counted per grid block (Figure 6.2). Example values are filled in. The CFU assay for CB240118-02, well A2 was used as an example (green).....234

Table 6.3: Per-plate counting sheet used to record colonies in each grid block (blue numbers) of each well (black numbers) of 24-well plates. Well numbers were adjusted according to the plate layout specific to the experiment. The CFU assay for CB240118-02, well A2 are used as an example (green).235

Table 6.4: Final consolidation of experimental data for CFU assay data capture. The data captured in this sheet was recorded for each 24-well plate. Wells were adjusted according to the plate layout specific to the experiment. . The CFU assay for CB240118-02, wells A2-A5 are used as an example (green).236

Table 6.5: Absolute (total cell) counts for UCB-derived MNCs from which CD34⁺ HSPC sub-populations were sorted.....239

Table 6.6: Comparison of total colonies between sorted HSPC populations using a two-way ANOVA with Tukey correction for multiplicity. Significance indicated by asterisks denotes adjusted *p*-values as follows: **p*≤0.05, ***p*≤0.01, ****p*≤0.001, *****p*<0.0001.....249

Table 6.7: Final volumes of HIV CFS (HIV-exposed) or CM (HIV-unexposed) for each flask in the HSPC infection optimisation experiment.....253

Table 6.8: DNA concentrations and purity ratios for HSPC MOI optimisation experiments. 255

Table 6.9: Pilot HIV experiment HSPC DNA concentrations, protein purity (A₂₆₀/A₂₈₀ ratio), and salt purity (A₂₆₀/A₂₃₀ ratio).....262

Table 6.10: Post-precipitation pilot HIV experiment HSPC DNA concentrations, protein purity (A₂₆₀/A₂₈₀ ratio), and salt purity (A₂₆₀/A₂₃₀ ratio).264

List of Abbreviations

TMB	3,3',5,5'-tetramethylbenzidine
$\Delta 32$	32-base pair deletion in CCR5 gene
7-AAD	7-aminoactinomycin D
AIDS	Acquired immunodeficiency syndrome
A	Adenine
ADA-SCID	Adenosine deaminase severe combined immunodeficiency
ARC	AIDS-related complex
ACT	Alberts Cellular Therapy
APC	Allophycocyanin
ANOVA	Analysis of Variance
ART	Antiretroviral therapy
AZT	Azido-deoxythymidine
E	Burst/colony-forming unit erythroid (data representations)
bp	Base pairs
BR	Biological replicate
BSL	Bio-safety level
BV605	Brilliant Violet 605™
B/CFU-E	Burst/colony forming unit erythroid
BFU-E	Burst-forming unit erythroid
cRNA	carrier RNA
CCR5	C-C motif chemokine receptor type 5
R5-tropic	CCR5-tropic HIV

CFS	Cell-free supernatant
G	Colony-forming unit granulocyte (data representations)
GEMM	Colony-forming unit granulocyte-erythroid-macrophage-megakaryocyte (data representations)
M	Colony-forming unit macrophage (data representations)
Mk	Colony-forming unit megakaryocyte (data representations)
CRF	Circulating recombinant form
CPD	Citrate phosphate dextrose
CRU	Clinical research unit
CD	Cluster of differentiation
CFU	Colony-forming unit
CFU-E	Colony-forming unit erythroid
CFU-G	Colony-forming unit granulocyte
CFU-GEMM	Colony-forming unit granulocyte-erythroid-macrophage-megakaryocyte
CFU-GM	Colony-forming unit granulocyte-macrophage
CFU-M	Colony-forming unit macrophage
CFU-Mk	Colony-forming unit megakaryocyte
CSF	Colony-stimulating factor
CLP	Common lymphoid progenitor
CMP	Common myeloid progenitor
cDNA	Complementary DNA
CROI	Conference on Retroviruses and Opportunistic Infections
CSIR	Council for Scientific and Industrial Research
CXCR4	C-X motif chemokine receptor type 4

CXCL12; SDF-1	C-X-C motif chemokine ligand 12; Stromal-derived factor 1
CAR	CXCL12-abundant reticular
X4-tropic	CXCR4-tropic HIV
Cy7	Cyanine 7
C	Cytosine
DNA	Deoxyribonucleic acid
dNTPs	Deoxyribonucleic acid triphosphates
DMSO	Dimethyl sulphoxide
dsDNA	Double-stranded DNA
DMEM	Dulbecco's modified Eagle medium
ESCRT	Endosomal sorting complexes required for transport
EF	Endotoxin-free
EPO	Erythropoietin
EtBr	Ethidium bromide
EDTA	ethylenediamine tetra-acetic acid
FITC	Fluorescein isothiocyanate
FL	Fluorescence detection channel
FACS	Fluorescence-activated cell sorting
FLT3-L	Fms-like tyrosine kinase 3 ligand
FBS	Foetal bovine serum
FS	Forward scatter
G ₀	G ₀ cell cycle phase indicating quiescence
GHOST cells	GHOST (3) R5X4
GvHD	Graft-versus-host disease

G-CSF	Granulocyte colony-stimulating factor
GM	Granulocyte-macrophage
GM-CSF	Granulocyte-macrophage colony-stimulating factor
GFP	Green fluorescent protein
G	Guanine
HPCs	Haematopoietic progenitor cells
HSPCT	Haematopoietic stem and progenitor cell transplant
HSPCs	Haematopoietic stem and progenitor cells
HSCs	Haematopoietic stem cells
HiFi	High fidelity
HIV-1B	HIV-1 subtype B
HIV-1C	HIV-1 subtype C
HRP	Horse radish peroxidase
HEK293T	Human embryonic kidney 293T cell line
HIV	Human immunodeficiency virus
HLA	Human leukocyte antigen
iPSCs	Induced pluripotent stem cells
IU	Infectious units
ICMM	Institute for Cellular and Molecular Medicine
IDT	Integrated DNA Technologies
IL-2	Interleukin-2
IL-3	Interleukin-3
IL-6	Interleukin-6
IL-7	Interleukin-7

ISCT	International Society for Cellular Therapy
ISHAGE	International Society for Hematotherapy and Graft Engineering
IC	Intracellular
IMDM	Iscove's modified Dulbecco's medium
KO	Krome-Orange™
Ltag	Large tumour antigen
Lin	Lineage marker cocktail (CD3, CD14, CD16, CD19, CD20, CD45)
LTR	Long terminal repeat
LB	Luria-Bertani
M-CSF	Macrophage colony-stimulating factor
MACS	Magnetic-activated cell sorting
CD117; SCFR	Mast/stem cell growth factor receptor
MFI	Mean fluorescence intensity
ME	Megakaryocyte-erythrocyte
T _M	Melting temperature
MSCs	Mesenchymal stem/stromal cells
mRNA	Messenger RNA
MOI	Multiplicity of infection
NCBI	National Centre for Biotechnology Information
NICD	National Institute for Communicable Disease
NIH	National Institutes of Health
NK	Natural killer
ND	Neutral density
NRC	No reverse transcriptase control

NTC	No template control
NEDB	Non-enzymatic dissociation buffer
OD	Optical density
P	Passage
CM	PBMC-conditioned medium
Pen/strep	Penicillin and streptomycin cocktail
PBMCs	Peripheral blood mononuclear cells
PBS	Phosphate-buffered saline
PE	Phycoerythrin
PHA-P	Phytohaemagglutinin-P
PEI	Polyethyleneimine
PCR	Polymerase chain reaction
CD45; PTPRC	Protein tyrosine phosphatase receptor type C
QC	Quality control
qPCR	Quantitative PCR
RANKL	Receptor activator of nuclear factor kappa-B ligand
rh	Recombinant human
RT	Reverse transcription
RPMI	Roswell Park Memorial Institute-1640 medium
SSC	Side scatter
SV40	Simian virus 40
ssRNA	Single-stranded RNA
SDS	Sodium dodecyl sulphate
SOPs	Standard operating procedures

SCF	Stem cell factor
SOC	Super optimal broth with catabolite suppression
Taq	Thermus aquaticus
TPO	Thrombopoietin
T	Thymine
TP ₄ buffer	TP buffer (40 µg/mL human albumin)
TAR	Trans-activator-responsive
TGF-β	Transforming growth factor-beta
TAE	Tris-acetate EDTA
UV	Ultraviolet
UCB	Umbilical cord blood
VSV-G	Vesicular stomatitis virus G protein
VPR	Viral protein R

Introduction, aims, and objectives

1.1 Introduction

Infection by the human immunodeficiency virus (HIV) remains a global pandemic, with millions of people being infected (almost 37 million in 2017)¹. Millions more people are affected by HIV due to the cost-burden of life-long treatment and HIV-associated disease². South Africa is the country most affected by the pandemic, with an estimated 7.2 million people living with HIV according to the latest (2017) available statistic¹. Infection with HIV remains incurable, despite continuous efforts resulting in improved antiretroviral therapy (ART) agents³ and regimens⁴ which can afford HIV-infected individuals an improved quality of life.

The rapid turnover of HIV in terms of replication causes the accumulation of mutations, which has resulted in distinct types of HIV being present globally⁵⁻⁸. The most prevalent is HIV-1 group M, which can be further divided into subtypes which arose from region-specific evolution⁹. With the migration of people between regions where different distinct subtypes are prevalent, recombination between subtypes of HIV-1 group M occurred^{8, 9}. HIV-1 subtype C (HIV-1C) is the most prevalent subtype of HIV-1 worldwide, and predominates in southern Africa (including South Africa) and Asia⁶. However, HIV-1B (prevalent in Europe and North America) is the most well-researched subtype¹⁰. This is an important point because of differences between HIV-1 group M subtypes with respect to virulence, drug response, and the emergence of escape mutants resulting in drug resistance^{6, 10}. The differences between HIV-1 group M subtypes means that ART, most often developed against and tested on HIV-1B, may not be effective against non-B subtypes.

Viral tropism contributes another paradigm to HIV diversity. Viral tropism refers to the preferred mechanism of receptor-dependent HIV entry into host cells, which is restricted by the affinity of the HIV envelope protein gp120 for specific host cell surface proteins¹¹. The most frequent tropism of HIV (across subtypes) is C-C motif chemokine receptor type 5 (CCR5)-tropic (R5-tropic) HIV¹². A naturally-occurring homozygous 32 base-pair deletion ($\Delta 32$)

in the CCR5 gene results in mutant cells being phenotypically CCR5 null, and consequently resistant to R5-tropic HIV¹³. Engineering HIV resistance through transplant of HIV-positive patients with CCR5-null haematopoietic stem and progenitor cells (HSPCs)¹⁴⁻¹⁸ has been demonstrated once in the Berlin patient¹⁸, and more recently in a second patient (known as the “London patient”)¹⁹. The Berlin patient remains HIV-free several years after receiving an HSPC transplant using cells from a donor homozygous for the $\Delta 32$ CCR5 mutation, used to treat his leukaemia^{18,20}. The London patient has thus far been in HIV remission for 18 months following homozygous $\Delta 32$ -mutant donor HSPC transplant to treat leukaemia¹⁹. This second patient who is in remission from HIV following CCR5-null HSPC transplantation provides hope for future patients. Other attempts to recreate the proof-of-concept gene therapy cure have been complicated by the emergence of C-X motif chemokine receptor type 4 (CXCR4)-tropic (X4-tropic) HIV moieties in mice²¹ and in human trials²², ultimately resulting in viral load rebound.

Haematological abnormalities in HIV patients are well-described, ranging from blood cell depletions (cytopenias) to haematological cancers, even in optimally treated patients^{23, 24}. These features point towards an effect of HIV infection and ART on the HSPC compartment which is responsible for reconstituting the haematopoietic system (consisting of blood and immune cells). This effect could be the result of direct infection of HSPCs with HIV²⁵, or an indirect effect of aberrant cell signalling by HIV-infected cells in the bone marrow disrupting HSPC homeostasis^{23, 26, 27}. Whether or not HSPCs are susceptible to HIV infection remains unclear, as research to date reflects conflicting data on *in vitro* and *in vivo* infection of HSPCs with HIV. HIV subtype diversity and tropism seem to contribute to the uncertainty, with articles suggesting that HIV-1C but not HIV-1B²⁸, and X4-tropic but not R5-tropic HIV²⁹ are capable of infecting HSPCs. Therefore, the interactions between HIV and HSPCs are not well understood and require further investigation.

HSPC susceptibility to HIV infection has two implications for potential HSPC-based anti-HIV gene therapies. The first is that clonal expansion may expand the proposed HSPC reservoir following the reinfusion of infected, gene-edited HSPCs³⁰. The second is that HSPCs can become infected with X4-tropic HIV²⁹ if they express CXCR4³¹, which a CCR5-null phenotype would not protect against.

The reduced colony-forming capacity of HSPCs obtained from HIV patients indicates that the suppressive effects of HIV infection and ART have a long-lasting impact on HSPC function²⁶. The suppression of haematopoiesis in HIV-infected patients has been proposed to be caused by viral replication, as impaired multilineage HSPC function can be restored with combination ART³². Haematopoietic suppression has also been linked to the presence of HIV proteins and anti-gp120 antibodies, which suppress the function of HSPCs from HIV patients but not from HIV-uninfected patients²³. In addition to the functional effects of HIV infection on HSPCs, bone marrow abnormalities (hypercellularity and dysplasia) are also present in HIV patients³³ suggesting a local effect of HIV infection on bone marrow cells. Whether these effects result from the presence of HIV, HIV proteins, and anti-HIV antibodies, or as a bystander effect from the presence of infected cells is unclear, as HIV-susceptible lymphocytes infiltrate into the bone marrow of HIV-infected patients³³. The complex effects of HIV on the haematopoietic system are often additive, resulting in chronic inflammation³⁴ and dysregulation of haematopoietic cytokine pathways^{24, 35}. These effects can be exacerbated by multidrug regimes used to treat HIV and HIV-associated conditions such as anaemia²⁴. In addition to the direct effects of HIV proteins, aberrant cell-signalling by infected cells³⁵, and multidrug treatment complications, co-infections (e.g. *Plasmodium falciparum* and *Cryptococcus*) can also deleteriously impact haematopoiesis²⁴.

In summary, a better understanding of the impact of HIV, more specifically, HIV-1C, on HSPC function is important for the continued development of improved treatment strategies.

1.2 Aim and Objectives

1.2.1 Aim

The overall aim of this project was to evaluate the effects of HIV infection on the colony-forming capacity of HSPCs, as a measure of HSPC function. Two HIV-1 subtypes (HIV-1C and HIV-1B) of three tropisms were to be evaluated.

1.2.2 Objectives

In order to achieve the aim, the project was divided into the following five objectives.

- (1) Produce three tropisms of HIV-1C primary isolates, and three tropisms of HIV-1B molecular clones for experimental purposes.
- (2) Detect HIV and titrate infectious virus for experimental purposes.
- (3) Isolate HSPCs obtained from umbilical cord blood (UCB) and leukapheresis product for experimental purposes.
- (4) Optimise the CFU assay and acquire the skills required to consistently identify, count, and categorise haematopoietic colonies.
- (5) Expose HSPCs to three tropisms of HIV-1C and three tropisms of HIV-1B, to evaluate the effect of HIV-1 infection on HSPC colony formation.

1.3 References

1. UNAIDS. UNAIDS Fact Sheet July 2018 2017 [Available from: <http://www.unaids.org/en/resources/fact-sheet>].
2. Taraphdar, P., Guha, R.T., Haldar, D., Chatterjee, A., Dasgupta, A., Saha, B., et al. Socioeconomic consequences of HIV/AIDS in the family system. *Nigerian medical journal : journal of the Nigeria Medical Association*. 2011;52(4):250-3.
3. Kirtane, A.R., Abouzid, O., Minahan, D., Bensel, T., Hill, A.L., Selinger, C., et al. Development of an oral once-weekly drug delivery system for HIV antiretroviral therapy. *Nature Communications*. 2018;9(1):2.
4. Antiretroviral Therapy Cohort, C. Survival of HIV-positive patients starting antiretroviral therapy between 1996 and 2013: a collaborative analysis of cohort studies. *The lancet HIV*. 2017;4(8):e349-e56.
5. Abecasis, A.B., Wensing, A.M.J., Paraskevis, D., Vercauteren, J., Theys, K., Van de Vijver, D.A.M.C., et al. HIV-1 subtype distribution and its demographic determinants in newly diagnosed patients in Europe suggest highly compartmentalized epidemics. *Retrovirology*. 2013;10(1):7.
6. Spira, S., Wainberg, M.A., Loemba, H., Turner, D., Brenner, B.G. Impact of clade diversity on HIV-1 virulence, antiretroviral drug sensitivity and drug resistance. *The Journal of antimicrobial chemotherapy*. 2003;51(2):229-40.
7. Lynch, R.M., Shen, T., Gnanakaran, S., Derdeyn, C.A. Appreciating HIV Type 1 Diversity: Subtype Differences in Env. *AIDS Research and Human Retroviruses*. 2009;25(3):237-48.
8. Ward, M.J., Lycett, S.J., Kalish, M.L., Rambaut, A., Leigh Brown, A.J. Estimating the Rate of Intersubtype Recombination in Early HIV-1 Group M Strains. *Journal of Virology*. 2013;87(4):1967-73.
9. Castro-Nallar, E., Pérez-Losada, M., Burton, G.F., Crandall, K.A. The evolution of HIV: Inferences using phylogenetics. *Molecular Phylogenetics and Evolution*. 2012;62(2):777-92.
10. Taylor, B.S., Sobieszczyk, M.E., McCutchan, F.E., Hammer, S.M. The challenge of HIV-1 subtype diversity. *The New England journal of medicine*. 2008;358(15):1590-602.
11. McGowan, J.P., Shah, S. Understanding HIV Tropism New York: Physicians' Research Network Inc.; 2010 [Volume 15, January 2010 - based on a live meeting.]. Available from: http://www.prn.org/index.php/management/article/hiv_tropism_1002.
12. Morner, A., Bjorndal, A., Albert, J., Kewalramani, V.N., Littman, D.R., Inoue, R., et al. Primary human immunodeficiency virus type 2 (HIV-2) isolates, like HIV-1 isolates, frequently use CCR5 but show promiscuity in coreceptor usage. *J Virol*. 1999;73(3):2343-9.
13. Galvani, A.P., Novembre, J. The evolutionary history of the CCR5-Δ32 HIV-resistance mutation. *Microbes and Infection*. 2005;7(2):302-9.
14. Barmania, F., Pepper, M.S. C-C chemokine receptor type five (CCR5): An emerging target for the control of HIV infection. *Applied & Translational Genomics*. 2013;2:3-16.

15. Hutter, G., Bodor, J., Ledger, S., Boyd, M., Millington, M., Tsie, M., et al. CCR5 Targeted Cell Therapy for HIV and Prevention of Viral Escape. *Viruses*. 2015;7(8):4186-203.
16. Symons, J., Vandekerckhove, L., Hütter, G., Wensing, A.M.J., van Ham, P.M., Deeks, S.G., et al. Dependence on the CCR5 Coreceptor for Viral Replication Explains the Lack of Rebound of CXCR4-Predicted HIV Variants in the Berlin Patient. *Clinical Infectious Diseases*. 2014;59(4):596-600.
17. Allers, K., Hütter, G., Hofmann, J., Loddenkemper, C., Rieger, K., Thiel, E., et al. Evidence for the cure of HIV infection by CCR5 Δ 32/ Δ 32 stem cell transplantation. *Blood*. 2011;117(10):2791-9.
18. Hütter, G., Nowak, D., Mossner, M., Ganepola, S., Müßig, A., Allers, K., et al. Long-Term Control of HIV by CCR5 Delta32/Delta32 Stem-Cell Transplantation. *New England Journal of Medicine*. 2009;360(7):692-8.
19. Gupta, R.K., Abdul-jawad, S., McCoy, L.E., Mok, H.P., Peppas, D., Salgado, M., et al. HIV-1 remission following CCR5 Δ 32/ Δ 32 haematopoietic stem-cell transplantation. *Nature*. 2019.
20. Hütter, G., Bodor, J., Ledger, S., Boyd, M., Millington, M., Tsie, M., et al. CCR5 Targeted Cell Therapy for HIV and Prevention of Viral Escape. *Viruses*. 2015;7(8):2816.
21. Myburgh, R., Ivic, S., Pepper, M.S., Gers-Huber, G., Li, D., Audigé, A., et al. Lentivector Knockdown of CCR5 in Hematopoietic Stem and Progenitor Cells Confers Functional and Persistent HIV-1 Resistance in Humanized Mice. *Journal of Virology*. 2015;89(13):6761-72.
22. Verheyen, J., Thielen, A., Lubke, N., Dirks, M., Widera, M., Dittmer, U., et al. Rapid Rebound of a Preexisting CXCR4-tropic Human Immunodeficiency Virus Variant After Allogeneic Transplantation With CCR5 Delta32 Homozygous Stem Cells. *Clinical infectious diseases : an official publication of the Infectious Diseases Society of America*. 2019;68(4):684-7.
23. Donahue, R.E., Johnson, M.M., Zon, L.I., Clark, S.C., Groopman, J.E. Suppression of in vitro haematopoiesis following human immunodeficiency virus infection. *Nature*. 1987;326(6109):200-3.
24. Vishnu, P., Aboulafia, D.M. Haematological manifestations of human immune deficiency virus infection. *British Journal of Haematology*. 2015;171(5):695-709.
25. Trono, D., Marzetta, F. Profaning the Ultimate Sanctuary: HIV Latency in Hematopoietic Stem Cells. *Cell Host & Microbe*. 2011;9(3):170-2.
26. Geissler, R.G., Ottmann, O.G., Kleiner, K., Mentzel, U., Bickelhaupt, A., Hoelzer, D., et al. Decreased haematopoietic colony growth in long-term bone marrow cultures of HIV-positive patients. *Research in Virology*. 1993;144:69-73.
27. Li, G., Zhao, J., Cheng, L., Jiang, Q., Kan, S., Qin, E., et al. HIV-1 infection depletes human CD34+CD38- hematopoietic progenitor cells via pDC-dependent mechanisms. *PLOS Pathogens*. 2017;13(7):e1006505.
28. Redd, A.D., Avalos, A., Essex, M. Infection of hematopoietic progenitor cells by HIV-1 subtype C, and its association with anemia in southern Africa. *Blood*. 2007;110(9):3143-9.

29. Carter, Christoph C., McNamara, Lucy A., Onafuwa-Nuga, A., Shackleton, M., Riddell Iv, J., Bixby, D., et al. HIV-1 Utilizes the CXCR4 Chemokine Receptor to Infect Multipotent Hematopoietic Stem and Progenitor Cells. *Cell Host & Microbe*. 2011;9(3):223-34.
30. Younan, P., Kowalski, J., Kiem, H.-P. Genetically Modified Hematopoietic Stem Cell Transplantation for HIV-1-infected Patients: Can We Achieve a Cure? *Mol Ther*. 2014;22(2):257-64.
31. Majka, M., Rozmyslowicz, T., Honczarenko, M., Ratajczak, J., Wasik, M.A., Gaulton, G.N., et al. Biological significance of the expression of HIV-related chemokine coreceptors (CCR5 and CXCR4) and their ligands by human hematopoietic cell lines. *Leukemia*. 2000;14(10):1821-32.
32. Koka, P.S., Fraser, J.K., Bryson, Y., Bristol, G.C., Aldrovandi, G.M., Daar, E.S., et al. Human Immunodeficiency Virus Inhibits Multilineage Hematopoiesis In Vivo. *Journal of Virology*. 1998;72(6):5121-7.
33. Calenda, V., Chermann, J.C. The effects of HIV on hematopoiesis. *European journal of haematology*. 1992;48(4):181-6.
34. Vandergeeten, C., Fromentin, R., Chomont, N. The role of cytokines in the establishment, persistence and eradication of the HIV reservoir. *Cytokine & Growth Factor Reviews*. 2012;23(4–5):143-9.
35. Alexaki, A., Wigdahl, B. HIV-1 Infection of Bone Marrow Hematopoietic Progenitor Cells and Their Role in Trafficking and Viral Dissemination. *PLoS Pathog*. 2008;4(12):e1000215.

Chapter 2 Literature review

2.1 Stem cells

2.1.1 Introduction to stem cells

2.1.1.1 Definition

Stem cells are present from the moment of conception to the moment of death in any multicellular organism and play an essential role in replacing cells and restoring tissues throughout an organism's life. The ability to undergo asymmetric division is one of the defining characteristics of stem cells. Asymmetric division refers to cell division in which one daughter cell replaces the parent (self-renewal), and the other daughter cell has a separate fate (differentiation). The second defining characteristic of stem cells is the ability to differentiate into multiple cell lineages¹⁻⁴. The ability of stem cells to self-renew and differentiate into multiple lineages results from (i) the absence of lineage-defining epigenetic marks^{1, 3, 5}, and (ii) specialised environments⁶ (niches) which support quiescence and orchestrate differentiation of stem cells^{1-3, 5, 7-10}.

2.1.1.2 Cradle to grave

Genes in the genome are expressed or repressed by the opening and closing of chromatin, which is determined by molecular additions (such as methylation) to the genome, globally termed epigenetic marking¹¹. Epigenetic marks modulate gene expression between different cell types by silencing or activating genes in varying degrees of permanence, resulting in cells with different forms and functions. These marks are not encoded by the genome, but rather determine how the genome is read during transcription and translation, by obstructing or assisting the opening of chromatin and promoter regions¹¹. Epigenetic markings govern the ability of a stem cell to self-renew and differentiate^{1, 12, 13}. The accumulation of epigenetic marks (epimarking) in stem cell populations confers lineage specificity, consequently reducing the potential of the cell to differentiate indiscriminately.

The potential of a stem cell to divide and differentiate into multiple different cell types rather than just an identical daughter cell (cell division), termed potency, is inversely proportionate to the amount of epigenetic marking. Stem cells can be divided into three classes of potency¹⁴, summarised in Table 2.1¹⁵. Potency is measured by the number of distinct lineages a stem cell can clonally expand and differentiate into, with totipotent stem cells having the highest potency, and multipotent stem cells having the lowest potency^{16, 17}. Lineage restriction, commitment, or priming, are terms used to describe the gradual loss of potency accompanying the accumulation of epigenetic marks with differentiation. Epimarking begins at the first step of embryogenesis¹², when a single totipotent cell divides to form a cell mass with distinct layers with different pre-determined fates, such as to become supporting tissue for embryo growth or to form part of the embryo itself. Epimarking continues to occur during development, well into the formation of complex tissue structures and adult stem cell pools present in most tissues.

Table 2.1: Classes of stem cell potency explained.

	Totipotent/omnipotent stem cells	Pluripotent stem cells	Multipotent stem cells
Differentiation potential	● Extra-embryonic and embryonic tissues	● Embryonic tissues	● Subset of embryonic tissues
Source tissues	● Zygote/morula – early stages post-fertilisation	● Inner cell mass of the blastocyst	● Various tissues
Examples	● Embryonic stem cells	● Induced pluripotent stem cells	● Adult stem cells

Self-renewal is a critical part of the function of stem cells, but does not occur indefinitely. Aging has been described as a consequence of stem cell deterioration both in number and in differentiation potential due to the deoxyribonucleic acid (DNA) damage and telomere shortening which accumulates with division¹⁸. Sufficient DNA damage will cause a self-renewing stem cell to undergo apoptosis, reducing the pool of self-renewing stem cells, and

affecting the ability of a body to respond sufficiently to stimuli initiating cell replacement or tissue restoration¹⁸. This gradual depletion of self-renewing stem cell pools with time (as a function of number of divisions and relative amount of DNA damage) reduces adequate regeneration of tissues and contributes to the slow decline of health characteristic of advanced age¹⁹. Stem cells are therefore critical not only for the development and maintenance of tissue structures by differentiating and regenerating cells as they cycle, but also for longevity.

2.1.1.3 The stem cell niche

During embryogenesis, the totipotent zygote divides to form daughter cells destined to generate the embryo or extra-embryonic tissues, which then divide and differentiate into the many tissues of the foetus¹⁵. Concerted cell division and differentiation continues throughout gestation to form organs and eventually, when the gestational period is complete, the organism is a mass of neatly stacked, terminally or near-terminally differentiated cells. However, pools of stem cells which did not lose all potency due to epimarking are maintained to regenerate tissues over the lifetime of the organisms^{20, 21}. These stem cells are termed “adult stem cells” and are not totipotent, but rather multipotent and tissue-specific.

Adult stem cells are maintained over an organism’s lifetime in specialised microenvironments called niches. These stem cell pools respond to micro-environmental stimuli, which regulate quiescence, division, or mobilisation as required for tissue maintenance^{22, 23}. Stem cell niches facilitate physical, neural, metabolic, and humoral feedback while providing structure for stem cells to be housed²⁰. Niches are formed by stromal cells and extracellular matrix proteins, and are typically well-vascularised microenvironments closely associated with neuronal networks for cellular signalling²⁴. The stem cell niche regulates the function of stem cells, which is to self-renew and differentiate into cell lineages in response to paracrine, nervous, and metabolic signalling delivered by niche cells^{4, 20, 25}. Thus, stem cell niches orchestrate the mobilisation and differentiation of specific stem cells, resulting in dynamic tissue regeneration.

2.1.2 Types of stem cells

2.1.2.1 Embryonic stem cells

Embryonic stem cells are well known pluripotent stem cells and are the main source of much of the controversy associated with stem cell research. These cells are obtained from the inner cell mass of the blastocyst formed during embryonic development^{17, 26}. Harvesting these cells therefore requires the sacrifice of an embryo *in vitro*, which is the subject of ethical contention.

2.1.2.2 Adult stem cells

Adult stem cells are multipotent cells which exist in niches in the adult body and carry out stem-like functions towards the regeneration of cells and tissues. These cells, also called tissue-specific stem cells, are epigenetically primed for self-renewal, clonal expansion, and differentiation into a few specific cell lineages^{20, 21}. The two most prominent categories of adult stem cells are haematopoietic stem cells (HSCs) and mesenchymal stem/stromal cells (MSCs)^{27, 28}.

2.1.2.2.1 Haematopoietic stem cells

HSCs are well-studied adult stem cells which reside in the bone marrow niche⁶. HSCs are responsible for the maintenance of the haematopoietic system, which includes all cells of the blood and immune systems, and can be sourced from bone marrow, peripheral blood, and UCB²⁹.

2.1.2.2.2 Mesenchymal stem cells

MSCs are a class of adult stem cell first identified as stromal cells in the bone marrow with osteogenic potential^{30, 31}. This class of stem cells was later expanded to include any stem or progenitor cell with trilineage potential, in other words, able to form osteoblasts,

chondrocytes, and adipocytes³². Sources of MSCs include bone marrow, adipose tissue, blood vessels, umbilical cord, and placenta³³.

2.1.2.2.3 Other adult stem cells

The category of adult stem cells also includes highly specialised stem cells which regenerate single tissues in the body. These include satellite cells which regenerate muscle, neural stem cells which regenerate neurons, and epithelial stem cells which regenerate skin cells²⁰.

2.1.2.3 *Induced pluripotent stem cells*

Induced pluripotent stem cells (iPSCs) are stem cells derived from somatic cells which have been reprogrammed to pluripotency by treatment with a cocktail of transcription factors which erase epigenetic marks on the DNA of reverted cells³⁴. These cells are gaining popularity in research and clinical settings as they are (i) relatively easily obtained, (ii) carry a patient's specific genetic make-up (important in personalised medicine), and (iii) can be generated from a variety of sources. Examples of cells from which iPSCs can be generated include skin fibroblasts, keratinocytes from the hair follicle, and epithelial cells passed in urine³⁵.

2.1.3 Stem cells in regenerative medicine

Regenerative medicine is a branch of medicine dedicated to the functional restoration of dysfunctional processes resulting in disease or debilitation³⁶. Restoration can be mechanical (prostheses, pacemakers, insulin pumps), chemical (iron tablets, insulin), or biological (protein- or cell-based therapies)³⁶. Stem cell therapies with great potential for long-term reconstitutive gene therapies and patient-specific tissue engineering are at the leading edge of regenerative medicine. Applications range from Parkinson's disease³⁷, diabetes³⁸, and HIV infection^{39, 40} in varying stages of realisation.

2.2 Haematopoietic stem cells

2.2.1 Biology and function

2.2.1.1 Purpose

Lifelong haematopoietic reconstitution through haematopoiesis is maintained by HSCs in the bone marrow niche of the iliac crest, spinal column, and long-bones. The process of haematopoietic reconstitution is achieved by the stimulation of quiescent HSCs to effect asymmetric cell division, resulting in clonal expansion and differentiation of HSCs^{5, 41}. The expansion and differentiation occurs through a series of lineage-primed haematopoietic progenitor cells (HPCs), which are capable of switching between lineages with the correct stimulus⁴¹. Clonal expansion is the ability of cells to exponentially multiply and divide into identical daughter cells. The ability of HSCs to simultaneously maintain the pool of quiescent HPCs through self-renewal, while giving rise to a pool of HPCs (which expand and differentiate), allows for life-long haematopoietic reconstitution and maintenance. Haematopoietic “stem” cells isolated from different sources are truly a heterogeneous population of HSCs and HSPCs, collectively termed HSPCs.

2.2.2 Haematopoietic stem/progenitor cell therapy

2.2.2.1 Haematopoietic system reconstitution – a clinical first

Transplant of HSPCs to facilitate bone marrow reconstitution in patients receiving radiation or chemotherapy was first performed in 1956⁴². This was followed by the discovery and exploration of the human leukocyte antigen (HLA) as the self-recognising immune surveillance system, resulting in HLA typing being used to match organ and tissue donors, as many of the first transplants resulted in recipients succumbing to graft-versus-host disease (GvHd)⁴³. HLA-matching, also known as tissue-typing or tissue-matching, is routinely performed prior to solid organ and HSPC transplantation to ensure that donor tissue will not illicit an uncontrollable immune response in the recipient⁴³. Reconstitution of the haematopoietic

system by HSPC transplant (HSPCT) was the first cell-based transplantation therapy and heralded the arrival of regenerative medicine. To date, HSPCT is the only stem cell therapy approved for clinical use.

2.2.2.2 Haematopoietic stem/progenitor cell transplant

2.2.2.2.1 Background

HSPCT is used to treat haematopoietic disorders, and can be divided into two categories, allogeneic or autologous, based on the HLA-match between donor and recipient. Autologous HSPCT, where the patient's own cells are given back to them, has the least risk for GvHD development and transplant rejection as the transplanted cells are HLA-identical, but is not possible in all cases. A special case of allogeneic transplant, called haploidentical HSPCT, refers to transplant of HSPCTs from a close HLA match such as in siblings or close relatives, has the next-best chance of success. Where the donor and recipient are HLA-matched but are not siblings or closely related, the HSPCT is termed "allogeneic". Current indications for HSPCT include leukaemias, myelomas, lymphomas, and non-malignant disorders such as bone marrow aplasia and severe immunodeficiencies⁴⁴. HSPCT facilitates bone marrow reconstitution after ablation resulting from high-dose chemotherapy treatment. Donor HSPCs take up residence in the recipient's bone marrow in a process called "engraftment", whereafter a functional haematopoietic system is restored. HSPCT, similarly to organ and tissue transplant, is often hampered by challenges such as the number of donors worldwide, compounded by the relatively low probability of finding an unrelated tissue-matched donor⁴⁵.

⁴⁶.

2.2.2.2.2 Sources of haematopoietic stem/progenitor cells for haematopoietic stem/progenitor cell transplant

Mobilised peripheral blood (leukapheresis product) is currently the preferred HSPCT product, and consists of HSPCs harvested in the mononuclear cell fraction from the peripheral blood of patients. This harvest is performed after granulocyte colony-stimulating factor (G-CSF) treatment to mobilise HSPCs from the bone marrow into the peripheral circulation⁴⁷.

However, UCB is emerging as an alternate source of HSPCs for transplantation purposes, with the advantage of a lower associated risk of GvHd even with reduced HLA-matching⁴⁵. However, the HSPC yield from UCB is low due to the small volumes of blood typically present in the umbilical cord. This means that single UCB units are not usually sufficient to achieve therapeutic HSPC doses for transplantation⁴⁵. Therapeutic doses are achieved by pooling UCB units, which increases the risk of GvHd due to the use of multiple low HLA-matched units⁴⁶.

2.2.2.2.3 Haematopoietic stem/progenitor cell dose in haematopoietic stem/progenitor cell transplant

HSPC dose refers to the total number of HSPCs present in the transplant product, and is associated with engraftment success^{48, 49}. HSPCs are routinely quantified during patient and donor evaluation prior to transplantation to ensure that sufficient HSPCs ($\geq 5 \times 10^6$ per recipient kilogram body weight)⁵⁰ are transplanted for successful engraftment. The cluster of differentiation (CD)-34 phosphoglycoprotein expressed on the surface of HSPCs, in combination with the pan-leukocyte cell surface marker protein tyrosine phosphatase receptor type C (PTPRC; CD45), are used to identify and enumerate HSPCs. The internationally recommended cell surface phenotype for HSPC enumeration, developed by the International Society for Cellular Therapy (ISCT) (previously known as the International Society for Hematotherapy and Graft Engineering (ISHAGE)), is CD45^{dim}CD34⁺. The strategy for enumerating CD45^{dim}CD34⁺ HSPCs has become known as the ISHAGE protocol⁵¹.

The success of matched-donor transplants contrasting with the chances of donor-recipient matching from current bone marrow registries and the low HSPC yield from UCB units coalesced into the field of *ex vivo* HSPC expansion⁵²⁻⁵⁴. Expansion aims to increase the absolute number of HSPCs while maintaining short- and long-term engraftment potential^{55, 56}, to achieve therapeutically significant HSPC numbers from UCB. This would contribute to alleviating donor insufficiency as HSPCT of UCB-derived HSPCs requires less stringently matched donors.

2.2.2.3 Haematopoietic stem/progenitor cells in gene therapy

The generation of functional blood and immune systems in patients previously afflicted by haematopoietic disorders or disease by HSPCT shifted the paradigm of regenerative medicine from restoration to reprogramming. Contrary to HSPCT, gene therapy approaches infuse recipients with a purified HSPC population⁵⁷, usually isolated using techniques which rely on identification of the cell-surface sialomucin stem cell marker, CD34⁵⁸. CD34⁺ HSPCs are isolated from the heterogenous HSPC-containing source by fluorescence-activated cell sorting (FACS)⁵⁹ or magnetic-activated cell sorting (MACS)⁶⁰. A patient's own cells could be harvested by mobilisation, gene-edited, and gene-edited cells expanded to generate a transplanted product which is non-immunogenic – eliminating the risk of GvHd – and curative in cases where disease or cancer is the result of mutation in the HSPC populations. This has been achieved with success in patients to treat adenosine deaminase severe combined immunodeficiency (ADA-SCID)⁶¹, X-linked SCID⁶², sickle cell anaemia⁶³, and cerebral adrenoleukodystrophy⁶⁴. Gene therapies in development based on haematopoietic reconstitution post-HSPCT include the generation of HIV resistance^{40, 65-72}, and reconstituting functional phenotype disrupted in thalassemia⁷³, and a subset of Fanconi anaemias⁷⁴.

2.2.3 Phenotype and heterogeneity

The precise cell surface phenotype of self-renewing “true” HSCs is a matter of contention owing in part to the long-standing dogma regarding CD34 cell surface expression. While CD34 is known as “the stem cell marker” and is associated with various types of stem cells⁵⁸, the CD34⁺ leukocyte population containing HSPCs is quite heterogenous^{41, 75, 76}. For this reason, CD34⁺ “HSCs” are more accurately referred to as CD34⁺ HSPCs, as the CD34⁺ population contains cells expressing various CD-markers including CD38^{41, 77}, CD133⁷⁸⁻⁸⁰, and CD90⁸¹. These subpopulations of CD34⁺ HSPCs have distinct differentiation potentials^{78, 80, 82-85}.

The heterogeneity of the HSPC population has been described transcriptomically and phenotypically^{41, 80, 81, 86-88}. The level of heterogeneity, coupled with functional similarities and differences between phenotypes contributes to the challenges which come with selecting

HSPC populations by phenotype. A summary of HSPC phenotypes in relation to potency and haematopoiesis is illustrated in Figure 2.1.

In form, HSPCs resemble leukocytes, and are small, round cells with a single nucleus. HSPCs from sources containing leukocytes, such as UCB, leukapheresis product, and bone marrow, these cells are characterised first by CD45 expression. This protein is involved in haematopoietic cell differentiation and activation, as well as homing and trafficking⁸⁹.

It is generally accepted that inclusion of lineage markers (Lin) expressed by terminally differentiated haematopoietic cells assists in excluding late-stage progenitors of limited potency and terminally differentiated cells during HSPC characterisation.

CD34 has long been used as the positive marker for HSPC identification⁹⁰, and the proportion of CD34⁺ HSPCs in transplant products are correlated to engraftment success in HSPCT^{48,49}. Its function is largely dependent on tissue-specific post-transcriptional and post-translational modifications which result in diverse functions depending on the tissue⁹¹.

The CD34⁺ HSPC population is divided into primitive progenitors and committed progenitors by the expression of CD38, a leukocyte activation marker effecting calcium signalling and involved in signal transduction and cell adhesion⁹². Co-expression of CD38 and CD34 denotes less primitive HPCs committed to differentiation⁴¹, observed on the single-cell phenotype, function, and transcriptome level. The common lymphoid progenitor (CLP) and common myeloid progenitor (CMP) both express CD38, and are destined for differentiation into lymphoid and myeloid cells, respectively (Figure 2.1).

Cell-surface expression of CD90 is mutually exclusive to CD38 expression, and indicates HSPC primitivity (Figure 2.1). CD90 plays important but varied roles in intercellular interactions and molecular signalling responses between cell types due to differential glycosylation⁹³. Expression of CD90 on CD34⁺ HSPCs has been associated with improved long-term engraftment and myeloid reconstitution success in mice⁸¹. In addition to expression on fibroblasts, keratinocytes, epithelial cells, and thymocytes⁹³, CD90 is a stem cell marker for

MSCs⁹⁴ and has been proposed as an identifying marker for the self-renewing HSPC in combination with CD34 and absence of CD38^{81, 82} (CD34⁺CD90⁺CD38⁻).

CD133 is proposed as an alternate primitivity marker to be used in conjunction with^{83, 87} and independently of CD34^{78, 80, 85, 95} to identify the self-renewing HSPC population. CD133 is also expressed on a wide variety of cell types, most notably cancer stem cells⁷⁹, and appears to have glycosylation-dependent functions including organising plasma membrane topology⁹⁶. CD133 is reportedly expressed on most-primitive HSPCs^{78, 85-87}. CD117 is reportedly expressed on most-primitive HSPCs for retention in the bone marrow niche, described in 2.2.4.1.2 *Cytokine profile of the bone marrow niche*.

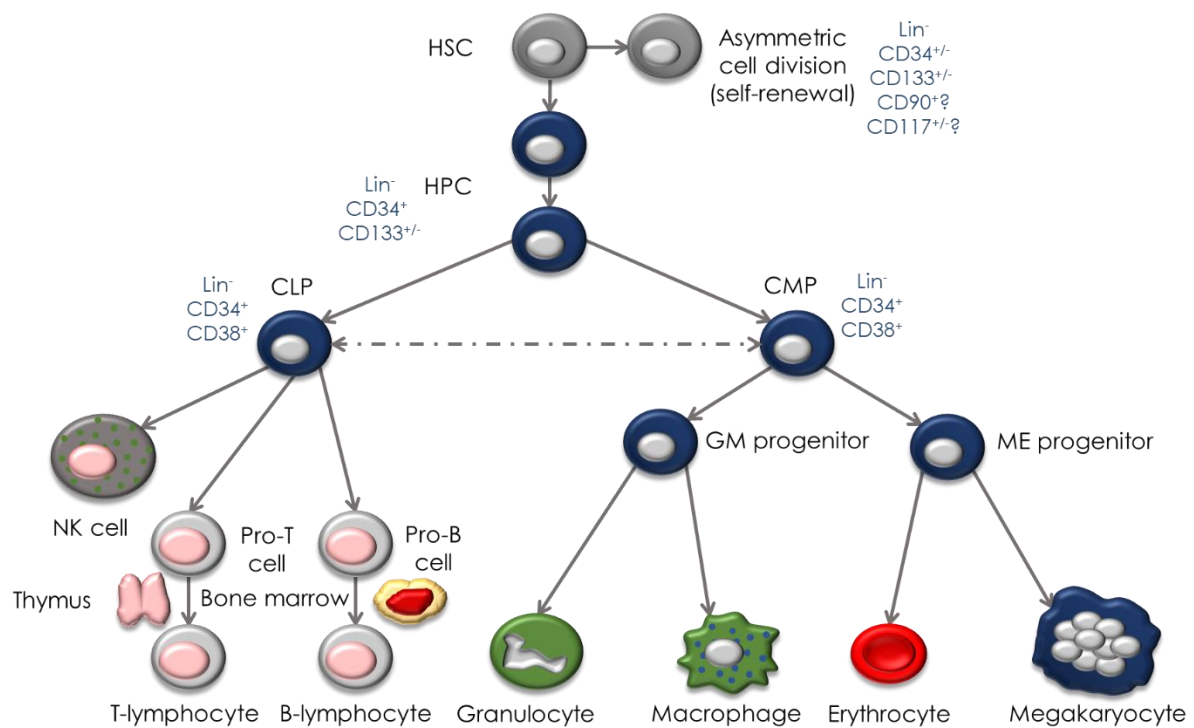


Figure 2.1: Classical model of haematopoiesis, compiled and adapted from literature^{5, 55, 97}. The model depicts unidirectional differentiation of an HSC into terminally differentiated haematopoietic cells following asymmetric, self-renewing cell division through a series of progenitors (HPCs). Cell surface phenotypes are indicated in blue; the dotted grey line indicates trans-differentiation, where sufficient stimulus allows the CLP or CMP to overcome lineage restriction to produce cells of the other lineage. The different markers supposed to be expressed by the true, self-renewing HSC are CD34, CD133, CD90, and CD117, which are under discussion in literature. The consensus is that all HSPCs are negative for lineage-specific (Lin)-markers until well-committed to a particular lineage. The common lymphoid progenitor (CLP) and common myeloid progenitor (CMP) are distinguished from more primitive HSPCs by expression of CD38, and only after differentiation do lineage markers become expressed.

2.2.4 Haematopoiesis

2.2.4.1 Stem cell maintenance – the bone marrow niche

Haematopoiesis describes the genesis of all blood and immune cells from a single HSC undergoing asymmetric cell division and subsequent clonal expansion and differentiation. Through the process of haematopoiesis, a single HSC is responsible for the generation of millions of terminally differentiated blood and immune cells of different lineages including T-cells, natural killer (NK) cells, dendritic cells, monocyte/macrophages (Figure 2.1). The infinite nuances of maintaining quiescent HSCs and nudging lineage-committed progenitors to their eventual purpose is orchestrated by a complex system of cells, cytokines, and microenvironment architecture in the bone marrow niche. Cytokines are small molecules important in cell signalling, which effect cascades of intracellular processes⁹⁸.

2.2.4.1.1 Cellular profile of the bone marrow niche

The bone marrow niche can be crudely divided into endosteal and perivascular stem cell niches in the long bones, vertebrae, and iliac crest of the hip (Figure 2.2). Different cell types dominate in each niche region, which are involved in support and signalling to maintain HSC quiescence and support HSPC mobilisation and differentiation. The endosteal niche is located closest to the endosteum layer of bone enclosing the bone marrow, made up primarily of osteoblasts and osteoclasts. Recent studies indicate that osteoblasts of the endosteal niche play a supporting rather than pivotal role in HSC maintenance, but are key to the maintenance and differentiation of lymphoid progenitors^{99, 100}.

The perivascular niche refers to the cells surrounding blood vessels in the bone marrow, including perivascular stem/stromal cells, endothelial cells, and nerve fibres including non-myelinating Schwann cells^{101, 102}. These cells contribute to the direct maintenance of HSC quiescence and retention in the bone marrow niche through intercellular interaction and paracrine (cell-to-cell) signalling. The perivascular niche is located closest to blood vessels permeating the bone marrow, and consists of a perivascular stem/stromal cells, endothelial

cells, and nerve cells. The endosteal and perivascular niches, while described separately, are difficult to distinguish due to cell heterogeneity and vascularisation in the tissue.

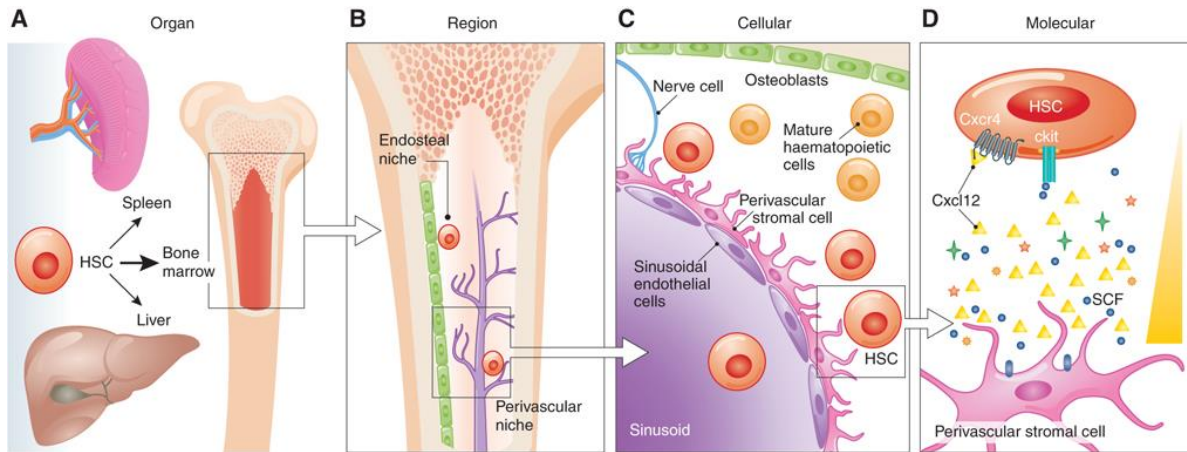


Figure 2.2: The bone marrow niche shown in windows of increasing resolution, used with permission from the corresponding author¹⁰⁰. The primary residential organ of HSCs is the bone marrow, but they may also home to the liver and spleen (A). The bone marrow niche consists of the endosteal and perivascular niches (B), which function to maintain HSC quiescence and retain HSPCs in the bone marrow niche (C) through the maintenance of critical cytokine gradients (D).

2.2.4.1.2 Cytokine profile of the bone marrow niche

Two cytokines in particular play a pivotal role in HSC maintenance in the bone marrow niche, namely C-X-C motif chemokine ligand 12 (CXCL12), also known as stromal-derived factor 1 (SDF-1), and stem cell factor (SCF) (Figure 2.2D). Soluble SCF, secreted by perivascular stem/stromal cells and endothelial cells, is a ligand for mast/stem cell growth factor receptor (SCFR; CD117) on the surface of HSCs which activates anti-apoptotic pathways¹⁰³. Cell membrane-bound SCF facilitates CD117-mediated interaction between HSCs and niche cells, providing a physical anchor to niche cells¹⁰⁴. Endosteal osteolineage cells facilitate HSC mobilisation by expression of receptor activator of nuclear factor kappa-B ligand (RANKL) which results in reduced cell-surface expression of SCF and the dissolution of SCF-CD117-mediated anchoring of HSCs to niche cells⁹⁹.

CXCL12, produced by perivascular stem/stromal cells, CXCL12-abundant reticular (CAR) cells, and sinusoidal endothelial cells is a ligand for C-X-C motif chemokine receptor type 4

(CXCR4)¹⁰⁰. Interaction between CXCR4 and CXCL12 induces HSC quiescence and facilitates HSPC migration and homing^{48, 94}. Migration of CXCR4-expressing HSPCs along a positive CXCL12 gradient induces quiescence with increasing local CXCL12 concentration, drawing primitive HSPCs towards niche cells such as CAR cells and perivascular stem/stromal cells¹⁰¹. In addition to molecular regulation, sympathetic nerve fibre synapsis on perivascular stem/stromal cells regulates secretion of CXCL12 in a circadian fashion¹⁰⁵.

Non-myelinating Schwann cells are also suspected to have niche modulation properties by regulating transforming growth factor-beta (TGF- β) activation, which helps maintain HSC quiescence and self-renewal¹⁰². These regulatory networks allow for the proper cycling of HSPCs in and out of quiescence, to bring about dynamic reconstitution of haematopoietic cells.

Several other cytokines are reported to support HSC maintenance in the bone marrow niche, including thrombopoietin (TPO) mainly synthesised in the liver and kidney, and pleiotrophin produced by sinusoidal endothelial cells and CAR cells¹⁰⁴. Maintenance of HSC self-renewal capacity by TPO is an example of exogenous niche regulation as only low levels are produced by bone marrow stroma.

2.2.4.2 Haematopoiesis – dynamic reconstitution

Blood and immune cells are constantly replenished by the clonal expansion and differentiation of HSCs through a discrete set of progenitors, with reducing potency as terminal differentiation is approached¹⁰. Although haematopoiesis is presented as a unidirectional process with early, rigid lineage commitment (Figure 2.1), recent research indicates that lineage commitment is suggestive rather than restrictive in more primitive progenitors⁴¹ (Figure 2.1, dotted grey line). Lineage commitment is therefore proposed as a function of probability with the probability of escaping lineage priming declining with increased differentiation⁷⁵. For illustrative purposes, the classical model of haematopoiesis is used throughout this dissertation (Figure 2.1).

The self-renewing HSC divides asymmetrically, with one daughter cell maintaining quiescent and being retained in the niche, and with the second daughter cell going on to clonal expansion and differentiation¹⁰⁶. In this way, haematopoiesis is achieved while maintaining the self-renewing HSC pool. The multipotent HPC undergoes transcriptomic lineage priming towards lymphoid or myeloid cell production, forming the CLP or CMP, respectively.

In the laboratory, the differentiation potential of lineage-primed progenitors can be assayed by colony forming unit (CFU) assays, where single cells are seeded in semisolid medium where they form colonies resulting from clonal expansion and differentiation in the presence of defined cytokine cocktails¹⁰⁷. The variety of cells in each colony is determined by the potency of the progenitor, which depends on the degree of lineage priming⁴¹.

2.2.4.2.1 Haematopoiesis – a symphony of cytokines

Much like quiescence and self-renewal capacity in the bone marrow niche, HSPC differentiation is orchestrated by a symphony of cytokines⁹⁷ (Figure 2.3). Together with cell-surface cytokine receptor expression (modulated by lineage priming) and degree of mobilisation from the perivascular and endosteal niches (facilitated by SCF and CXCL12 regulation), cytokine stimulation effects lineage priming and differentiation of the HSPC pool. Only cytokines relevant in CFU assays of HSPCs will be discussed here.

In addition to its role in niche homeostasis, SCF has been reported to accelerate cell cycling, promote survival of HSPCs *in vitro*, and to synergise with other cytokines for HSPC differentiation and proliferation¹⁰⁸. Colony-stimulating factors (CSF), originally grouped together, include granulocyte-CSF (G-CSF), macrophage-CSF (M-CSF), and granulocyte-macrophage-CSF (GM-CSF). These cytokines were found to stimulate the formation of granulocyte colonies (CFU-G), macrophage colonies (CFU-M), and granulocyte-macrophage colonies (CFU-GM) when culturing HSCs in semisolid media¹⁰⁹ (Figure 2.3).

The category of CSF also includes interleukin-3 (IL-3), which is a prominent cytokine in haematopoietic development¹⁰⁹. As a group, CSFs promote myeloid lineage priming in multipotent HPCs, and facilitate clonal expansion and differentiation into granulocytes,

monocyte/macrophages, megakaryocytes and erythrocytes¹⁰⁹. Although IL-3 has little effect when added singly, it plays an important synergising role throughout myeloid differentiation by enhancing cell proliferation prior to differentiation^{110, 111}. In addition to its role in haematopoiesis, G-CSF is also used in the clinic to mobilise HSPCs from the bone marrow to peripheral blood circulation for transplant purposes, the mechanisms of which are not clear⁴⁷.

Erythropoietin (EPO) and TPO are responsible for the production of erythrocytes and megakaryocytes respectively. These cytokines play a role only in the terminal stages of differentiation into these lineages, and are crucial to the maintenance of erythrocytes and megakaryocytes (and as a result, platelets) in the circulation⁹⁷. Genetic deletion of the genes encoding EPO and TPO or their receptors proved lethal in the case of EPO, and resulted in drastically reduced megakaryocyte production and thrombocytopenia in the case of TPO⁹⁷.

Interleukin-6 (IL-6) in the bone marrow niche plays a role in differentiating osteoblasts into osteoclasts¹¹², and has also been critically implicated in the self-renewal and maintenance of HSPCs in the bone marrow⁹⁸. Additionally, IL-6 plays a role in granulocyte-macrophage differentiation¹¹³ and megakaryocyte maturation¹¹⁴. Furthermore, expansion of UCB-derived CD133⁺ and CD34⁺ HSPCs show improved maintenance of primitive HSPCs when using cytokine cocktails including IL-6^{115, 116}.

The first distinct step of lineage priming occurs with the cell-surface upregulation of CD38⁴¹ which correlates with transcriptomic priming towards myeloid (CMP) or lymphoid (CLP) progenitors. The cytokine fms-like tyrosine kinase 3 ligand (FLT3-L) is thought to be responsible for repression of myeloid lineage priming, resulting in production of the CLP¹¹⁷. Inclusion of FLT3-L in *ex vivo* expansion cocktails is used to encourage lymphoid lineage priming. In addition to inducing CLP differentiation, FLT3-L synergises with interleukin-7 (IL-7) to produce pro-B cells and natural killer (NK) cells¹¹⁸. The lymphoid cytokine IL-7 is responsible for the survival of lymphoid precursors and plays a supporting but synergistic role in lymphoid, particularly T-cell, lineage priming and resulting differentiation¹¹⁹.

The capacity of the cytokine combinations described above to induce cytokine-specific differentiation patterns in HSPCs is exploited in CFU assays. The CFU assay evaluates HSPC

function by assessing the colony-forming capacity of HSPCs seeded in semisolid medium with defined cytokine cocktails. Colonies are formed by clonal expansion and differentiation into single-lineage colonies originating from lineage-restricted progenitors, or multi-lineage colonies originating from progenitors with increased potency (Figure 2.3). The CFU assay is explained in more detail below.

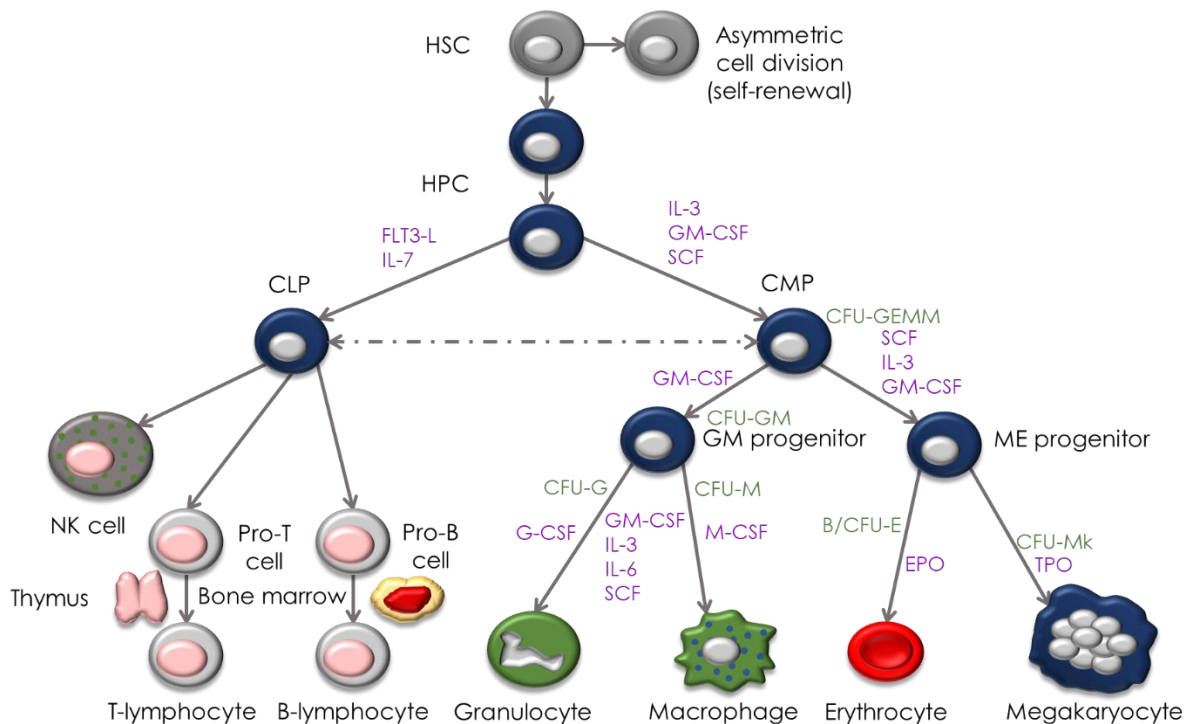


Figure 2.3: Major haematopoietic cytokines and their roles in haematopoiesis, adapted for re-use^{5, 120}. Cytokines are indicated in purple next to the differentiation path they promote^{97, 104}. Colonies produced in CFU assays of myeloid lineages are shown in green¹⁰. FLT3-L and IL-7 facilitate the differentiation of HSPCs into lymphoid cells (natural killer cells, and T- and B-lymphocytes) through the CLP. Myeloid differentiation is initiated in HSPCs by IL-3, GM-CSF, and SCF stimulation, forming the CMP. The CMP forms multilineage colonies consisting of granulocytes, erythrocytes, macrophages, and megakaryocytes (CFU-GEMM). The CMP can differentiate into the granulocyte-macrophage (GM) progenitor with GM-CSF stimulation, which form granulocyte-macrophage colonies (CFU-GM), or the megakaryocyte-erythrocyte (ME) progenitor with SCF, IL-3, and GM-CSF stimulation. GM progenitors stimulated with GM-CSF, IL-6, IL-3, and SCF can also produce single-lineage macrophage (CFU-M) or granulocyte (CFU-G) colonies when additionally stimulated with M-CSF and G-CSF, respectively. ME progenitors form either erythroid colonies in burst-forming units (BFU-E) or CFUs (together called B/CFU-E), or megakaryocyte colonies (CFU-Mk) when stimulated with EPO or TPO, respectively.

2.2.4.2.2 Colony-forming unit assays

As previously mentioned, CFU assays are used to assess HSPC function for diagnostic and research purposes. CFU assays are performed by plating HSPCs in a semisolid medium composed of methylcellulose in Iscove's Modified Dulbecco's medium (IMDM) containing growth factors important for cell proliferation, as well as salts, vitamins, minerals, amino acids, and glucose^{107, 121}. Cytokines are added to support differentiation appropriate to the nature of the experiment (Figure 2.3).

Methylcellulose-based medium is viscous enough to support differentiating cells in a three-dimensional space rather than in suspension as in liquid medium, preventing panmixia of expanded cells. This results in discrete colonies being formed by clonal expansion and differentiation of HSPCs. The seeding cell potency can be determined by the size of the colony and the variety of cells that make up the colony (Figure 2.3). Such assays are useful in potentially detecting the underlying causes of haematological abnormalities resulting from HSPC dysfunction¹²², and for determining the quality of HSPCs harvested for transplant purposes¹²³.

Colonies which can typically be identified using CFU assays are shown in Figure 2.3. Multilineage colonies such as granulocyte-erythrocyte-macrophage-megakaryocyte colonies (CFU-GEMM) and CFU-GM are produced by the multipotent CMP and GM progenitor, respectively. Single-lineage colonies originate from cells which are more lineage-committed, producing CFU-M, CFU-G, megakaryocyte colonies (CFU-Mk), and burst-forming unit (BFU) or erythroid colonies (grouped together as B/CFU-E). The spread of colonies produced by HSPCs evaluated using the CFU assay can be used to determine if heterogenous HSPCs are capable of forming all myeloid lineages in culture, as a proxy for normal HSPC function.

2.3 Human immunodeficiency virus and haematopoiesis

2.3.1 Human immunodeficiency virus – a global view

2.3.1.1 Background

HIV is a global problem, with almost 37 million people worldwide being infected in 2017 (according to the latest available statistic), of which less than 22 million were receiving antiretroviral therapy (ART)¹²⁴. In 2018, approximately 7.5 million people in South Africa were living with HIV¹²⁵. Despite the efficacy of current ART in controlling viral load and improving the lifespan of infected individuals, HIV is still incurable¹²⁶.

Although the virus is relatively well-characterised, immune evasion, reservoir establishment, and the evolution of drug resistance contribute to the persistence of HIV¹²⁷⁻¹³⁰. Since the discovery of HIV as the causative agent of acquired immunodeficiency syndrome (AIDS) in the early 1980s^{131, 132}, the virus is categorised into two types, HIV-1 and HIV-2, of which the former is the most prevalent. HIV-1 has been divided into three groups (M, N, and O) and approximately eight distinct clades within the main group (group M) based on sequencing, with various circulating recombinant forms (CRF) also being documented^{132, 133}.

2.3.1.2 Replication and persistence

2.3.1.2.1 Replication

HIV is classified as a single-stranded ribonucleic acid (ssRNA) lentivirus of the family *Retroviridae*¹³⁴ and is an intracellular virus requiring host cell machinery to replicate. The HIV genome is relatively small, consisting of approximately 9.5 kilobases (kb) of RNA, with three distinct reading frames of overlapping coding regions¹³⁴ (Figure 2.4).

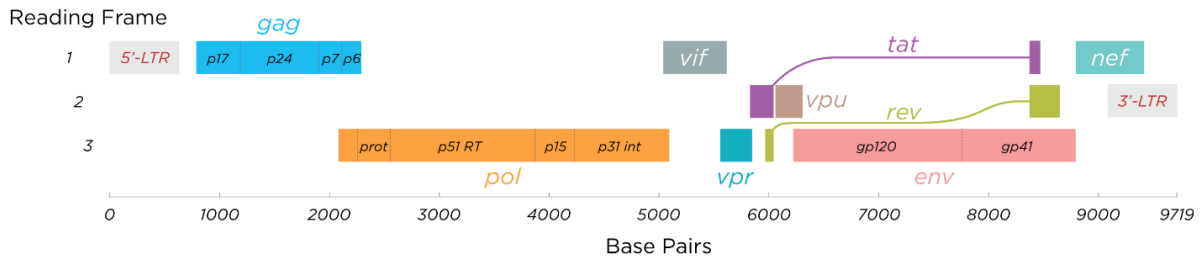


Figure 2.4: The HIV genome with three distinct reading frames. HIV proteins are indicated as encoded in colour-coded genes, with links indicating the trans-frame protein-coding regions. Figure used with permission¹³⁵.

The HIV life cycle¹³⁶ involves host cell receptor-dependent infection using viral envelope proteins, fusion of the virion to the host cell and injection of the internal capsid containing viral genetic material and proteins critical to viral replication (Figure 2.5). Receptor-mediated entry is facilitated by the viral envelope glycoprotein gp120 binding to CD4 and either CXCR4 or C-C motif chemokine receptor type 5 (CCR5) present on the surface of subsets of T-cells, macrophages, and dendritic cells. Receptor/gp120 binding activates the fusogenic properties of the viral gp120 protein complex, resulting in the fusion of host cell and virus¹³⁴.

Upon fusion, the viral capsid, containing the viral genome and consisting primarily of the viral protein p24, is injected into the host cell cytoplasm¹³⁷. The capsid slowly disassembles as the viral genome is reverse transcribed into double-stranded DNA (dsDNA), forming the proviral genome. The proviral genome associated with viral integrases (forming the pre-integration complex) is released into the cytoplasm when sufficient capsid disassembly has occurred¹³⁷. The pre-integration complex is imported into the nucleus by viral protein R (VPR)¹³⁴, and the proviral genome is inserted into the host cell genome¹³⁸ by the viral integrase.

Transcription of the provirus is encouraged by the viral trans-activator of transcription (Tat) protein binding to the trans-activator-responsive (TAR) sequence located in the 5'-long terminal repeat (LTR) region of the HIV genome, a strong promoter of transcription¹³⁴. Binding of Tat to the TAR region recruits RNA polymerases and elongation factors required for the production of long polyprotein-encoding messenger RNA (mRNA) transcripts from proviral DNA¹³⁹. Polyprotein-encoding viral mRNAs are exported to the cytoplasm with the help of the

viral protein Rev¹⁴⁰ for translation into proteins using host ribosomes and processing into functional proteins by proteases. A subset of full-length transcripts are enveloped in capsid proteins, directed by Rev¹⁴⁰. Release of the HIV particle occurs when packaged capsids reach regions of the host cell membrane into which viral gp120 proteins have been inserted. Gag-mediated recruitment of endosomal sorting complexes required for transport (ESCRT) proteins is poorly understood, but is postulated to facilitate the fission of assembled viral particles from the host cell plasma membrane¹⁴¹. ESCRT-mediated fission results in the infectious viral particle budding off from the host cell membrane¹⁴¹. The host cell is lysed when a critical mass of budding virions is released, and the host cell can no longer repair the damage to the plasma membrane (Figure 2.5). The hallmark depletion of CD4⁺ T-cells in the peripheral blood of HIV-infected patients is therefore a consequence of the lytic cycle of HIV replication.

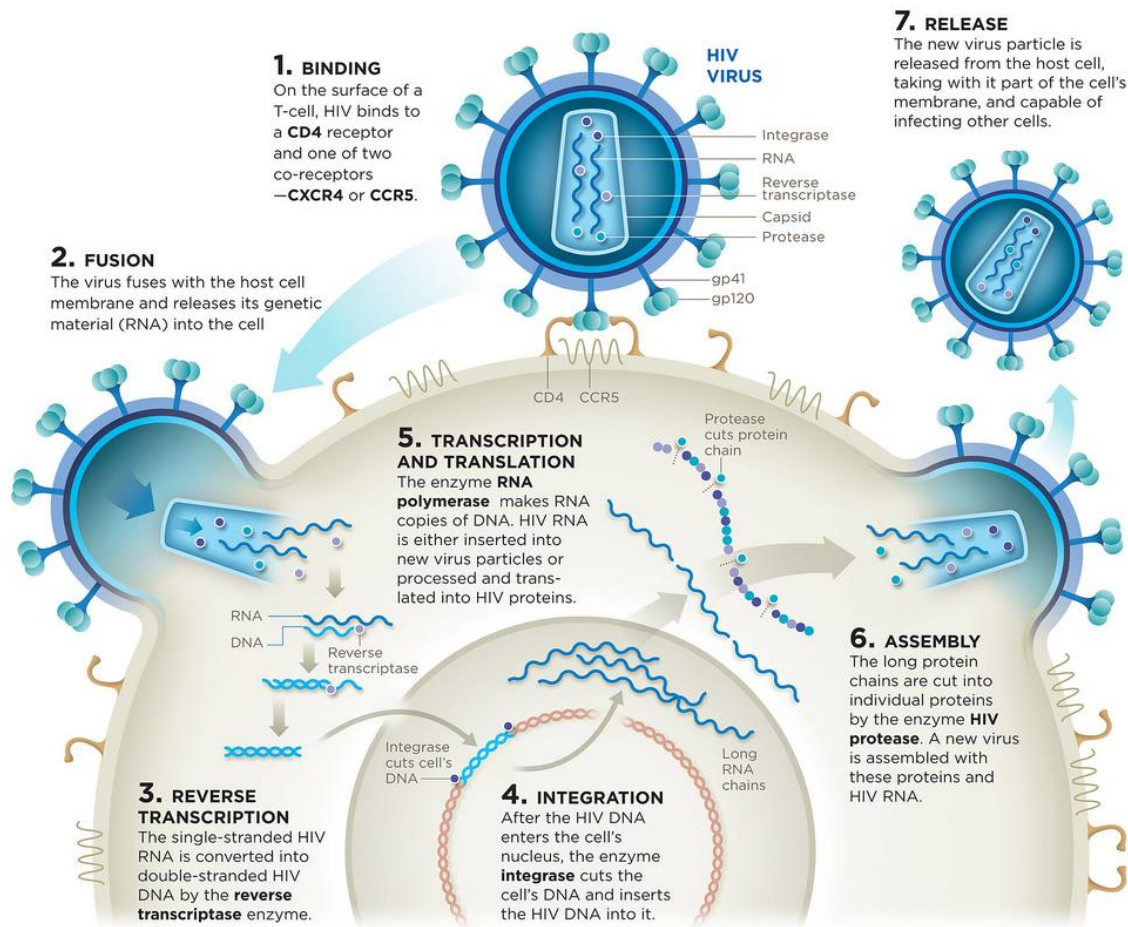


Figure 2.5: Representation of the HIV life cycle, designed by 5W Infographic and reused with permission¹³⁶. HIV-1 binding to target cell receptors CD4 and CCR5/CXCR4 begins the cycle of replication consisting of reverse transcription of the viral genome to proviral DNA which is integrated into the host cell genome. Transcription and translation of the proviral genome results in the assembly and release of newly-packaged virions by budding from the host cell membrane.

2.3.1.2.2 Persistence

HIV persists in the host by evolution, facilitated by the error-prone reverse transcriptase which is responsible for synthesising the proviral genome¹⁴². This results in a diverse viral population within the host, termed quasispecies, which provide variance supporting evasion of tropism restriction, and drug pressure¹⁴³. Also critical to the evolution of escape mechanisms is viral tropism, conferred by the affinity of gp120 for different host cell receptor/co-receptor combinations¹⁴⁴. Cells expressing receptor/co-receptor combinations

to which a particular gp120 moiety can bind are therefore susceptible to infection. Viral tropism changes throughout the course of infection from being primarily CD4/CCR5-utilising virus (R5-tropic HIV), to a combination of alternate tropisms, among which is the CD4/CXCR4-utilising virus (X4-tropic HIV)¹⁴⁵. Changes in tropism expand the pool of susceptible host cells, which is a major driver of HIV persistence. Additionally to receptor-mediated infection, cell-to-cell transfer of HIV facilitated by a variety of mechanisms including endocytosis of infected cells by phagocytes and fusion of infected and uninfected cells¹⁴⁶ have been described.

Another driver of persistence is the ability of HIV to exist in cells in a latent form. These pools of latently infected cells comprise the HIV reservoir. Cells of the reservoir harbour provirus but do not produce HIV for long periods of time, and may be distributed throughout host tissues¹⁴⁷. The reservoir includes the gastrointestinal mucosa, liver, central nervous system (including the brain)¹⁴⁷, and bone marrow¹⁴⁸⁻¹⁵⁰. Reservoir cells are not usually actively dividing or transcribing proteins. Cells of the reservoir contribute to viral persistence when they become transcriptionally active, which results in viral production. Dormant reservoir cells can be extremely long-lived, adding to the need for life-long suppressive ART¹²⁷.

2.3.2 Towards a cure: human immunodeficiency virus gene therapy

Life-long suppressive ART is a short-term solution to a long-term problem, which is the eradication of HIV. To date, the Berlin patient (Timothy Brown), has been completely cured of HIV. This was achieved with allogeneic haematopoietic stem cell transplant (HSCT) from a CCR5-null donor, homozygous for the loss-of-function $\Delta 32$ mutation in the CCR5 gene³⁹ during treatment of acute myeloid leukaemia. The reconstituted immune system of the Berlin patient was resistant to R5-tropic HIV, who has since been screened for tissue reservoirs and been found to be completely HIV-free in the absence of ART several years after the transplant¹⁵¹. A second patient (the London patient) has recently been declared in remission from HIV after 18 months of undetectable viral load (viral count in blood) in the absence of ART, also following allogeneic CCR5-null HSCT, to treat Hodgkin's lymphoma¹⁵². A third patient (Düsseldorf patient), announced at the Conference on Retroviruses and Opportunistic

Infections (CROI) 2019, could also have been cured¹⁵³. The Düsseldorf patient underwent allogeneic CCR5-null HSCT five years ago to treat acute myeloid leukaemia, interrupted ART four months ago. No viral load rebound has yet occurred¹⁵³. While this is too soon to declare remission, this is promising for the future treatment of HIV patients. While gene therapy and HSCT to treat HIV had been proposed prior to the success of the Berlin patient, proof of principle brought the field to life. The prospect of a cure for HIV has seen important points affecting the feasibility of the cure coming to the fore, specifically regarding viral load rebound post-CCR5-null HSCT due to tropism switching from R5-tropic virus to X4-tropic virus^{40, 154}. The tropism switch from predominantly R5-tropic to X4-tropic virus has been correlated with poorer patient prognosis¹⁴⁵.

2.3.3 Human immunodeficiency virus and haematopoietic stem/progenitor cells

The negative impact of HIV infection on haematopoiesis observed since 1987¹⁵⁵, with cytopenia (blood cell depletion) *in vivo* and deficient HPC growth *in vitro* being observed¹⁵⁶. This led to the search for detectable HIV infection in CD34⁺ HSPCs *in vivo* and *in vitro*, which continues to yield conflicting reports.

2.3.3.1 Haematopoietic stem/progenitor cell susceptibility to human immunodeficiency virus

Long-lived reservoirs of HIV contribute to viral persistence, as discussed previously. Haematological abnormalities associated with HIV infection and the prospect of HSPC-based gene therapy cures for HIV constitute two of the reasons for exploring HSPCs as an HIV reservoir.

HIV diversity has contributed to the dialogue concerning the conflicting reports regarding the susceptibility of HSPCs to HIV infection both *in vivo* and *in vitro*. Historically, HIV-1B was the most studied viral subtype due to its geographic prevalence in Northern America and much of Europe^{132, 157, 158}. However, phylogeographic subtype distribution is becoming less defined

with migration. Differences between subtypes in terms of virulence^{129, 159}, drug susceptibility¹⁵⁹, and drug resistance have become more apparent with research^{129, 160, 161}, and as a result, research into non-B subtypes is improving. The historically southern African subtype, HIV-1C, is the most prevalent form of HIV occurring in sub-Saharan Africa and Asia¹³², and is more recently occurring in recombinant forms with HIV-1B in South America¹⁶². Understanding the link between HIV-1 subtype and the likelihood of establishing certain reservoirs, such as the HSPC reservoir, is important for understanding HIV-associated co-morbidities in the clinic, and for the development of cell-based treatment strategies.

2.3.3.1.1 Human immunodeficiency virus-associated haematological abnormalities

HIV-associated haematological abnormalities include a variety of conditions previously termed “AIDS-related complex” (ARC)¹⁶³, encompassing everything from myelodysplasia (bone marrow defects) to various cytopenias (blood cell depletions). Considering the complexities of maintaining bone marrow homeostasis and orchestrating HSPC differentiation, it is not surprising that infiltration of the bone marrow niche has far-reaching consequences.

Cytopenias are driven by cell depletion and/or deficient production, both of which are multifactorial. With the progression of HIV disease, single- or multi-lineage cytopenias manifest and can be the consequence of direct infection, indirect effects of infection, or due to treatment. Leukopenia (white blood cell depletion) is the defining hallmark of HIV infection as a result of the lytic cycle of HIV infection depleting CD4⁺ T-cells. This depletion indirectly increases naïve CD8⁺ T-cell proportions, which require CD4⁺ T-cells for activation, hindering the cytotoxic T-cell immune response. The three most common cytopenias that HIV-patients present with are anaemia (erythrocyte depletion), thrombocytopenia (platelet deficiency), and neutropenia (neutrophil depletion)¹⁶⁴; these are described below.

Anaemia in HIV patients remains a complex and persistent issue in managing HIV disease, with causes ranging from myelosuppressive medication to haemolysis in the spleen¹⁶⁵. Anaemia is associated with poor prognosis¹⁶⁶ and mortality in resource-poor settings^{167, 168}.

Thrombocytopenia is relatively common in HIV patients and can manifest early in HIV disease, with bleeding episodes in severe cases resulting from platelet deficiency. This may also contribute to pancytopenia (depletion of all blood lineages)¹⁶⁹.

Megakaryocyte infection resulting in insufficient platelet production and accelerated platelet clearance contribute to thrombocytopenia in infected patients, but are restored with azido-deoxythymidine (AZT)-containing ART regimens¹⁷⁰.

The extent and severity of neutropenia in HIV patients is correlated with advanced disease progression^{171, 172}. Neutrophils are a subset of granulocytes which make up the majority of blood cells and are pivotal in the first-line inflammatory response and antimicrobial immunity. Neutropenia therefore results in impaired microbial immunity and infection with opportunistic pathogens¹⁷² such as *Mycobacterium tuberculosis*, the causative organism for tuberculosis¹⁷¹.

In addition to cytopenias, HIV-associated haematological abnormalities include several haematological cancers including B-cell lymphomas and leukaemias, as well as bone marrow hyper- or hypo-cellularity¹⁷³. These abnormalities are more prevalent in late-stage HIV disease, the biggest contributing factor being dysregulation of the bone marrow niche¹⁷⁴. As treatment options and time to diagnosis improve, HIV-associated haematological normalities decrease in frequency except in late-stage disease¹⁶⁴. However, with the high burden of HIV in resource-poor settings such as the South African public health sector, understanding the prevalence and causes of HIV-associated haematological abnormalities is paramount to sustained quality of life of our HIV patients.

2.3.3.1.2 Conflicting literature

Despite constitutive expression of CXCR4 on primitive HSPCs, and CD4 and CCR5 expression on HSPCs in varying stages of differentiation, it remains unclear whether HSPCs are susceptible to HIV infection. The susceptibility of HSPCs to HIV infection has been extensively researched (Table 2.2), but variation in (i) experimental design, (ii) HSPC source and

phenotype, and (iii) the nature of virus being examined, creates a discordant tapestry of results.

General consensus (Table 2.2) indicates that less primitive progenitors (CMP and CLP; CD34⁺CD38⁺) are susceptible to infection, and can be directly associated with at least some HIV-associated cytopenias. This alone has consequences for autologous HSCT proposed for anti-HIV gene therapy, in that the CD34⁺ fraction used for HSCT includes HIV-susceptible and possibly infected cells. Determining whether or not primitive HSPCs are susceptible to infection is vital, considering autologous HSPCT is practiced with HIV-infected patients as with uninfected patients¹⁷⁴. Infection of more primitive HSPCs would have a great capacity to re-establish the HIV reservoir and contribute to viral load due to the clonal expansion capacity of more primitive HSPCs compared to less primitive HSPCs. In HIV patients undergoing autologous transplant for the purpose of gene therapy, viral load rebound and expansion of the reservoir (resulting from increased viral load) are important concerns¹⁷⁵.

Table 2.2: Summary of literature regarding HIV infection of HSPCs. Where HIV derived from patients was used but not evaluated for subtype, the country in which patients were recruited is stated if known.

Article	Outcome	Infection in vivo or in vitro	HSPCs	HIV
Davis <i>et al.</i> , 1991 ¹⁵⁶	HIV infection of CD34 ⁺ HSPCs is absent or rare <i>in vivo</i> .	In vivo	Bone marrow-derived CD34 ⁺ HSPCs purified by immunomagnetic selection.	Patient virus (USA).
Louache <i>et al.</i> , 1992 ¹⁷⁶	HIV infection inhibits HSPC colony forming capacity, but direct infection was not detected.	In vivo	Bone marrow-derived CD34 ⁺ HSPCs purified by immunomagnetic selection.	Patient virus.
Stanley <i>et al.</i> , 1992 ¹⁷⁷	A subset of HIV individuals had detectable HIV in CD34 ⁺ cells, correlated with worsened disease state. HIV infection suppresses HSPC colony formation regardless of CD34 ⁺ infection.	In vivo	Bone marrow-derived CD34 ⁺ HSPCs purified by immunomagnetic selection.	Patient virus (Zaire and USA).
Chelucci <i>et al.</i> , 1995 ¹⁷⁸	A minority of primitive but not multipotent HSPCs are susceptible to HIV infection.	In vitro	Peripheral blood-derived CD34 ⁺ HSPCs.	HIV-1 HTL VIII B and NL4-3 molecular clones (HIV-1B).

<p>Marandin <i>et al.</i>, 1996¹⁷⁹</p>	<p>Direct infection of CD34⁺ HSPCs is not likely responsible for haematological disorders observed in HIV patients, although the CD34⁺CD38⁻ and CD34⁺CD90⁺ primitive HSPC fractions were significantly reduced in HIV patients.</p>	<p>In vivo</p>	<p>Bone marrow-derived CD34⁺, CD34⁺CD38⁻, and CD34⁺CD90⁺ HSPCs purified by fluorescence-activated cell sorting (FACS).</p>	<p>Patient virus (France).</p>
<p>Weichold <i>et al.</i>, 1998¹⁸⁰</p>	<p>Neither HIV-1 nor HIV-2 infect primitive CD34⁺CD38⁻ HSPCs <i>in vitro</i>.</p>	<p>In vitro</p>	<p>Bone marrow-derived CD34⁺CD38⁻ and CD34⁺CD38⁺ HSPCs purified by immunomagnetic selection followed by FACS</p>	<p>HIV-1 BAL and RF molecular clones (HIV-1B), and HIV-2 ST and ROD molecular clones. Two primary isolates (MN and 571) were also used in some experiments.</p>
<p>Shen <i>et al.</i>, 1999¹⁸¹</p>	<p>Despite expression of CCR5 and CXCR4, quiescent CD34⁺ HSCs (G₀) resist HIV infection through pre-entry blocks. Less primitive HSPCs (CD34⁺, not at G₀) have detectable proviral DNA after infection.</p>	<p>In vitro and in vivo</p>	<p>Bone marrow-derived CD34⁺CD38⁻ and CD34⁺CD38⁺ HSPCs purified by immunomagnetic selection and FACS. Quiescent (G₀) HSPCs derived from CD34⁺ HSPCs after 7 days in culture. Bone marrow-derived G₀ HSPCs were compared to bone marrow- and peripheral blood-derived mononuclear cells from HIV-infected patients.</p>	<p>HIV-1 BAL and IIIB molecular clones (HIV-1B), as well as vesicular stomatitis virus G (VSV-G), HXB2, Yu2, or 89.6 pseudotyped reporter HIV construct pHvec2.GFP containing green fluorescence protein (GFP).</p>

<p>Redd <i>et al.</i>, 2007¹⁸²</p>	<p>HSPCs can be infected <i>in vivo</i> and <i>in vitro</i> by HIV-1C, but not (or rarely) by HIV-1B. HSPC infection with HIV-1C correlates with anaemia.</p>	<p>In vitro and in vivo</p>	<p>UCB-derived CD34⁺ HSPCs, and peripheral blood-derived CD34⁺ HSPCs purified by immunomagnetic selection from HIV-1C infected patients (Botswana).</p>	<p>Molecular clones MJ4, MHX-13, and HXB2RU3CI (HIV-1B). Lab-adapted HIV-1B strain MN, and primary isolates 30165, 92US657, 92US712, 92US714, and 92US727. Primary HIV-1C isolates obtained from patients in Botswana: BW-1841, BW-2031, BW-2036, BW-2041, and BW-5042.</p>
<p>Carter <i>et al.</i>, 2010¹⁸³</p>	<p>Multipotent HSPCs are susceptible to HIV infection. Downregulation of human leukocyte antigen class I (HLA-I) is observed in infected CD34⁺ HSPCs. Active HIV replication is cytotoxic to HSPCs. CD34⁺ HSPCs can be infected in virally suppressed patients.</p>	<p>In vitro and in vivo</p>	<p>Bone marrow- and UCB-derived CD34⁺, CD133⁺, and Lin⁻CD34⁺ CD133⁺ CD38⁻ HSPCs purified by immunomagnetic selection. Bone marrow-derived CD34⁺ cells from HIV-infected patients were purified by immunomagnetic selection.</p>	<p>An HIV reporter construct, HIV-7SF-GFP pseudotyped with the HIV-1B 89.6 envelope (R5X4-tropic). Patient virus (USA).</p>
<p>Carter <i>et al.</i>, 2011¹⁸⁴</p>	<p>Multipotent HSPCs (CD34⁺CD133⁺) can be infected with X4- and R5X4-tropic HIV, but not by R5-tropic HIV.</p>	<p>In vitro</p>	<p>Bone marrow- and UCB-derived CD34⁺ HSPCs purified by immunomagnetic selection.</p>	<p>An HIV reporter construct, HIV-7SF-GFP was pseudotyped with the X4-tropic envelope of HXB, the R5X4-tropic envelope of 89.6, and the R5-tropic envelopes of Yu2 (HIV-1B) and ZM53M (HIV-1C) molecular clones. Full-length molecular clones of NL4-3</p>

				(X4-tropic; HIV-1B) and 94UG (R5-tropic; HIV-1D) were also used.
Durand <i>et al.</i> , 2012 ¹⁴⁹	The bone marrow fraction containing CD4 ⁺ T-cells is infected with HIV, but purified CD34 ⁺ populations are not.	In vivo	Bone marrow-derived HSPCs and CD4 ⁺ T-cells purified by immunomagnetic selection followed by FACS.	Patient virus (USA).
Josefsson <i>et al.</i> , 2012 ¹⁸⁵	Lin ⁻ CD34 ⁺ and Lin ⁻ CD34 ⁻ HSPC fractions from patients on long-term (>3 years) suppressive therapy do not carry HIV. Lin ⁻ CD4 ⁺ cells from bone marrow harbour HIV which is genetically similar to HIV found in peripheral blood lymphoid cells, indicating exchange of infected cells between bone marrow and peripheral blood.	In vivo	Bone marrow-derived Lin ⁻ CD34 ⁻ , Lin ⁻ CD34 ⁺ , and Lin ⁻ CD4 ⁺ HSPC fractions as well as Lin ⁺ CD4 ⁺ fractions purified by FACS. Peripheral blood memory CD4 ⁺ T-cell fraction purified from peripheral blood by FACS.	Patient virus (USA).
McNamara <i>et al.</i> , 2012 ¹⁸⁶	Multipotent CD133 ⁺ CD34 ⁺ HSPCs are susceptible to HIV-1 infection and form part of the latent reservoir.	In vitro	Bone marrow- and UCB-derived CD133 ⁺ cells purified by magnetic selection. CD133 ⁺ CD34 ⁺ CD45 ^{+/-} CD38 ^{+/-} HSPCs sorted from magnetically purified cells by FACS.	HIV-1B-derived reporter constructs NL4-3-ΔGPE-GFP and HXB-ePLAP pseudotyped with VSV-G or HXB envelopes.

Mullis <i>et al.</i> , 2012 ¹⁸⁷	HIV-1 subtypes A and D rarely infect HSPCs <i>in vivo</i> .	In vivo	Peripheral blood mononuclear cells from HIV-1A- and HIV-1D-infected patients. Single-colony CFU assays were performed to identify colony-forming HSPCs and test for HIV infection.	Patient virus (Uganda).
McNamara <i>et al.</i> , 2013 ¹⁸⁸	HIV genomes can be harboured in CD133 ⁺ HSPCs in patients with long-term (>6 months) viral suppression.	In vivo	Bone marrow-derived CD133 ⁺ HSPCs and CD133-depleted bone marrow cell fractions purified by immunomagnetic selection.	Patient virus (USA).
Nixon <i>et al.</i> , 2013 ¹⁸⁹	Intermediate HPCs (CD34 ⁺ CD38 ⁺) are susceptible to HIV infection, and infection results in impaired haematopoietic potential <i>in vitro</i> and in humanised mice.	In vitro and in vivo	Foetal liver and UCB-derived CD34 ⁺ HSPCs purified by immunomagnetic selection.	An HIV reporter construct, NL4 _{HSA-eGFP} , pseudotyped with the VSV-G envelope, and HIV-1B molecular clones 89.6, NL4-3, and JR-CSF (HIV-1B).
Bordoni <i>et al.</i> , 2015 ¹⁹⁰	HIV-1 is harboured in CD34 ⁺ Lin ⁻ HSPCs in the bone marrow of ART-treated and -untreated patients. The extent of infection may be correlated with viral load.	In vivo	Bone marrow-derived Lin ⁻ CD34 ⁺ HSPCs purified by immunomagnetic selection.	Patient virus.

Griffin and Goff, 2015 ¹⁹¹	CD34 ⁺ HSPCs from UCB resist HIV infection by means of a pre-integration block.	In vitro	UCB-derived CD34 ⁺ cells purified by immunomagnetic selection.	An HIV-1B-derived reporter construct, NL4.3.mCherry.R ⁻ E ⁻ pseudotyped with the VSV-G envelope. The red fluorescent protein mCherry was used to identify infected cells.
Araínga <i>et al.</i> , 2016 ¹⁹²	HIV infects, integrates, and transcribes in humanised mouse bone marrow- and spleen-derived CD34 ⁺ Lin ⁻ HSPCs.	In vivo	Bone marrow- and spleen-derived CD34 ⁺ Lin ⁻ HSPCs purified by immunomagnetic selection followed by FACS.	HIV-1B isolate HIV-1 ADA (R5-tropic).
Sebastian <i>et al.</i> , 2017 ¹⁹³	More primitive (CD133 ⁺ CD34 ⁺ CD38 ^{+/-} CD90 ^{+/-}) and less primitive (CD34 ⁺ CD38 ^{+/-} CD90 ^{+/-}) HSPC populations that express CD4 harbour R5- and X4-tropic provirus in subsets of HIV-infected patients.	In vivo	Bone marrow-derived CD133 ⁺ CD34 ⁺ CD38 ^{+/-} CD90 ^{+/-} and CD34 ⁺ CD38 ^{+/-} CD90 ^{+/-} HSPCs purified by immunomagnetic selection for CD133 ⁺ and CD34 ⁺ HSPCs, respectively, followed by FACS.	Patient virus (USA).
Zaikos <i>et al.</i> , 2018 ¹⁹⁴	Infected HSPCs are a persistent source of plasma virus in a subset of virally suppressed HIV-1 patients.	In vivo	Bone marrow-derived CD133 ⁺ and CD34 ⁺ CD133 ⁻ HSPCs purified by immunomagnetic selection.	Patient virus (USA).

2.4 Summary

The effects of HIV-1 infection on the haematopoietic system have devastating consequences in HIV patients, including the risk of developing HIV-associated haematological cancers and cytopenias which can be life-threatening. In addition, the development of AIDS further suppresses immune responses to oncogenesis (cancer) and microbial, viral, fungal, and parasitic infections. While HIV can be successfully treated with ART, HIV-associated pathologies are often aggravated by ART and can severely impact quality of life.

In the interest of understanding haematological abnormalities which present in HIV patients, and towards bringing HSCT gene therapy cures for HIV closer to the clinic, the effect of HIV infection on HSPCs must be explored. Extensive research indicates that HIV infection negatively impacts haematopoiesis, which could be caused by direct infection or as an indirect consequence of infection. Literature reports both direct and indirect mechanisms of HIV-mediated haematopoietic dysfunction, but there is still no consensus as to the susceptibility of HSPCs to HIV, and whether susceptibility is confined to identifiable subsets of HSPCs. Elucidating the direct and indirect effects of HIV infection on HSPCs is therefore important for understanding the haematological abnormalities HIV patients present with, as well as having consequences for anti-HIV gene therapy strategies.

2.5 References

1. Kosan, C., Godmann, M. Genetic and Epigenetic Mechanisms That Maintain Hematopoietic Stem Cell Function. *Stem Cells International*. 2016;2016:5178965.
2. Seita, J., Weissman, I.L. Hematopoietic Stem Cell: Self-renewal versus Differentiation. *Wiley interdisciplinary reviews Systems biology and medicine*. 2010;2(6):640-53.
3. Lim, W.F., Inoue-Yokoo, T., Tan, K.S., Lai, M.I., Sugiyama, D. Hematopoietic cell differentiation from embryonic and induced pluripotent stem cells. *Stem Cell Research & Therapy*. 2013;4(3):71-81.
4. Kanji, S., Pompili, V.J., Das, H. Plasticity and Maintenance of Hematopoietic Stem Cells During Development. *Recent Patents on Biotechnology*. 2011;5(1):40-53.
5. Bryder, D., Rossi, D.J., Weissman, I.L. Hematopoietic stem cells: the paradigmatic tissue-specific stem cell. *The American journal of pathology*. 2006;169(2):338-46.
6. Schofield, R. The relationship between the spleen colony-forming cell and the haemopoietic stem cell. *Blood cells*. 1978;4(1-2):7-25.
7. Mendelson, A., Frenette, P.S. Hematopoietic stem cell niche maintenance during homeostasis and regeneration. *Nature medicine*. 2014;20(8):833-46.
8. Ahmadzadeh, A., Kast, R.E., Ketabchi, N., Shahrabi, S., Shahjahani, M., Jaseb, K., et al. Regulatory effect of chemokines in bone marrow niche. *Cell and Tissue Research*. 2015;361(2):401-10.
9. Alexaki, A., Wigdahl, B. HIV-1 Infection of Bone Marrow Hematopoietic Progenitor Cells and Their Role in Trafficking and Viral Dissemination. *PLoS Pathog*. 2008;4(12):e1000215.
10. Hoffbrand, V., Moss, P.A.H. *Hoffbrand's Essential Haematology*. 7 ed. West Sussex, United Kingdom: Wiley; 2015. p. 1-9.
11. Bird, A. Perceptions of epigenetics. *Nature*. 2007;447:396-398.
12. Hu, Q., Rosenfeld, M.G. Epigenetic regulation of human embryonic stem cells. *Frontiers in genetics*. 2012;3:238-.
13. Yagi, M., Yamanaka, S., Yamada, Y. Epigenetic foundations of pluripotent stem cells that recapitulate in vivo pluripotency. *Laboratory investigation; a journal of technical methods and pathology*. 2017;97(10):1133-41.
14. Singh, V.K., Saini, A., Kalsan, M., Kumar, N., Chandra, R. Describing the Stem Cell Potency: The Various Methods of Functional Assessment and In silico Diagnostics. *Frontiers in cell and developmental biology*. 2016;4:134-.
15. Mitalipov, S., Wolf, D. Totipotency, pluripotency and nuclear reprogramming. *Advances in biochemical engineering/biotechnology*. 2009;114:185-99.
16. Rich, I.N., Potency, Proliferation and Engraftment Potential of Stem Cell Therapeutics: The Relationship between Potency and Clinical Outcome for Hematopoietic Stem Cell Products. *Journal of Cell Science & Therapy*. 2013;04(02).

17. Chagastelles, P.C., Nardi, N.B. Biology of stem cells: an overview. *Kidney international supplements*. 2011;1(3):63-7.
18. Ermolaeva, M., Neri, F., Ori, A., Rudolph, K.L. Cellular and epigenetic drivers of stem cell ageing. *Nature Reviews Molecular Cell Biology*. 2018;19(9):594-610.
19. Choudry, F.A., Frontini, M. Epigenetic Control of Haematopoietic Stem Cell Aging and Its Clinical Implications. *Stem Cells International*. 2016;2016:9.
20. Ferraro, F., Celso, C.L., Scadden, D. Adult stem cells and their niches. *Advances in experimental medicine and biology*. 2010;695:155-68.
21. Xin, T., Greco, V., Myung, P. Hardwiring Stem Cell Communication through Tissue Structure. *Cell*. 2016;164(6):1212-25.
22. Shi, Y., Cao, J., Wang, Y. Rethinking regeneration: empowerment of stem cells by inflammation. *Cell Death And Differentiation*. 2015;22:1891-2.
23. Bauer, S. Cytokine control of adult neural stem cells. *Annals of the New York Academy of Sciences*. 2009;1153:48-56.
24. Scadden, D.T. The stem-cell niche as an entity of action. *Nature*. 2006;441:1075-9.
25. Sperber, H., Mathieu, J., Wang, Y., Ferreccio, A., Hesson, J., Xu, Z., et al. The metabolome regulates the epigenetic landscape during naive-to-primed human embryonic stem cell transition. *Nature Cell Biology*. 2015;17:1523-32.
26. de Miguel-Beriain, I. The ethics of stem cells revisited. *Advanced Drug Delivery Reviews*. 2015;82:176-80.
27. Mahla, R.S. Stem Cells Applications in Regenerative Medicine and Disease Therapeutics. *International journal of cell biology*. 2016;2016:6940283.
28. Fortier, L.A. Stem cells: classifications, controversies, and clinical applications. *Veterinary surgery: VS*. 2005;34(5):415-23.
29. Haspel, R.L., Miller, K.B. Hematopoietic stem cells: source matters. *Current stem cell research & therapy*. 2008;3(4):229-36.
30. Friedenstein, A.J., Petrakova, K.V., Kurolesova, A.I., Frolova, G.P. Heterotopic of bone marrow. Analysis of precursor cells for osteogenic and hematopoietic tissues. *Transplantation*. 1968;6(2):230-47.
31. Liao, H.-T., Chen, C.-T. Osteogenic potential: Comparison between bone marrow and adipose-derived mesenchymal stem cells. *World journal of stem cells*. 2014;6(3):288-95.
32. Dominici, M., Le Blanc, K., Mueller, I., Slaper-Cortenbach, I., Marini, F., Krause, D., et al. Minimal criteria for defining multipotent mesenchymal stromal cells. The International Society for Cellular Therapy position statement. *Cytotherapy*. 2006;8(4):315-7.
33. Elahi, K.C., Klein, G., Avci-Adali, M., Sievert, K.D., MacNeil, S., Aicher, W.K. Human Mesenchymal Stromal Cells from Different Sources Diverge in Their Expression of Cell Surface Proteins and Display Distinct Differentiation Patterns. *Stem Cells Int*. 2016;2016:5646384.
34. Takahashi, K., Yamanaka, S. Induction of Pluripotent Stem Cells from Mouse Embryonic and Adult Fibroblast Cultures by Defined Factors. *Cell*. 2006;126(4):663-76.

35. Raab, S., Klingenstein, M., Lieban, S., Linta, L. A Comparative View on Human Somatic Cell Sources for iPSC Generation. *Stem cells International*. 2014;2014.
36. Mason, C., Dunnill, P. A brief definition of regenerative medicine. *Regenerative Medicine*. 2007;3(1):1-5.
37. Garitaonandia, I., Gonzalez, R., Sherman, G., Semechkin, A., Evans, A., Kern, R. Novel Approach to Stem Cell Therapy in Parkinson's Disease. *Stem Cells and Development*. 2018;27(14):951-7.
38. Sneddon, J.B., Tang, Q., Stock, P., Bluestone, J.A., Roy, S., Desai, T., et al. Stem Cell Therapies for Treating Diabetes: Progress and Remaining Challenges. *Cell Stem Cell*. 2018;22(6):810-23.
39. Hütter, G., Nowak, D., Mossner, M., Ganepola, S., Müßig, A., Allers, K., et al. Long-Term Control of HIV by CCR5 Delta32/Delta32 Stem-Cell Transplantation. *New England Journal of Medicine*. 2009;360(7):692-8.
40. Myburgh, R., Ivic, S., Pepper, M.S., Gers-Huber, G., Li, D., Audigé, A., et al. Lentivector Knockdown of CCR5 in Hematopoietic Stem and Progenitor Cells Confers Functional and Persistent HIV-1 Resistance in Humanized Mice. *Journal of Virology*. 2015;89(13):6761-72.
41. Velten, L., Haas, S.F., Raffel, S., Blaszkiewicz, S., Islam, S., Hennig, B.P., et al. Human haematopoietic stem cell lineage commitment is a continuous process. *Nat Cell Biol*. 2017;19(4):271-81.
42. Thomas, E.D., Lochte, H.L., Jr., Lu, W.C., Ferrebee, J.W. Intravenous infusion of bone marrow in patients receiving radiation and chemotherapy. *The New England journal of medicine*. 1957;257(11):491-6.
43. Juric, M.K., Ghimire, S., Ogonek, J., Weissinger, E.M., Holler, E., van Rood, J.J., et al. Milestones of Hematopoietic Stem Cell Transplantation - From First Human Studies to Current Developments. *Front Immunol*. 2016;7:470.
44. Holowiecki, J. Indications for hematopoietic stem cell transplantation. *Polskie Archiwum Medycyny Wewnętrznej*. 2008;118(11):658-63.
45. Barker, J.N., Weisdorf, D.J., DeFor, T.E., Blazar, B.R., McGlave, P.B., Miller, J.S., et al. Transplantation of 2 partially HLA-matched umbilical cord blood units to enhance engraftment in adults with hematologic malignancy. *Blood*. 2005;105(3):1343-7.
46. Wagner, J.E., Jr., Eapen, M., Carter, S., Wang, Y., Schultz, K.R., Wall, D.A., et al. One-unit versus two-unit cord-blood transplantation for hematologic cancers. *The New England journal of medicine*. 2014;371(18):1685-94.
47. Hoggatt, J., Pelus, L.M. Mobilization of hematopoietic stem cells from the bone marrow niche to the blood compartment. *Stem Cell Res Ther*. 2011;2(2):13.
48. Perez-Simon, J.A., Caballero, M.D., Corral, M., Nieto, M.J., Orfao, A., Vazquez, L., et al. Minimal number of circulating CD34+ cells to ensure successful leukapheresis and engraftment in autologous peripheral blood progenitor cell transplantation. *Transfusion*. 1998;38(4):385-91.

49. Siena, S., Schiavo, R., Pedrazzoli, P., Carlo-Stella, C. Therapeutic relevance of CD34 cell dose in blood cell transplantation for cancer therapy. *Journal of clinical oncology: official journal of the American Society of Clinical Oncology*. 2000;18(6):1360-77.
50. Gianni, A.M. Where do we stand with respect to the use of peripheral blood progenitor cells? *Annals of Oncology*. 1994;(5)9:781-4.
51. Sutherland, D.R., Anderson, L., Keeney, M., Nayar, R., Chin-Yee, I. The ISHAGE guidelines for CD34+ cell determination by flow cytometry. *International Society of Hematotherapy and Graft Engineering. Journal of hematotherapy*. 1996;5(3):213-26.
52. Wagner, J.E., Brunstein, C., McKenna, D., Sumstad, D., Maahs, S., Laughlin, M.J., et al. Acceleration of Umbilical Cord Blood (UCB) Stem Engraftment: Results of a Phase I Clinical Trial with Stemregenin-1 (SR1) Expansion Culture. *Biology of Blood and Marrow Transplantation*. 2015;21(2):S48-S9.
53. Nikiforow, S., Ritz, J. Dramatic Expansion of HSCs: New Possibilities for HSC Transplants? *Cell Stem Cell*. 2015;18(1):10-2.
54. Park, B., Yoo, K.H., Kim, C. Hematopoietic stem cell expansion and generation: the ways to make a breakthrough. *Blood research*. 2015;50(4):194-203.
55. Kode, J., Khattry, N., Bakshi, A., Amrutkar, V., Bagal, B., Karandikar, R., et al. Study of stem cell homing & self-renewal marker gene profile of ex vivo expanded human CD34(+) cells manipulated with a mixture of cytokines & stromal cell-derived factor 1. *The Indian journal of medical research*. 2017;146(1):56-70.
56. Dmitrieva, R.I., Anisimov, S.V. Optimal protocols of hematopoietic stem cell expansion in vitro. *Cell and Tissue Biology*. 2013;7(3):207-11.
57. Morgan, R.A., Gray, D., Lomova, A., Kohn, D.B. Hematopoietic Stem Cell Gene Therapy: Progress and Lessons Learned. *Cell Stem Cell*. 2017;21(5):574-90.
58. Sidney, L.E., Branch, M.J., Dunphy, S.E., Dua, H.S., Hopkinson, A. Concise Review: Evidence for CD34 as a Common Marker for Diverse Progenitors. *Stem Cells (Dayton, Ohio)*. 2014;32(6):1380-9.
59. Fritsch, G., Stimpfl, M., Kurz, M., Leitner, A., Printz, D., Buchinger, P., et al. Characterization of hematopoietic stem cells. *Annals of the New York Academy of Sciences*. 1995;770:42-52.
60. Kekarainen, T., Mannelin, S., Laine, J., Jaatinen, T. Optimization of immunomagnetic separation for cord blood-derived hematopoietic stem cells. *BMC cell biology*. 2006;7:30.
61. Aiuti, A., Slavin, S., Aker, M., Ficara, F., Deola, S., Mortellaro, A., et al. Correction of ADA-SCID by stem cell gene therapy combined with nonmyeloablative conditioning. *Science*. 2002;296(5577):2410-3.
62. Hacein-Bey-Abina, S., Le Deist, F., Carlier, F., Bouneaud, C., Hue, C., De Villartay, J.P., et al. Sustained correction of X-linked severe combined immunodeficiency by ex vivo gene therapy. *The New England journal of medicine*. 2002;346(16):1185-93.
63. Ribeil, J.-A., Hacein-Bey-Abina, S., Payen, E., Magnani, A., Semeraro, M., Magrin, E., et al. Gene Therapy in a Patient with Sickle Cell Disease. *New England Journal of Medicine*. 2017;376(9):848-55.

64. Eichler, F., Duncan, C., Musolino, P.L., Orchard, P.J., De Oliveira, S., Thrasher, A.J., et al. Hematopoietic Stem-Cell Gene Therapy for Cerebral Adrenoleukodystrophy. *New England Journal of Medicine*. 2017;377(17):1630-8.
65. DiGiusto, D.L., Krishnan, A., Li, L., Li, H., Li, S., Rao, A., et al. RNA-based gene therapy for HIV with lentiviral vector-modified CD34(+) cells in patients undergoing transplantation for AIDS-related lymphoma. *Sci Transl Med*. 2010;2(36):36ra43.
66. Kambal, A., Mitchell, G., Cary, W., Gruenloh, W., Jung, Y., Kalomoiris, S., et al. Generation of HIV-1 Resistant and Functional Macrophages From Hematopoietic Stem Cell-derived Induced Pluripotent Stem Cells. *Mol Ther*. 2011;19(3):584-93.
67. Younan, P., Kowalski, J., Kiem, H.-P. Genetically Modified Hematopoietic Stem Cell Transplantation for HIV-1-infected Patients: Can We Achieve a Cure? *Mol Ther*. 2014;22(2):257-64.
68. Armijo, E., Soto, C., Davis, B.R. HIV/AIDS: modified stem cells in the spotlight. *Cellular and molecular life sciences : CMLS*. 2014;71(14):2641-9.
69. Esmaeilzadeh, A., Farshbaf, A., Erfanmanesh, M. Autologous Hematopoietic Stem Cells transplantation and genetic modification of CCR5 m303/m303 mutant patient for HIV/AIDS. *Medical Hypotheses*. 2015;84(3):216-8.
70. Kang, H., Minder, P., Park, M.A., Mesquitta, W.-T., Torbett, B.E., Slukvin, I.I. CCR5 Disruption in Induced Pluripotent Stem Cells Using CRISPR/Cas9 Provides Selective Resistance of Immune Cells to CCR5-tropic HIV-1 Virus. *Mol Ther Nucleic Acids*. 2015;4:e268.
71. Mehta, V., Chandramohan, D., Agarwal, S. Genetic Modulation Therapy Through Stem Cell Transplantation for Human Immunodeficiency Virus 1 Infection. *Cureus*. 2017;9(3):e1093.
72. Khamaikawin, W., Shimizu, S., Kamata, M., Cortado, R., Jung, Y., Lam, J., et al. Modeling Anti-HIV-1 HSPC-Based Gene Therapy in Humanized Mice Previously Infected with HIV-1. *Molecular Therapy - Methods & Clinical Development*. 2018;9:23-32.
73. Wang, H., Georgakopoulou, A., Psatha, N., Li, C., Capsali, C., Samal, H.B., et al. In vivo hematopoietic stem cell gene therapy ameliorates murine thalassemia intermedia. *The Journal of Clinical Investigation*. 2018;129(2).
74. Adair, J.E., Chandrasekaran, D., Sghia-Hughes, G., Haworth, K.G., Woolfrey, A.E., Burroughs, L.M., et al. Novel lineage depletion preserves autologous blood stem cells for gene therapy of Fanconi anemia complementation group A. *Haematologica*. 2018;103(11):1806-14.
75. Haas, S., Trumpp, A., Milsom, M.D. Causes and Consequences of Hematopoietic Stem Cell Heterogeneity. *Cell Stem Cell*. 2018;22(5):627-38.
76. Ivanovic, Z. Hematopoietic stem cells in research and clinical applications: The "CD34 issue". *World journal of stem cells*. 2010;2(2):18-23.
77. Cimato, T.R., Furlage, R.L., Conway, A., Wallace, P.K. Simultaneous measurement of human hematopoietic stem and progenitor cells in blood using multicolor flow cytometry. *Cytometry Part B, Clinical cytometry*. 2016;90(5):415-23.

78. Kobari, L., Giarratana, M.C., Pflumio, F., Izac, B., Coulombel, L., Douay, L. CD133+ cell selection is an alternative to CD34+ cell selection for ex vivo expansion of hematopoietic stem cells. *Journal of Hematotherapy and Stem Cell Research*. 2001;10(2):273-81.
79. Li, Z. CD133: a stem cell biomarker and beyond. *Experimental hematology & oncology*. 2013;2(1):17-.
80. Takahashi, M., Matsuoka, Y., Sumide, K., Nakatsuka, R., Fujioka, T., Kohno, H., et al. CD133 is a positive marker for a distinct class of primitive human cord blood-derived CD34-negative hematopoietic stem cells. *Leukemia*. 2014;28(6):1308-15.
81. Majeti, R., Park, C.Y., Weissman, I.L. Identification of a hierarchy of multipotent hematopoietic progenitors in human cord blood. *Cell Stem Cell*. 2007;1(6):635-45.
82. Craig, W., Kay, R., Cutler, R.L., Lansdorp, P.M. Expression of Thy-1 on human hematopoietic progenitor cells. *The Journal of experimental medicine*. 1993;177(5):1331-42.
83. de Wynter, E.A., Buck, D., Hart, C., Heywood, R., Coutinho, L.H., Clayton, A., et al. CD34+AC133+ cells isolated from cord blood are highly enriched in long-term culture-initiating cells, NOD/SCID-repopulating cells and dendritic cell progenitors. *Stem Cells*. 1998;16(6):387-96.
84. Goodell, M.A. CD34+ or CD34-: Does it Really Matter? *Blood*. 1999;94(8):2545-7.
85. Sumide, K., Matsuoka, Y., Kawamura, H., Nakatsuka, R., Fujioka, T., Asano, H., et al. A revised road map for the commitment of human cord blood CD34-negative hematopoietic stem cells. *Nature Communications*. 2018;9(1):2202.
86. Radtke, S., Görgens, A., Kordelas, L., Schmidt, M., Kimmig, K.R., Königer, A., et al. CD133 allows elaborated discrimination and quantification of haematopoietic progenitor subsets in human haematopoietic stem cell transplants. *British Journal of Haematology*. 2015;169(6):868-78.
87. Drake, A.C., Khoury, M., Leskov, I., Iliopoulou, B.P., Fragoso, M., Lodish, H., et al. Human CD34+ CD133+ Hematopoietic Stem Cells Cultured with Growth Factors Including Angptl5 Efficiently Engraft Adult NOD-SCID Il2ry-/- (NSG) Mice. *PLOS ONE*. 2011;6(4):e18382.
88. Carrelha, J., Meng, Y., Kettle, L.M., Luis, T.C., Norfo, R., Alcolea, V., et al. Hierarchically related lineage-restricted fates of multipotent haematopoietic stem cells. *Nature*. 2018;554:106.
89. Shvitiel, S., Lapid, K., Kalchenko, V., Avigdor, A., Goichberg, P., Kalinkovich, A., et al. CD45 regulates homing and engraftment of immature normal and leukemic human cells in transplanted immunodeficient mice. *Exp Hematol*. 2011;39(12):1161-70.e1.
90. Berardi, A.C., Wang, A., Levine, J.D., Lopez, P., Scadden, D.T. Functional isolation and characterization of human hematopoietic stem cells. *Science*. 1995;267(5194):104-8.
91. Nielsen, J.S., McNagny, K.M. Novel functions of the CD34 family. *Journal of cell science*. 2008;121(Pt 22):3683-92.

92. Mehta, K., Shahid, U., Malavasi, F. Human CD38, a cell-surface protein with multiple functions. *FASEB journal : official publication of the Federation of American Societies for Experimental Biology*. 1996;10(12):1408-17.
93. Kisselbach, L., Merges, M., Bossie, A., Boyd, A. CD90 Expression on human primary cells and elimination of contaminating fibroblasts from cell cultures. *Cytotechnology*. 2009;59(1):31-44.
94. Haack-Sorensen, M., Friis, T., Bindslev, L., Mortensen, S., Johnsen, H.E., Kastrup, J. Comparison of different culture conditions for human mesenchymal stromal cells for clinical stem cell therapy. *Scandinavian journal of clinical and laboratory investigation*. 2008;68(3):192-203.
95. Handgretinger, R., Kuci, S. CD133-Positive Hematopoietic Stem Cells: From Biology to Medicine. *Advances in experimental medicine and biology*. 2013;777:99-111.
96. Irollo, E., Pirozzi, G. CD133: to be or not to be, is this the real question? *American journal of translational research*. 2013;5(6):563-81.
97. Metcalf, D. Hematopoietic cytokines. *Blood*. 2008;111(2):485-91.
98. Bernad, A., Kopf, M., Kulbacki, R., Weich, N., Koehler, G., Gutierrez-Ramos, J.C. Interleukin-6 is required in vivo for the regulation of stem cells and committed progenitors of the hematopoietic system. *Immunity*. 1994;1(9):725-31.
99. Kollet, O., Dar, A., Shivtiel, S., Kalinkovich, A., Lapid, K., Sztainberg, Y., et al. Osteoclasts degrade endosteal components and promote mobilization of hematopoietic progenitor cells. *Nat Med*. 2006;12(6):657-64.
100. Ugarte, F., Forsberg, E.C. Haematopoietic stem cell niches: new insights inspire new questions. *The EMBO Journal*. 2013;32(19):2535-47.
101. Morrison, S.J., Scadden, D.T. The bone marrow niche for haematopoietic stem cells. *Nature*. 2014;505(7483):327-34.
102. Yamazaki, S., Ema, H., Karlsson, G., Yamaguchi, T., Miyoshi, H., Shioda, S., et al. Nonmyelinating Schwann cells maintain hematopoietic stem cell hibernation in the bone marrow niche. *Cell*. 2011;147(5):1146-58.
103. Hassan, H.T., Zander, A. Stem cell factor as a survival and growth factor in human normal and malignant hematopoiesis. *Acta haematologica*. 1996;95(3-4):257-62.
104. Zhang, C.C., Lodish, H.F. Cytokines regulating hematopoietic stem cell function. *Current opinion in hematology*. 2008;15(4):307-11.
105. Katayama, Y., Battista, M., Kao, W.M., Hidalgo, A., Peired, A.J., Thomas, S.A., et al. Signals from the sympathetic nervous system regulate hematopoietic stem cell egress from bone marrow. *Cell*. 2006;124(2):407-21.
106. Moore, M.A.S. Chapter 47 - Hematopoietic Stem Cells. In: Lanza R, Langer R, Vacanti J, editors. *Principles of Tissue Engineering (Fourth Edition)*. Boston: Academic Press; 2014. p. 989-1040.
107. Pereira, C., Clarke, E., Damen, J. Hematopoietic colony-forming cell assays. *Methods Mol Biol*. 2007;407:177-208.
108. Broudy, V.C. Stem Cell Factor and Hematopoiesis. *Blood*. 1997;90(4):1345-64.

109. Metcalf, D. The colony-stimulating factors and cancer. *Cancer immunology research*. 2013;1(6):351-6.
110. Ihle, J.N. Interleukin-3 and hematopoiesis. *Chemical immunology*. 1992;51:65-106.
111. Donahue, R.E., Seehra, J., Metzger, M., Lefebvre, D., Rock, B., Carbone, S., et al. Human IL-3 and GM-CSF act synergistically in stimulating hematopoiesis in primates. *Science*. 1988;241(4874):1820.
112. Udagawa, N., Takahashi, N., Katagiri, T., Tamura, T., Wada, S., Findlay, D.M., et al. Interleukin (IL)-6 induction of osteoclast differentiation depends on IL-6 receptors expressed on osteoblastic cells but not on osteoclast progenitors. *The Journal of experimental medicine*. 1995;182(5):1461-8.
113. Chomarat, P., Banchereau, J., Davoust, J., Palucka, A.K. IL-6 switches the differentiation of monocytes from dendritic cells to macrophages. *Nature immunology*. 2000;1(6):510-4.
114. Ishibashi, T., Kimura, H., Uchida, T., Kariyone, S., Friese, P., Burstein, S.A. Human interleukin 6 is a direct promoter of maturation of megakaryocytes in vitro. *Proceedings of the National Academy of Sciences of the United States of America*. 1989;86(15):5953-7.
115. Feng, J.F., Zhuang, M., Zhu, L.J., Sheng, Z.L., Zhu, Y.Q., Li, C.P. Effect of IL-6/sIL-6R on ex vivo expansion of human cord blood derived CD34+ cells. *Ai zheng = Aizheng = Chinese journal of cancer*. 2004;23(6):715-8.
116. Bordeaux-Rego, P., Luzo, A., Costa, F.F., Olalla Saad, S.T., Crosara-Alberto, D.P. Both interleukin-3 and interleukin-6 are necessary for better ex vivo expansion of CD133+ cells from umbilical cord blood. *Stem Cells Dev*. 2010;19(3):413-22.
117. Sitnicka, E., Bryder, D., Theilgaard-Monch, K., Buza-Vidas, N., Adolfsson, J., Jacobsen, S.E. Key role of flt3 ligand in regulation of the common lymphoid progenitor but not in maintenance of the hematopoietic stem cell pool. *Immunity*. 2002;17(4):463-72.
118. Tsapogas, P., Mooney, C.J., Brown, G., Rolink, A. The Cytokine Flt3-Ligand in Normal and Malignant Hematopoiesis. *International journal of molecular sciences*. 2017;18(6):1115.
119. Fry, T.J., Mackall, C.L. Interleukin-7: from bench to clinic. *Blood*. 2002;99(11):3892-3904.
120. Häggström, M., Rad, A. Hematopoietic growth factors. In: *factors.svg Hg*, editor. Wikimedia Commons. 235469199 ed. Online: Wikimedia Commons; 2017.
121. Gordon, M.Y. Human haemopoietic stem cell assays. *Blood reviews*. 1993;7(3):190-7.
122. Li, B., Liu, J., Qu, S., Gale, R.P., Song, Z., Xing, R., et al. Colony-forming unit cell (CFU-C) assays at diagnosis: CFU-G/M cluster predicts overall survival in myelodysplastic syndrome patients independently of IPSS-R. *Oncotarget*. 2016;7(42):68023-32.
123. Pamphilon, D., Selogie, E., McKenna, D., Cancelas-Peres, J.A., Szczepiorkowski, Z.M., Sacher, R., et al. Current practices and prospects for standardization of the hematopoietic colony-forming unit assay: a report by the cellular therapy team of the Biomedical Excellence for Safer Transfusion (BEST) Collaborative. *Cytotherapy*. 2013;15(3):255-62.

124. UNAIDS. UNAIDS Fact Sheet July 2018 2017 [Available from: <http://www.unaids.org/en/resources/fact-sheet>].
125. Africa, S.S. Mid-year population estimates, 2018. In: Africa SS, editor. Pretoria: Statistics South Africa; 2018.
126. Hoxie, J.A., June, C.H. Novel Cell and Gene Therapies for HIV. *Cold Spring Harbor perspectives in medicine*. 2012;2(10).
127. Alexaki, A., Liu, Y., Wigdahl, B. Cellular reservoirs of HIV-1 and their role in viral persistence. *Current HIV research*. 2008;6(5):388-400.
128. Coiras, M., Lopez-Huertas, M.R., Perez-Olmeda, M., Alcamí, J. Understanding HIV-1 latency provides clues for the eradication of long-term reservoirs. *Nat Rev Microbiol*. 2009;7(11):798-812.
129. Spira, S., Wainberg, M.A., Loemba, H., Turner, D., Brenner, B.G. Impact of clade diversity on HIV-1 virulence, antiretroviral drug sensitivity and drug resistance. *The Journal of antimicrobial chemotherapy*. 2003;51(2):229-40.
130. Menéndez-Arias, L. Molecular basis of human immunodeficiency virus drug resistance: An update. *Antiviral Research*. 2010;85(1):210-31.
131. Levy, J.A. HIV pathogenesis: 25 years of progress and persistent challenges. *AIDS (London, England)*. 2009;23(2):147-60.
132. Castro-Nallar, E., Pérez-Losada, M., Burton, G.F., Crandall, K.A. The evolution of HIV: Inferences using phylogenetics. *Molecular Phylogenetics and Evolution*. 2012;62(2):777-92.
133. Gnanakaran, S., Lang, D., Daniels, M., Bhattacharya, T., Derdeyn, C.A., Korber, B. Clade-Specific Differences between Human Immunodeficiency Virus Type 1 Clades B and C: Diversity and Correlations in C3-V4 Regions of gp120. *Journal of Virology*. 2007;81(9):4886-91.
134. Frankel, A.D., Young, J.A. HIV-1: fifteen proteins and an RNA. *Annual review of biochemistry*. 1998;67:1-25.
135. Splettstoesser, T. HIV-genome. In: HIV-genome, editor. Adobe ImageReady. online: Wikimedia Commons; 2014. p. Structure of the HIV-1 genome. It has a size of roughly 10.000 base pairs and consists of nine genes, some of which are overlapping.
136. Infographic, W. HIV life cycle. In: 5w-sample-020-hiv-lifecycle, editor. Unknown. Online - Wordpress: 5W Infographics; 2014. p. Life cycle of HIV.
137. Arhel, N. Revisiting HIV-1 uncoating. *Retrovirology*. 2010;7(1):96.
138. Craigie, R., Bushman, F.D. HIV DNA integration. *Cold Spring Harbor perspectives in medicine*. 2012;2(7):a006890.
139. Roof, P., Ricci, M., Genin, P., Montano, M.A., Essex, M., Wainberg, M.A., et al. Differential regulation of HIV-1 clade-specific B, C, and E long terminal repeats by NF-kappaB and the Tat transactivator. *Virology*. 2002;296(1):77-83.
140. Hope, T.J. The Ins and Outs of HIV Rev. *Archives of Biochemistry and Biophysics*. 1999;365(2):186-91.

141. Freed, E.O. HIV-1 assembly, release and maturation. *Nat Rev Micro*. 2015;13(8):484-96.
142. Bebenek, K., Abbotts, J., Wilson, S.H., Kunkel, T.A. Error-prone polymerization by HIV-1 reverse transcriptase. Contribution of template-primer misalignment, miscoding, and termination probability to mutational hot spots. *The Journal of biological chemistry*. 1993;268(14):10324-34.
143. Sguanci, L., Bagnoli, F., Liò, P. Modeling HIV quasispecies evolutionary dynamics. *BMC Evolutionary Biology*. 2007;7(Suppl 2):S5-S.
144. McGowan, J.P., Shah, S. Understanding HIV Tropism New York: Physicians' Research Network Inc.; 2010 [Volume 15, January 2010 - based on a live meeting.]. Available from: http://www.prn.org/index.php/management/article/hiv_tropism_1002.
145. Delobel, P., Sandres-Saune, K., Cazabat, M., Pasquier, C., Marchou, B., Massip, P., et al. R5 to X4 switch of the predominant HIV-1 population in cellular reservoirs during effective highly active antiretroviral therapy. *Journal of acquired immune deficiency syndromes (1999)*. 2005;38(4):382-92.
146. Bracq, L., Xie, M., Benichou, S., Bouchet, J. Mechanisms for Cell-to-Cell Transmission of HIV-1. *Front Immunol*. 2018;9:260.
147. Svicher, V., Ceccherini-Silberstein, F., Antinori, A., Aquaro, S., Perno, C.F. Understanding HIV Compartments and Reservoirs. *Current HIV/AIDS Reports*. 2014;11(2):186-94.
148. McNamara, L.A., Collins, K.L. Hematopoietic stem/precursor cells as HIV reservoirs. *Current opinion in HIV and AIDS*. 2011;6(1):43-8.
149. Durand, C.M., Ghiaur, G., Siliciano, J.D., Rabi, S.A., Eisele, E.E., Salgado, M., et al. HIV-1 DNA is detected in bone marrow populations containing CD4+ T cells but is not found in purified CD34+ hematopoietic progenitor cells in most patients on antiretroviral therapy. *J Infect Dis*. 2012;205(6):1014-8.
150. Trono, D., Marzetta, F. Profaning the Ultimate Sanctuary: HIV Latency in Hematopoietic Stem Cells. *Cell Host & Microbe*. 2011;9(3):170-2.
151. Hutter, G., Bodor, J., Ledger, S., Boyd, M., Millington, M., Tsie, M., et al. CCR5 Targeted Cell Therapy for HIV and Prevention of Viral Escape. *Viruses*. 2015;7(8):4186-203.
152. Gupta, R.K., Abdul-jawad, S., McCoy, L.E., Mok, H.P., Peppia, D., Salgado, M., et al. HIV-1 remission following CCR5 Δ 32/ Δ 32 haematopoietic stem-cell transplantation. *Nature*. 2019;568(7751):244-8.
153. Jensen, B.-E.O., Knops, E., Lübke, N., Wensing, A., Martinez-Picado, J., Kaiser, R., et al. Analytic treatment interruption (ATI) after allogeneic CCR5-D32 HSCT for AML in 2013. In: Foundation/IAS–USA C, editor. CROI 2019; Seattle, Washington: Conference for Retroviruses and Infectious Diseases; 2019.
154. Henrich, T.J., Hanhauser, E., Marty, F.M., Sirignano, M.N., Keating, S., Lee, T.-H., et al. Antiretroviral-free HIV-1 remission and viral rebound after allogeneic stem cell transplantation: report of 2 cases. *Annals of internal medicine*. 2014;161(5):319-27.
155. Donahue, R.E., Johnson, M.M., Zon, L.I., Clark, S.C., Groopman, J.E. Suppression of in vitro haematopoiesis following human immunodeficiency virus infection. *Nature*. 1987;326(6109):200-3.

156. Davis, B.R., Schwartz, D.H., Marx, J.C., Johnson, C.E., Berry, J.M., Lyding, J., et al. Absent or rare human immunodeficiency virus infection of bone marrow stem/progenitor cells in vivo. *Journal of Virology*. 1991;65(4):1985-90.
157. Abecasis, A.B., Wensing, A.M.J., Paraskevis, D., Vercauteren, J., Theys, K., Van de Vijver, D.A.M.C., et al. HIV-1 subtype distribution and its demographic determinants in newly diagnosed patients in Europe suggest highly compartmentalized epidemics. *Retrovirology*. 2013;10(1):7.
158. Bulla, I., Schultz, A.-K., Schreiber, F., Zhang, M., Leitner, T., Korber, B., et al. HIV classification using the coalescent theory. *Bioinformatics*. 2010;26(11):1409-15.
159. Easterbrook, P.J., Smith, M., Mullen, J., O'Shea, S., Chrystie, I., de Ruiter, A., et al. Impact of HIV-1 viral subtype on disease progression and response to antiretroviral therapy. *Journal of the International AIDS Society*. 2010;13:4-.
160. Koning, F.A., Castro, H., Dunn, D., Tilston, P., Cane, P.A., Mbisa, J.L. Subtype-specific differences in the development of accessory mutations associated with high-level resistance to HIV-1 nucleoside reverse transcriptase inhibitors. *The Journal of antimicrobial chemotherapy*. 2013;68(6):1220-36.
161. Herrera-Carrillo, E., Berkhout, B. The impact of HIV-1 genetic diversity on the efficacy of a combinatorial RNAi-based gene therapy. *Gene therapy*. 2015;22(6):485-95.
162. Gräf, T., Pinto, A.R. The increasing prevalence of HIV-1 subtype C in Southern Brazil and its dispersion through the continent. *Virology*. 2013;435(1):170-8.
163. Calenda, V., Chermann, J.C. The effects of HIV on hematopoiesis. *European journal of haematology*. 1992;48(4):181-6.
164. Vishnu, P., Aboulafia, D.M. Haematological manifestations of human immune deficiency virus infection. *British Journal of Haematology*. 2015;171(5):695-709.
165. Volberding, P.A., Levine, A.M., Mitsuyasu, R., Dieterich, D., Mildvan, D., Saag, M. Anemia in HIV Infection: Clinical Impact and Evidence-Based Management Strategies. *Clinical Infectious Diseases*. 2004;38(10):1454-63.
166. Kaner, J., Thibaud, S., Sridharan, A., Assal, A., Polineni, R., Zingman, B., et al. HIV Is Associated with a High Rate of Unexplained Multilineage Cytopenias and Portends a Poor Prognosis in Myelodysplastic Syndrome (MDS) and Acute Myeloid Leukemia (AML). *Blood*. 2016;128(22):4345.
167. Vaughan, J.L., Wiggill, T.M., Alli, N., Hodgkinson, K. The prevalence of HIV seropositivity and associated cytopenias in full blood counts processed at an academic laboratory in Soweto, South Africa. *SAMJ: South African Medical Journal*. 2017;107:264-9.
168. Kyeyune, R., Saathoff, E., Ezeamama, A.E., Löscher, T., Fawzi, W., Guwatudde, D. Prevalence and correlates of cytopenias in HIV-infected adults initiating highly active antiretroviral therapy in Uganda. *BMC infectious diseases*. 2014;14(1):496.
169. Nascimento, F.G., Tanaka, P.Y. Thrombocytopenia in HIV-Infected Patients. *Indian journal of hematology & blood transfusion : an official journal of Indian Society of Hematology and Blood Transfusion*. 2012;28(2):109-11.
170. Scaradavou, A. HIV-related thrombocytopenia. *Blood reviews*. 2002;16(1):73-6.

171. Shi, X., Sims, M.D., Hanna, M.M., Xie, M., Gulick, P.G., Zheng, Y.-H., et al. Neutropenia during HIV infection: adverse consequences and remedies. *International reviews of immunology*. 2014;33(6):511-36.
172. Levine, A.M., Karim, R., Mack, W., Gravink, D.J., Anastos, K., Young, M., et al. Neutropenia in Human Immunodeficiency Virus Infection: Data From the Women's Interagency HIV Study. *Archives of Internal Medicine*. 2006;166(4):405-10.
173. Katsarou, O., Terpos, E., Patsouris, E., Peristeris, P., Viniou, N., Kapsimali, V., et al. Myelodysplastic features in patients with long-term HIV infection and haemophilia. *Haemophilia : the official journal of the World Federation of Hemophilia*. 2001;7(1):47-52.
174. Little, R.F., Dunleavy, K. Update on the treatment of HIV-associated hematologic malignancies. *ASH Education Program Book*. 2013;2013(1):382-8.
175. Verheyen, J., Thielen, A., Lubke, N., Dirks, M., Widera, M., Dittmer, U., et al. Rapid Rebound of a Preexisting CXCR4-tropic Human Immunodeficiency Virus Variant After Allogeneic Transplantation With CCR5 Delta32 Homozygous Stem Cells. *Clinical infectious diseases : an official publication of the Infectious Diseases Society of America*. 2019;68(4):684-7.
176. Louache, F., Henri, A., Bettaieb, A., Oksenhendler, E., Raguin, G., Tulliez, M., et al. Role of human immunodeficiency virus replication in defective in vitro growth of hematopoietic progenitors. *Blood*. 1992;80(12):2991-9.
177. Stanley, S.K., Kessler, S.W., Justement, J.S., Schnittman, S.M., Greenhouse, J.J., Brown, C.C., et al. CD34+ bone marrow cells are infected with HIV in a subset of seropositive individuals. *J Immunol*. 1992;149(2):689-97.
178. Chelucci, C., Hassan, H.J., Locardi, C., Bulgarini, D., Pelosi, E., Mariani, G., et al. In vitro human immunodeficiency virus-1 infection of purified hematopoietic progenitors in single-cell culture. *Blood*. 1995;85(5):1181-7.
179. Marandin, A., Katz, A., Oksenhendler, E., Tulliez, M., Picard, F., Vainchenker, W., et al. Loss of primitive hematopoietic progenitors in patients with human immunodeficiency virus infection. *Blood*. 1996;88(12):4568-78.
180. Weichold, F.F., Zella, D., Barabitskaja, O., Maciejewski, J.P., Dunn, D.E., Sloand, E.M., et al. Neither Human Immunodeficiency Virus-1 (HIV-1) nor HIV-2 Infects Most-Primitive Human Hematopoietic Stem Cells as Assessed in Long-Term Bone Marrow Cultures. *Blood*. 1998;91(3):907-15.
181. Shen, H., Cheng, T., Preffer, F.I., Dombkowski, D., Tomasson, M.H., Golan, D.E., et al. Intrinsic human immunodeficiency virus type 1 resistance of hematopoietic stem cells despite coreceptor expression. *J Virol*. 1999;73(1):728-37.
182. Redd, A.D., Avalos, A., Essex, M. Infection of hematopoietic progenitor cells by HIV-1 subtype C, and its association with anemia in southern Africa. *Blood*. 2007;110(9):3143-9.
183. Carter, C.C., Onafuwa-Nuga, A., McNamara, L.A., Riddell, J., Bixby, D., Savona, M.R., et al. HIV-1 Infects Multipotent Progenitor Cells Causing Cell Death and Establishing Latent Cellular Reservoirs. *Nature medicine*. 2010;16(4):446-51.

184. Carter, Christoph C., McNamara, Lucy A., Onafuwa-Nuga, A., Shackleton, M., Riddell Iv, J., Bixby, D., et al. HIV-1 Utilizes the CXCR4 Chemokine Receptor to Infect Multipotent Hematopoietic Stem and Progenitor Cells. *Cell Host & Microbe*. 2011;9(3):223-34.
185. Josefsson, L., Eriksson, S., Sinclair, E., Ho, T., Killian, M., Epling, L., et al. Hematopoietic precursor cells isolated from patients on long-term suppressive HIV therapy did not contain HIV-1 DNA. *J Infect Dis*. 2012;206(1):28-34.
186. McNamara, L.A., Ganesh, J.A., Collins, K.L. Latent HIV-1 infection occurs in multiple subsets of hematopoietic progenitor cells and is reversed by NF-kappaB activation. *J Virol*. 2012;86(17):9337-50.
187. Mullis, C.E., Oliver, A.E., Eller, L.A., Guwatudde, D., Mueller, A.C., Eller, M.A., et al. Short Communication: Colony-Forming Hematopoietic Progenitor Cells Are Not Preferentially Infected by HIV Type 1 Subtypes A and D in Vivo. *AIDS Research and Human Retroviruses*. 2012;28(9):919-23.
188. McNamara, L.A., Onafuwa-Nuga, A., Sebastian, N.T., Riddell, J.t., Bixby, D., Collins, K.L. CD133+ hematopoietic progenitor cells harbor HIV genomes in a subset of optimally treated people with long-term viral suppression. *J Infect Dis*. 2013;207(12):1807-16.
189. Nixon, C.C., Vatakis, D.N., Reichelderfer, S.N., Dixit, D., Kim, S.G., Uittenbogaart, C.H., et al. HIV-1 infection of hematopoietic progenitor cells in vivo in humanized mice. *Blood*. 2013;122(13):2195-204.
190. Bordoni, V., Bibas, M., Abbate, I., Viola, D., Rozera, G., Agrati, C., et al. Bone marrow CD34+ progenitor cells may harbour HIV-DNA even in successfully treated patients. *Clinical Microbiology and Infection*. 2015;21(3):290.e5-.e8.
191. Griffin, D.O., Goff, S.P. HIV-1 Is Restricted prior to Integration of Viral DNA in Primary Cord-Derived Human CD34+ Cells. *J Virol*. 2015;89(15):8096-100.
192. Araínga, M., Su, H., Poluektova, L.Y., Gorantla, S., Gendelman, H.E. HIV-1 cellular and tissue replication patterns in infected humanized mice. *Scientific Reports*. 2016;6:23513.
193. Sebastian, N.T., Zaikos, T.D., Terry, V., Taschuk, F., McNamara, L.A., Onafuwa-Nuga, A., et al. CD4 is expressed on a heterogeneous subset of hematopoietic progenitors, which persistently harbor CXCR4 and CCR5-tropic HIV proviral genomes in vivo. *PLOS Pathogens*. 2017;13(7):e1006509.
194. Zaikos, T.D., Terry, V.H., Sebastian Kettinger, N.T., Lubow, J., Painter, M.M., Virgilio, M.C., et al. Hematopoietic Stem and Progenitor Cells Are a Distinct HIV Reservoir that Contributes to Persistent Viremia in Suppressed Patients. *Cell Rep*. 2018;25(13):3759-73.e9.

Chapter 3 Human immunodeficiency virus detection, quantitation, and infectivity

3.1 Introduction

The HIV virus is a small particle¹ (Figure 3.1) which spends the bulk of its lifecycle inside a host cell² (Figure 2.5). Detecting HIV is important for research and clinical purposes and can be achieved by direct or indirect testing methods. Direct testing assays target viral proteins, viral protein-encoding mRNA transcripts³, and ssRNA/dsDNA forms of the viral genome⁴, where indirect testing targets anti-HIV antibodies⁵. HIV-reporter cell lines can also be used to detect HIV⁶⁻⁸. Reporter cell lines, predominantly used in the research setting, are transgenic immortalised cells which display virus-specific, measurable responses to the presence of HIV. The ability to reliably detect and quantify virus is not only paramount for experiment standardisation, but also an important endpoint in research studies⁹.

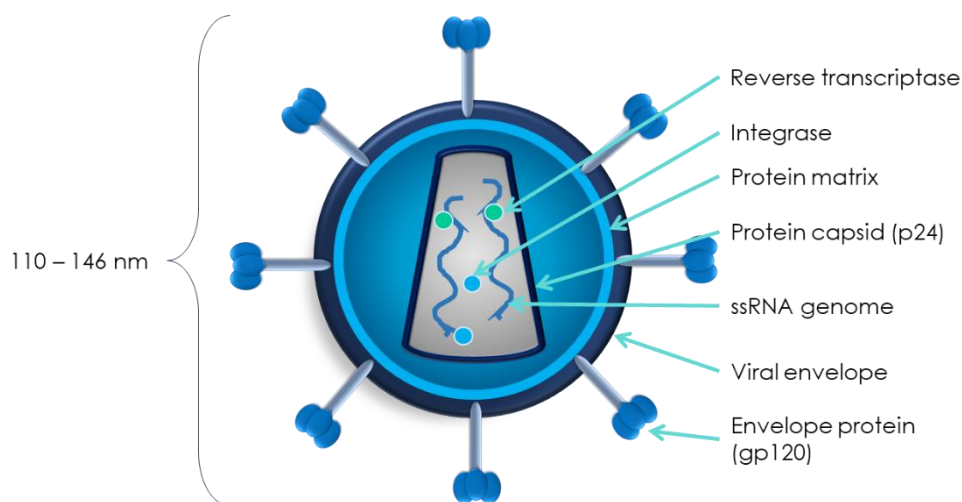


Figure 3.1: An HIV virus particle, adapted from literature^{1, 2, 10}, indicating the size range of HIV particles, and the location of various viral proteins and nucleic acids which can be used to detect HIV.

3.1.1 Viral genome detection

3.1.1.1 Background

Nucleic acids make up the genomes of all entities capable of self-maintenance, growth, and adaptation. These nucleic acids are called DNA or RNA depending on the type of sugar linking the nitrogenous base to the phosphodiester backbone¹¹. Nitrogenous bases, namely, adenine (A), cytosine (C), guanine (G), and thymine (T; in DNA)/uracil (U; in RNA), comprise nucleic acids¹². Each base is bound to a ribose sugar which may contain either an alcohol group (ribose) or a hydrogen in its place (deoxyribose) to form a nucleotide. Nucleotides are bound to each other through a phosphodiester bond linking the 5'-phosphate group of one nucleotide to the 3'-hydroxyl (alcohol) group of another. The phosphodiester bonds occur in a polar fashion, resulting in a 5'-end and 3'-end of a string of nucleotides¹³.

Base-pairing refers to hydrogen bonding between single strands (ss) of complementary nucleotides (A-T/A-U, and G-C) to form a double-stranded (ds) antiparallel nucleic acid molecule¹¹. This ds-nucleic acid molecule is twisted into the characteristic helical shape caused by the interplay of torsion and tension in the phosphodiester backbone and hydrogen bonds between base pairs (bp)¹⁴.

3.1.1.1.1 Nucleic acid polymerisation

Nucleic acid polymerisation is important in cell replication, where the genome is duplicated and split between two daughter cells¹⁵. Nucleic acid polymerisation also features in genome translations from RNA to DNA genomes such as reverse transcription of the HIV genome from ssRNA to dsDNA. Polymerase enzymes synthesise nucleic acid polymers by sequestering complementary deoxyribonucleic acid triphosphates (dNTPs) from solution, guided by a DNA template¹⁶. DNA polymerases synthesise new dsDNA from a ssDNA template (cell division), while RNA polymerases synthesise messenger RNA (mRNA) transcripts from a ssDNA template (transcription)¹⁷. Nucleic acid polymerisation for the purposes of transcription and replication is tightly regulated by genome architecture and molecular activation or suppression of transcription or replication¹⁷, but the enzymatic process is reasonably simple.

3.1.1.2 Detecting human immunodeficiency virus nucleic acids

Replication polymerisation is only performed by DNA polymerases requiring a dsDNA template, RNA to be amplified must first be converted to DNA before it can be amplified. Conversion from RNA to DNA is facilitated by reverse transcriptase enzymes, which reverse transcribe an RNA template to complementary DNA (cDNA). The polymerase chain reaction (PCR), involves the amplification of DNA by DNA polymerase enzymes in the presence of sufficient dNTPs and appropriate salt-containing buffers¹⁸. This amplification allows the detection of very small amounts of nucleic acids, either quantitatively (qPCR) or semi-quantitatively (PCR). Amplified products can be detected by the incorporation of fluorescent dyes¹⁹ or fluorescent dye-bound probes which bind to target sequences by base-pairing²⁰. Detection of fluorescence can either be achieved by laser/detector systems, or by exposure to ultraviolet (UV) light^{19, 20}.

The HIV genome can be detected at two stages of replication using PCR techniques, namely the ssRNA stage (free-floating virus), or the dsDNA stage (proviral genome inside infected cells) (Figure 2.5) by targeted nucleic acid amplification⁴.

3.1.2 Viral protein detection

3.1.2.1 Background

Ribosomes in the cell cytoplasm translate mRNA transcripts into proteins by incorporating the amino acids encoded by mRNA into a peptide²¹. Peptides are folded into functional proteins using amino acid-sequence specific cues to form active sites and functional domains responsible for the unique activity of each protein²¹. Viral proteins are produced by host cell ribosomes after viral mRNA is transcribed from the proviral genome (Figure 2.5). Some viral proteins, such as the capsid protein p24, are transcribed in large amounts, while other proteins, such as the integrase, are transcribed in smaller amounts. The amount of protein synthesised depends on the (i) proximity of the viral gene to the LTR promoter, and (ii) relative abundance of the protein in the packaged virion²². Detection of viral proteins is therefore a measure of productive infection rather than latent infection, as proteins are being produced

for packaging into virions. Cells harbouring provirus and producing sufficient quantities of viral proteins to package and release virions are termed “productively infected”. Latent infection refers to cells harbouring provirus but not producing virus²³.

3.1.2.2 Detecting viral proteins

Viral proteins can be detected on the infected cell surface, inside infected cells, and in virus-containing suspensions such as blood or cell culture medium, using viral antigen-specific antibodies. These antibodies bind to viral proteins of interest and can be detected colorimetrically, using fluorescent tags, or enzymatically depending on the technique^{24, 25}.

3.1.3 Indirect detection

Indirect detection of virus relies on detecting a variable which responds to viral presence⁷. Indirect detection methods are often used in clinical settings for HIV diagnosis⁵ (anti-HIV antibody tests) and in research settings for a plethora of applications, including, but not limited to functional HIV titration, efficacy testing of anti-HIV therapies, and functional HIV tropism assessment.

Engineered, immortalised cell lines are valuable research tools when it comes to the indirect detection of virus. Cell lines are clonally expanded, immortalised cells often derived from primary cancer cells, which grow predictably and can be stably gene-edited to respond to certain stimuli. A few examples are HIV reporter cell lines which express GFP (GHOST (3) cell line⁸), luciferase (LuSIV cell line⁷), and β -galactosidase (TZM-bl cell line⁶), as detectable reporter proteins in the presence of HIV.

3.2 Ethical and safety considerations

3.2.1 Ethical approval

Research undertaken throughout this dissertation received approval from the Faculty of Health Sciences Research Ethics Committee under protocol number 207/2016.

Written informed consent was obtained at the time of donation from anonymous peripheral blood donors by qualified personnel of the Clinical Research Unit (CRU) at the University of Pretoria's Prinshof Campus. Peripheral blood units were provided by the CRU staff after being coded to preserve donor anonymity. Donors consented to donate 250 mL peripheral blood collected into a sterile 450 mL blood bag (Jiaxing Tianhe Pharmaceutical Co. Ltd, China) containing 60 mL citrate phosphate dextrose (CPD) as an anticoagulant. Only donors who declared to be HIV-negative were included in the study.

3.2.2 Safety considerations

All HIV experiments described in this dissertation, with the exception of transformation and culturing of bacteria and uninfected cells (Chapter 4 *Human immunodeficiency virus* production), were performed under strict bio-safety level (BSL) 2+ conditions in a self-contained BSL2+ facility. All HIV-contaminated waste was decontaminated in 1% Virkon™S (Lanxess, Germany) as recommended by manufacturers and exposed to ultraviolet light for 15 min before being discarded in liquid biohazardous waste containers.

The BSL2+ Operations and Safety Manual and associated standard operating procedures (SOPs) established and written during the completion of work described in this dissertation are attached in Appendix I *BSL2+ Operations and Safety Manual*.

3.3 Donor testing

Although HIV-negative donors (self reported) were included in the study, the Ethics Committee, Faculty of Health Sciences, University of Pretoria requested confirmation of HIV status prior to use of the cells in experiments. Donor samples were tested for HIV using the GeneXpert® GX-I (Cepheid, USA) instrument platform. The GeneXpert® GX-I is a closed-system making use of self-contained reagent cartridges loaded with the appropriate test material. HIV-1 Qual cartridges are validated for whole blood samples or rehydrated dry blood spots. A cartridge consists of separate compartments containing reagents for (i) internal quality controls (QC), (ii) sample amplification, (iii) detection of amplified products.

3.3.1 Principles

The GeneXpert® GX-I is a closed automated system that is able to detect the presence of HIV-1 nucleic acid in blood samples, with a limit of detection of approximately 203 copies of viral nucleic acid per millilitre whole blood. The system detects both free-floating HIV (ssRNA genomes) and HIV provirus inside infected cells using fluorescent dyes incorporated during HIV-specific PCR, which are excited by in-built lasers and detector systems. This microfluidic test allows small volumes of sample to be tested using small amounts of reagents compacted in the form of dry beads. Dry reagent beads in different chambers of the cartridge are rehydrated by sample moving through these chambers as the test is being performed.

3.3.2 Test and quality control

3.3.2.1 Sample preparation

HIV-1 Qual cartridges were loaded by dispensing 700 µL loading buffer (supplied with the cartridges) into the loading chamber, and carefully layering 100 µL whole blood sample on top of the buffer as per manufacturer's instructions. Bubbles in the loading chamber were removed after adding each component to the loading chamber using a sterile 10 µL pipette tip, as bubbles disrupt the fluidics and result in QC step failures. Once loaded, the cartridge was placed inside the docking bay of the GeneXpert® GX-I instrument and the test was run.

3.3.2.2 Quality control steps

Several QC steps are built into the The GeneXpert® GX-I platform, and are performed with each cartridge (Table 3.1). Failure at any of the QC steps is indicated in the test report generated for each cartridge run, and results in an invalid test result. Three QC parameters are measured over the course of the test: sample volume adequacy, probe check control, and the sample processing control which contains the positive reaction control ²⁶.

Table 3.1: GeneXpert in-built QC steps, what they control for, and the reasons for failure, measured with each test run.

QC step	Control measure	Reason(s) for failure
Sampe volume adequacy	Ensures that the sample volume is adequate. Inadequate sample volume introduces bubbles into the microfluidics system of the cartridge and compromises the test.	Inadequate volume.
Probe check control	Internal control to ensure that the probe and detectors on the instrument, and the reagents in the cartridge are functional.	Reagent bead rehydration inadequate. Nucleic acid detection dyes not stable. Reaction microtube not filling. Probe integrity compromised. Fluorescence detectors on instrument not working.
Sample processing control	Built-in positive control in the form of Armoured RNA® dry beads (HIV-RNA packaged in bacteriophage coat proteins) ²⁷ . Verifies lysis, successful PCR reagent rehydration, RT-PCR and fluorescence detection in sample.	Positive control compromised and does not amplify.

3.4 P24 Enzyme-linked immunosorbent assay

3.4.1 Introduction

Absolute titre and productive infection were measured with p24 enzyme-linked immunosorbent assay (ELISA) using the Lenti-X™ Rapid Titre p24 ELISA kit (ClonTech, USA). The p24 protein is a lentiviral capsid protein used as a proxy for virion assembly and is often used as a marker of productive infection. This is because HIV must have achieved entry, reverse transcription, nuclear presence, transcription, translation, and polyprotein processing for p24 to be detected. According to the Lenti-X™ Rapid Titre p24 ELISA kit manufacturers, 1 ng of p24 protein is stoichiometrically equivalent to approximately 1.25×10^7 lentiviral particles in suspension. This correlation allows the number of viral particles in a suspension to be estimated using a standard curve.

P24 ELISAs were performed during optimisation and modification of HIV propagation according to standard protocols, and were performed according to the manufacturer's instructions.

3.4.2 Principles

In a sandwich ELISA such as the Lenti-X Rapid Titre p24 ELISA kit, p24 is quantified based on p24-specific antibodies recognising and binding p24 antigen, followed by a colorimetric assay quantifying secondary-antibody binding. The bottoms of the Lenti-X™ plate wells are pre-coated with anti-p24 primary antibody (capture antibody) which binds p24 protein present in lysed cell or virus suspensions. Unbound proteins and cell/virus lysates are removed by washing. A secondary biotin-conjugated anti-p24 antibody (detection antibody) is added and incubated to allow for binding, after which unbound detection antibody is removed by washing. A streptavidin-horse radish peroxidase (HRP) conjugate is then added, and binds with high specificity to the biotin conjugate on the p24-bound detection antibody (Figure 3.2).

The HRP substrate, 3,3',5,5'-tetramethylbenzidine (TMB; colourless) is added, in excess, resulting in the HRP-catalysed reduction of hydrogen peroxide to water. This reaction forms

3,3',5,5'-tetramethylbenzidine diimine (blue-green). The reaction is time-sensitive and is halted by the addition of a "stop solution" containing sulphuric acid. The "stop solution" stops the reaction and results in a colour change, converting the blue-green colour into yellow. The optical density (OD) of the yellow reaction product is analysed by spectrophotometry at 450 nm. The p24 concentration in the test sample is estimated using a standard curve prepared with known concentrations of p24 protein.

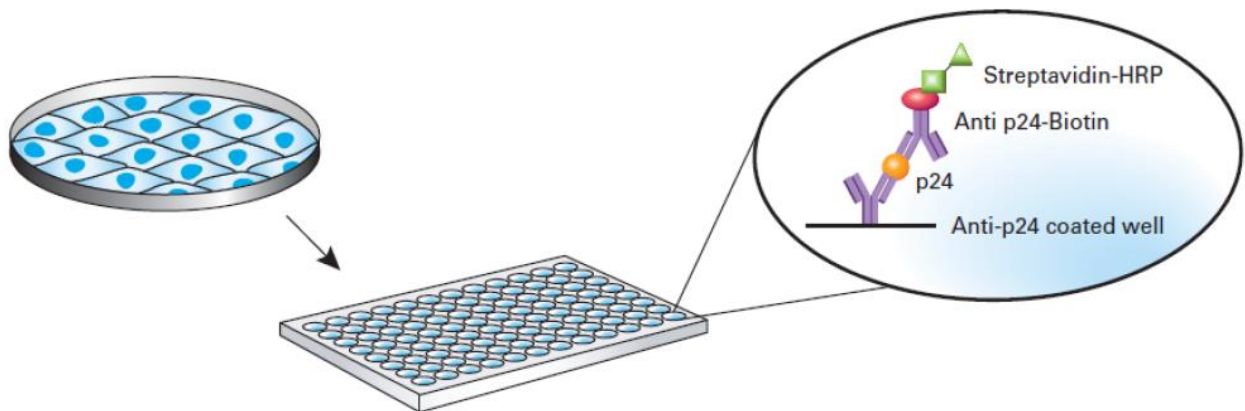


Figure 3.2: Schematic representation of the Lenti-X™ Rapid Titre p24 ELISA kit; image available from the Lenti-X™ Rapid Titre p24 ELISA kit user manual.

3.4.3 Methods

3.4.3.1.1 Enzyme-linked immunosorbent assay protocol

The Lenti-X™ Rapid Titre p24 ELISA kit plate consists of convenient, separable 8-well strips, which were used individually as required. Before each use, 20 x wash buffer provided with the kit was diluted to 1 x wash buffer in distilled water. Positive p24 controls were prepared by diluting the p24 protein standard provided with the kit to 12.5 pg/mL (low concentration control) and or 200 pg/mL (high concentration control) respectively, in Roswell Park Memorial Institute-1640 medium (RPMI; ThermoFisher Scientific, USA). A standard 8-well strip layout is indicated in Figure 3.3, showing the position of the blank, known concentration p24

standards, and samples. Undiluted samples and 1/10 dilutions of samples were subjected to p24 ELISA to ensure that p24 could be detected. Undiluted samples were assayed to make sure that low-levels of p24 could be detected, and 1/10 dilutions (in RPMI) were used to avoid insufficient conversion of the TMB reaction product (blue-green) to the yellow product (partially seen in Figure 3.3 sample C) in wells with high concentrations of p24.

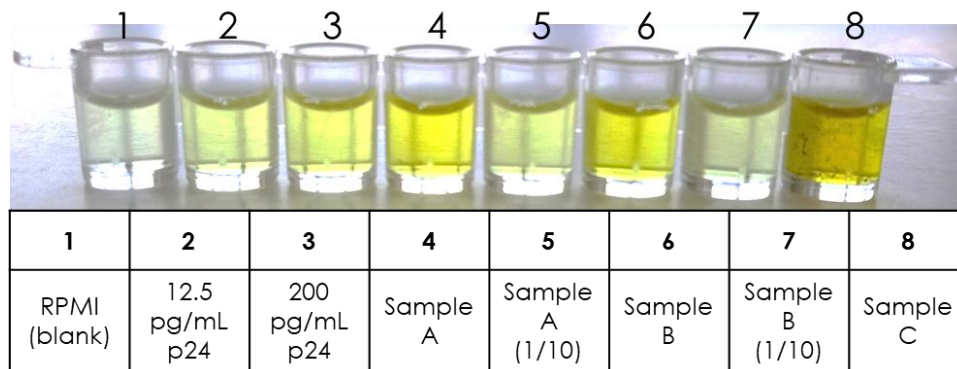


Figure 3.3: Typical sample layout in an 8-well strip of Lenti-X™ Rapid Titre p24 ELISA kits.

Two hundred microlitres (200 μ L) of sample, followed by 20 μ L of lysis buffer, was added to each well. Lysed cells or virus particles released p24 protein, which then bound to anti-p24 capture antibodies by incubating the 8-well strips at 37°C for 60 min. After incubation, cell lysates were removed by tipping the 8-well strip over onto paper towel. The wells were washed six times by adding 200 μ L per well wash buffer and then tipping the buffer out. Capture antibody-bound p24 was tagged with detection antibody by adding 100 μ L biotinylated anti-p24 detection antibody per well, and incubating the 8-well strip at 37°C for 60 min. Unbound detection antibody was removed by tipping the wells once again, followed by washing six times with 200 μ L wash buffer per well as described above. Streptavidin-HRP conjugate (100 μ L per well) was added to each well and incubated at room temperature for 30 min. After incubation, wells were again emptied and washed six times as described above.

Colorimetric detection of p24 was initiated by adding 100 μ L TMB substrate to each well, and incubating the wells in the dark for 20 min to allow substrate binding and prevent light-

mediated degradation of the reaction product (3,3',5,5'-tetramethylbenzidine diimine; blue-green). After 20 min incubation, the reaction was stopped by adding 100 µL stop solution to each well. The OD of the end products were measured at 450 nm on a PowerWaveX spectrophotometer (Bio-Tek, USA).

3.4.3.1.2 Standard curve preparation

A standard curve for p24 was established for each ELISA kit received, using serial dilutions of the p24 protein standard provided with the kit. Serial dilutions were prepared in RPMI. The p24 ELISA was performed as described in 3.4.3.1.1 *Enzyme-linked immunosorbent assay* protocol, and the ODs measured by spectrophotometry at 450 nm. OD values obtained were used to set up the p24 standard curve shown in Table 3.2 and Figure 3.4.

Table 3.2: An example of results obtained during setup of a standard curve for the Lenti-X™ Rapid Titre p24 ELISA (kit lot number KCL05161; plate lot number P1094).

Well	p24 (pg/mL)	OD	Normalised
1	0	0.17	0
2	12.5	0.244	0.074
3	25	0.292	0.122
4	50	0.454	0.284
5	100	0.649	0.479
6	200	1.208	1.038
7	400	2.263	2.093
8	600	3.026	2.856

p24 Standard curve

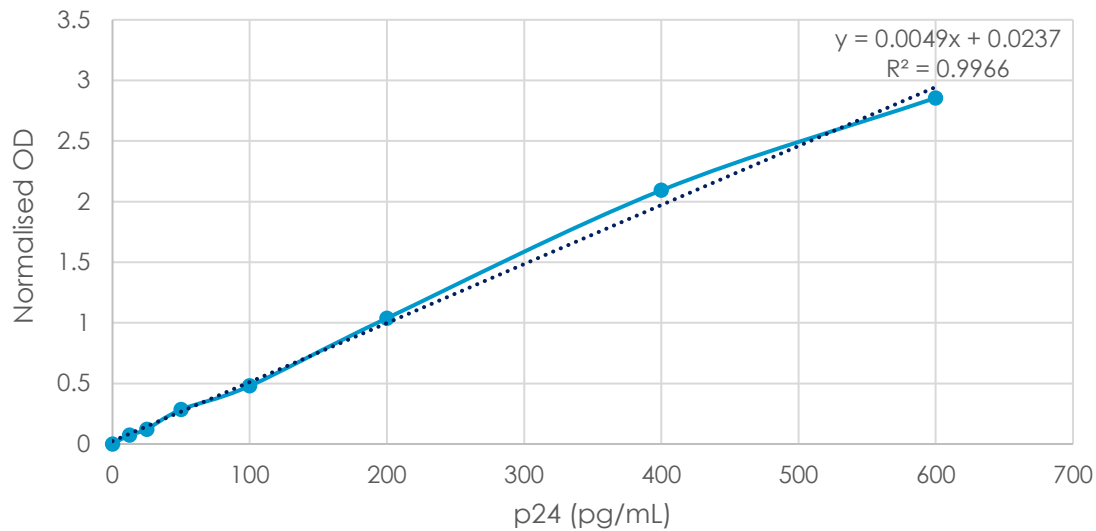


Figure 3.4: p24 Standard curve generated using the Lenti-X™ Rapid Titre p24 ELISA kit (lot number KCL05161; plate lot number P1094). The equation of the line of best fit (dotted line) used to estimate p24 concentrations relative to the standard curve is shown on the graph.

3.4.4 Data processing

A report was prepared for each p24 ELISA performed, containing qualitative data (photograph of 8-well strip), absorbance values obtained (ODs), and normalised absorbance values. Absorbance values were normalised to 0 by subtracting the blank OD from the measured OD. Normalised OD values were used to estimate the absolute amount of p24 (and thus absolute HIV titre) using the standard curve (Figure 3.4).

According to the manufacturer's instructions, valid ELISA results require OD readouts of ≤ 0.10 for the blank (negative control), and ≥ 0.60 for the 100 pg/mL p24 standard. However, these values were validated using Dulbecco's modified Eagle medium (DMEM; ThermoFisher Scientific, USA) as a diluent. In this setting, p24 ELISAs were performed on HIV produced in cells cultured in RPMI. Therefore, the blank cut-off value were adjusted to $0.15 \leq x \leq 0.18$, based on the reproducibility of successive blank readings obtained using RPMI instead of DMEM as the blank.

3.5 Nucleic acid detection

3.5.1 Introduction

3.5.1.1 Background

PCR, first described for target DNA amplification in 1985 by Mullis and colleagues¹⁸, is summarised in Figure 3.5. Today, various forms of PCR principles are routinely used for the detection and sequencing of nucleic acid targets. The technique exploits the DNA replication enzyme DNA polymerase to replicate specific segments of DNA by the binding of sequence-specific DNA primers. The principles of nucleic acid polymerisation explained in 3.1.1.1.1 *Nucleic acid polymerisation* apply to the PCR technique. Reactions to amplify DNA of interest contain heat-stable DNA polymerase, sufficient quantities of pure DNA template, an abundance of dNTPs and a salt-balanced buffer containing divalent chloride salts like MgCl₂ which enhance DNA polymerase activity²⁸.

Short ssDNA oligonucleotides, known as primers, are required to give the DNA polymerase starting points for DNA synthesis. Forward (5' - 3') and reverse (3' - 5') target-sequence-specific primers constitute the 5' and 3' boundaries of the region of interest. The region of interest is amplified by DNA polymerase on both the sense (5' - 3') and antisense (3' - 5') DNA strands. These ssDNA amplicons hybridise by complementation to form dsDNA amplicons of interest. PCR is achieved by thermocycling, which rapidly brings the reaction mixture to specific temperatures to achieve annealing of primers and denaturation of dsDNA complexes in cycles of amplification and re-priming (Figure 3.5). In this way, a specific length of DNA is exponentially amplified for downstream applications included specific target detection (such as HIV), sequencing, transcript quantification, or cloning.

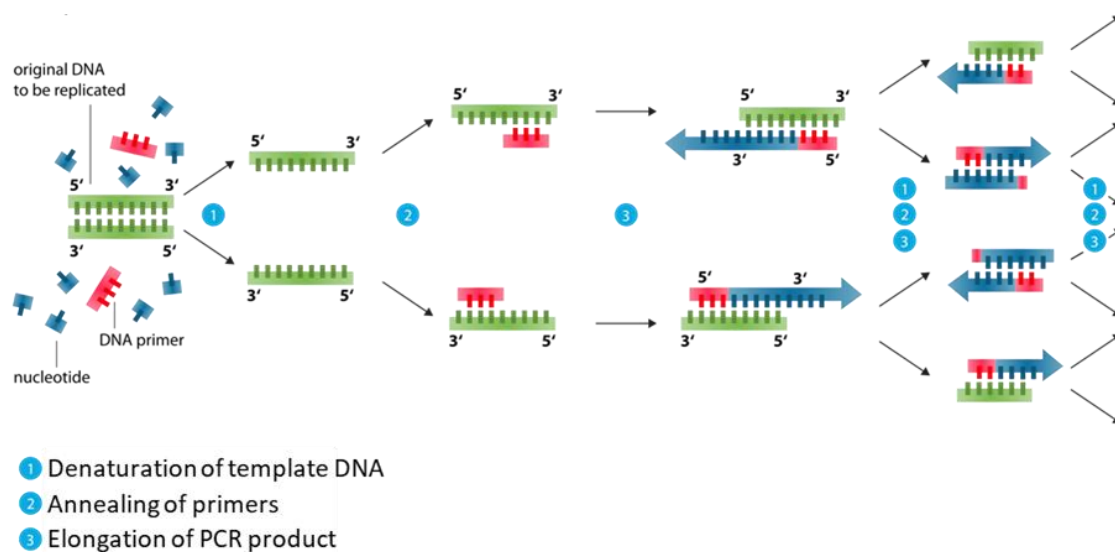


Figure 3.5: A schematic representation of the principles of PCR, used with permission²⁹. Cycles of denaturing DNA templates followed by primer annealing and polymerisation (elongation) of target DNA regions selected by primers is shown.

3.5.1.2 Amplicon analysis

To determine whether amplification has taken place, reaction products are subject to agarose gel electrophoresis, where an electric current is applied to PCR products loaded in wells cast into an agarose gel (Figure 3.6). This causes the negatively charged DNA to migrate through pores in the gel matrix towards the positive terminal¹⁹. This allows separation of linear DNA fragments by length, as longer fragments take longer to migrate through the gel matrix pores than shorter fragments. Resolution of amplicons of different sizes in the gel allows estimation of fragment size relative to known-size fragments in commercial DNA ladders¹⁹.

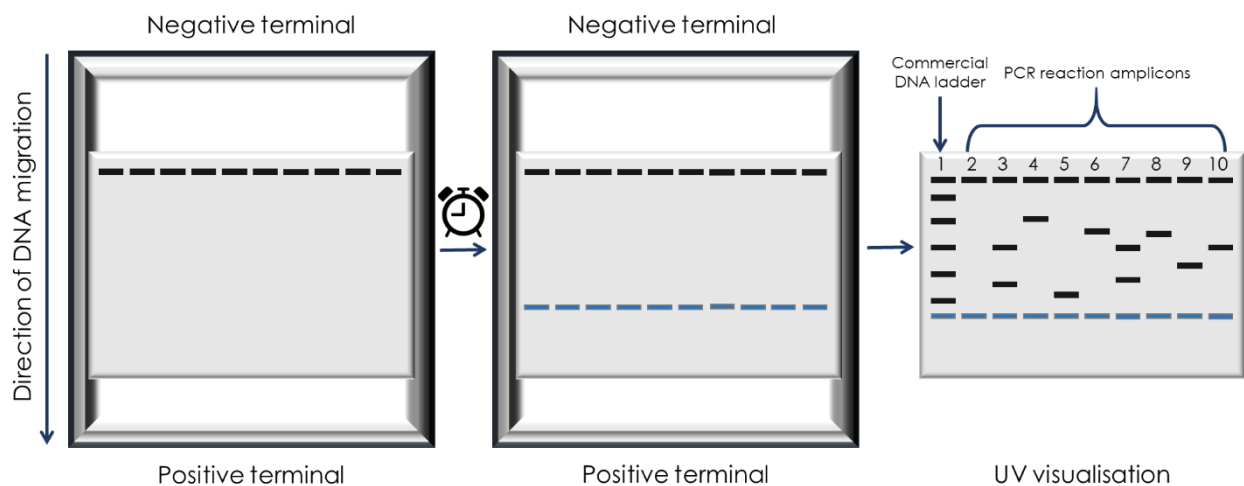


Figure 3.6: PCR amplicon analysis by agarose gel electrophoresis. The direction of DNA migration is from the negative terminal to the positive terminal, as a result of the applied electric current. Over time, colorimetric tracking (blue band near positive terminal) indicates that the DNA amplicons have migrated through the length of the gel and will likely be resolved. Visualisation by UV light shows DNA amplicons stained by fluorescent dyes on the gel not visible with the naked eye.

3.5.2 Primer design

In order to perform PCR, oligonucleotide primers specific to the region of interest must be designed *in silico* and validated by showing that PCR performed using those primers amplifies only the region of interest with high specificity. Primers targeting various regions of the HIV genome were designed using CLC Main Workbench 7 v7.9.1 (QIAGEN, Germany). Primer sequences were analysed for specificity and suitability using the National Centre for Biotechnology Information (NCBI) Primer-BLAST³⁰, OligoCalc version 3.27³¹, and the Integrated DNA Technologies (IDT) OligoAnalyzer online tools.

3.5.2.1 Important factors in primer design

Priming, the binding of primers to DNA in a sequence-specific manner, requires primers to be long enough to confer target sequence specificity, but short enough to not require extreme annealing temperatures to bind to target DNA. Primer pairs should have (i) similar melting and annealing temperatures, (ii) high specificity at the elongation end (3'-end), and (iii)

limited ability to form secondary structures³². Primer nucleotide composition influences each of the aforementioned criteria, and is important to consider during primer design.

3.5.2.1.1 Melting temperatures

Melting temperature (T_M) refers to the temperature at which hydrogen bonds between complementary nucleotides in dsDNA are dissociated³³. T_M therefore depends on factors which increase the number of hydrogen bonds in a fragment of dsDNA, namely GC content, and the length of the fragment³³. This is because base-pairing between G and C forms three hydrogen bonds, which are more stable than the two hydrogen bonds formed by A-T base-pairing. Optimal PCR primers have 40-60% GC content^{32, 34}. Priming fidelity in a PCR reaction is linked to T_M in that the annealing temperature in the thermocycling process is selected based on the temperature which disrupts interactions between non-complementary bases, but not more stable interactions between complementary bases³⁴. To maintain priming fidelity, T_M for each primer in a pair should be similar. This avoids potential non-specific priming for the primer with the highest T_M .

3.5.2.1.2 Secondary structures

Secondary structures are formed by ssDNA primers when self-complementation or complementation with other primers occurs. Self-complementation (hairpin or dimerisation; Figure 3.7) or complementarity between primers in a primer pair prevents primers from binding to the target sequence, unless the secondary structure has a lower T_M than the primer-target complex³⁴. Hairpin secondary structures are formed by primers binding partially to themselves, and dimerisation occurs when primers of the same sequence can bind to each other. Primers which can form secondary structures with overhangs should be avoided as DNA polymerase cannot distinguish between primer secondary structures and primer-target complexes, resulting in amplification of secondary structures (Figure 3.7B and D). Polymerisation of secondary structures uses up nitrogenous bases in the form of dNTPs in the PCR reaction and produces short non-target amplicons which can limit the efficacy of target amplification. In order to increase specificity and prevent mis-priming, it is recommended that the last three to five nucleotides on the 3'-end contain a GC clamp, which

is a combination of two to three nucleotides in a row being G or C³². This helps to prevent non-target amplification which, as explained earlier, contributes to reaction exhaustion and sub-optimal amplification.

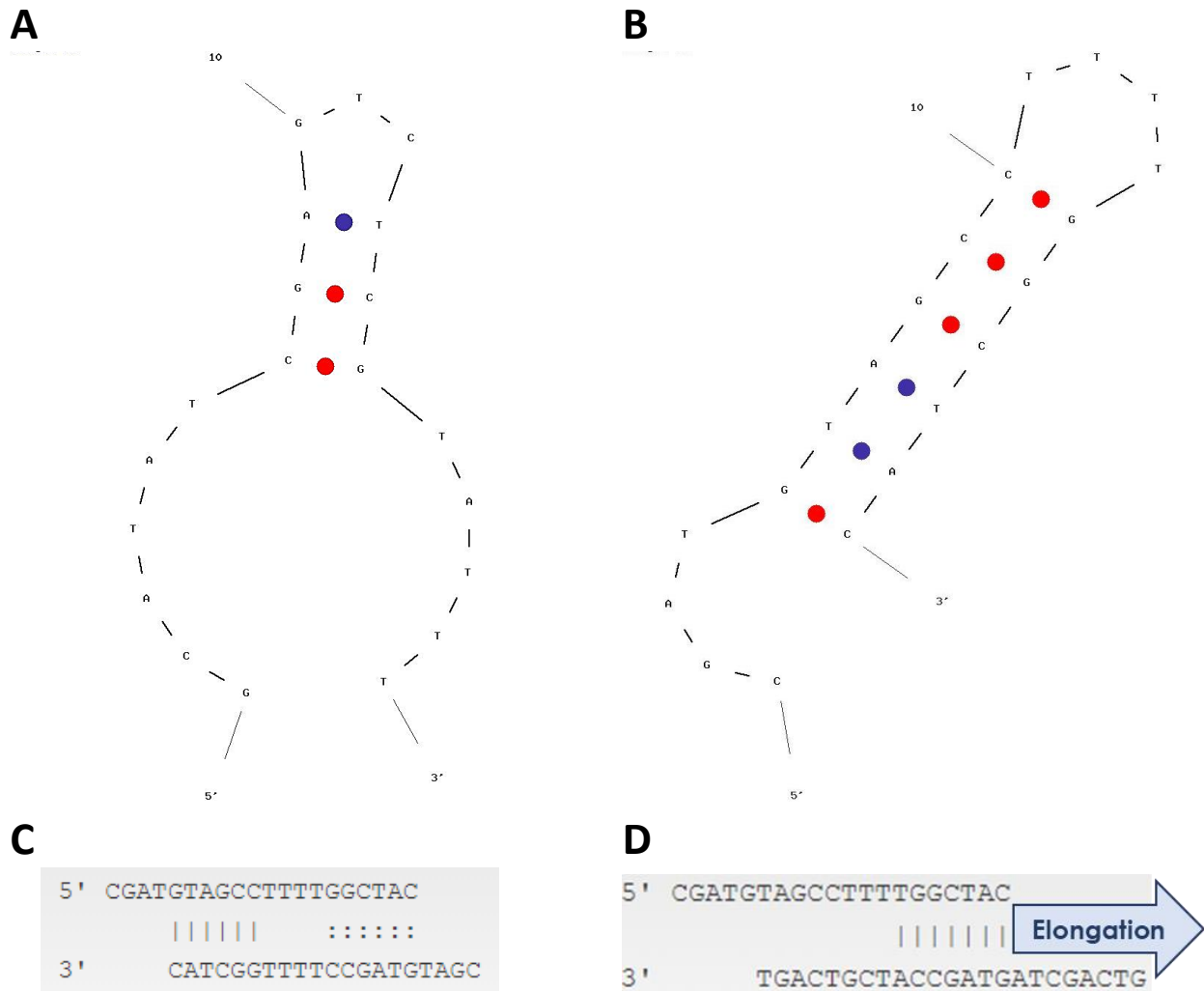


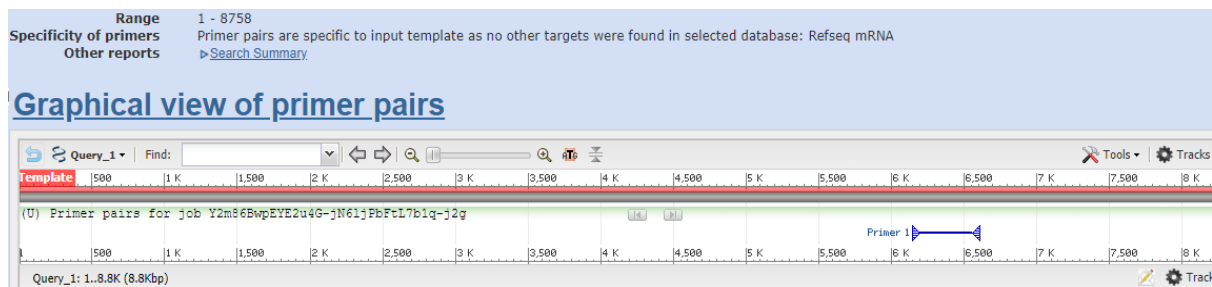
Figure 3.7: Examples of primer secondary structures, generated using the IDT OligoAnalyzer online tool. (A) Hairpin structure which does not result in elongation but prevents primer from binding to target. (B) Hairpin structure with a 3'-overhang which will result in elongation. (C) Homodimer between primers of the same sequence with a 3'-overhang which could result in elongation. (D) Heterodimer between two primers in a primer pair with a 3'-overhang which will result in elongation.

3.5.2.2 *In silico* primer design

Primers were manually designed for HIV-1C isolates by generating multiple sequence alignments of HIV-1 genes and genomes in CLC Main Workbench. HIV-1 gene and genome sequences were obtained from the Los Alamos National Laboratory HIV Sequence Database

(available from <https://www.hiv.lanl.gov/content/sequence/HIV/mainpage.html>). Curation of search results was performed by selecting one sequence per patient derived from full-length or near full-length sequence deposits. Primers were first designed on the consensus sequence exported from the alignment, and then queried on the alignment. Primers which matched at least 90% of aligned HIV-1 sequences were evaluated for secondary structure formation, T_M , and specificity using the online tools mentioned previously in 3.5.2 *Primer design*.

Target specificity was determined using the Primer-BLAST tool, which queries the primer pair against a user-selected database (in this case, RefSeq mRNA) to determine off-target annealing. Figure 3.8 shows the Primer-BLAST output of a primer pair designed to target the V3-loop of the HIV-1C gp120 protein complex responsible for conferring HIV tropism. The T_M difference between the primers in the pair was within three degrees of each other, and the GC content was similar, as is desirable. The primer pair was predicted to be specific to the consensus HIV-1C consensus input sequence, with no off-target priming using the Refseq mRNA database as a reference.

A**B**

Detailed primer reports

Primer pair 1

	Sequence (5'→3')	Template strand	Length	Start	Stop	T _m	GC%	Self complementarity	Self 3' complementarity
Forward primer	GGACCATGCAATAATGTCAGC	Plus	21	6180	6200	57.64	47.62	4.00	2.00
Reverse primer	GTGTTGTAATTTCTAGTCCCC	Minus	22	6585	6564	56.42	45.45	4.00	1.00
Product length	406								

Figure 3.8: Example output of NCBI primer analysis (Primer-BLAST) using the full-length consensus sequence for HIV-1C generated in CLC Main Workbench for a primer pair designed to amplify a portion of the HIV-1C *Env* gene. (A) Specificity of primers to target relative to the Refseq mRNA database, and the location of the amplicon resulting from PCR using these primers is shown. (B) Primer details returned in the same primer analysis report, indicating the amplicon (product) length, and T_M, GC-content, and self-complementarity values of the primer pair. The values for self- and self-3'-complementarity correspond to the propensity for self-complementation. Lower values (≤3) are therefore preferred.

Primer design parameters, such as secondary structure formation, T_M, and specificity, are illustrated in Figure 3.9. OligoAnalyzer and OligoCalc both make use of the BLAST function (linked to the NCBI) to determine specificity. Secondary structure was analysed primarily in OligoAnalyzer and OligoCalc, as the Primer-BLAST tool output is not as detailed. OligoAnalyzer shows T_M for hairpins, which was useful in determining whether the secondary structure would impede primer binding during the annealing step in the thermocycling reaction.

A

Minimum base pairs required for single primer self-dimerization: 4.
Minimum base pairs required for a hairpin: 3.

Potential hairpin formation :

5' GGACCATGCAATAATGTCAGC 3'
5' GGACCATGCAATAATGTCAGC 3'

3' Complementarity:
None !

All potential self-annealing sites are marked in red (allowing 1 mis-match):





5' GGACCATGCAATAATGTCAGC 3'
3' CGACTGTAATAACGTACCAGG 5'

5' GGACCATGCAATAATGTCAGC 3'
3' CGACTGTAATAACGTACCAGG 5'

5' GGACCATGCAATAATGTCAGC 3'
3' CGACTGTAATAACGTACCAGG 5'

5' GGACCATGCAATAATGTCAGC 3'
3' CGACTGTAATAACGTACCAGG 5'

B

structure	Image	T _m (°C)
1		30.6
2		23.5
3		23.3
4		20.8

C

Physical Constants	Melting Temperature (T _M) Calculations
Length: <input type="text" value="21"/> Molecular Weight: <input type="text" value="6439.34"/> GC content: <input type="text" value="48%"/>	<u>1</u> <input type="text" value="52.4"/> °C (Basic)
1 ml of a sol'n with an Absorbance of <input type="text" value="1"/> at 260 nm	<u>2</u> <input type="text" value="59.5"/> °C (Salt Adjusted)
is <input type="text" value="4.25"/> microMolar <u>5</u> and contains <input type="text" value="27.4"/> micrograms.	<u>3</u> <input type="text" value="51.73"/> °C (Nearest Neighbor)
Thermodynamic Constants Conditions: 1 M NaCl at 25°C at pH 7.	
RlnK <input type="text" value="33.404"/> cal/(°K* ² mol)	deltaH <input type="text" value="166.2"/> Kcal/mol
deltaG <input type="text" value="25.8"/> Kcal/mol	deltaS <input type="text" value="436.8"/> cal/(°K* ² mol)
Deprecated Hairpin/self dimerization calculations	
<input type="text" value="4"/> (Minimum base pairs required for single primer self-dimerization)	<input type="button" value="Check Self-Complementarity"/>
<input type="text" value="3"/> (Minimum base pairs required for a hairpin)	

Figure 3.9: OligoAnalyzer and OligoCalc primer analysis tool outputs for the forward primer indicated in Figure 3.8B, as a supplement to Primer-BLAST analysis. Within-primer potential secondary structures best illustrated by the OligoAnalyzer tool (A), ranked from most likely to least likely. Potential self-annealing (B) and primer specifics (C) calculated by OligoCalc show similar results to both Primer-Blast and OligoAnalyzer outputs.

3.5.2.3 Primer design output

Primers designed and synthesised for validation purposes adhered to the suggested criteria previously discussed. Primers were 18-28 nucleotides, and PCR amplicon lengths ranged between 400 and 1000 bp. Self-complementarity on the 3'-end was negligible (≤ 4 on PrimerBLAST, and none on OligoCalc for the criteria shown in Figure 3.9). Hairpins returned by the OligoAnalyzer tool were expected to denature at temperatures at least 15°C lower than T_M calculated for the primer binding to its complementary target.

The primers selected for future experiments are shown in Table 3.3. Primers amplifying a portion of the gp10-encoding *env* gene responsible for conferring tropism (V3 loop) were included for possible sequencing applications to confirm the tropism of primary HIV-1C isolates. Primers spanning the LTR-*gag* region were included to detect the presence of HIV.

The reverse primer for the LTR-*gag* primer pair used for HIV detection was obtained from literature³⁵. The primer was originally used as a forward primer for a *gag-pol* primer pair, and was reverse-complemented to obtain the primer ts5'-Gag_R, which was modified at single bases to bind to HIV-1C isolate CM9 and HIV-1B molecular clone 89.6 (Table 3.3).

Table 3.3: Primer pairs and sequences for detecting HIV nucleic acids. Primers highlighted in grey indicate primers taken from or adapted from literature.

Primer name	Sequence (5' - 3')	HIV isolate specificity	T_A (°C)	Product size (bp)
V3_fwd2	GGACCATGCAATAATGTCAGC	CM9	58	406
V3_rvs1.2	GTGTTGTAATTTCTAGGTCCCC	CM9		
V3_fwd3	GGACCATGCCATAATGTCAGC	SW7	58	551
V3_rvs2	CCTACCCCCTGCCACATG	SW7		
LTR_fwd5	CCCTCAGATGCTGCATATAAGCAGC	Yu2; 89.6	58	978-988
ts5'Gag_R	TCTTTTAACATTTGCATGGCTGCTTG	Yu2; NL4-3; SW7		
LTR_fwd5 NL4-3	CCCTCAGATGCTACATATAAGCAGC	NL4-3		
ts5'Gag_R 89.6	TCTTTTAACATTTGCATGGCTGCCTG	89.6		
LTR_fwd6	CCCTCAGATGCTGCATATAAGCAGCTGC	CM9; SW7		
ts5'Gag_R CM9	TCCTTTAACATTTGCATGGCTGCTTG	CM9		

Primer validation and determination of annealing temperatures shown in Table 3.3 is described in 3.5.3 *Primer validation*.

3.5.3 Primer validation

3.5.3.1 Introduction

Primer validation was performed by PCR and gel electrophoresis. Proviral DNA was assayed by extracting DNA from HIV-exposed GHOST cells. The GHOST HIV-permissive cell line was cultured and infected with HIV as described in 3.6.6.2.2 *Infection*.

3.5.3.2 Primer synthesis

Primers were synthesised by Inqaba Biotec™ (Inqaba Biotechnical Industries, South Africa). Lyophilised primers were resuspended in the volume of molecular grade distilled water (QIAGEN, Germany) recommended by manufacturers to obtain a 100 µM stock solution. Working solutions of 10 µM were made for each primer with molecular grade water, which were used to set up PCR reactions. Primer working solutions were stored at -20°C.

3.5.3.3 Sample material preparation

CD4^{high} GHOST cells were resuscitated from liquid nitrogen at low passage and cultured in T75 flasks until confluence in complete DMEM supplemented with puromycin, hygromycin, and G418 as described in 3.6.2 *Cell culture and maintenance*. GHOST cells were enzymatically dissociated and seeded at 3×10^5 cells per well in a 6-well plate (Greiner Bio-One, Austria) and allowed to adhere overnight at 37°C, 5%CO₂. After overnight incubation, cells were infected with HIV CFS containing approximately 5×10^5 IU of the appropriate HIV isolate (indicated in Table 3.4), as determined by functional titration using the GHOST GFP assay. GHOST cells were exposed to approximately 5×10^5 IU of neat HIV CFS for 2 hr before topping up the medium to 2 mL complete DMEM. After 24 hr exposure to virus, the medium was aspirated from wells and replaced with 2 mL DMEM and incubated for another day. Exact virus to cell ratios were not considered here as the only requirement was the presence of infected cells. Cells were enzymatically dissociated as described in 3.6.2.2.1 *Enzymatic dissociation*.

3.5.3.4 DNA extraction and quantification

DNA extraction was performed according to QIAamp DNA Micro kit (QIAGEN, Germany) according to manufacturer's instructions.

3.5.3.4.1 QIAamp DNA micro kit reagent preparation

Before the first use, buffer AW1 and AW2 were reconstituted by the addition of 25 mL and 30 mL absolute ethanol (Sigma-Aldrich, USA) respectively. Lyophilized carrier RNA (cRNA) was dissolved in AE buffer to a final cRNA concentration of 1 µg/µL, and aliquoted for storage at -20°C until use. ATL and AL buffers may form precipitates over time. Therefore, precipitates were dissolved by heating the buffers to 70°C with agitation before each use. All reagents were inverted several times to mix before use.

3.5.3.4.2 DNA extraction procedure

Cells for DNA extraction were pelleted in 1.5 mL Safe-Lock microcentrifuge tubes (microcentrifuge tubes; Eppendorf, Germany) by centrifugation at 300 x g for 10 min and resuspended in 50 µL PBS. ATL buffer was added to each sample to a final volume of 100 µL. To lyse cell membranes and digest proteins which could influence optimal DNA extraction, 10 µL proteinase K and 100 µL AL buffer containing 0.1 µg/µL cRNA and guanidine thiocyanate were added to each sample. Samples were vortexed and incubated for 10 mins in a 56°C pre-heated water bath to allow for proteinase K digestion. To precipitate proteins, 50 µL absolute ethanol was added and samples were incubated for 3 min. Lysates and precipitated proteins were transferred to QIAamp MinElute columns in 2 mL collection tubes and centrifuged at 6000 x g for 1 min.

Flow-through containing buffer remnants and proteins was discarded. AW buffer (1500 µL) was applied to the silica membrane of the column and centrifuged for 1 min at 6000 x g to wash bound nucleic acids. The column was washed once more with 500 µL AW2 buffer. Column silica membranes were dried by centrifuging columns for 1 min at 14 000 x g in a new 2 mL collection tube. DNA was eluted by applying 20-50 µL nuclease-free water (supplied with the kit) to the membrane and incubating for 5 min, followed by centrifugation for 1 min at

14 000 x g. The eluate was placed back on the membrane for 1 min and centrifuged again for 1 min at 14 000 x g to increase DNA recovery from the membrane.

3.5.3.4.3 Nucleic acid quantification by NanoDrop®

DNA concentrations and purity analyses were determined by NanoDrop® ND-1000 (NanoDrop®; ThermoFisher Scientific, USA) spectrophotometry (Table 3.4). Absorbance is a measure of OD, defined as the amount of light of a given wavelength which is not transmitted through a liquid sample. Different types of molecules achieve maximal absorbance at unique wavelengths, where absorbed light can be related to the absolute amount of substance³⁶. Therefore, classes of molecules such as nucleic acids and proteins can be quantified in relation to contaminants by spectrophotometry. The maximal light absorbance of nucleic acids is achieved at 260 nm, proteins at 280 nm, and salts and small molecule contaminants at 230 nm³⁶. Ratios of light absorbance at these three wavelengths indicate the proportion of nucleic acids to protein (A_{260}/A_{280}), and nucleic acids to contaminating salts and small molecules (A_{260}/A_{230}), respectively. Both these measurements are used as indicators of DNA purity and consequently successful DNA extraction. Generally, A_{260}/A_{280} values of approximately 1.8 and A_{260}/A_{230} values approaching 2 are considered adequate for downstream applications such as PCR, although higher ratio values are better tolerated than lower ratio values. DNA extractions with A_{260}/A_{280} ratios ≥ 1.8 and A_{260}/A_{230} ratios ≥ 2 were accepted for PCR purposes. DNA extraction concentrations and purity values are indicated in (Table 3.4).

Table 3.4: Concentrations, protein purity (A_{260}/A_{280} ratio), and salt purity (A_{260}/A_{230} ratio) of HIV-exposed GHOST DNA extracted for HIV-1 primer validations.

Sample ID	DNA concentration (ng/ μ L)	A_{260}/A_{280} ratio	A_{260}/A_{230} ratio
HIV exposed Ghost DNA CM9-290118	19.08	2.25	2.02
HIV exposed Ghost DNA SW7-010818	55.97	2.09	2.18
HIV exposed Ghost DNA Yu2-041217	70.31	2.10	2.16
HIV exposed Ghost DNA 89.6-041217	115.62	2.09	2.14
HIV exposed Ghost DNA NL4-3-041217	102.14	2.05	2.21

3.5.3.5 Polymerase chain reaction

3.5.3.5.1 Reaction preparation

PCR reactions to detect HIV proviral DNA were set up in thin-walled Corning® Thermowell GOLD 0.2 mL PCR tubes (PCR tubes; Corning Inc., USA) on ice. The 2 x Kapa Taq ReadyMix PCR kit (Kapa RM; Kapa Biosystems, USA) PCR reagent system was used. The *Thermus aquaticus* (Taq)-derived heat-stable DNA polymerase is provided already optimally buffered with $MgCl_2$ and containing dNTPs. In a final volume of 25 μ L, 12.5 μ L Kapa RM was supplemented with 0.75 μ L of each relevant forward and reverse primer, 50 ng DNA template of interest (variable volumes), and molecular grade water (variable volumes). Isolate-specific primers for both LTR-*gag* and V3 primer pairs (Table 3.3) were used to set up reactions for each DNA extract (Table 3.4).

3.5.3.5.2 Thermocycling specifications

Annealing temperature optimisation was simultaneously performed by preparing reaction cocktails for PCR in multiple thermocyclers along a gradient of annealing temperatures (Figure 3.10, blue). Annealing temperatures ranged between 54°C to 64.5°C increasing in 1.5°C increments. Thermocycling was performed using two GeneAmp™ PCR System 9700 machines (GeneAmp™; ThermoFisher Scientific, USA). Amplification of target DNA usually occurs between twenty five to thirty cycles of denaturation, primer annealing, and elongation (Figure 3.10) depending on the amount of target template expected¹⁶. As the DNA template of interest (HIV proviral genome) was only present in infected cells and the DNA extract is from a mixture of infected and uninfected cells, a higher number of denaturation/primer annealing/elongation cycles was preferred.

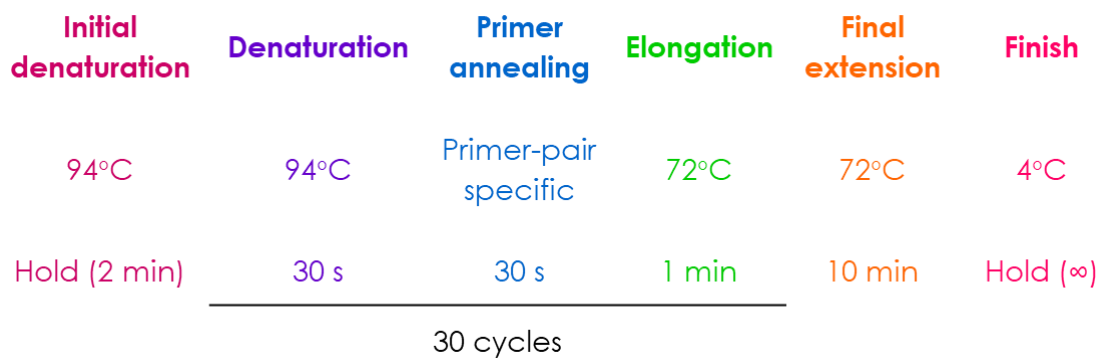


Figure 3.10: Thermocycling conditions and their respective descriptions applied during PCR reactions.

3.5.3.6 Agarose gel electrophoresis

3.5.3.6.1 Gel preparation

To prepare the agarose gel, 1% mass-by-volume molecular grade agarose LE (agarose; Benchmark Scientific Inc., USA) was dissolved in 1 x Tris-acetate-ethylenediaminetetraacetic acid (EDTA) (TAE) buffer. TAE (1 x) was prepared from UltraPure™ 10 x TAE buffer

(ThermoFisher Scientific, USA) by diluting with distilled water. Agarose was dissolved in TAE buffer by heating and swirling until completely clear and homogenous. To visualise DNA, ethidium bromide (EtBr; Promega, USA) was diluted 1:20 000 from 10 mg/mL stock in the agarose gel immediately prior to casting. Gels were cast in a casting tray containing well-moulds. EtBr is a fluorescent small molecular DNA intercalator which binds between bp of dsDNA which can be visualised under UV light. As the DNA migrates through pores of the agarose gel matrix, EtBr cast in the gel matrix binds to the DNA¹⁹. Once set, the opaque gel was placed in a gel electrophoresis tank filled with 1 x TAE and samples were immediately loaded in the wells.

3.5.3.6.2 Sample preparation for gel loading

To prepare samples for agarose gel electrophoresis, 10 x BlueJuice™ Gel Loading Buffer (BlueJuice™; ThermoFisher Scientific, USA) was diluted to 1 x concentration by adding to PCR reactions. Each well of the agarose gel was loaded with 15 µL BlueJuice™/PCR reaction (sample). In addition to facilitating colorimetric tracking, BlueJuice™ contains glycerol which makes DNA heavy enough to sink to the bottom of the wells while loading. This prevents sample DNA from floating out of the wells once loaded¹⁹. FastRuler™ Low-range DNA ladder (FastRuler™ LR; ThermoFisher Scientific, USA) was loaded in the first lane of each set of wells for amplicon size estimation.

3.5.3.6.3 Electrophoresis

Agarose gel electrophoresis was performed by applying a constant voltage of 90 V for 60 min, to the gel tank (Figure 3.6) causing DNA to migrate through the gel from the negative terminal where the wells are located, towards the positive terminal. Electrophoretic separation of DNA is possible due to the net negative charge on the DNA backbone¹⁹. Like-charge repulsion forces DNA to migrate through pores formed by the set agarose gel matrix, which provide resistance to migration proportional to the length of DNA fragments. Longer fragments therefore migrate slower than smaller fragments.

3.5.3.6.4 Visualisation and interpretation of gel images

Gel-stained DNA was visualised under UV light in a Gel Doc™ XR+ Gel Documentation System (Gel Doc™; Bio-Rad Laboratories Inc., USA). Gel images for the validation of primers (Table 3.3) targetting HIV are shown in Figure 3.11.

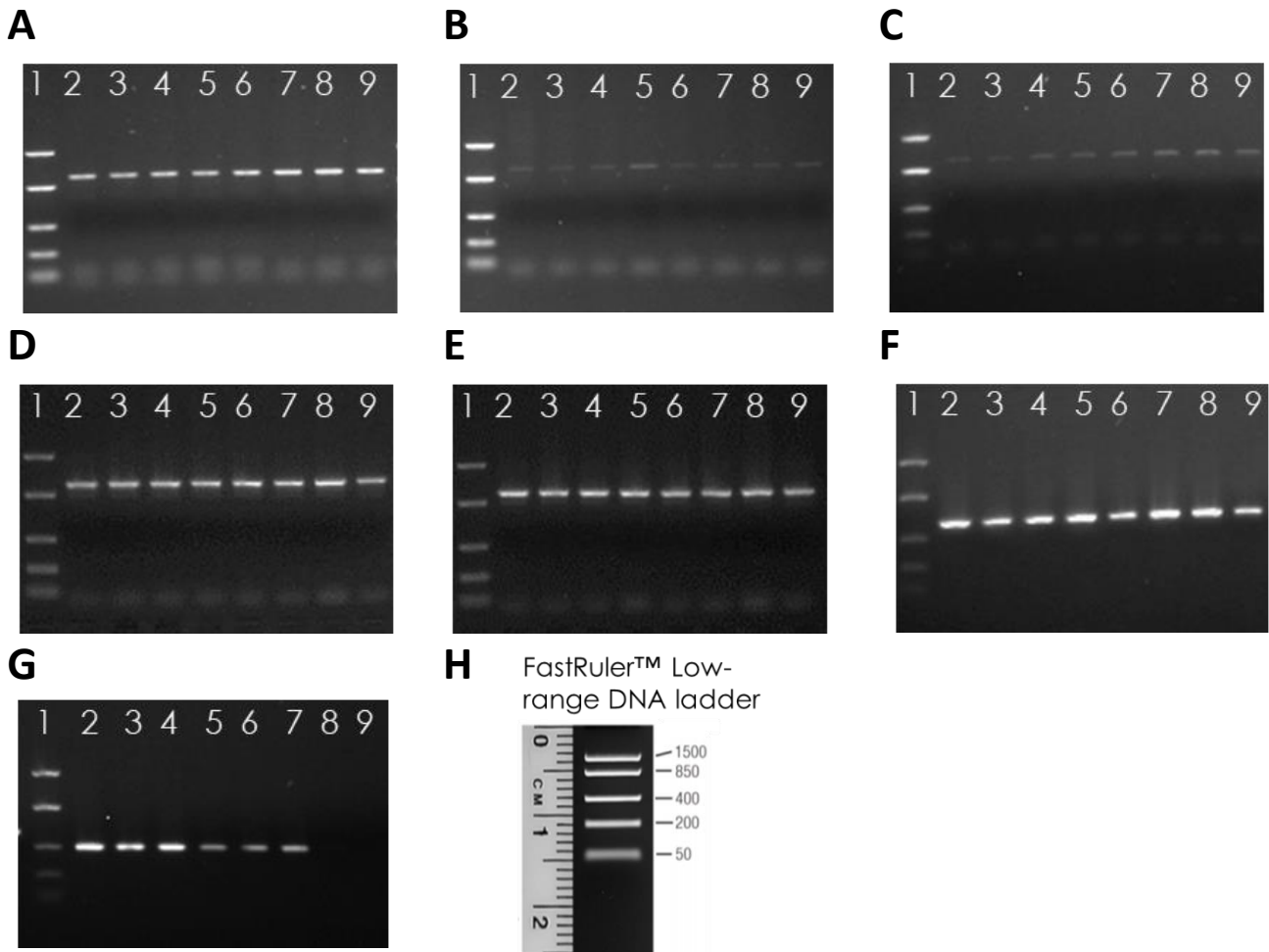


Figure 3.11: HIV LTR-*gag* and V3 primer validation and annealing temperature optimisation. (H) The FastRuler™ LR loaded in lane 1 for each gel, indicating known fragment sizes of 1500, 850, 400, 200, 50 bp. (A-G) Lanes 2-9 for each gel show PCR products generating using annealing temperatures 54 (lane 2), 55.5 (lane 3), 57 (lane 4), 58.5 (lane 5), 60 (lane 6), 61.5 (lane 7), 63 (lane 8), and 64.5°C (lane 9) respectively. DNA extracted from GHOST cells exposed to the following HIV-1 isolates: Yu2 (A), 89.6 (B), NL4-3 (C), SW7 (D), and CM9 (E) was amplified using isolate-specific primers against the LTR-*gag* region of the HIV proviral genome. DNA extracted from GHOST cells exposed to only primary HIV-1C isolates SW7 (F) and CM9 (G) was amplified using isolate-specific primers against the V3-encoding region of the HIV proviral genome.

Primer validation (Figure 3.11) indicated that both the LTR-*gag* and V3 primer pairs amplified the expected products in GHOST cells infected with the corresponding virus. These amplicon sizes were approximately 978-988 bp for all LTR-primer containing reactions (Figure 3.11A-E), approximately 551 bp for SW7-infected-, and approximately 406 bp for CM9-infected-GHOST cell DNA amplified with V3-loop primers specific to SW7 and CM9, respectively.

Respective amplicon sizes were estimated relative to the FastRuler™ LR ladder (Figure 3.11H). Single amplicons in each lane indicate good specificity of the primer pair to the target. The difference between the gel images in terms of the brightness of bands observed is due to the amount of amplicon, which relates back to the amount of target (HIV) DNA present in DNA extractions from HIV-exposed GHOST cells. Brighter bands on the same gel indicate temperatures at which amplification was more successful (Figure 3.11B, lane 5 and Figure 3.11C, lanes 5-8). This could be due to the small volumes of target DNA added resulting in different amounts of HIV DNA per reaction (pipetting error), or due to more efficient amplification at certain temperatures^{16, 34}. Alternatively, it could be due to efficacy of viral entry into GHOST cells being reduced in isolates where dimmer bands are observed, resulting in fewer infected cells being present than in stocks with a greater efficacy of entry. As GFP was not analysed for the infected cells before DNA extraction, the true reasons for the differences in amplicon intensity cannot be resolved without further experimentation.

The annealing temperature selected for future amplifications using all primer pairs validated above was 58°C. This was selected as the amplicons in lanes 4 and 5 for each image (corresponding to PCR at annealing temperatures of 57 and 58.5°C, respectively) amplified well in cases of poor amplification, such as against NL4-3 (Figure 3.11B), and good amplification, such as SW7 (Figure 3.11D).

3.5.4 Limit of detection determination

3.5.4.1 Rationale

The limit of detection describes the lower limit of an assay to detect its target³⁷. This is an important qualifier when presenting results, as failure to detect target may be a limitation of the assay rather than indicating absolute absence of target. In the case of PCR, template DNA and primer concentrations, cycle number, and DNA polymerase specifications all contribute to the limit of detection.

Determining the limit of detection can be approached in two ways, either by setting a lower limit and optimising reaction conditions to achieve the limit, or by running the assay with different amounts of target and determining where target is no longer detectable. Isolate-specific primers may have resulted in slightly different optimal reaction conditions being required for HIV-detection PCR. In order to avoid using different PCR conditions to detect different HIV isolates, different ratios of HIV-infected (GFP⁺) to HIV-uninfected (HIV-unexposed) GHOST cells were used to establish the limit of detection. The pre-established PCR protocol for which the limit of detection was investigated is described in 3.5.3.5 *P*.

3.5.4.2 Method

3.5.4.2.1 Sample material preparation

CD4^{high} GHOST cells were thawed, cultured, and enzymatically dissociated as described in 3.6.2 *Cell culture and maintenance*. GHOST cells were seeded at 3×10^5 cells per well of a 6-well plate, and were allowed to adhere by overnight incubation at 37°C, 5% CO₂. After overnight incubation, GHOST cells were infected with 2×10^5 IUs of the appropriate HIV isolates (Table 3.3) as described in 3.5.3.3 *Sample material preparation*. The following HIV CFS stocks were used in this series of experiments: CM9-020518, SW7-010818, Yu2-041217, 89.6-041217, and NL4-3-041217.

Three days post-infection, cells were enzymatically dissociated as described in 3.6.2.2.1 *Enzymatic dissociation* and prepared to sort GFP⁺ (from HIV-exposed GHOST cells) and GFP⁻ (from HIV-unexposed GHOST cells) GHOST cells by FACS. Sample preparation for FACS and sorting was performed as described in 3.6.3.6 *GHOST cell sorting*. Since HIV-infected GHOST cells express GFP, 10⁵ GFP⁺ HIV-exposed GHOST cells were sorted from each tube of HIV-infected cells, into 15 mL Falcon™ centrifuge tubes (15 mL centrifuge tubes; Corning Inc., USA) containing 2 mL PBS.

Sorted GFP⁺ and GFP⁻ GHOST cells were pelleted by centrifugation at 300 x g for 10 min. The supernatant was aspirated and the pellets were resuspended in PBS to a final concentration of 1000 cells/μL. Different proportions of sorted GFP⁺ GHOST cells relative to HIV-unexposed GFP⁻ GHOST cells were prepared by adding the correct volume of the respective cells to 1.5 microcentrifuge tubes as shown in Table 3.5. Each tube was made up to 100 μL with PBS.

Table 3.5: Cell ratios for each set of HIV-infected (GFP+) sorted GHOST cells to HIV unexposed GHOST cells for DNA extraction.

	0.1% HIV+	1% HIV+	5% HIV+	10% HIV+	20% HIV+
GFP⁺ GHOST cells	100	1000	5000	10 000	20 000
HIV unexposed GHOST cells	99 900	99 000	95 000	90 000	80 000

3.5.4.2.2 DNA extraction

DNA was extracted and quantified (as described in 3.5.3.4 *DNA extraction and quantification*) from each HIV⁺ proportion described in Table 3.5 for each HIV isolate described in 3.5.4.2.1 *Sample material preparation*. NanoDrop® results for these extractions are shown in Table 3.6.

Table 3.6: Concentrations, protein purity (A260/A280 ratio), and salt purity (A260/A230 ratio) of GHOST cell DNA extracted to determine the limit of detection of the in-house PCR protocol.

Sample ID	DNA concentration (ng/μL)	A₂₆₀/A₂₈₀ ratio	A₂₆₀/A₂₃₀ ratio
Yu2 0.1% HIV+ cells	40.99	2.69	1.52
Yu2 1% HIV+ cells	47.57	2.46	1.14
Yu2 5% HIV+ cells	48.32	2.77	2.01
Yu2 10% HIV+ cells	51.83	2.8	1.61
Yu2 20% HIV+ cells	56.6	2.62	1.8
89.6 0.1% HIV+ cells	47.65	2.4	1.2
89.6 1% HIV+ cells	36.72	3.11	1.51
89.6 5% HIV+ cells	43.13	2.75	0.96
89.6 10% HIV+ cells	51.39	2.7	1.6
89.6 20% HIV+ cells	51.95	2.66	1.77
NL4-3 0.1% HIV+ cells	41.74	2.79	1.56
NL4-3 1% HIV+ cells	35.06	3.25	1.27
NL4-3 5% HIV+ cells	42.28	3.02	1.91
NL4-3 10% HIV+ cells	43.9	2.81	1.86
NL4-3 20% HIV+ cells	14.97	2.48	0.68
CM9 0.1% HIV+ cells	53.47	2.41	1.72
CM9 1% HIV+ cells	55.26	2.64	2.23

CM9 5% HIV+ cells	44.08	2.74	1.93
CM9 10% HIV+ cells	49.91	2.42	1.38
CM9 20% HIV+ cells	51.5	2.47	1.87
SW7 0.1% HIV+ cells	53.92	2.5	1.98
SW7 1% HIV+ cells	54.14	2.29	1.62
SW7 5% HIV+ cells	57.04	2.35	1.53
SW7 10% HIV+ cells	51.71	2.66	1.08
SW7 20% HIV+ cells	58.54	2.24	1.56

3.5.4.2.3 Limit of detection polymerase chain reaction

The limit of detection PCR was set up as described in 3.5.3.5.1 *Reaction preparation* using 50 ng DNA per reaction and the appropriate HIV isolate-specific LTR-*gag* primer pair indicated in Table 3.3. HIV-unexposed GHOST DNA (Table 3.4) was included for each isolate-specific primer pair and served as a negative control. The negative control showed that the target amplified by PCR was specific to HIV-infected cells. No-template controls (NTC), where molecular grade water replaced the DNA volume, were not prepared for each primer pair. This was because the HIV unexposed control served the same purpose, showing that amplification was not due to contaminated PCR reagents.

A positive PCR control containing primers targeting the human large ribosomal subunit (L32) was included for HIV unexposed DNA extracted previously (Table 3.3), to confirm the integrity of the DNA and to show that the Kapa RM was still functioning after freeze-thawing. Primer sequences for the L32 primer pair were obtained from Dr Patrick Salmon's Lentiviral Vectors Lab at the University of Geneva, Switzerland. The forward primer sequence is 5'- GTG AAG

CCC AAG ATC GTC AA -3' (L32F), and the reverse primer sequence is 5'- TTG GTG ACT CTG ATG GCC AG -3' (L32R), available from <http://lentilab.unige.ch/mycoplasmaassay.html>.

3.5.4.2.4 Agarose gel electrophoresis

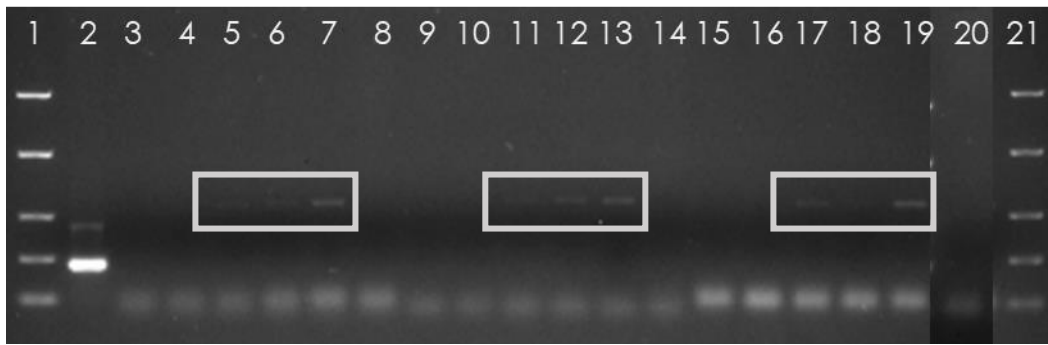
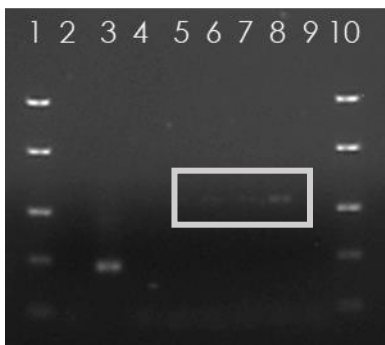
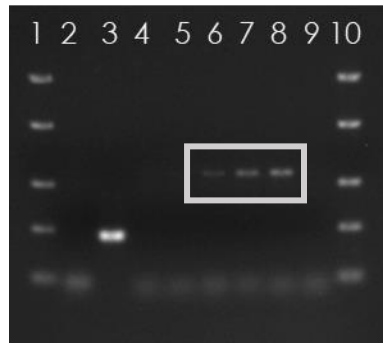
Agarose gel electrophoresis was performed as described in 3.5.3.6 *Agarose gel electrophoresis*. In summary, a 1% agarose gel (w/v) was prepared in 1 x TAE supplemented with EtBr for visualisation. Gels were run at 90 V for 60 min prior to analysis on the GelDoc™. Samples were prepared for electrophoretic analysis as described in 3.5.3.6.2 *Sample preparation for gel loading*. Wells were loaded with 10 µL (small gel) or 15 µL (large gel) sample, and DNA ladder lanes (Figure 3.12) were loaded with the same volume of FastRuler™ Middle-range DNA ladder (FastRuler™ MR; ThermoFisher Scientific, USA).

3.5.4.3 Results and interpretation

Gel images for the limit of detection PCR are shown in Figure 3.12. Gel image quality could not be improved due to malfunctioning of the focus function on the GelDoc™ system. Due to the number of wells in each row, the image for HIV-1B isolates (Figure 3.12A) was edited to include the HIV-unexposed DNA PCR reaction for the NL4-3-specific LTR-*gag* primer pair in the same image (Figure 3.12A, well 20).

The limit of detection for the in-house HIV-detection PCR reaction was established using LTR-*gag*-targetting HIV-specific primers. The limit of detection was found to be 5000 infected cells in 10⁵ total cells, corresponding to 5 HIV proviral genome copies per 100 cells, and thus 1 copy in 20 cells. Bands are highlighted in the grey boxes in Figure 3.12.

Primer dimers can reduce the limit of detection if the primers are not added in excess. The intensity of the primer dimer bands (approximately 100 bp) is comparable across HIV proportions for each isolate (Figure 3.12 A and C). This suggests that the amplification of primer dimers did not reduce amplification here, as the intensity of primer dimer bands did not noticeably reduce with increasing amplification of HIV target.

A**B****C****D**

FastRuler™ Middle-range DNA ladder

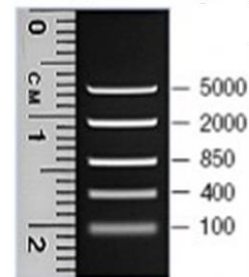


Figure 3.12: Limit of detection PCR gel images. Grey boxes in each image indicate where amplification of the LTR-*gag* region was observed. (A) Limit of detection PCR reactions for HIV-1B isolates. FastRuler™ MR ladder (D) was loaded in lanes 1 and 21, and the L32 positive amplification control for HIV negative DNA was loaded in lane 2. Lanes 3-7 were loaded with 0.1%, 1%, 5%, 10%, 20% Yu2-infected GHOST cell LTR-*gag* PCR product respectively, and lane 8 with the HIV unexposed GHOST cell LTR-*gag* PCR product. The same pattern was repeated for 89.6-infected GHOST cell LTR-*gag* PCR products (lanes 9-14) and NL4-3-infected GHOST cell LTR-*gag* PCR products (lanes 15-19). HIV-unexposed PCR products for the LTR-*gag* amplification was loaded in lane 20 as the negative control. (B & C) Limit of detection PCR reactions for HIV-1C isolates SW7 (B) and CM9 (C). Lanes 1 and 10 were loaded with FastRuler™ MR, lane 2 was loaded with the no template control for each primer pair, and lane 3 was loaded with the L32 positive amplification control performed on HIV-unexposed GHOST cell DNA. Lanes 4-9 were loaded with the respective isolate-specific LTR-*gag* PCR products containing 0.1%, 1%, 5%, 10%, 20%, and no HIV-infected cell DNA respectively.

3.6 GHOST green fluorescent protein assay

3.6.1 Introduction

The infectivity of each HIV isolate was determined after every production using the GHOST HIV-reporter cell line. The GHOST (3) cell line is a plastic-adherent osteosarcoma-derived HIV reporter cell line used for HIV titration and infection studies. The value of these cells lies in their expression of GFP upon infection with HIV, as they are stably transduced with an HIV-1 Tat-responsive HIV-2-LTR-driven GFP reporter gene⁸. GHOST cells are stably transduced with GFP under the control of the HIV-2-derived LTR, responsive to the HIV-1 transcription factor Tat. Upon HIV infection, the Tat protein of infecting virus activates expression of GFP in infected GHOST cells, which can be detected by fluorescence microscopy and flow cytometry⁸. GHOST (3) cells used in this study have been genetically modified to express HIV receptor/coreceptors CD4, CXCR4, and CCR5, and are therefore denoted GHOST (3) R5X4, referred to hereafter as “GHOST cells”. The Ghost cell line was obtained through the National Institutes of Health (NIH) AIDS Reagent Program, Division of AIDS, NIAID, NIH from Dr V.N. KewalRamani and Dr D.R. Littman.

Infectivity of each HIV isolate was determined after every production using the GHOST GFP assay. Functional titration (using the GHOST GFP assay) rather than absolute titration was used to maintain consistency between virus production techniques (PBMC-propagated versus molecular cloning). Functional titration refers to the titration of infectious virus, which excludes non-infectious virus present due to deleterious mutation or packaging. In contrast, absolute titration refers to the viral load per volume of virus-containing suspension, and thus includes infectious and non-infectious virus. Absolute titre and functional titre are therefore not necessarily equal. One of the main advantages of functional titration is the potential for reproducibility in downstream infection experiments.

3.6.2 Cell culture and maintenance

During the culture and maintenance of GHOST cells, the cell surface phenotype was checked by flow cytometry. This resulted in sorting low-passage GHOST cells expressing high levels of CD4, denoted CD4^{high} GHOST cells, which were used in HIV experiments. This was to maintain a GHOST population with uniform HIV receptor and coreceptor expression, allowing for reproducible titration of HIV. The culture and maintenance of GHOST cells described below applies to both sorted (CD4^{high}) and unsorted GHOST cells.

3.6.2.1 GHOST cell thawing

Cryopreserved GHOST cells were obtained from the NIH and stored in liquid nitrogen until use. GHOST cells were frozen in freezing medium made up of 90% foetal bovine serum (FBS) and 10% dimethyl sulfoxide (DMSO). Cryoprotectants, such as DMSO, are miscible in water and reduce the formation of damaging ice crystals by disrupting the crystal structure of pure water³⁸. However, DMSO is toxic to metabolising cells and should be removed as soon as possible after thawing to prevent loss of viability³⁸.

GHOST cell stocks (2×10^6 GHOST cells per cryovial) were thawed in 50 mL pre-warmed DMEM in 50 mL Falcon™ centrifuge tubes (50 mL centrifuge tubes; Corning Inc., USA) and pelleted by centrifugation at 300 x g for 10 min. The supernatant containing DMSO was aspirated, before seeding the cells in T75 culture flasks (Greiner Bio-One, Austria) at 2×10^6 cells per flask, in 8 mL complete DMEM (DMEM with 10% FBS (ThermoFisher Scientific, USA) and 2% penicillin and streptomycin cocktail (pen/strep; ThermoFisher Scientific, USA)). Complete DMEM was supplemented with 1 µg/mL puromycin (Sigma-Aldrich, USA), 100 µg/mL hygromycin (Sigma-Aldrich, USA), and 500 µg/mL G418 (Roche, Switzerland) to drive the CCR5 and CXCR4 expression cassettes and select CD4-expressing cells, as per the supplier's instructions. GHOST cells were cultured to confluence at 37°C and 5% CO₂ in a Forma® Series II water jacketed CO₂ incubator (ThermoFisher Scientific, USA).

3.6.2.2 *GHOST passaging*

Passage number (P) of GHOST cells increased by 1 each time cells were dissociated from culture vessels, and was recorded on cells returned to liquid nitrogen storage.

3.6.2.2.1 **Enzymatic dissociation**

At confluence, GHOST cells were dissociated from the culture plate surface by aspirating the culture medium, rinsing the flask with phosphate-buffered saline (PBS; 137 mM NaCl, 2.7 mM KCl, 4.3 mM Na₂HPO₄, 1.47 mM KH₂PO₄; Sigma-Aldrich, USA), and adding 4 mL pre-warmed 0.25% Trypsin-EDTA (trypsin; ThermoFisher Scientific, USA) to the flask. GHOST cells were incubated at 37°C with trypsin until visibly detached (approximately 5 min). To neutralise the proteolytic activity of trypsin which could damage proteins on the cell surface, 4 mL complete DMEM was added to the flask of dissociated cells. Dissociated GHOST cells were collected into 15 mL centrifuge tubes. The flasks were washed with 4 mL PBS to collect any remaining cells, which were pooled with the dissociated GHOST cell suspensions in the 15 mL centrifuge tubes. Cells were pelleted by centrifugation at 300 x g for 10 min, and the supernatant was aspirated. The cells were resuspended in 2 mL complete DMEM per T75 flask dissociated for enumeration by flow cytometry as described in 3.6.3.3 *Enumeration*.

3.6.2.2.2 **Non-enzymatic dissociation**

For certain experiments (3.6.4.4 *Effect of dissociation and detection method on CD4 phenotype*), GHOST cells were thawed and grown to confluence as described above, and dissociated with non-enzymatic dissociation buffer (NEDB; Sigma-Aldrich, USA) instead of trypsin. Cells were dissociated by aspirating the culture medium, rinsing the flask with 5 mL PBS, and adding 5 mL pre-warmed NEDB to the flask. Cells were incubated with NEDB at 37°C for 5 min, after which the culture flasks were tapped firmly to dislodge the cells. The dissociation buffer contains EDTA, which compromises cell viability with lengthy exposure. To minimise loss of viability, 5 mL complete DMEM was added to the flask after 5 min with NEDB and stubborn cells were dislodged by gentle pipetting across the culture surface. Dislodged cells were transferred to 50 mL centrifuge tubes and the flask was rinsed with 10 mL cold PBS

to collect any remaining cells. The PBS was added to the cell suspension in the 50 mL centrifuge tube. Cells were pelleted by centrifugation at 300 x g for 10 min and resuspended in 2 mL complete DMEM per T75 flask dissociated for enumeration by flow cytometry as described in 3.6.3.3 *Enumeration*.

3.6.2.3 *GHOST cell cryopreservation*

After enumeration and seeding for experiments, remaining GHOST cells were pelleted by centrifugation at 300 x g for 10 min, after which the supernatant was aspirated. Cells were resuspended in 1 mL freezing medium (FBS containing 10% DMSO (Sigma-Aldrich, USA)) per 2×10^6 GHOST cells. Aliquots of 1 mL cell suspension were transferred to 1.5 mL cryovials on ice (Greiner Bio-One, Austria) and stored in liquid nitrogen.

3.6.3 Flow cytometry

3.6.3.1 *Introduction*

Flow cytometers use a hydrodynamic, focussed liquid stream to analyse the characteristics of individual cells as they move past a light source, usually a laser, in single file. There are two types of flow cytometers, namely benchtop analyzers, and cell sorters. Both of these types of flow cytometers operate on the same principles. The only difference is that cell sorters have the ability to break the core stream into micro-droplets containing cells. FACS involves the separation of these droplets by charged plates, deflecting droplets containing the cells of interest into collection tubes. Cells are identified and/or sorted based on detected emission spectra of laser-excited dyes. These dyes (fluorochromes) are often conjugated to protein antigen-specific antibodies. Lasers of different wavelengths have the capacity to excite different fluorochromes, each of which emit unique spectra upon excitation. Emission spectra are detected by optic and computational components of the instrument and are interpreted using software linked to the instrument. Cells can be stained with a panel of antibodies, each conjugated to a fluorochrome with a unique emission spectrum. Fluorochrome-conjugated antibodies specific to the cell surface protein(s) of interest are typically monoclonal, meaning

they bind with high specificity to a single epitope of a protein antigen. This allows single-cell analysis or sorting of discrete cell populations based on selected cell-surface phenotypes³⁹.

Cell surface phenotypes are determined by immunofluorescent staining, whereby fluorochrome-conjugated antibodies bound to specific cell-surface protein antigen are detected using laser excitation as described above³⁹. These fluorochrome-labelled protein (antigen)-antibody complexes allow for quantitative or semi-quantitative analysis of phenotype. The two measurements that can be obtained from a flow cytometer are (i) an indication of the proportion (%) of cells with a specific phenotype (based on binding of the antibodies to the cells; quantitative) and (ii) an indication of the relative number of epitopes present on the cell surface of a specific cell (mean fluorescence intensity (MFI); semi-quantitative)⁴⁰. The more protein of interest is present on the cell surface, the more antibody will bind, the more fluorescence will be emitted upon laser-excitation, which corresponds to a higher MFI.

3.6.3.2 Instruments

3.6.3.2.1 Instruments and configurations

Flow cytometry was performed using a Gallios™ 3 Laser 10 Colour flow cytometer (Table 3.7; Gallios™; Beckman Coulter, USA) to phenotype and enumerate cells and conduct GFP assays. Flow-Check™ Pro fluorospheres (Beckman Coulter, USA) were used to verify optical alignment and instrument performance prior to sample analysis. Flow-Check™ Pro consists of fluorescent 10 µm polystyrene microspheres with fluorescence emission in the range 525 nm to 700 nm when excited at 488 nm. Cell sorting and some of the phenotypic analysis was performed on a BD FACSAria™ Fusion cell sorter (FACSAria™; BD Biosciences, USA). The FACSAria™ is equipped with 6 lasers (of which 4 can be used simultaneously) and 18 detectors. The additional detectors available on the FACSAria™ allow for the optimal detection of some of the monoclonal antibodies used for phenotypic characterization. Cells stained with fluorochrome-conjugated monoclonal antibodies not compatible with the detectors available on the Gallios™ were analysed on the FACSAria™.

The FACS Aria™ laser/detector configuration used during sorting and phenotyping of GHOST cells is shown in Figure 3.13. A neutral density (ND)-1 filter was used to visualise the cells on forward scatter (FS) versus side scatter (SSC) plots. Different ND filter configurations may be used on the FACS Aria™ cell sorter. Selection of the appropriate ND filter depends on the characteristics of the cells to be analysed, particularly their size. The function of a ND filter is to adjust the FS signal generated by the scattering of light, to allow for optimal display on FS versus SSC plots. This was necessary because FS can vary greatly between different cell types analysed, as it is a function of the amount of light scattered due to cell size³⁹.

Table 3.7: Gallios™ laser and filter configurations including fluorescent detection channels (FL) used to detect emission spectra of laser-excited fluorochromes.

Laser	Filter	Channel
488nm, 22mW (BLUE)	525/40	FL1
	575/30	FL2
	620/30	FL3
	695/30	FL4
	755 LP	FL5
638nm, 25mW (RED)	660/20	FL6
	725/20	FL7
	755 LP	FL8
405nm, 40mW (VIOLET)	450/40	FL9
	550/40	FL10

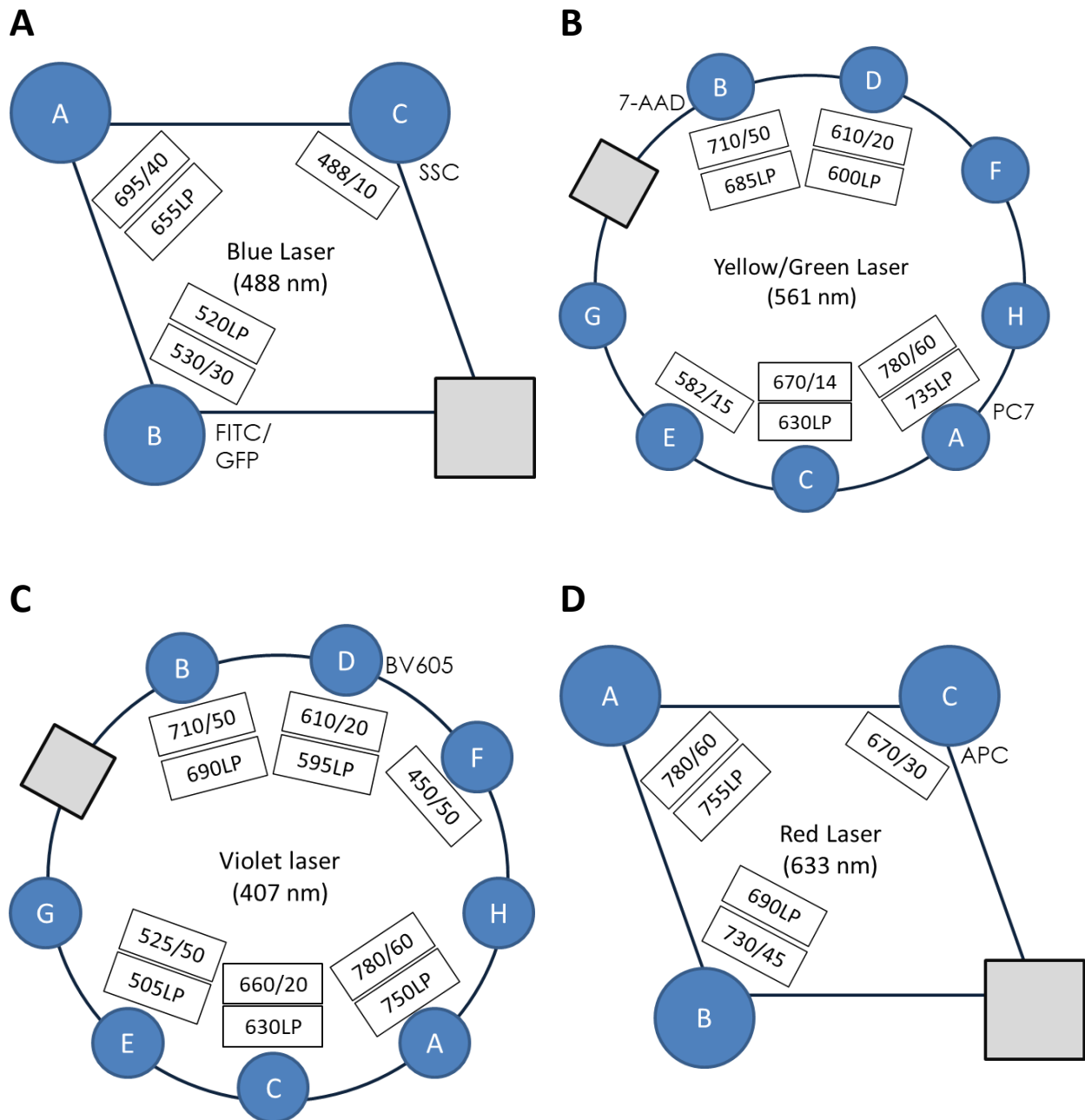


Figure 3.13: FACS Aria™ laser/detector configuration used for GHOST cell phenotype and sorting experiments. (A) The blue laser excites fluorochromes at 488 nm and was used to detect FITC and GFP on B, and SSC on C. (B) The yellow/green laser excites fluorochromes at 561 nm and was used to detect PC7 on A and 7-AAD on B. (C) The violet laser excites fluorochromes at 407 nm and was used to detect BV605 on D. (D) The red laser excites fluorochromes at 633 nm and was used to detect APC on C.

3.6.3.2.2 Protocols

Flow cytometry acquisition protocols were set up using Kaluza version 1.0 (Beckman Coulter, USA) software for acquisition on the Gallios, and FACSDiva™ version 8.0 (BD Biosciences, USA) software for acquisition on the FACS Aria™.

Generally, FS Lin and SSC Log two-parameter plots were used to distinguish cells from debris, and cells of different size and complexity from each other. Membrane-permeable 7-aminoactinomycin D (7-AAD; Beckman Coulter, USA) was used to determine cell viability by negative staining, as live cells with intact membranes are not permeable to the DNA-intercalating dye, preventing the dye from entering cells and binding to dsDNA. Protocols for each type of experiment were kept consistent between runs post-set up. Post-acquisition analysis was performed using Kaluza Analysis version 2.1. Protocol set-up, gating strategies followed, and antibody staining protocols are described for each cell type used.

3.6.3.3 Enumeration

3.6.3.3.1 General sample preparation

Aliquots of samples (100 µL unless stated otherwise) were stained with relevant fluorochrome-conjugated antibodies or fluorescent stains for at least 10 min in the dark prior to flow cytometric analysis. When absolute cell count enumeration assays were required, the same volume of Flow-Count™ fluorospheres (Beckman Coulter, USA) as sample volume (100 µL unless stated otherwise) was added to the flow cytometry tube, followed by the addition of 400 µL PBS. The Gallios™ flow cytometer is known to have a dead volume, referring to the volume between the bottom of the sample tube and the end of the sample pick-up probe. The addition of PBS was therefore to ensure that adequate sample was aspirated by the probe during analysis.

3.6.3.3.2 General enumeration

Flow-Count™ fluorospheres are fluorescent beads of uniform size (10 µm) and have an emission spectrum ranging between 525 nm and 700 nm when excited by the 488 nm (blue) laser. This means that Flow-Count™ is detectable in any of the first four blue laser detection channels (FL1-FL4) of the Gallios™ flow cytometer. Thus, during flow cytometer protocol setup, an unused blue laser detection channel can be used to detect Flow-Count™ beads. As Flow-Count™ fluorospheres are similar in size to some cells, the beads can overlap with the cells in FS versus SSC plots, compromising results. Flow-Count™ beads were therefore removed from analysis of cells using a Boolean gating strategy. A Boolean gating strategy allows a selected population to be included or excluded from subsequent plots in sequential gating strategies, depending on the character string used to set up the gating strategy. Flow-Count™ fluorospheres were captured in a region labelled “BEADS” on a single-parameter plot, appearing as a relatively tight peak (due to uniform size) to the right (due to brightness) of plots used to visualise Flow-Count™ fluorospheres. A Boolean gate “NOT BEADS” allowed subsequent plots to exclude Flow-Count™ fluorospheres appearing in the region BEADS from the gated plot, removing the beads during down-stream data analysis.

Flow-Count™ serves as a concentration calibrator to calculate the number of cells per unit volume. Lot number-specific calibration (Cal) factors are provided with each vial of Flow-Count™ fluorospheres. This is an important parameter when calculating absolute counts on non-volumetric flow cytometers, in which the aspiration volume is difficult to quantify. The absolute count calculation is based on the assumption of equal-volume distribution of Flow-Count™ fluorospheres and cell suspension to be analysed. Absolute counts (cells/µL) were obtained on the Gallios by relating number of cells in a gated region (*events in region of interest*) to the number of Flow-Count™ beads (*cal region*) of known concentration per unit volume (*cal factor*). The equation used to calculate absolute count (Equation 3.1) is illustrated below with an example calculation (Figure 3.14).

Equation 3.1: Cell enumeration using the Flow-Count™ calibrator.

$$\text{Cells per } \mu\text{L} = \frac{\text{Number of events in region of interest}}{\text{Number of Flow - count bead events (Cal region)}} \times \text{Cal factor}$$

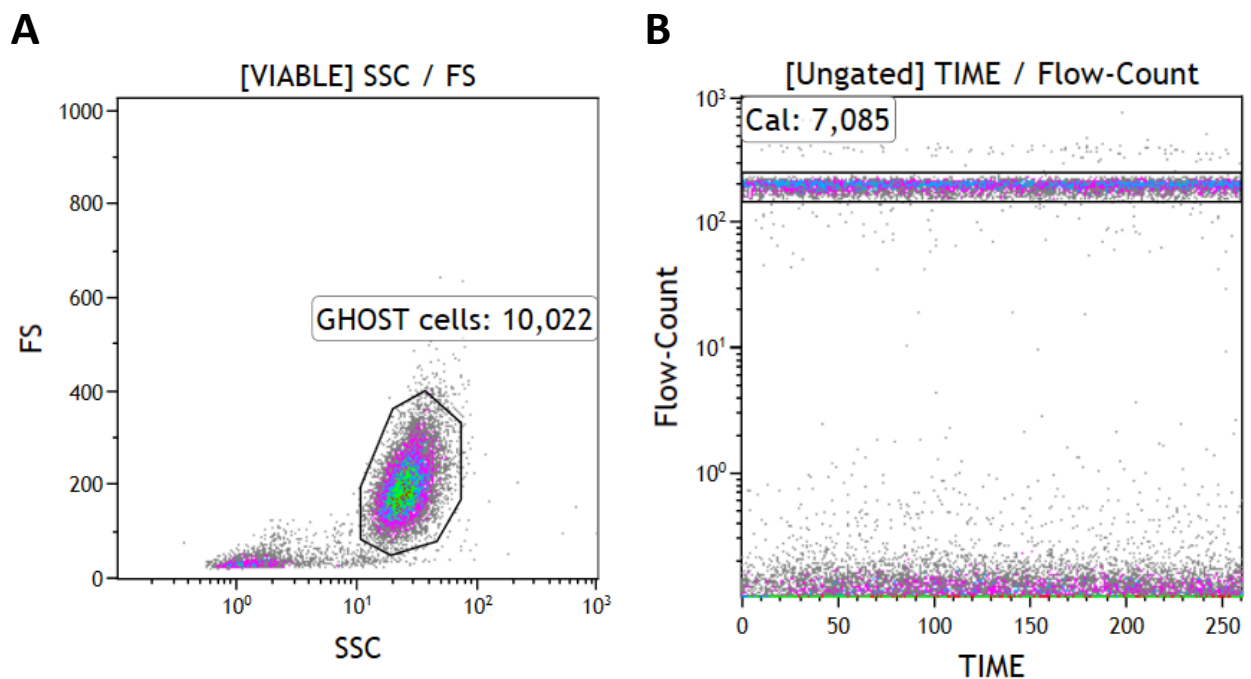


Figure 3.14: Enumeration of GHOST cells using Flow-Count™ fluorospheres. (A) 10 022 intact, viable GHOST cells are selected in the region GHOST cells. (B) 7085 Flow-Count™ beads are detected in the Cal region.

The lot number-specific calibration factor supplied with this batch of Flow-Count™ was 1002. The number of GHOST cells counted on the Gallios™ flow cytometer was 10 022, and the number of Flow-Count™ beads which were counted at the same time as the cells was 7085. To obtain the absolute cell count per unit volume in the cell suspension, Equation 3.1 was applied as follows.

$$\text{Count per } \mu\text{L cell suspension} = ((10\ 022) / (7085)) \times 1002 = \underline{1417.36 \text{ cells}/\mu\text{L}}.$$

$$\text{Count in total volume (2 mL)} = 1417.36 \times 2000 (\mu\text{L in 2 mL}) = \underline{2.83 \times 10^6 \text{ viable GHOST cells in 2 mL cell suspension.}}$$

3.6.3.4 *Post-sort purity*

Post-sort purity was evaluated for each sort by sorting a small number of cells into a plate or tube maintaining the same sort set-up and experiment layout, resuspending the sorted cells in PBS, and re-analysing the sorted population. This was done to ensure the sort setup was optimal before proceeding with experiments. Post-sort purities above 95% were considered acceptable in most applications.

3.6.3.5 *GHOST cell gating strategies*

3.6.3.5.1 **Sample preparation**

A single protocol was used to obtain absolute counts of viable GHOST cells, and to determine the proportion of GHOST cells (i) expressing CD4, and (ii) expressing GFP after being challenged with HIV (Figure 3.15). Methods used in HIV exposure are described in section 3.6.6 *GHOST green fluorescent protein assay – method*.

Phenotyping and enumeration

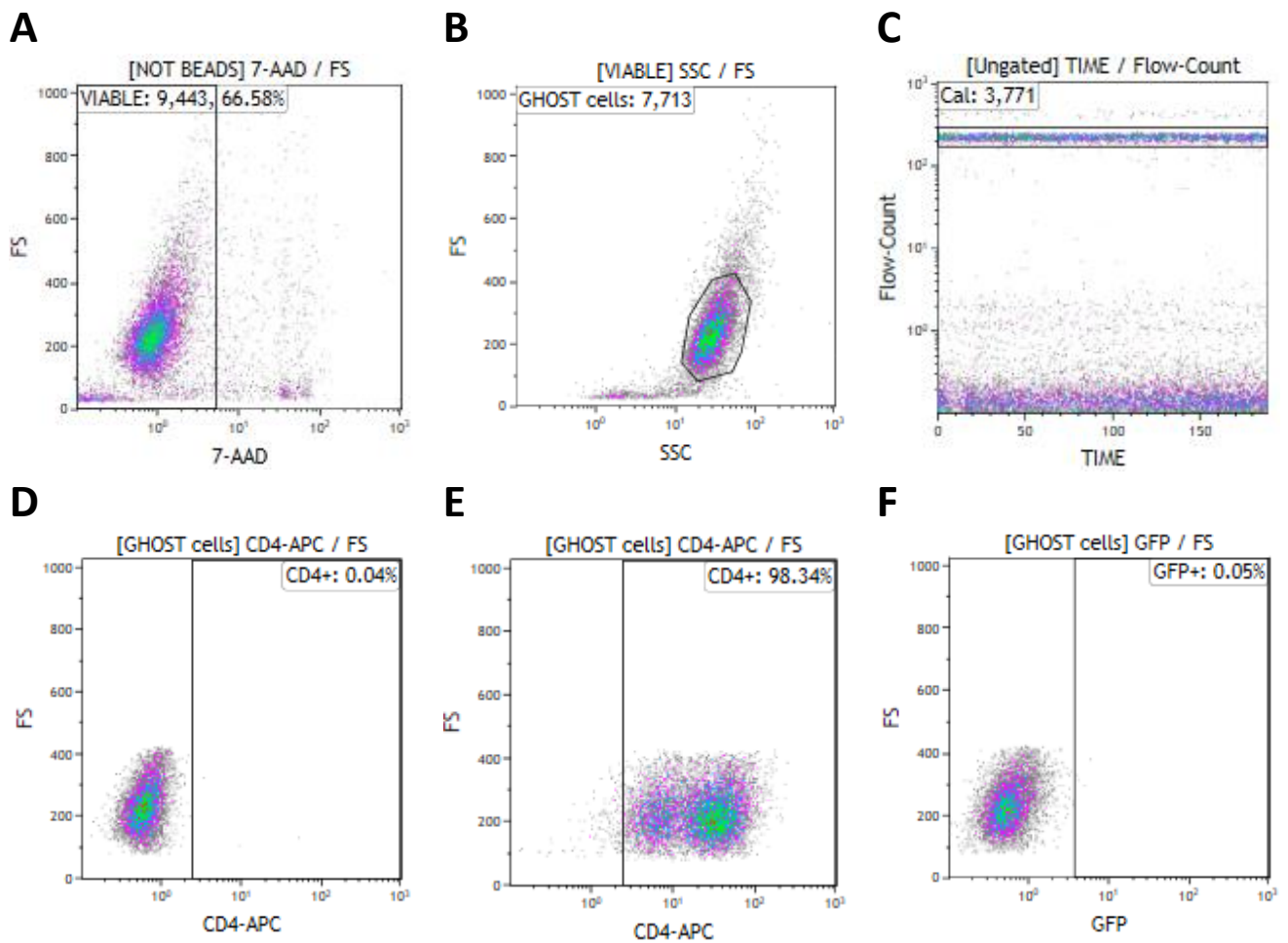
One (enumeration) or two (phenotyping) 100 μ L aliquots of GHOST cells were stained as outlined in 3.6.3.3.1 *General sample preparation* with 3 μ L 7-AAD added to each aliquot. For phenotyping, one aliquot was then stained with mouse anti-human CD4 conjugated to allophycocyanin (APC) (CD4-APC; clone 13B8.2; Beckman Coulter, USA), and the second aliquot was stained with the appropriate isotype control (CD4-APC iso; mouse IgG₁; Beckman Coulter, USA). Cells were stained for 10 min in the dark before adding 100 μ L Flow-Count™ fluorospheres and 400 μ L PBS for volume, and then analysed on the Gallios™.

GFP expression analysis

Flow cytometry was used to determine the proportion of HIV-exposed cells infected with HIV, and therefore that expressed GFP. GHOST cells exposed to HIV were prepared for flow cytometry as described in 3.6.6.3 *Green fluorescent protein detection*.

3.6.3.5.2 Gating strategy

The sequential gating strategy of GHOST cells is shown in Figure 3.15. To enumerate GHOST cells, plots A-C (Figure 3.15) were used, for CD4-phenotyping, plots A-E (Figure 3.15) were used, and for HIV infection experiments, plots A,B, and F/G (Figure 3.15) were used. The CD4+ region was set according to the isotype control, and the GFP+ region was set relative to an HIV-unexposed control, or according to HIV-exposed cells not expressing GFP (Figure 3.15G).



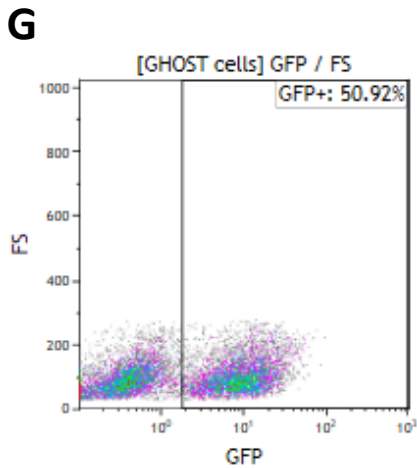


Figure 3.15: Gating strategy routinely used for GHOST cell enumeration, CD4 phenotype, and GFP expression. (A) A FS Lin versus 7-AAD two-parameter plot with Flow-Count™ beads excluded was used to select viable cells, which stain negative for 7-AAD and are indicated in the VIABLE region. (B) A two-parameter FS Lin versus SSC Log plot gated on the “VIABLE” region to identify viable, intact cell GHOST cells (GHOST cells region). (C) A two-parameter plot of Flow-Count versus time, with the number of beads captured indicated in the Cal region. (D & E) Two-parameter FS Lin versus CD4-APC plots gated on “GHOST cells” were used to enumerate CD4⁺ GHOST cells. (D) GHOST cells stained with CD4-APC iso, used to set the “CD4+” region. (E) GHOST cells stained with CD4-APC. (F) A two-parameter FS Lin versus GFP plot of HIV-unexposed GHOST cells which do not express GFP. (G) The same two-parameter plot as in F showing HIV-exposed GHOST cells expressing GFP.

3.6.3.6 GHOST cell sorting

3.6.3.6.1 Purpose

GHOST cells were independently sorted by FACS for GFP and CD4 expression for experimental purposes. GFP⁺ GHOST cells were sorted from HIV-exposed GHOSTs prepared as described in 3.5.4.2 *Method* for HIV nucleic acid detection experiments. CD4^{high} GHOST cells were sorted from HIV-unexposed GHOST cells cultured for the purpose of obtaining a population with uniform CD4 expression for HIV titration, discussed in detail in 3.6.4.1 *GHOST cell CD4 expression*.

3.6.3.6.2 Sample preparation

CD4 sort

GHOST cells were sorted for CD4 expression using CD4-APC in two instances. The first instance was in the optimisation of the GHOST GFP assay, described in 3.6.4 *GHOST green fluorescent protein assay setup* and optimisation. The second instance was after determining that CD4^{high} GHOST cells should be used for functional titration of HIV, when a single low-passage stock was sorted for CD4 expression as described below. CD4^{high} GHOST cells sorted in the second instance were used to titrate virus and were used for all experimental purposes.

Low-passage (P0) GHOST cells were resuscitated from liquid nitrogen and cultured for one passage as described in 3.6.2 *Cell culture and maintenance*. GHOST cells were non-enzymatically dissociated as described in 3.6.2.2.2 *Non-enzymatic dissociation*. Approximately 20×10^6 GHOST cells at P1 were stained with 2 μ L 7-AAD and 2 μ L CD4-APC per 10^6 cells in 100 μ L PBS, and incubated for 10 min in the dark. Cells were pelleted by centrifugation at 300 x g for 10 min to remove unbound and weakly-bound (resulting from non-specific staining) antibody, and resuspended in 1 mL PBS for sorting.

A post-sort purity of 98.07% viable, intact CD4^{high} GHOST cells was achieved (Figure 3.16E and F) for the CD4^{high} GHOST cells used for functional titration after optimisation experiments (described in 3.6.4 *GHOST green fluorescent protein assay setup* and optimisation). CD4^{high} GHOST cells were seeded at 5×10^5 cells per T75 flask in complete DMEM with puromycin, hygromycin, and G418 as described in 3.6.2 *Cell culture and maintenance* for one passage. Cells were then dissociated enzymatically as described in 3.6.2.2.1 *Enzymatic dissociation* before cryopreservation, as described in 3.6.2.3 *GHOST cell cryopreservation*.

GFP sort

HIV-exposed and -unexposed GHOST cells (3.5.4 *Limit of detection determination*) were prepared by centrifugation at 300 x g for 10 min and resuspended in 100 μ L and 200 μ L PBS for HIV-exposed and HIV-unexposed GHOST cells, respectively. A post-sort purity of 99.95% viable, intact, GFP⁻ HIV-unexposed GHOST cells was achieved.

3.6.3.6.3 Gating strategy

GHOST cells were sorted into 15 mL centrifuge tubes containing 2 mL DMEM for CD4-sorted cells, or 1 mL PBS for GFP-sorted cells. The flow cytometry protocol and sequential gating strategies used during sorts are indicated in Figure 3.16.

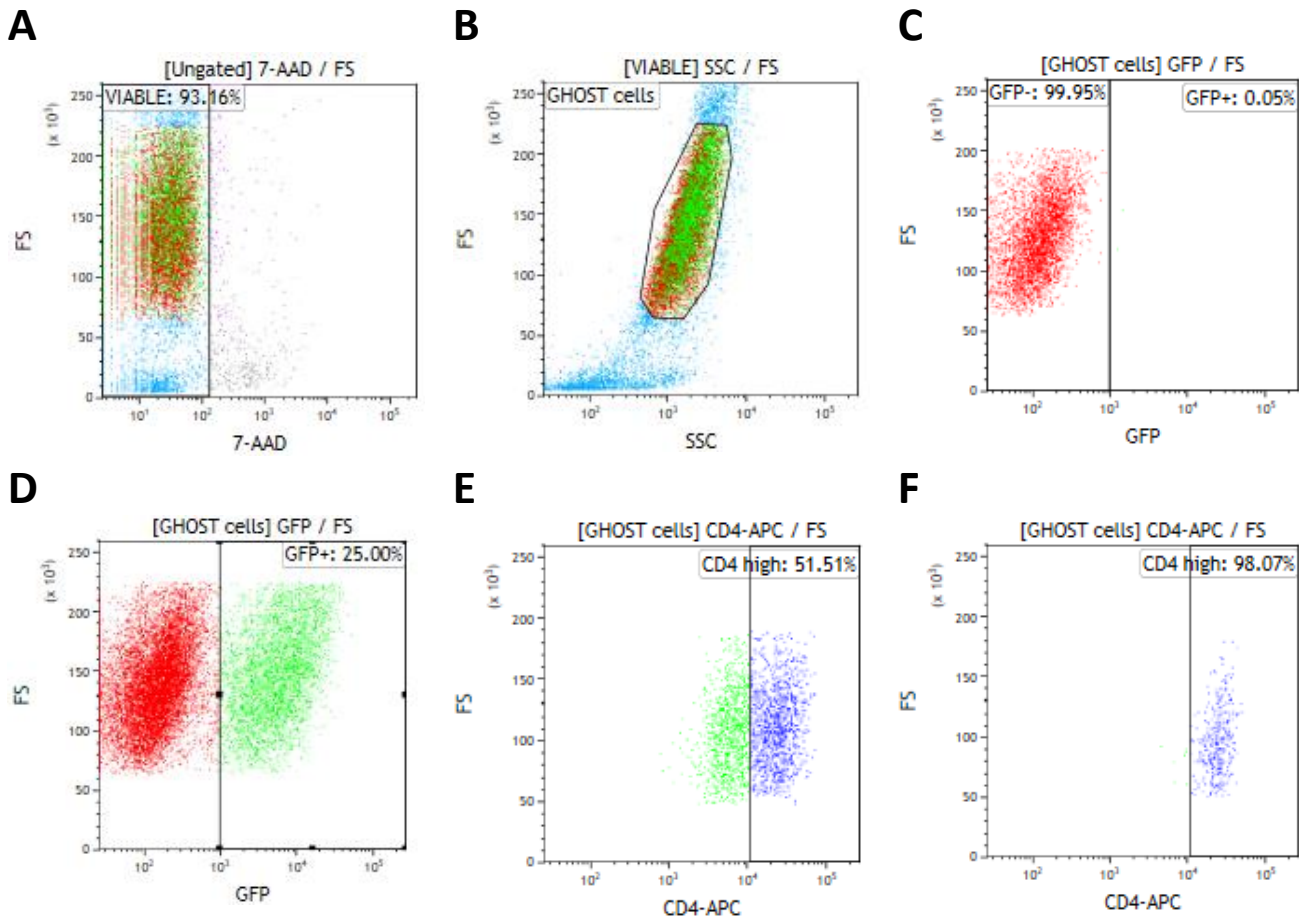


Figure 3.16: Flow cytometry and gating strategies used for GHOST cell sorts. (A) A two-parameter FS Lin versus 7-AAD was used to select viable (7-AAD negative) GHOST cells, captured in the “VIABLE” region. (B) A two-parameter FS Lin versus SSC plot gated on viable GHOST cells (“VIABLE” region) was used to capture intact GHOST cells. (C) A two-parameter FS Lin versus GFP plot gated on “GHOST cells” was used to sort GFP⁻ GHOST cells (“GFP-“region) from HIV-unexposed GHOST cells. (D) The same two-parameter FS Lin versus GFP plot without the “GFP-“ gate was used to sort GFP⁺ GHOST cells (“GFP+”) from HIV-exposed GHOST cells. (E) A two-parameter FS Lin versus CD4-APC plot gated on “GHOST cells” was used to sort CD4^{high} low-passage GHOST cells. (F) Representative post-sort purity achieved after sorting CD4^{high} GHOST cells.

3.6.4 GHOST green fluorescent protein assay setup and optimisation

3.6.4.1 GHOST cell CD4 expression

3.6.4.1.1 Introduction

Immunophenotyping of GHOST cells used in GFP assays was introduced as a quality control step to monitor possible changes in phenotype as the cells approach the passage range (P10-P15) where the transgenic construct expression could become unstable according to suppliers (GHOST (3) R5X4 datasheet – NIH). Construct destabilisation could result in unstable expression of CD4, CXCR4, and CCR5, which are required for HIV entry and reliable functional titration. Initial phenotyping of CD4, CXCR4, and CCR5 showed stable expression of CCR5 and CXCR4, but CD4 was not detectable by flow cytometry using the reagents initially available. The apparent lack of expression of CD4 (Figure 3.17D) using mouse anti-human CD4 conjugated to fluorescein isothiocyanate (FITC) (CD4-FITC; clone Okt 4; BioLegend, USA) was investigated by procuring a new CD4 detection antibody with a different fluorochrome (CD4-APC), and by assessing the expression of CD4 on the transcriptomic level.

3.6.4.2 GHOST cell phenotype

3.6.4.2.1 Sample preparation for phenotype

Unsorted GHOST cells were resuscitated from liquid nitrogen and cultured to confluence in complete DMEM supplemented with puromycin, hygromycin, and G418 (described in 3.6.2 *Cell culture and maintenance*). Cells were enzymatically dissociated as described in 3.6.2.2.1 *Enzymatic dissociation*, pelleted by centrifugation at 300 x g for 10 min, and resuspended in 5 mL complete DMEM for immunophenotyping. Two 100 µL aliquots were prepared for staining as follows.

One of the 100 µL aliquots of GHOST cell suspension was stained with 3 µL of each of the following: 7-AAD; CD4-FITC; rat anti-human CCR5 conjugated to phycoerythrin- (PE)-cyanine-

7 (Cy7) (PC7) (CCR5-PC7; clone 359106; BioLegend, USA); and mouse anti-human CXCR4 conjugated to Brilliant Violet 605™ (CXCR4-BV605; clone 12G5; BioLegend, USA). The second 100 µL aliquot was stained with 3 µL of each of the following: 7-AAD; rat IgG2b conjugated to PC7 (CCR5-PC7 iso; BioLegend, USA); and mouse IgG2a conjugated to Brilliant Violet 605™ (CXCR4-BV605 iso; clone 12G5; BioLegend, USA).

The second tube served as the non-specific/unstained control containing the appropriate isotypes for CXCR4-BV605 and CCR5-PC7. The appropriate CD4 isotype was not available at the time and was thus not added to the tubes. Unbound and weakly-bound antibody was washed off by adding 1 mL PBS to each tube and pelleting cells by centrifugation at 300 x g for 10 min. Cells were resuspended in 500 µL PBS before analysing on the FACS Aria™ cell sorter.

3.6.4.2.2 Results and outcome

Figure 3.17 shows the co-expression of CCR5 and CXCR4 on GHOST cells (using the same gating strategy to obtain viable GHOST cells as in Figure 3.16A and B) relative to the corresponding isotype controls. The isotype tube did not contain an isotype control for CD4. Consequently, the negative/positive delineation was set up using autofluorescence emitted by the cells in the FL1 channel (Figure 3.17C). Figure 3.17D shows negligible difference between the unstained control sample (Figure 3.17C) and stained sample in terms of CD4-FITC detection.

From Figure 3.17B, 2% of GHOST cells did not express either CXCR4 or CCR5 (Figure 3.17B “CXCR4- CCR5-“ region). This could be explained by partial construct breakdown in these cells, or, more likely, that construct-driving antibiotics could have been replaced more frequently in culture. More than 80% of the GHOST cells expressed both CCR5 and CXCR4 (Figure 3.17B “CXCR4+ CCR5+“ region), and less than 15% expressed one co-receptor but not the other. This could, again, be due to partial construct breakdown, or the depletion of construct-driving antibiotics during culture resulting in these constructs being lost during rapid cell division.

Reliable titration of HIV on GHOST cells using the GHOST GFP assay requires the cells to be susceptible to HIV, ie. the majority (>80%) of the cells should express CCR5, CXCR4, and CD4. While CCR5 and CXCR4 were repeatedly shown to be satisfactorily expressed on GHOST cell surfaces, the proportion of GHOST cells expressing CD4 varied between 0% and 60% (see Figure 3.23 showing CD4-FITC phenotypes of five GHOST cell stocks), despite culturing the cells in construct-driving antibiotics. The apparent lack of CD4 expression was concerning and was investigated in follow-up experiments. Construct stability was assessed by CD4 mRNA expression, protein stability during culture was assessed by testing dissociation methods and protein recovery, and flow cytometric detection of protein was compared using different fluorochromes.

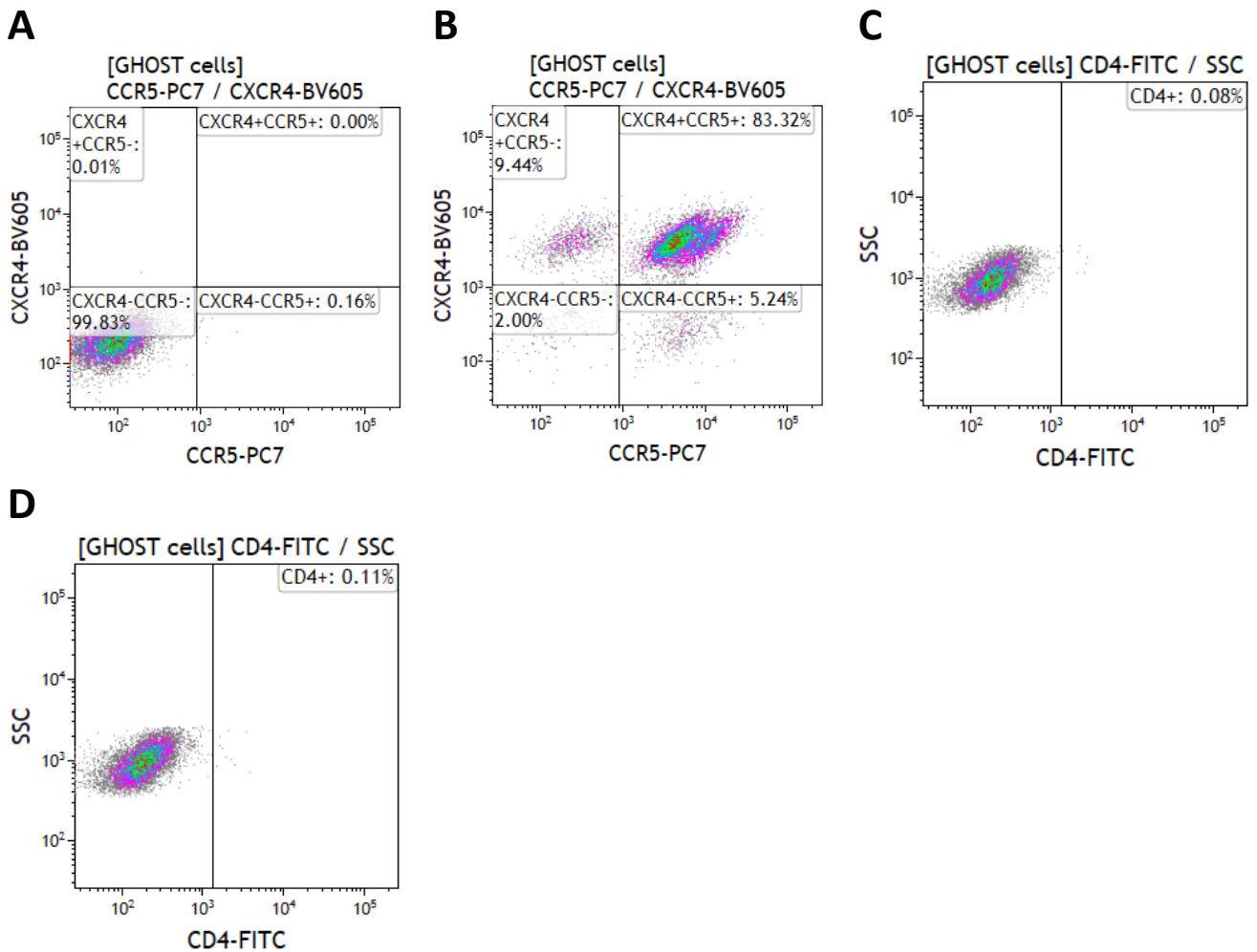


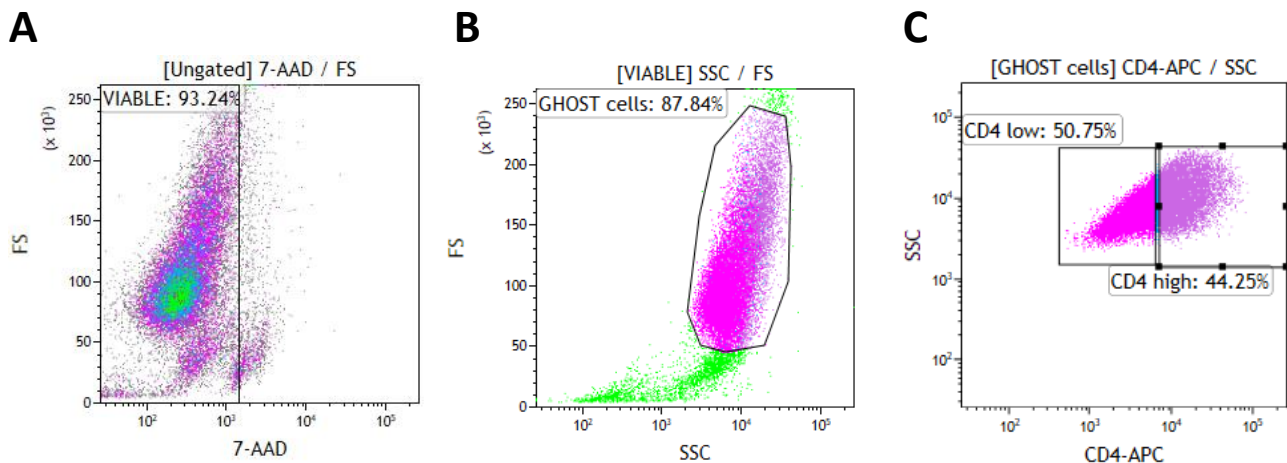
Figure 3.17: GHOST cell phenotype analysis using CCR5-PC7, CXCR4-BV605, and CD4-FITC. (A) A representative two-parameter plot of CXCR4-BV605 versus CCR5-PC7 of GHOST cells stained with the isotype combination used to set the four quadrants indicated on the plot. **(B)** Same plot as A, representing data obtained for GHOST cells stained with CXCR4-BV605 and CCR5-PC7. Subpopulations of GHOST cells with different co-receptor expression profiles are shown. **(C)** A representative two-parameter plot of SSC Log versus CD4-FITC for the isotype tube (unstained for CD4-FITC) used to set the “CD4+” region. **(D)** Same plot as C for GHOST cells stained with CD4. GHOST cells expressing CD4 should have appeared in the “CD4+” region.

3.6.4.3 CD4 messenger RNA expression

In order to determine whether expression of CD4 was compromised in GHOST cells due to construct destabilisation, mRNA was isolated to perform reverse-transcription (RT)-PCR. TZM-bl cells (HeLa-derived cells known to express high levels of CD4) and peripheral blood mononuclear cells (PBMCs) were used as positive controls. GHOST cells of a single frozen stock were thawed, cultured, and non-enzymatically dissociated before sorting into CD4^{high} and CD4^{low} fractions using the CD4-APC antibody (described in 3.6.3.5 *GHOST cell gating*

strategies) procured for this experiment, as described in 3.6.3.6 *GHOST cell sorting*. Briefly, dissociated cells from one T75 flask were stained with 7-AAD and CD4-APC as described in 3.6.3.6 *GHOST cell sorting*. Sorting was performed according to the sequential gating strategy shown in Figure 3.18. CD4^{low} GHOST cells were sorted with a purity of 96.36%, and CD4^{high} GHOST cells with a purity of 81.13%. Approximately 2x10⁶ GHOST cells were sorted for each fraction, into 15 mL centrifuge tubes containing 1 mL PBS.

The CD4-APC monoclonal antibody was initially procured to establish whether the relative brightness of the fluorochrome could be responsible for the lack of CD4 detection using CD4-FITC (Figure 3.17C and D). Dim fluorochromes (such as FITC) are suitable when adequate resolution of the positive population is expected due to the abundance of target protein. Brighter fluorochromes (such as APC) should be used when the protein of interest is not necessarily abundant⁴¹. The CD4-APC iso antibody was procured at a later stage. It was found that detection of CD4 using CD4-APC was markedly better when compared to CD4-FITC, discussed in 3.6.4.4.3 *Fluorochrome comparison and CD4-recovery over time*. For these reasons, CD4-APC was used to sort different GHOST cell sub-populations based on CD4 expression.



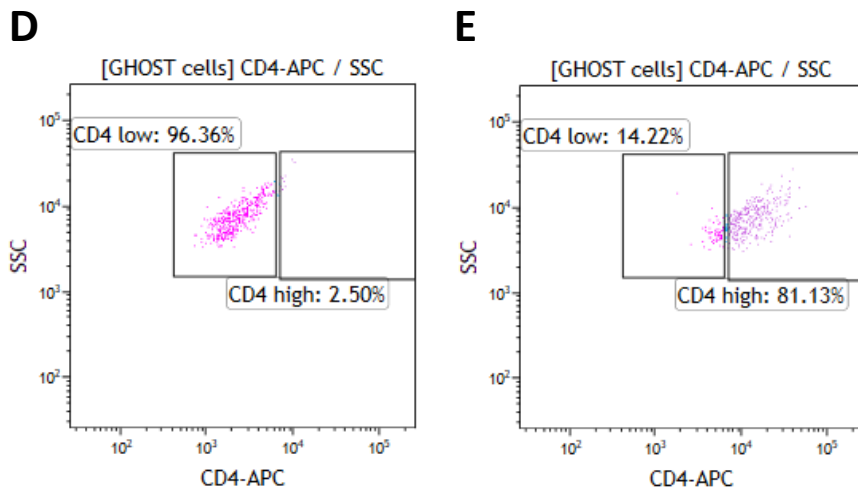


Figure 3.18: Sequential gating strategy used to sort CD4^{high} and CD4^{low} GHOST cells for mRNA evaluation. (A) Viability of GHOST cells negative for 7-AAD captured in the “Viable” region on a FS Lin versus 7-AAD two-parameter plot. (B) Viable, intact GHOST cells were selected in the region “GHOST cells” on a two-parameter FS Lin versus SSC Log plot. (C) The pre-sort CD4 population shown on a two-parameter SSC Log versus CD4-APC plot. The regions “CD4 low” (pink) and “CD4 high” (purple) were sorted. (D) Post-sort purity for CD4^{low} GHOST cells is shown on the same plot as in C. (E) The same two-parameter plot as in C shows the post-sort purity of CD4^{high} GHOST cells.

3.6.4.3.1 RNA extraction

RNA was isolated from TZM-bl cells (positive control), HEK293T cells (negative control), PBMCs (positive control), CD4^{low} GHOST cells, and CD4^{high} GHOST cells. Extractions were performed using the QIAGEN RNeasy Mini Kit (QIAGEN, Germany) according to the manufacturer’s instructions. Prior to each use, RLT buffer was prepared by adding β -mercaptoethanol (Sigma-Aldrich, USA) to a final concentration of 1%, as per manufacturer’s instructions.

Approximately 2×10^6 cells of each type were transferred to 1.5 mL microcentrifuge tubes and pelleted by centrifugation at 300 x g for 10 min. The supernatant was discarded and the pellets each resuspended in 350 μ L RLT buffer per extraction, followed by vortexing for 1 min to homogenise. RLT buffer contains β -mercaptoethanol and guanidine thiocyanate to lyse cells and inactivate nucleases. To precipitate proteins from the cell lysates, 350 μ L 70% ethanol was added to a final concentration of 35%. Cell lysate and precipitated proteins were transferred to the silica membrane of RNeasy spin columns assembled in 2 mL collection tubes and centrifuged for 15 s at 8000 x g to remove liquids.

Flow-through containing buffer remnants and proteins was discarded, and 700 μL RW1 buffer was applied to each column. The columns were centrifuged for 15 s at 8000 x g to wash membrane-bound nucleic acids. Flow-through was discarded once again and the silica membranes washed twice with 500 μL RPE buffer by incubating the tube for 1 min at room temperature to allow salts to dissolve in the buffer followed by centrifugation for 15 s and 2 min at 8000 x g. The salt-containing flow-through was discarded and the columns were placed in sterile 2 mL microcentrifuge tube. RNase-free water (20 – 30 μL) provided with the kit was incubated on the column membranes for 2 min prior to elution by centrifugation for 1 min at 8000 x g. The eluates were placed back on the respective column membranes, incubated for 1 min, and eluted again by centrifugation for 1 min at 8000 x g. This was done to improve the RNA yield.

RNA concentrations and purity analyses were determined by NanoDrop® as previously described in 3.5.3.4.3 *Nucleic acid quantification by NanoDrop®*, and are summarised in Table 3.8. Preferred purity values for reverse transcription of RNA to cDNA before PCR were $A_{260/280}$ and $A_{260/230}$ ratios ≥ 2 . Samples not meeting this criteria (PBMCs and HEK293T cells) were converted to cDNA on the basis that the purity values were very close to 2 (PBMCs), or that the RNA concentration was high and protein purity met the criteria (HEK293T cells).

Table 3.8: RNA concentrations, protein purity ($A_{260/280}$), and salt purity ($A_{260/230}$) for RNA extracted from PBMCs, TZM-bl cells, GHOST cells sorted for low- and high-CD4 expression, and HEK293T cells.

Sample	[RNA] (ng/ μL)	$A_{260/280}$	$A_{260/230}$
PBMCs	436.9	1.98	1.95
TZM-bl	1109.9	2.04	2.24
Ghosts (CD4 ^{high})	1021.19	2.07	1.87
Ghosts (CD4 ^{low})	1388.99	2.06	2.05
HEK293T	1487.91	2.07	0.50

3.6.4.3.2 Reverse transcription

RNA (Table 3.8) was reverse transcribed to cDNA using the Bioline SensiFast cDNA Synthesis kit (Meridian Life Sciences, Inc, USA) according to manufacturer's instructions. Reactions were set up on ice in PCR tubes as summarized in Table 3.9. A NTC and no reverse transcriptase control (NRC) were included (Table 3.9). Approximately 1 µg RNA was added per reaction, which were set up in thin-walled 0.2 mL PCR tubes on ice. The SensiFAST cDNA reagent kit uses a high-fidelity (HiFi) reverse transcriptase enzyme and optimised buffer systems which maximise the activity of the enzyme even in the presence of enzyme inhibitors such as salts.

GeneAmp™ thermocycler conditions for reverse transcription were as follows: 25°C for 10 min to anneal primers; 42°C for 15 min for reverse transcription; 85°C for 5 min to inactivate reverse transcriptase; 4°C hold to prepare for sample storage.

Table 3.9: Reverse transcription reactions set-up using the SensiFAST cDNA reverse transcription kit.

Sample ID	5x TransAmp buffer (μL)	Reverse Transcriptase (μL)	RNA (μL)	Nuclease-free water (V _f 20μL)
NTC	4	1	-	15
NRC	4	-	1 (TZM-bl RNA)	15
PBMCs	4	1	2	13
TZM-bl	4	1	1	14
Ghosts (CD4 ^{high})	4	1	1	14
Ghosts (CD4 ^{low})	4	1	0.7	14.3
HEK293T	4	1	0.7	14.3

*The purpose of the NRC was to confirm removal of genomic DNA during the RNA isolation, and to ensure that reagents used to prepare reverse transcription reactions were not contaminated with cDNA synthesis kit reagents. Since all the RNA extractions were performed in one isolation, the RNA isolation with the highest $A_{260/280}/A_{260/230}$ ratio combination (TZM-bl cells) was used for this control. The high ratios were used to select the NRC RNA sample as the higher ratios indicate greater potential for genomic DNA contamination of the RNA during isolation. Genomic DNA contamination would result in the amplification of CD4-targetting PCR reactions from the DNA rather than mRNA-derived cDNA, and would not be useful in determining whether CD4 is differentially expressed between CD4^{high} and CD4^{low} GHOST cells.

3.6.4.3.3 CD4 messenger RNA detection polymerase chain reaction

Forward (CD4F) 5'- GTC CCT TTT AGG CAC TTG CTT CT -3' and reverse (CD4R) 5'- TCT TTC CCT GAG TGG CTG CT -3' primers for a region of CD4 mRNA previously described for qPCR were obtained from literature⁴² and manufactured by IDT (Integrated DNA Technologies, Inc, USA). Lyophilised primers were resuspended in molecular grade water to 100 μM stocks as recommended by manufacturers and diluted to 10 μM working stocks in molecular grade water.

PCR reactions for amplification of CD4 from cDNA were set up as described in 3.5.3.5 *P* on ice. All reactions (shown in Table 3.10) were set up using the CD4F and CD4R primer pair, except the L32 PCR control which contained the L32F and L32R primer pair previously described in 3.5.4.2.3 *Limit of detection* . Reactions were prepared with 1 μL cDNA as approximately 1 μg RNA was used for the preparation of cDNA. Uniform, efficient conversion of 1 μg RNA to approximately 1 μg cDNA in each 20 μL reverse transcription reaction was assumed, which would result in a concentration of approximately 50 ng/ μL cDNA per reaction. The PCR protocol described in 3.5.3.5 *P* requires 50 ng DNA per reaction, and therefore 1 μL cDNA was used per PCR reaction (Table 3.10). Thermocycling was performed as indicated in Figure 3.10, with primer annealing temperatures for CD4-amplifying reactions set at 65°C, and the annealing temperature for the L32 primer pair set at 55°C. Controls for the PCR include NTC for the PCR and an L32 positive PCR control.

Table 3.10: PCR reactions set up for CD4 mRNA detection.

Sample ID	2x Kapa RM (μL)	Forward primer (μL)	Reverse primer (μL)	cDNA (μL)	Distilled water (μL)
NTC _{PCR} (PCR control)	12.5	0.75	0.75	-	11
L32 (PCR control)	12.5	0.75	0.75	1	10
NTC _{RT} (cDNA control)	12.5	0.75	0.75	1	10
NRC (cDNA control)	12.5	0.75	0.75	1	10
TZM-bl	12.5	0.75	0.75	1	10
PBMCs	12.5	0.75	0.75	1	10
Ghost CD4 ^{high}	12.5	0.75	0.75	1	10
Ghost CD4 ^{low}	12.5	0.75	0.75	1	10
HEK293T	12.5	0.75	0.75	1	10

3.6.4.3.4 CD4 polymerase chain reaction amplicon analysis

Amplicons were analysed by agarose gel electrophoresis (described in 3.5.3.6 *Agarose gel electrophoresis*), using 1% agarose gels made with TAE. Samples were prepared for electrophoretic analysis as described in 3.5.3.6.2 *Sample preparation for gel loading*, and wells were loaded with 10 μ L of PCR reactions. Electrophoresis was performed by applying 90V for 80 min. Band sizes were estimated relative to 5 μ L FastRuler™ LR DNA ladder loaded in lanes 1 and 11 (Figure 3.19).

3.6.4.3.5 Results and interpretation

None of the three negative reaction controls (NTC_{PCR}, NTC_{RT}, and NRC) produced any amplicons, as expected. The NTC_{PCR} controlled for PCR reagent contamination with DNA fragments, the NTC_{RT} controlled for reverse transcription reagent contamination with RNA fragments, and the NRC controlled for genomic DNA contamination in the RNA preparation.

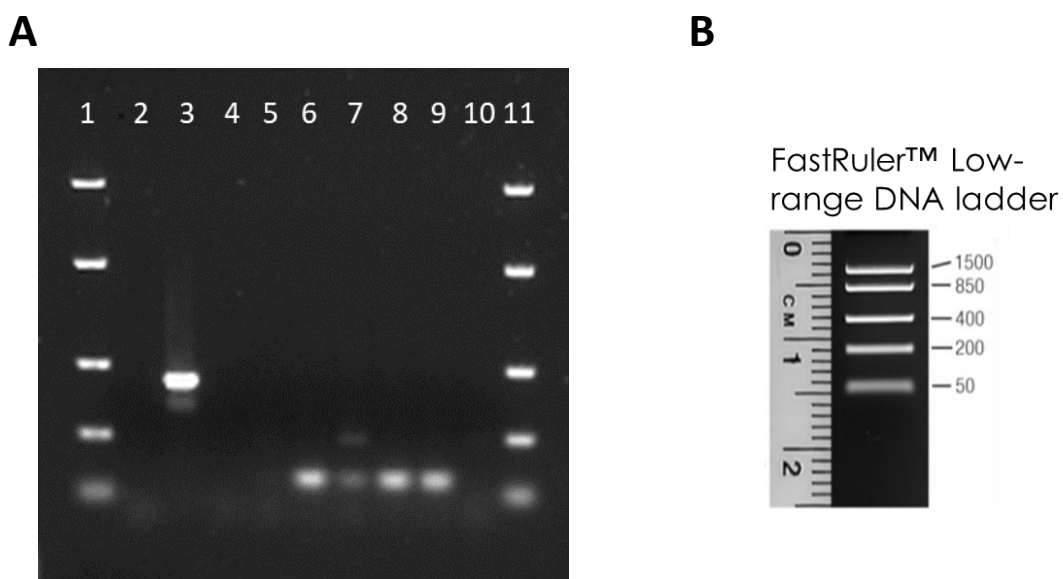


Figure 3.19: Gel image of CD4 cDNA PCR to assess the CD4-expressing construct in GHOST cells. (A) Lanes 1 and 11 were loaded with FastRuler™ LR DNA ladder shown in B for amplicon size estimation. Lanes 2 and 3 were loaded with the NTC_{PCR} and L32 PCR positive controls respectively. Lanes 4 and 5 were loaded with the NTC_{RT} and NRC reverse transcription controls respectively. Lanes 6-10 contained CD4 PCR products for TZM-bl (lane 6), PBMC (lane 7), Ghost CD4^{high} (lane 8), Ghost CD4^{low} (lane 9), and HEK293T (lane 10) cells.

The CD4 PCR was expected to yield a single amplicon of 67 bp from mRNA transcripts. Bands observed in TZM-bl cells, PBMCs, CD4^{high} Ghosts, and CD4^{low} GHOST cells were of the expected size (Figure 3.19). The CD4 expression negative control, HEK293T cells, did not amplify the desired band, although a faint band was observed ~200 bp. This additional ~200 bp band was also present in PBMCs.

The CD4 primers span the exon 2/intron/exon 3 boundary of the CD4 gene (Figure 3.20), which is a region of 186 bp including the intron and 67 bp excluding the intron. The band of approximately 200 bp in length fits with the size of the amplicon including the intron. It is therefore likely that the approximately 200 bp amplicons originate from transcripts which have not been completely processed. This is possible in cells producing low-levels of transcripts which are not translated into proteins⁴³ (possibly HEK293T cells), or in cells with a high turnover of CD4 resulting in abundant CD4 transcripts in varying stages of processing. The heterogenous population of PBMCs could fall into either category.

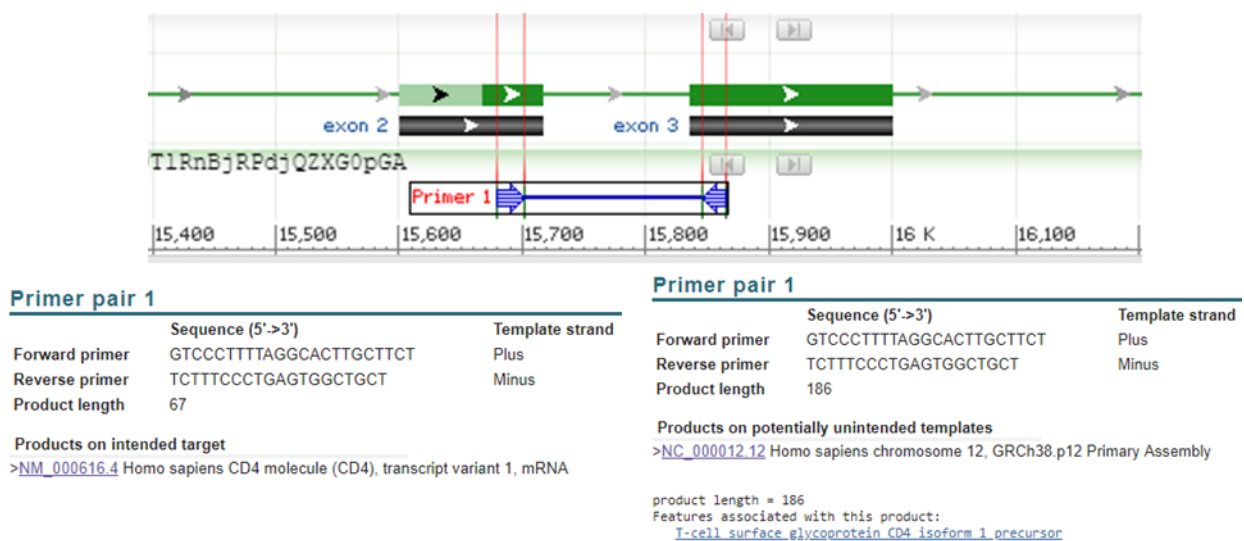


Figure 3.20: *In silico* CD4 mRNA transcript prediction explaining the presence of the 186 bp amplicon observed in HEK293T and PBMC mRNA pools assayed by RT-PCR.

Similar intensities of CD4 amplicons were observed for CD4^{low} and CD4^{high} GHOST cells, suggesting that insufficient expression of CD4 on the cell surface observed by flow cytometry was not due to CD4 construct destabilisation.

3.6.4.4 *Effect of dissociation and detection method on CD4 phenotype*

Since the GHOST cells sorted for CD4^{high} and CD4^{low} showed comparable expression of CD4 mRNA, the effect of cell culture treatment and detection methods on CD4 expression was investigated. The effects of cell culture and detection methods on CCR5 and CXCR4 were not explored as stable expression was observed regardless of GHOST cell stock and dissociation method used.

3.6.4.4.1 **Dissociation method investigation - rationale**

Virtual cleavage of the CD4 protein by trypsin (used in enzymatic dissociation) was performed using PeptideCutter⁴⁴ (open source: ExPASy, Swiss Institute of Bioinformatics, Switzerland). Trypsin is predicted to cleave human CD4 at 57 sites with probability of higher than 80%, and 62 sites in total based on protein sequence analysis using the SwissProt human CD4 protein sequence (ref: P01730). Two dissociation methods were investigated, enzymatic dissociation (described in 3.6.2.2.1 *Enzymatic dissociation*) and non-enzymatic dissociation (described in 3.6.2.2.2 *Non-enzymatic dissociation*). Preliminary results comparing enzymatic and non-enzymatic dissociation on multiple GHOST cell stocks using CD4-FITC indicated that trypsinised cells expressed less CD4. However, this preliminary finding was obscured by poor resolution of positive and negative populations using CD4-FITC.

3.6.4.4.2 **Detection method investigation – rationale**

As previously mentioned (3.6.4.2.1 *Sample preparation for phenotype*), detection of CD4 using CD4-FITC showed that positive and negative populations could not be resolved using an unstained control to set the positive region. As CD4 expression at the mRNA level and the protein expression level was discordant, the fluorochrome used to detect CD4 on GHOST cells was investigated. The discrepancy in detection of CD4 on aliquots of the same unsorted GHOST cells using CD4-FITC and CD4-APC is shown in Figure 3.21. The sequential gating strategy described in 3.6.3.5 *GHOST cell gating strategies* (Figure 3.15) was used to obtain the

data below. CD4-FITC was detectable using that same protocol as FITC is detected in the same channel as GFP on the Gallios™ (FL1).

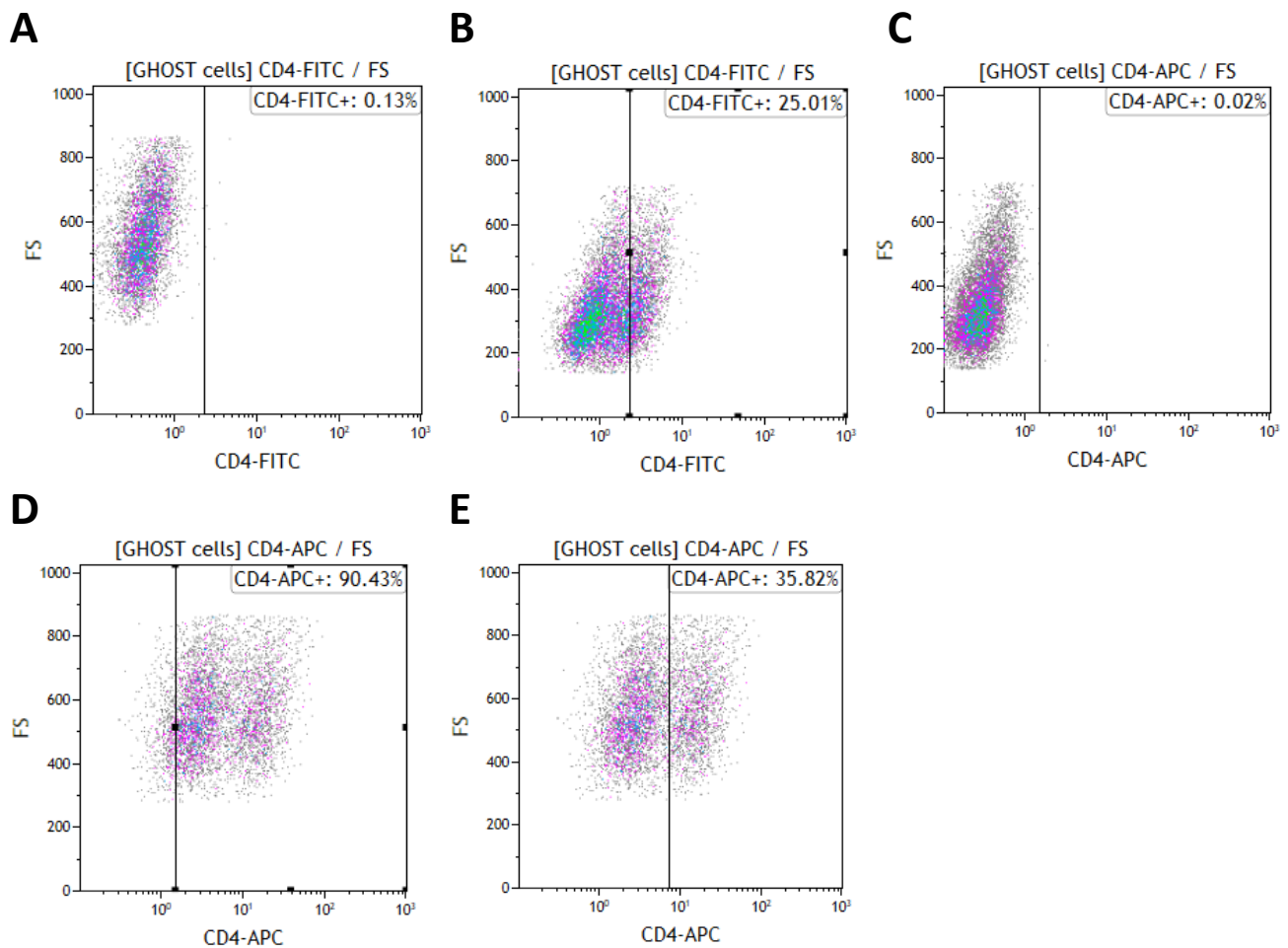


Figure 3.21: The discrepancy in CD4 detection between unsorted GHOST cells stained with CD4-FITC and CD4-APC. (A) Two-parameter FS Lin versus CD4-FITC plot unstained for CD4-FITC, used to set the “CD4-FITC+” region. (B) The same plot as A, using cells stained with CD4-FITC. (C) Two-parameter FS Lin versus CD4-APC plot unstained for CD4-APC used to set the “CD4-APC+” region. (D) The same plot as C, using cells stained with CD4-APC and the “CD4-APC+” region set on the unstained control. (E) The same plot as D, with the “CD4-APC+” region set on the division between the two populations of CD4-APC expression, as the “CD4-FITC+” region divides the two populations. The difference between D and E illustrates the need for an isotype control for CD4-APC, in order to correctly resolve the CD4⁺ population from the CD4⁻ population.

3.6.4.4.3 Fluorochrome comparison and CD4-recovery over time

Following preliminary results indicating that detection of CD4 on enzymatically dissociated GHOST cells was reduced compared to the detection of CD4 on non-enzymatically dissociated GHOST cells using CD4-FITC, a multi-parameter experiment was designed. This experiment simultaneously compared FITC and APC fluorochromes for the detection of CD4 on GHOST cells, and determined how long CD4 expression on trypsinised cells takes to recover. The rate of CD4 recovery on trypsinised GHOST cells was measured using CD4-FITC and CD4-APC in 24 hr intervals until a plateau in CD4 expression was reached.

Method

Five replicates of GHOST cells from different sources (Table 3.11) resuscitated from liquid nitrogen at different passages were analysed, including two replicates donated for this purpose by Dr Janine Scholefield (Council for Scientific and Industrial Research (CSIR), South Africa).

Table 3.11: Biological replicate (BR) designation of different GHOST cell stocks for the CD4 recovery and fluorochrome detection experiment.

Replicate	Passage	Source	Date frozen
BR1	P5	ICMM	09/03/2017
BR2	P8	ICMM	23/07/2017
BR3	P6	ICMM	29/06/2016
BR4	P15	CSIR	01/2017
BR5	P12	CSIR	08/09/2014

GHOST cells were thawed and cultured for one passage in 1 x T75 flask per culture as described in 3.6.2 *Cell culture and maintenance* in complete DMEM supplemented with puromycin, hygromycin, and G418. GHOST cells were then dissociated enzymatically as described in 3.6.2.2.1 *Enzymatic dissociation*. Cells were pelleted by centrifugation at 300 x g for 10 min, resuspended in 2 mL complete DMEM, and enumerated as described in 3.6.3.5 *GHOST cell gating strategies*. GHOST cells from each replicate were seeded at a density of 1.5×10^5 cells per well in 12-well plates, in 1 mL complete DMEM per well. Every 24 hr, two wells (R1 and R2) of each biological replicate were non-enzymatically dissociated as described in 3.6.2.2.2 *Non-enzymatic dissociation*. Dissociated cells were pelleted by centrifugation at 300 x g for 10 min, and resuspended in 200 μ L per tube (corresponding to each well). Each 200 μ L GHOST cell suspension was divided into two 100 μ L aliquots. One aliquot was stained with 3 μ L each of 7-AAD and CD4-FITC, and the other aliquot was stained with 3 μ L each of 7-AAD and CD4-APC. The CD4-APC-stained tube was used as an unstained tube for CD4-FITC, and vice-versa, to set the regions “CD4-FITC+” and “CD4-APC+”, respectively. The gating strategy used to perform flow cytometric analysis was described in 3.6.3.5 *GHOST cell gating strategies* and 3.6.4.4.2 *Detection method investigation – rationale* (Figure 3.21).

Results and outcome

The average CD4 recovery over time assessed by CD4-APC (Figure 3.22) and CD4-FITC (Figure 3.23) illustrates (i) improved detection of CD4 with a brighter fluorochrome (APC), (ii) CD4 expression recovers post-trypsinisation, and (iii) that non-enzymatic dissociation is an alternative to enzymatic dissociation which retains cell surface CD4 for flow cytometric detection.

Contrasting the detection of CD4 based on unstained controls for two fluorochromes highlights the importance of selecting fluorochromes specific to the sample of interest. CD4-FITC analysis indicated that GHOST cells expressing CD4 peaked between 20-60%, where CD4-APC analysis indicated that GHOST cells expressing CD4 was not significantly reduced by enzymatic dissociation and reached plateaus above 99%.

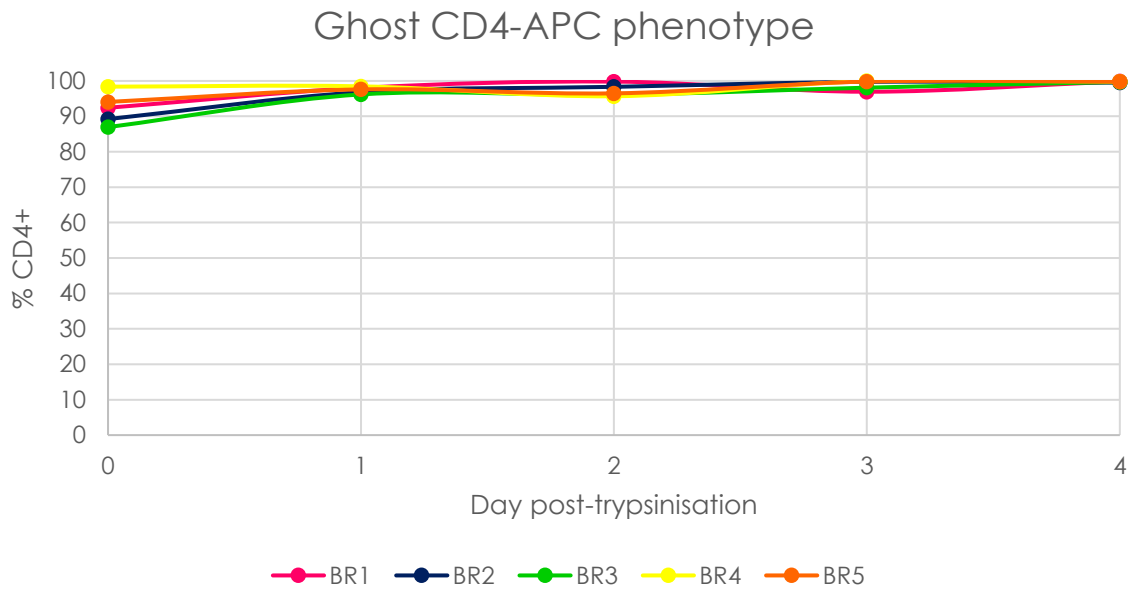


Figure 3.22: CD4 recovery on five biological replicates (BR) of GHOST cells post-trypsinisation, detected using CD4-APC.

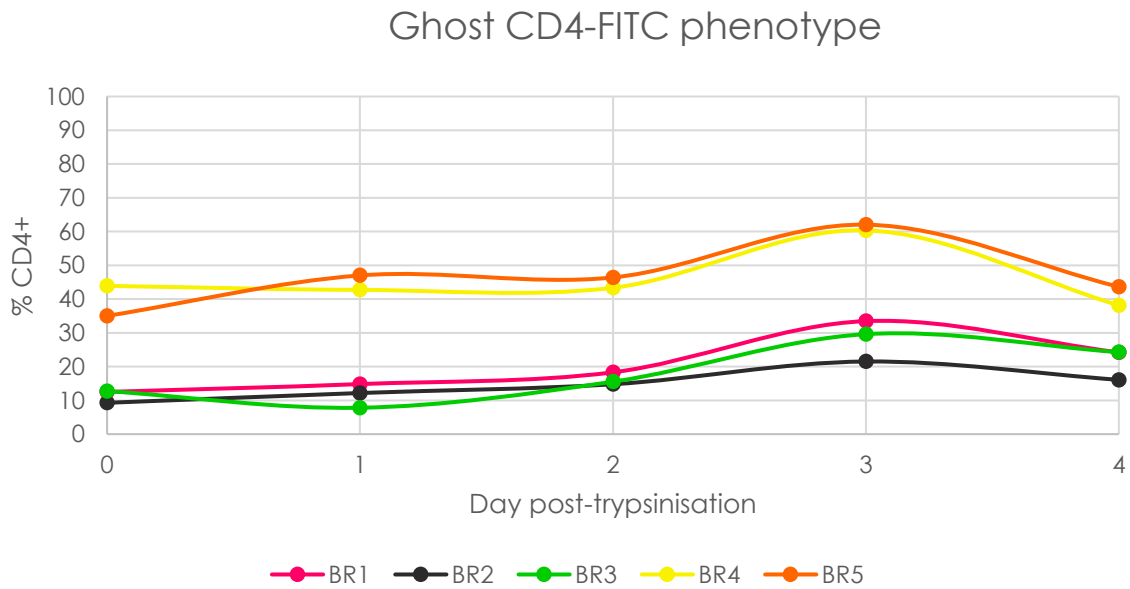


Figure 3.23: CD4 recovery on five biological replicates (BR) of GHOST cells post-trypsinisation, detected using CD4-FITC.

3.6.4.5 Validation of CD4 expression on CD4^{high} GHOST cells

Low-passage CD4^{high} GHOST cells were resuscitated, cultured, and sorted as described in 3.6.3.6 *GHOST cell sorting* for all future GHOST GFP assays and HIV experiments using GHOST cells. The stability of CD4 expression on CD4^{high} GHOST cells during culture and dissociation was validated using a slightly modified version of the CD4 recovery over time assay (described in 3.6.4.4.3 *Fluorochrome comparison and CD4-recovery over time*). CD4^{high} GHOST cells were thawed and cultured for one passage (described in 3.6.2 *Cell culture and maintenance*), and dissociated enzymatically prior to enumeration as described in 3.6.3.5 *GHOST cell gating strategies*.

3.6.4.5.1 Effect of dissociation method on CD4^{high} GHOST cell CD4

Method

One hundred and fifty thousand (1.5×10^5) dissociated CD4^{high} GHOST cells per well were seeded at P3 in complete DMEM (3 mL complete DMEM per well) in a 6-well plate. After three days in culture in complete DMEM at 37°C, 5% CO₂, three wells were dissociated enzymatically using 500 µL trypsin, and the remaining three wells were dissociated non-enzymatically using 500 µL NEDB. Trypsinised and NEDB-dissociated CD4^{high} GHOST cells were pooled by dissociation method, and cells were pelleted by centrifugation at 300 x g for 10 min. The pellets were each resuspended in 1 mL complete DMEM, and analysed for CD4 expression as described in 3.6.3.5 *GHOST cell gating strategies*. Two 100 µL aliquots were stained for each dissociation method. The first aliquot was stained with 3 µL each of 7-AAD and CD4-APC iso, and the second was stained with 3 µL each of 7-AAD and CD4-APC as described in 3.6.3.5.1 *Sample preparation*.

Results and outcome

Figure 3.24 shows the difference between enzymatically (Figure 3.24C and D) and non-enzymatically (Figure 3.24A and B) dissociated CD4^{high} GHOST cells. There was no significant difference in detection of CD4⁺ CD4^{high} GHOST cells dissociated enzymatically or non-

enzymatically, although CD4 on non-enzymatically dissociated cells was more clearly not affected by dissociation.

CD4 expression on CD4^{high} GHOST cells shows two distinct subpopulations. While the reasons for the presence of these subpopulations were not experimentally explored, these populations could result from recently divided cells (less CD4) and cells about to divide (more CD4) due to the accumulation of forced CD4 expression. To evaluate this, CD4 expression and cell cycling could be co-analysed using a nuclear stain or proliferation-associated proteins.

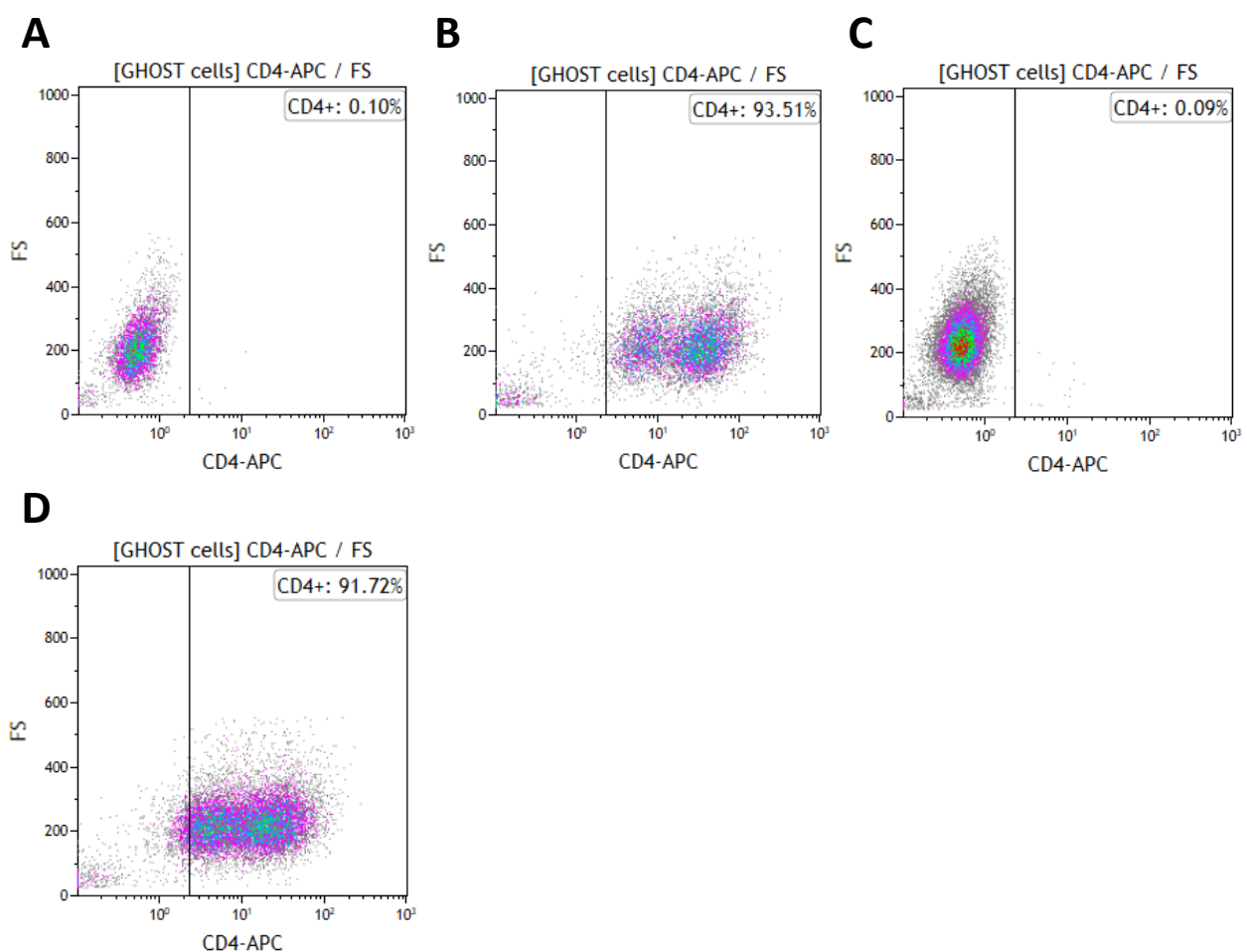


Figure 3.24: Effect of dissociation method on CD4 detection of sorted CD4^{high} GHOST cells. (A) A two-parameter FS Lin versus CD4-APC plot used to set the “CD4+” region on non-enzymatically dissociated CD4^{high} GHOST cells stained with CD4-APC iso. (B) The same two-parameter plot as in A, for non-enzymatically dissociated CD4^{high} GHOST cells stained with CD4-APC. (C) A two-parameter FS Lin versus CD4-APC plot used to set the “CD4+” region on enzymatically dissociated CD4^{high} GHOST cells stained with CD4-APC iso. (D) The same two-parameter plot as in C, for enzymatically dissociated CD4^{high} GHOST cells stained with CD4-APC.

3.6.4.5.2 CD4 recovery in culture on sorted CD4^{high} GHOST cells

Method

Enzymatically dissociated CD4^{high} GHOST cells remaining from 3.6.4.5.1 *Effect of dissociation method on CD4^{high} GHOST cell CD4* were seeded at 1.5×10^5 cells per well in 3 mL complete DMEM in a 6-well plate. At three time points post-trypsinisation and seeding (24 hr, 48 hr, and 72 hr), two wells were non-enzymatically dissociated using 500 μ L NEDB (described in 3.6.4.4.3 *Fluorochrome comparison and CD4-recovery over time*). Dissociated cells were pelleted by centrifugation at 300 x g for 10 min and resuspended in 200 μ L PBS per tube, and split into two 100 μ L aliquots. The first aliquot was stained with 3 μ L each of 7-AAD and CD4-APC iso, and the second aliquot was stained with 3 μ L each of 7-AAD and CD4-APC, as described in 3.6.3.5 *GHOST cell gating strategies*. The proportion of CD4⁺ CD4^{high} GHOST cells was determined by flow cytometry as described in 3.6.3.5.2 *Gating strategy*.

Results and outcome

The results of the CD4 recovery assay on CD4^{high} GHOST cells are shown in Table 3.12. While enzymatic dissociation (trypsinisation) does have an effect on the CD4 expressed by CD4^{high} GHOST cells, more than 90% of these cells still express CD4. Furthermore, the expression of CD4 on CD4^{high} GHOST cells recovers to an average of 98.16% within 24 hr, 99.24% within 48 hr, and 98.97% within 72 hr of trypsinisation. CD4^{high} GHOST cells are therefore validated for stable CD4 expression despite enzymatic dissociation, and are optimal for use in GHOST GFP assays for HIV titration within 24 hr of seeding post-trypsinisation. All GHOST cell experiments were therefore performed with CD4^{high} sorted GHOST cells thawed, cultured, and passaged as described in 3.6.2 *Cell culture and maintenance*, and phenotyped for CD4 as described in 3.6.3.5 *GHOST cell gating strategies* prior to seeding for experiments. The acceptable level of viable, intact CD4-expressing CD4^{high} GHOST cells was $\geq 90\%$ for CD4^{high} GHOST cells seeded for experiments.

Table 3.12: CD4 recovery (indicated as %) post-trypsinisation of CD4^{high} GHOST cells.

	Time post-trypsinisation			
	0 hr	24 hr	48 hr	72 hr
R1	93.44	97.88	99.32	99.11
R2	NA	98.44	99.15	98.83
Average	NA	98.16	99.24	98.97

*R1 and R2 indicate two replicate wells dissociated at each time point.

3.6.5 GHOST green fluorescent protein assay optimisation

3.6.5.1 Introduction

The GHOST GFP assay is used for HIV titration and functional HIV tropism studies, and the protocol is quite standard^{9, 45}. Fundamentally, protocols recommend seeding 2.5×10^4 GHOST cells per well of 12-well plates in 1 mL complete DMEM per well. GHOST cells are allowed to adhere for 24 hr prior to infection, which are performed in duplicate serial dilutions. To sediment virus, it is recommended that infections are performed in the presence of 20 µg/mL Polybrene[®] for 2-18 hr, in a final volume of 300-500 µL. It is advised that the medium be changed to complete DMEM when the 2-18 hr exposure time is over. Protocols recommend that GFP expressed by HIV-infected cells be assayed 48-72 hr after exposure, by enzymatically dissociating HIV-exposed cells and pooling duplicate wells. Infectious titre is then determined by Equation 3.2, using a cell count obtained on the day of assaying GFP^{9, 46}.

Starting with the susceptibility of GHOST cells exposed to HIV for the purpose of functional titration (described in 3.6.4.1 *GHOST cell CD4 expression*), the GHOST GFP assay described in the literature was dissected to improve the reliability of functional titration. Aspects of the GHOST GFP assay which could contribute to variance between titrations were identified from Equation 3.2 to improve the statistical confidence in infectious titre estimations. These aspects included pooling of technical replicates, Polybrene[®] concentrations, and cell counts

and seeding density. The optimised GHOST GFP assay is described in 3.6.6 *GHOST green fluorescent protein* assay – method.

3.6.5.2 *Dissection of variables*

3.6.5.2.1 **Replicates and pooling**

GHOST GFP assay protocols recommend pooling duplicate wells exposed to the same virus dilution on the day of assay. Practically, this pooling is a way of averaging data before analysis to compensate for differences between wells of the same dilution. However, pooling cells before analysis could mask human error and skew results of the GHOST GFP assay. To improve confidence in GHOST GFP assay titrations with statistical measures such as standard deviation, infections were performed in triplicate and GFP assayed separately for each well. This way, outliers in the triplicate could be excluded from further analyses and the titre would not be skewed due to averaging prior to analysis. At least two wells of each dilution were required to calculate infectious titre, otherwise the GHOST GFP assay was repeated.

3.6.5.2.2 **Polybrene® concentrations**

Polybrene concentrations were adjusted from 20 µg/mL to 5-10 µg/mL, as literature reported that the plateau of Polybrene® efficiency on adherent cell lines was between 5-10 µg/mL⁴⁷. Molecular clones of HIV-1B produced in HEK293T cells (4.3 *Molecular clone production*) were titrated in the presence of 5 µg/mL Polybrene® as the initial infection volume was halved compared to PBMC-propagated HIV-1C isolates. PBMC-propagated HIV-1C isolates were titrated in 500 µL initial volume with 10 µg/mL Polybrene®. Visibly less cell death was observed in the uninfected control wells on day 3 of the GHOST GFP assay when Polybrene® concentrations were adjusted lower than recommended by standard protocols.

3.6.5.2.3 **Cell counts and seeding density**

Calculating infectious titre according to Equation 3.2 rests heavily on the number of cells exposed to virus dilutions. Error in infectious titre estimation due to assumptions made by

standard protocols are the result of two factors, namely seeding density, and cell proliferation between seeding and GFP detection.

While establishing the GHOST GFP assay and learning to culture the cells, it was observed that GHOST cells seeded in 12-well plates at densities of 2.5×10^4 and 1.5×10^5 cells per well reached similar levels of confluence over the same time course. This observation suggested that a lower seeding density may correspond to an increased proliferation rate in GHOST cells seeded for the GHOST GFP assay. Cell proliferation is a source of compound error in functional titrations as the rate of cell division between neighbouring cells is not necessarily similar. This error is exponentially increased in wells seeded at lower densities which reach similar confluence over three days as wells seeded at higher densities due to increased proliferation which must have occurred to achieve this. To limit error as a result of cell proliferation, the higher seeding density (1.5×10^5 cells per well) was used to seed CD4^{high} GHOST cells for GHOST GFP assays.

As a consequence of cell proliferation between seeding cells for the GHOST GFP assay and the day of GFP analysis, the absolute count used to calculate infectious titre, and the day of GFP analysis was explored. The absolute cell count used in Equation 3.2 reflects the number of cells which could have been infected by virus to be titrated. This was determined to be on the day of infection rather than the day of GFP assay, hence the introduction of “count” wells (see 3.6.6.2 *Day 1 count and infection*). The day of assay was determined by independently establishing growth curves for two stocks (A and B) of GHOST cells over a four-day time course.

GHOST stocks were thawed, cultured for one passage, and enzymatically dissociated as described in 3.6.2 *Cell culture and maintenance*. Dissociated cells were enumerated as described in 3.6.3.5 *GHOST cell gating strategies* and seeded at 1.5×10^5 cells in 1 mL DMEM per well of 12-well plates. Triplicate wells of each seeding stock were enzymatically dissociated (described in 3.6.2.2.1 *Enzymatic dissociation*) at 24 hr, 72 hr, and 96 hr post-seeding (day 1, 3, and 4 post-seeding) and enumerated by flow cytometry as described in 3.6.3.3.2 *General enumeration*. Briefly, dissociated cells were pelleted by centrifugation at 300 x g for 10 min and resuspended in 100 μ L PBS. Cells were stained with 3 μ L 7-AAD for

5 min in the dark before adding 100 μ L Flow-Count™ and 400 μ L PBS and analysing on the Gallios™. Table 3.13 shows the absolute counts of live, intact GHOST cells obtained as described in 3.6.3.5 *GHOST cell gating strategies*.

Figure 3.25 shows growth curves for GHOST cell stock A, B, and an average of A and B, derived from Table 3.13. The reproducibility of absolute counts between seeding stocks up to day 3 indicated reliability of the growth curve. The standard deviation reported for each triplicate is lower for day 1 and day 3 counts than for day 4 counts, where the absolute cell counts are visibly different between triplicates (Figure 3.25). For the GHOST GFP assay, enough time should be allowed for (i) HIV-infected cells to produce GFP, while (ii) maintaining reproducibility based on growth curves. For this reason, the latest time point where absolute counts were reliable (day 3 post-seeding) was used for GFP detection in the GHOST GFP assay.

Table 3.13: GHOST cell proliferation assayed in triplicate at three time points for two stocks of GHOST cells.

DAY	ID	Cells/well	Average count	Standard deviation
DAY 1	A_R1	222 333.64	218 884.82	20 221.84
	A_R2	197 170.46		
	A_R3	237 150.34		
DAY 3	A_R1	630 890.97	815 671.77	160 036.7
	A_R2	910 010.55		
	A_R3	906 113.80		
DAY 4	A_R1	808 543.99	828 221.82	174 815.8
	A_R2	1 012 043.90		
	A_R3	664 077.56		
DAY 1	B_R1	248 382.76	249 792.49	1739.82
	B_R2	251 736.89		
	B_R3	249 257.81		
DAY 3	B_R1	788 995.97	803 153.50	8675.02
	B_R2	724 352.04		
	B_R3	896 112.48		
DAY 4	B_R1	893 374.37	972 687.37	155 142.8
	B_R2	873 234.67		
	B_R3	1 151 453.08		

*R1, R2, and R3 are triplicate wells assayed individually at each time point.

GHOST cell growth curves for GHOST GFP assay optimisation

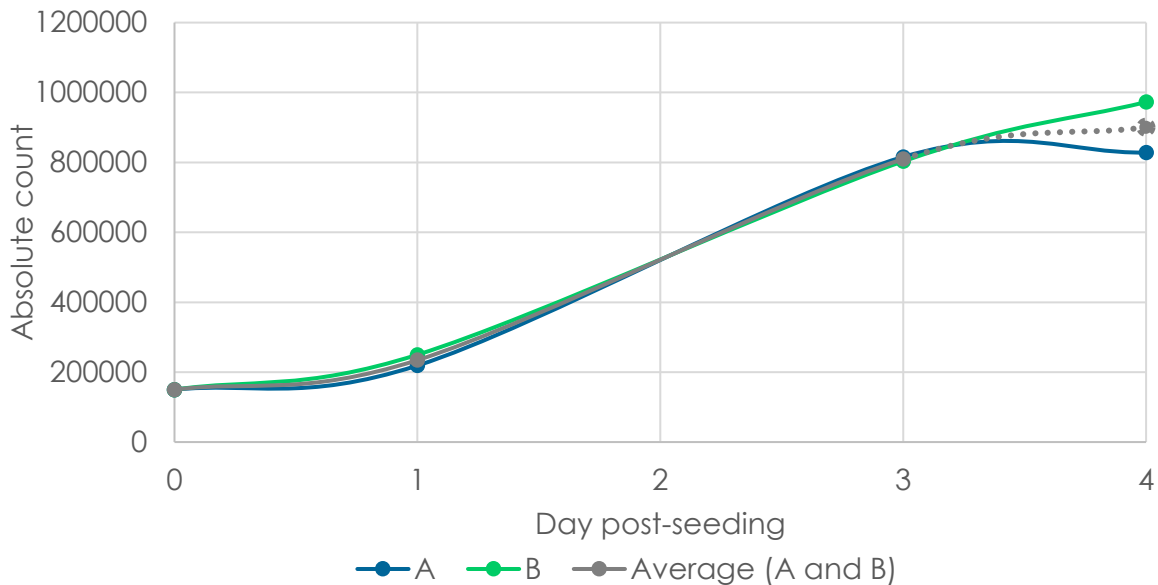


Figure 3.25: GHOST cell growth curves for GFP assay optimisation showing average cell counts of triplicate wells for two stocks (A and B) of GHOST cells assayed at three time points.

3.6.6 GHOST green fluorescent protein assay – method

Functional titration of HIV using the GHOST GFP assay was achieved by making serial dilutions of viral preparations and exposing HIV-susceptible CD4^{high} GHOST cells to the various viral suspension dilutions (Figure 3.26). Infectious titre was determined by relating the number of infected GHOST cells expressing GFP across dilutions, to the dilution factor. As the limiting dilution is approached, the accuracy of titration is improved as viral particles rather than cell number become the limiting factor. Both primary isolates of HIV-1C and molecular clones of HIV-1B were titrated using the GHOST GFP assay.

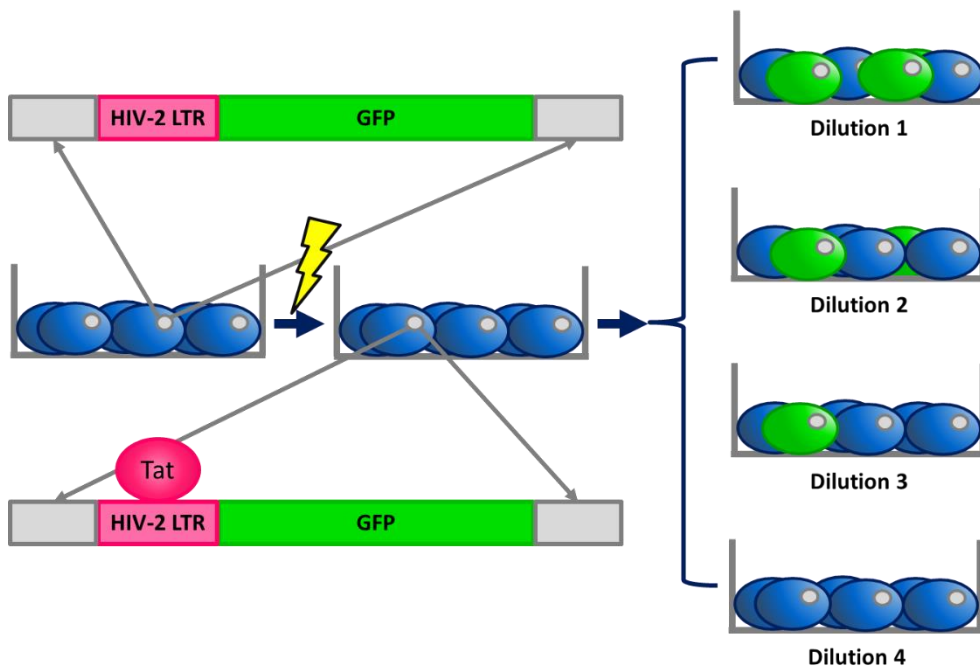
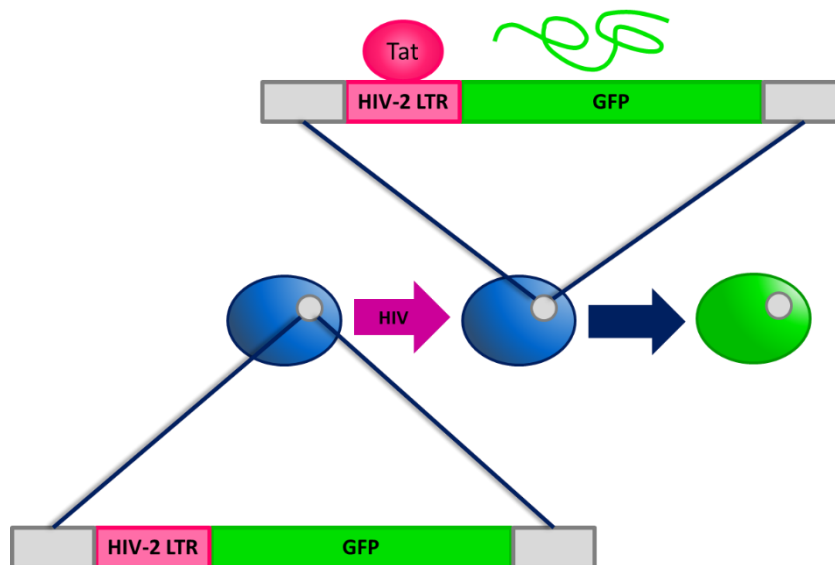
A**B**

Figure 3.26: Functional titration of HIV on GHOST cells by limiting dilution, based on GFP expression in HIV-infected GHOST cells. (A) Functional titration of HIV by exposing a known number of GHOST cells to known dilutions of virus (dilution 1 being the least dilute and dilution 4 being the most dilute). HIV-infected cells are detected by the expression of GFP (green cells), detectable 48 hr post-infection. (B) Transcription of the HIV-2 LTR-driven GFP transgene in GHOST cells, activated by the binding of Tat from infecting HIV-1 to the HIV-2 LTR, resulting in the expression of GFP in HIV-infected cells.

3.6.6.1 Preparation of CD4^{high} GHOST cells for infection

CD4^{high} GHOST cells were thawed, cultured to confluence for one passage, and enzymatically or non-enzymatically dissociated as described in 3.6.2 *Cell culture and maintenance*. Cells were enumerated as described in 3.6.3.3 *Enumeration* and 3.6.3.5 *GHOST cell gating strategies*. The GHOST GFP assay was performed in 12-well plates (Greiner Bio-One, Austria) at a seeding density of 1.5×10^5 cells per well in 1 mL complete DMEM. Seeded CD4^{high} GHOST cells were allowed to attach for 24 hr prior to infection. The plate layout for the GHOST GFP assay is indicated in Figure 3.27.

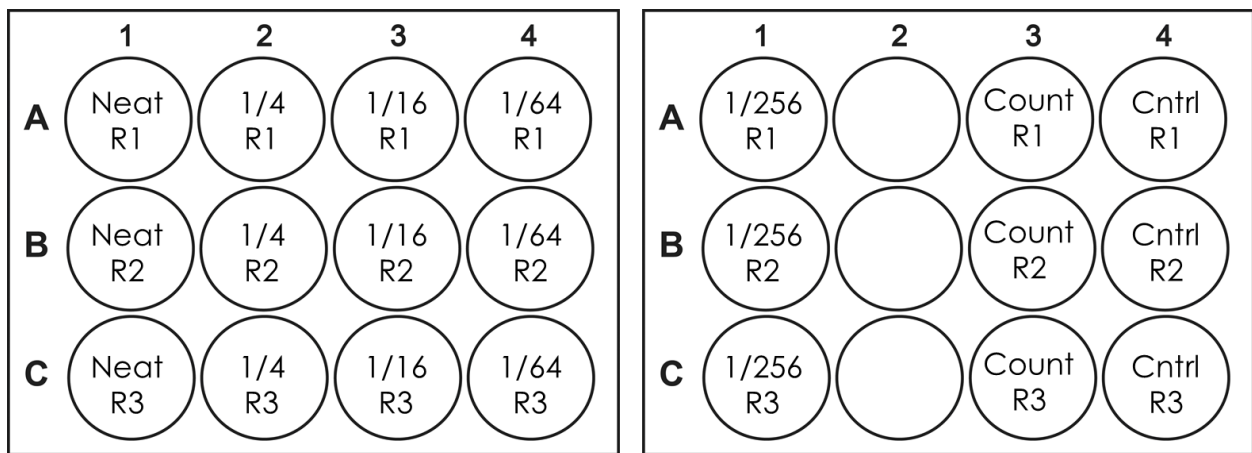


Figure 3.27: GHOST GFP assay plate layout. Dilutions of HIV to be added to each well are indicated in the wells. Empty wells contained 1 mL PBS. R1-3 represent technical replicates.

3.6.6.2 Day 1 count and infection

3.6.6.2.1 Day 1 count

The absolute counts of three wells seeded for the GHOST GFP assay (“Count” wells; Figure 3.27) were determined on day 1 of the GHOST GFP assay (day of infection). The cells in the “Count” wells were dissociated by aspirating the culture medium, rinsing the wells with 500 μ L PBS, aspirating the PBS, and dissociated with 200 μ L trypsin per well as described in 3.6.2.2.1 *Enzymatic dissociation*. Dissociated cells were pelleted by centrifugation at 300 x g

for 10 min, and the pellet was resuspended in 100 μ L PBS for enumeration as described in 3.6.3.3 *Enumeration* and 3.6.3.5 *GHOST cell gating strategies*.

3.6.6.2.2 Infection

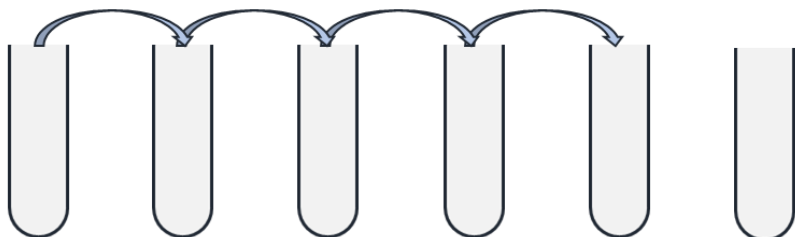
After day 1 counts were done, infections were performed overnight in the presence of Polybrene[®] (Sigma Aldrich, USA). Polybrene[®] is a branched cationic polymer which is used as an infection- or transduction-enhancing reagent⁴⁸. The mechanism of action is two-fold, the first being charge-shielding on the target cell membrane, and the second being aggregation of virus particles, facilitating their sedimentation⁴⁷. Multiple branches of positive charges allow Polybrene[®] to interact with the net negative charge on the plasma membrane of cells, resulting in regions of reduced negative charge. These islands of reduced negative charge facilitate the adsorption of negatively charged virus particles to the plasma membrane because of reduced like-charge repulsion between viral particles and the cell plasma membrane. This adsorption improves access to cell-surface receptors required for receptor-mediated virus entry⁴⁷. High molecular weight branched cationic polymers such as Polybrene[®] serve as sedimentation agents by interacting with negatively charged virus and forming virus/Polybrene[®] aggregates with sufficient molecular weight to sink down towards cells in suspension, which sink to the bottom of culture ware over time⁴⁷. This critically reduces the distance between virus and cells, which would otherwise be separated by volume due increased sedimentation of larger, heavier cells compared to much smaller, lighter virus. The use of Polybrene[®] as a sedimentation agent eliminates the requirement for spinoculation (centrifugation to bring cells closer to virus) or agitation during infection⁴⁷.

Infections were conducted in triplicate using HIV cell-free supernatant (HIV CFS), of which 1/4 serial dilutions were prepared in 15 mL centrifuge tubes. Serial dilutions ranged from neat (undiluted) virus to 1/256 dilutions (Figure 3.27). An HIV-unexposed control was also included in triplicate (“Cntrl” wells, Figure 3.27). The preparation of serial dilutions is summarised in Figure 3.28. To perform infections, medium was aspirated from GHOST GFP assay wells and replaced with the appropriate volume of HIV serial dilution as described below. Cells were incubated with the indicated volumes of HIV dilutions for 2 hr at 37°C, 5% CO₂ before topping the volume up to a final volume of 1 mL with complete DMEM.

The production protocols for HIV-1B molecular clones and HIV-1C primary HIV isolates differed (Chapter 4 *Human immunodeficiency virus production*). HIV-1B isolates were harvested in 8 mL batches of CFS, whereas HIV-1C isolates were harvested in 20-60 mL batches of CFS. In order to maximise smaller harvests, HIV-1B was titrated in half the volume compared to HIV-1C, reflected in Figure 3.28. Polybrene[®] concentrations were therefore halved in HIV-1B titrations, as half the sedimentation effect was required due to the initial infection volume being halved. Infections were performed in the presence of 20 µg/mL Polybrene[®] for 2 hr, and reduced to 5 µg/mL for HIV-1B and 10 µg/mL for HIV-1C isolates respectively, when the medium was topped up to 1 mL. Furthermore, dilutions for HIV-1B and HIV-1C GHOST GFP assays were performed in DMEM and RPMI, respectively. This was because HIV-1B molecular clones were harvested from cells grown in DMEM, and HIV-1C primary isolated were harvested from cells grown in RPMI.

At 24 hr post-infection, HIV-containing supernatants were aspirated from wells and replaced with 1 mL complete DMEM. Due to the susceptibility of GHOST cells to HIV, 24 hr is the recommended exposure time for virus entry to occur⁴⁶. Remaining non-infectious viral particles were removed after 24 hr as they may still contain Tat which can penetrate cells without infection and cause GFP expression in uninfected GHOST cells⁴⁹.

Dilution series:



	Tube 1	Tube 2	Tube 3	Tube 4	Tube 5	Tube 6
Dilution factor	Neat	1/4	1/16	1/64	1/256	Cntrl
Volume medium		1875µL/ 937.5µL	1875µL/ 937.5µL	1875µL/ 937.5µL	1875µL/ 937.5µL	2500µL/ 1250µL
Starting volume HIV	2500µL/ 1250µL					
Volume HIV transferred	625µL/ 312.5µL	625µL/ 312.5µL	625µL/ 312.5µL	625µL/ 312.5µL		
Final volume	1875µL/ 937.5µL	1875µL/ 937.5µL	1875µL/ 937.5µL	1875µL/ 937.5µL	2500µL/ 1250µL	2500µL/ 1250µL
Polybrene (20 mg/mL stock)	1.88µL/ 0.94µL	1.88µL/ 0.94µL	1.88µL/ 0.94µL	1.88µL/ 0.94µL	2.5µL/ 1.25µL	2.5µL/ 1.25µL
Volume per well (x3)	500µL/ 250µL	500µL/ 250µL	500µL/ 250µL	500µL/ 250µL	500µL/ 250µL	500µL/ 250µL

Figure 3.28: Illustration of the preparation of dilution series employed for the GHOST GFP assay. Blue values indicate volumes used for HIV-1C primary HIV-1 isolate titrations, and green values indicate volumes used for HIV-1B molecular clone titrations. Dilution series were prepared by adding medium to each tube (2-6) as indicated, then adding the starting volume of HIV to tube 1, and transferring the volumes of HIV indicated from tube 1 to tube 5 (illustrated by the dilution series tube transfer diagram). Polybrene® was added to a concentration of 20 µg/mL, and the volumes of each dilution (last row) were dispensed into the corresponding wells illustrated in Figure 3.27.

3.6.6.3 Green fluorescent protein detection

GFP expression in HIV-exposed GHOST cells was analysed on day 3 of the GHOST GFP assay (48 hr post-infection). Culture medium (supernatant) was collected into separate, labelled 2 mL microcentrifuge tubes (Eppendorf, Germany). Cells were dissociated enzymatically as described in 3.6.2.2.1 *Enzymatic dissociation* and 3.6.6.2.1 *Day 1 count* and pooled with their corresponding supernatants. Each well was rinsed with 400 µL PBS to collect any remaining

dissociated cells, which was pooled with the matching cell suspension. Cells were pelleted by centrifugation at 300 x g for 10 min. The supernatants were aspirated, and the cells were fixed by resuspending each pellet in 300 µL of 0.22 µm sterile-filtered intracellular (IC) fixation buffer (fixation buffer; ThermoFisher Scientific, USA). Cell suspensions were fixed by incubation for 10 min at 4°C, as per manufacturer's instructions.

Fixation buffer contains formaldehyde which penetrates cells and cross-links proteins, which preserves proteins from degradation over time and preserves protein localisation at the time of fixation^{50, 51}. Cells were fixed prior to analysing to (i) preserve GFP present in cells at the time of fixation, and (ii) render any possible HIV particles non-infectious due to the cross-linking of envelope proteins required for infection. After incubation, the fixation buffer was removed by adding 1 mL PBS to each tube, followed by centrifugation at 300 x g for 10 min. The supernatants were aspirated, and cells were resuspended in 400 µL PBS per tube before transferring the cell suspensions to correspondingly-labelled flow cytometry tubes (Beckman Coulter, USA). Fixed GHOST cells were evaluated for GFP expression by flow cytometry as described in 3.6.3.5.2 *Gating strategy*.

3.6.7 Results, calculations, and statistical considerations

3.6.7.1 *Flow cytometry*

The gating strategy used for counts and GFP analysis was described in 3.6.3.5 *GHOST cell gating strategies* (Figure 3.15).

3.6.7.2 *Statistical considerations*

Percentage GFP⁺ GHOST cells were averaged over triplicates for each dilution, excluding data points which caused the standard deviation to be greater than 10% of the mean. Means per triplicate were related to titre for each dilution by Equation 3.2. An average titre, measured in infectious units (IU) per unit volume of HIV CFS, was calculated using three consecutive dilution means where the calculated IU/mL fall within the same log value. The day 1 count

calculations (described in 3.6.6.2.1 *Day 1 count*) are summarised in Table 3.14. A breakdown of the IU/mL spreadsheet calculation is shown in Table 3.15, and an example of IU/mL determination of HIV-1C isolate SW7-010818 is shown in Table 3.16.

Equation 3.2: Infectious titre calculation using the GHOST GFP assay. IU refers to infectious units of virus.

$$\frac{IU}{mL} = \frac{cells}{mL} \times \frac{\%GFP\ positivity}{100} \times dilution\ factor$$

Table 3.14: Calculations used to obtain Day 1 absolute counts of HIV-unexposed GHOST cells. GHOST count, number of beads, and calibration factor were obtained as described in 3.6.3.5 *GHOST cell gating strategies* (Figure 3.15). Absolute counts were calculated according to Equation 3.1 as described in 3.6.3.3.2 *General enumeration*.

ID	GHOST count [A]	Number of beads [B]	Calibration factor [C]	Cells/ μ L [D]	Suspension volume (μ L)	Absolute cell count [E]	Mean absolute count [F]	Standard deviation [G]	% Standard deviation of mean
Day 1 Count R1	Events in GHOST cell region	Events in Cal region	Number of beads per μ L Flow-Count™	$\left(\frac{A}{B}\right) \times C$	100	$D \times 100$	$\frac{\sum(E)_{R1,R2,R3}}{n}$	$\sqrt{\frac{\sum(E_{Rx} - F)^2}{n - 1}}$	$\frac{G}{F} \times 100$
Day 1 Count R2	Events in GHOST cell region	Events in Cal region	Number of beads per μ L Flow-Count™	$\left(\frac{A}{B}\right) \times C$	100	$D \times 100$			
Day 1 Count R3	Events in GHOST cell region	Events in Cal region	Number of beads per μ L Flow-Count™	$\left(\frac{A}{B}\right) \times C$	100	$D \times 100$			

*R1, R2, and R3 refer to three technical repeats; n refers to the number of technical repeats used in calculations.

Table 3.15: Breakdown of calculations performed on Day 3 to obtain IU/mL (derived from Equation 3.2) from functional titration in the GHOST GFP assay.

ID	%GFP/100 [a]	Mean [b]	Normalised mean [c]	Dilution factor [d]	IU [e]	IU/mL [f]	Mean IU/mL
Day 3 Control/Dilution R1	a_{R1}	$\frac{\sum[a]_{R1,R2,R3}}{n}$	$[b] - [b]_{control}$	Dilution factor (1, 4, 16, 64, or 256)	$F \times c$ $\times d$	$e \times v$	Average of two to three consecutive dilutions (if possible) yielding an IU/ mL within one Log of each other.
Day 3 Control/Dilution R2	a_{R2}						
Day 3 Control/Dilution R3	a_{R3}						

* v refers to the proportion of 1 mL in which the initial 2 hr infection was performed; $v_{HIV-1B} = 1000 \mu\text{L} / 250 \mu\text{L} = 4$; $v_{HIV-1C} = 1000 \mu\text{L} / 500 \mu\text{L} = 2$. n indicates the number of technical repeats used to calculate the mean. F refers to the mean absolute count of GHOST cells exposed to HIV (Table 3.14).

Table 3.16: Example of an IU/mL calculation with real data obtained for the GHOST GFP assay of HIV-1C primary isolate SW7_010818. The green block indicates the mean day 1 cell count used in further calculations, pink blocks indicate the three closest IU/mL values used to calculate the average, and blue blocks indicate values excluded from further calculations.

PART 1: Day 1 Count								
	GHOST count	Cal	Cal factor	Cells/uL	uL	Abs count	Mean	Stdev
Day 1 count R1	10178	7085	1014	1456.67	100	145667	179398.56	2167.97
Day 1 count R2	10058	5734	1014	1778.66	100	177866		
Day 1 count R3	9978	5592	1014	1809.32	100	180932		
PART 2: Day 3 GFP Assay								
	%GFP	%GFP/ 100	Mean	Normalised mean	Stdev (norm)	Dilution factor	IU/ 500uL	IU/mL
Day 3 control R1	0.13	0.0013	0	0	0	0.00	0	0
Day 3 control R2	0.08	0.0008						
Day 3 control R3	0.13	0.0013						
Day 3 neat R1	52.96	0.5296	0.5448	0.54	0.02	1	97742.32	195484.63
Day 3 neat R2	54.28	0.5428						
Day 3 neat R3	56.21	0.5621						
Day 3 1/4 R1	36.83	0.3683	0.3503	0.35	0.02	4	251349.34	502698.68
Day 3 1/4 R2	32.24	0.3224						
Day 3 1/4 R3	36.01	0.3601						

Day 3 1/16 R1	6.84	0.0684	0.0727	0.07	0.01	16	208580.73	417161.45
Day 3 1/16 R2	7.06	0.0706						
Day 3 1/16 R3	7.90	0.0790						
Day 3 1/64 R1	1.94	0.0194	0.0215	0.02	0.00	64	246852.42	493704.84
Day 3 1/64 R2	2.06	0.0206						
Day 3 1/64 R3	2.45	0.0245						
Day 3 1/256 R1	0.75	0.0075	0.0071	0.01	0.00	256	324543.95	649087.91
Day 3 1/256 R2	0.71	0.0075						
Day 3 1/256 R3	0.66	0.0066						
Part 3: IU/mL								
Mean IU/mL						Stdev IU/mL		
4.71×10^5						4.7×10^4		

*R1, R2, and R3 refer to three technical repeats; Stdev refers to standard deviation.

*Day 1 count R1 was excluded from further calculations due to unacceptable deviation from the mean, which could have resulted from (i) human error during seeding, or (ii) unstable fluidics of the flow cytometer during sample analysis which was not corrected in time.

3.7 Summary

HIV detection for experimental purposes was achieved by optimising direct detection methods (PCR and p24 ELISA). An indirect detection method was instituted and optimised for the functional titration of HIV produced for experimental purposes (GHOST GFP assay).

3.8 References

1. Gentile, M., Adrian, T., Scheidler, A., Ewald, M., Dianzani, F., Pauli, G., et al. Determination of the size of HIV using adenovirus type 2 as an internal length marker. *Journal of virological methods*. 1994;48(1):43-52.
2. Shattock, R.J., Rosenberg, Z. *Microbicides: Topical Prevention against HIV*. Cold Spring Harbor perspectives in medicine. 2012;2(2).
3. Baxter, A.E., Niessl, J., Fromentin, R., Richard, J., Porichis, F., Charlebois, R., et al. Single-Cell Characterization of Viral Translation-Competent Reservoirs in HIV-Infected Individuals. *Cell Host Microbe*. 2016;20(3):368-80.
4. Stramer, S.L., Glynn, S.A., Kleinman, S.H., Strong, D.M., Caglioti, S., Wright, D.J., et al. Detection of HIV-1 and HCV Infections among Antibody-Negative Blood Donors by Nucleic Acid–Amplification Testing. *New England Journal of Medicine*. 2004;351(8):760-8.
5. Lennette, E.T., Karparkin, S., Levy, J.A. Indirect immunofluorescence assay for antibodies to human immunodeficiency virus. *Journal of Clinical Microbiology*. 1987;25(2):199.
6. Wei, X., Decker, J.M., Liu, H., Zhang, Z., Arani, R.B., Kilby, J.M., et al. Emergence of resistant human immunodeficiency virus type 1 in patients receiving fusion inhibitor (T-20) monotherapy. *Antimicrobial agents and chemotherapy*. 2002;46(6):1896-905.
7. Roos, J.W., Maughan, M.F., Liao, Z., Hildreth, J.E.K., Clements, J.E. LuSIV Cells: A Reporter Cell Line for the Detection and Quantitation of a Single Cycle of HIV and SIV Replication. *Virology*. 2000;273(2):307-15.
8. Morner, A., Bjorndal, A., Albert, J., Kewalramani, V.N., Littman, D.R., Inoue, R., et al. Primary human immunodeficiency virus type 2 (HIV-2) isolates, like HIV-1 isolates, frequently use CCR5 but show promiscuity in coreceptor usage. *J Virol*. 1999;73(3):2343-9.
9. Janas, A.M., Wu, L. HIV-1 interactions with cells: from viral binding to cell-cell transmission. *Current protocols in cell biology*. 2009;Chapter 26:Unit 26.5.
10. Frankel, A.D., Young, J.A. HIV-1: fifteen proteins and an RNA. *Annual review of biochemistry*. 1998;67:1-25.
11. Watson, J.D., Crick, F.H.C. Molecular Structure of Nucleic Acids: A Structure for Deoxyribose Nucleic Acid. *Nature*. 1953;171:737.
12. Lodish, H., Berk, A., Zipursky, S., al., e. Section 4.1 Structure of Nucleic Acids. *Molecular Cell Biology*. 4th edition ed. New York: W. H. Freeman; 2000.
13. Kennepohl, D.F., S.; Schaller, C.; Jakubowski, H. *Biomolecules*. LibreTexts Chemistry: Athabasca University; 2017.
14. Deweese, J.E., Osheroff, M.A., Osheroff, N. DNA Topology and Topoisomerases: Teaching a "Knotty" Subject. *Biochemistry and molecular biology education: a bimonthly publication of the International Union of Biochemistry and Molecular Biology*. 2008;37(1):2-10.

15. Lodish, H., Berk, A., Zipursky, S., al., e. Section 12.2 The DNA Replication Machinery. *Molecular Cell Biology*. 4th edition ed. New York: W. H. Freeman; 2000.
16. Lorenz, T.C. Polymerase chain reaction: basic protocol plus troubleshooting and optimization strategies. *Journal of visualized experiments: JoVE*. 2012(63):e3998-e.
17. Lodish, H., Berk, A., Zipursky, S., al., e. Section 4.3 Nucleic Acid Synthesis. *Molecular Cell Biology*. 4th edition ed. New York: W. H. Freeman; 2000.
18. Saiki, R.K., Scharf, S., Faloona, F., Mullis, K.B., Horn, G.T., Erlich, H.A., et al. Enzymatic amplification of beta-globin genomic sequences and restriction site analysis for diagnosis of sickle cell anemia. *Science*. 1985;230(4732):1350-4.
19. Lee, P.Y., Costumbrado, J., Hsu, C.-Y., Kim, Y.H. Agarose gel electrophoresis for the separation of DNA fragments. *Journal of visualized experiments: JoVE*. 2012(62):3923.
20. Arya, M., Shergill, I.S., Williamson, M., Gommersall, L., Arya, N., Patel, H.R.H. Basic principles of real-time quantitative PCR. 2005;(5)2:209-19.
21. Wruck, F., Katranidis, A., Nierhaus, K.H., Büldt, G., Hegner, M. Translation and folding of single proteins in real time. *Proceedings of the National Academy of Sciences of the United States of America*. 2017;114(22):E4399-E407.
22. Lefebvre, G., Desfarges, S., Uyttebroeck, F., Munoz, M., Beerenwinkel, N., Rougemont, J., et al. Analysis of HIV-1 expression level and sense of transcription by high-throughput sequencing of the infected cell. *J Virol*. 2011;85(13):6205-11.
23. Painter, M.M., Zaikos, T.D., Collins, K.L. Quiescence promotes latent HIV infection and resistance to reactivation from latency with histone deacetylase inhibitors. *Journal of Virology*. 2017.
24. Rychert, J., Strick, D., Bazner, S., Robinson, J., Rosenberg, E. Detection of HIV gp120 in plasma during early HIV infection is associated with increased proinflammatory and immunoregulatory cytokines. *AIDS research and human retroviruses*. 2010;26(10):1139-45.
25. Bystryak, S., Acharya, C. Detection of HIV-1 p24 antigen in patients with varying degrees of viremia using an ELISA with a photochemical signal amplification system. *Clinica chimica acta; international journal of clinical chemistry*. 2016;456:128-36.
26. WHO Prequalification of In Vitro Diagnostics. PUBLIC REPORT. In: Organisation WH, editor.: World Health Organisation; 2016.
27. Pasloske, B.L., Walkerpeach, C.R., Obermoeller, R.D., Winkler, M., DuBois, D.B. Armored RNA technology for production of ribonuclease-resistant viral RNA controls and standards. *Journal of clinical microbiology*. 1998;36(12):3590-4.
28. Davalieva, K., D. Efremov, G. Influence of salts and PCR inhibitors on the amplification capacity of three thermostable DNA polymerases. *Macedonian Journal of Chemistry and Chemical Engineering*. 2010;29(1):57-62.
29. Enzoklop. Schematic drawing of the PCR cycle. In: Reaction P editor. Online: *Wikimedia Commons, the free media repository*; 2014. Schematic drawing of the PCR cycle.

30. Ye, J., Coulouris, G., Zaretskaya, I., Cutcutache, I., Rozen, S., Madden, T.L. Primer-BLAST: a tool to design target-specific primers for polymerase chain reaction. *BMC bioinformatics*. 2012;13:134.
31. Kibbe, W.A. OligoCalc: an online oligonucleotide properties calculator. *Nucleic Acids Res.* 2007;35(Web Server issue):W43-6.
32. Dieffenbach, C.W., Lowe, T.M., Dveksler, G.S. General concepts for PCR primer design. *PCR methods and applications*. 1993;3(3):S30-7.
33. Owczarzy, R., Moreira, B.G., You, Y., Behlke, M.A., Walder, J.A. Predicting stability of DNA duplexes in solutions containing magnesium and monovalent cations. *Biochemistry*. 2008;47(19):5336-53.
34. Wu, D.Y., Ugozzoli, L., Pal, B.K., Qian, J., Wallace, R.B. The effect of temperature and oligonucleotide primer length on the specificity and efficiency of amplification by the polymerase chain reaction. *DNA and cell biology*. 1991;10(3):233-8.
35. Kaiser, P., Joos, B., Niederost, B., Weber, R., Gunthard, H.F., Fischer, M. Productive human immunodeficiency virus type 1 infection in peripheral blood predominantly takes place in CD4/CD8 double-negative T lymphocytes. *J Virol*. 2007;81(18):9693-706.
36. Gallagher, S. Quantitation of nucleic acids with absorption spectroscopy. *Current protocols in protein science*. 2001;Appendix 4:Appendix 4K.
37. Armbruster, D.A., Pry, T. Limit of blank, limit of detection and limit of quantitation. *The Clinical biochemist Reviews*. 2008;29 Suppl 1(Suppl 1):S49-S52.
38. Best, B.P. Cryoprotectant Toxicity: Facts, Issues, and Questions. *Rejuvenation Research*. 2015;18(5):422-36.
39. Adan, A., Alizada, G., Kiraz, Y., Baran, Y., Nalbant, A. Flow cytometry: basic principles and applications. *Critical Reviews in Biotechnology*. 2017; 37(2):163-76.
40. Mizrahi, O., Ish Shalom, E., Baniyash, M., Klieger, Y. Quantitative Flow Cytometry: Concerns and Recommendations in Clinic and Research. *Cytometry Part B: Clinical Cytometry*. 2018;94(2):211-8.
41. Njemini, R., Onyema, O.O., Renmans, W., Bautmans, I., De Waele, M., Mets, T. Shortcomings in the application of multicolour flow cytometry in lymphocyte subsets enumeration. *Scandinavian journal of immunology*. 2014;79(2):75-89.
42. Kolte, L., Gaardbo, J.C., Skogstrand, K., Ryder, L.P., Ersbøll, A.K., Nielsen, S.D. Increased levels of regulatory T cells (T(regs)) in human immunodeficiency virus-infected patients after 5 years of highly active anti-retroviral therapy may be due to increased thymic production of naive T(regs). *Clinical and Experimental Immunology*. 2009;155(1):44-52.
43. Djebali, S., Davis, C.A., Merkel, A., Dobin, A., Lassmann, T., Mortazavi, A., et al. Landscape of transcription in human cells. *Nature*. 2012;489:101.
44. Bairoch, E.G.C.H.A.G.S.e.D.M.R.W.R.D.A.A. Protein Identification and Analysis Tools on the ExPASy Server. In: Walker JM, editor. *The Proteomics Protocols Handbook*: Hamana; 2005. p. 571-607.
45. Vodros, D., Fenyo, E.M. Quantitative evaluation of HIV and SIV co-receptor use with GHOST(3) cell assay. *Methods Mol Biol*. 2005;304:333-42.

46. Vödrös, D., Fenyő, E.M. Quantitative Evaluation of HIV and SIV Co-Receptor Use With GHOST(3) Cell Assay. In: Zhu T, editor. Human Retrovirus Protocols: Virology and Molecular Biology. Totowa, NJ: Humana Press; 2005. p. 333-42.
47. Davis, H.E., Rosinski, M., Morgan, J.R., Yarmush, M.L. Charged Polymers Modulate Retrovirus Transduction via Membrane Charge Neutralization and Virus Aggregation. *Biophysical Journal*. 2004;86(2):1234-42.
48. Davis, H.E., Morgan, J.R., Yarmush, M.L. Polybrene increases retrovirus gene transfer efficiency by enhancing receptor-independent virus adsorption on target cell membranes. *Biophysical Chemistry*. 2002;97(2):159-72.
49. Ciobanasu, C., Siebrasse, J.P., Kubitscheck, U. Cell-penetrating HIV1 TAT peptides can generate pores in model membranes. *Biophysical journal*. 2010;99(1):153-62.
50. Thavarajah, R., Mudimbaimannar, V.K., Elizabeth, J., Rao, U.K., Ranganathan, K. Chemical and physical basics of routine formaldehyde fixation. *Journal of oral and maxillofacial pathology : JOMFP*. 2012;16(3):400-5.
51. Hobro, A.J., Smith, N.I. An evaluation of fixation methods: Spatial and compositional cellular changes observed by Raman imaging. *Vibrational Spectroscopy*. 2017;91:31-45.

Chapter 4 Human immunodeficiency virus production

4.1 Introduction

HIV is a ssRNA virus, which requires reverse transcription to a dsDNA proviral genome prior to integration into the host cell genome for propagation¹ (Figure 2.5). Transcription and translation of HIV proteins facilitated by host cell mechanisms results in the production and packaging of HIV in transcriptionally active cells^{2,3}.

To produce HIV, the *in vivo* replication cycle is exploited in a cell culture setting by exposing activated, susceptible cells to infected cells or infectious virus preparation. Virus production leads to host cell lysis due to budding of a critical mass of virions leaving the host cell unable to repair its cell membrane³. The depleted host cell population is then replaced with fresh activated susceptible cells at strategic intervals to ensure continued virus production. Released virus is harvested in cell culture supernatant⁴. PBMCs are often used as host cells to propagate HIV⁴.

An alternative strategy to produce HIV is to clone the relatively small HIV proviral genome (approximately 9 kb) into a plasmid which is replicated in bacteria and transferred to mammalian cells by transfection⁵. Successfully transfected cells produce virus from plasmid-encoded HIV proviral genomes without the requirement of reverse transcription or integration into the host genome⁶. Replication-competent HIV is then harvested in transfected cell supernatant. Figure 4.1 outlines primary virus and molecular clone production strategies.

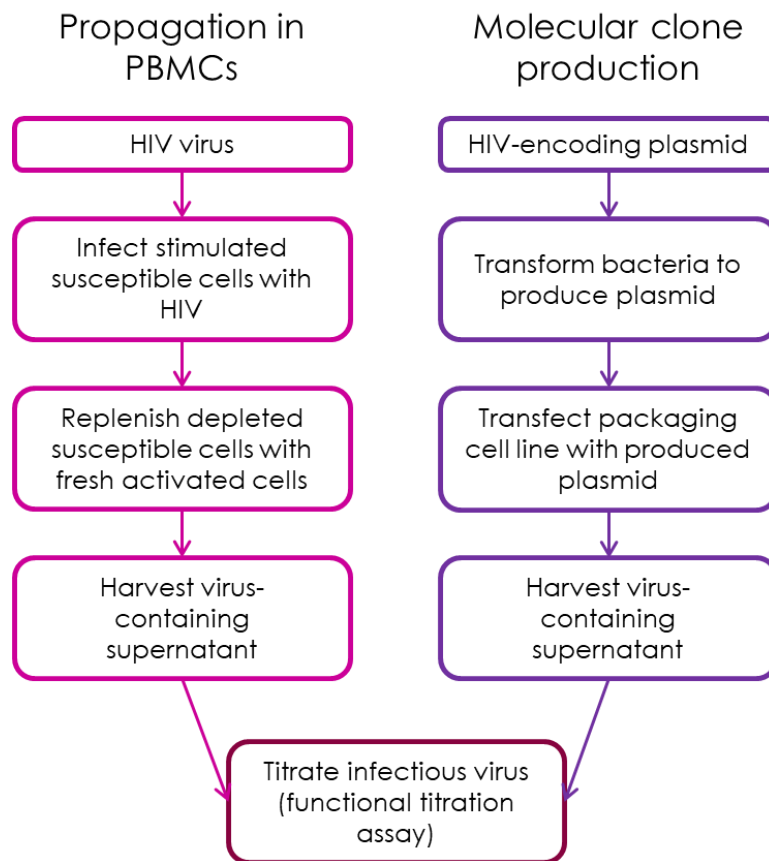


Figure 4.1: Outlines of strategies for the production of primary virus (propagation in PBMCs, pink) and molecular clones (molecular clone production, purple). Functional titration of virus produced by both strategies is described in 3.6.6 *GHOST green fluorescent protein assay – method*.

4.1.1 Virus used for experimental purposes

Three tropisms of HIV-1 (X4-tropic, R5-tropic, and R5X4-tropic) of two subtypes (HIV-1B and HIV-1C) were produced as outlined in Figure 4.1 for experimental purposes.

4.1.1.1 Primary human immunodeficiency virus-1C isolates

The following primary isolates of HIV-1C (Table 4.1) were propagated in phytohaemagglutinin-P (PHA-P)-activated PBMCs according to the Montefiori Laboratory protocol entitled “Protocol for HIV-1 Isolation by PBMC Co-culture”⁴, which was modified to increase yield and decrease production time (4.4 *Propagation of HIV in*). Primary isolates of

HIV-1C were kindly provided by Professor Lynn Morris from the National Institute for Communicable Disease (NICD).

Table 4.1: Details of HIV-1C primary isolates produced in PBMCs.

HIV-1C Isolate	Accession numbers	Tropism	Primary reference
CM1 ⁷	AY505003	R5	Cilliers <i>et al.</i> (2003)
CM9 ⁷	AF411967	R5X4	Cilliers <i>et al.</i> (2003)
SW7 ⁷	AF411966	X4	Cilliers <i>et al.</i> (2003)
Du422F ⁸	AY043175.1	R5	Williamson <i>et al.</i> (2003)
Du156 ⁸	AY529660	R5	Williamson <i>et al.</i> (2003)
Du123 ⁸	AF544007	R5	Williamson <i>et al.</i> (2003)
COT1 ⁹	DQ235624	R5	Choge <i>et al.</i> (2006)

4.1.1.2 Human immunodeficiency virus-1B molecular clones

Molecular clones of HIV-1B (Table 4.2) were produced by transformation into *E.coli*, transfection of HEK293T cells, and harvested in cell culture supernatant. Plasmids were kindly donated by Professor Roberto Speck (University Hospital Zurich, Switzerland), originally obtained from the NIH AIDS Reagents Program.

Molecular clones of HIV are replication-competent HIV-moieties which have been cloned into plasmids capable of containing full-length HIV genomes. These plasmids encode the proviral (DNA) genome of HIV and are used to generate large amounts of clonally identical infectious HIV virions when transfected into a suitable cell line for packaging⁵. Plasmid-based production reduces the proportion of non-infectious, or replication-incompetent viral quasispecies present in PBMC-propagated stocks by bypassing the error-prone reverse transcription and integration steps in the life cycle of primary HIV isolates¹⁰.

Table 4.2: Details of HIV-1B molecular clones produced in this study.

	Yu2	NL4-3	JRCFS	89.6
Plasmid name	pYu-2	pNL4-3	pYK-JRCFS	p89.6
HIV tropism	R5	X4	R5	R5X4
Plasmid vector	pTZ19R	pUC18	pBRN/B	pUC19
Plasmid size (bp)	~12 000	14 825	14 607	12 214
Antibiotic resistance	Ampicillin	Ampicillin	Ampicillin	Ampicillin
Accession number	M93258	AF324493	M38429	U39362
NIH reference	NIH AIDS Reagent Program, Division of AIDS, NIAID, NIH, from Dr. Beatrice Hahn and Dr. George Shaw (cat# 1350).	NIH AIDS Reagent Program, Division of AIDS, NIAID, NIH, from Dr. Malcolm Martin (cat# 114).	NIH AIDS Reagent Program, Division of AIDS, NIAID, NIH, from Dr. Irvin SY Chen and Dr. Yoshio Koyanagi (cat# 2708).	NIH AIDS Reagent Program, Division of AIDS, NIAID, NIH, from Ronald G. Collman, MD (cat# 3552).

4.2 Ethical considerations

Donors consented to donate 250 mL peripheral blood collected into a sterile 450 mL blood bag (Jiaxing Tianhe Pharmaceutical Co. Ltd, China) containing 60 mL CPD as an anticoagulant. Donor HIV-negative status was confirmed by testing an aliquot of donated whole blood on the GeneXpert® platform using Xpert® HIV-1 Qual cartridges before the isolated cells were used (described in 3.3 *Donor testing*). Ethical approval for consenting donors and collecting blood at the CRU was granted by the Faculty of Health Sciences Research Ethics Committee at the University of Pretoria under protocol number 204/2016.

4.3 Molecular clone production

4.3.1 Overview

Molecular clones of HIV-1B were obtained from Professor Speck's laboratory in the form of plasmid dry spots on blotting paper. Plasmids were recovered by cutting the dry spots out of the blotting paper using a new razor blade for each spot. One spot per plasmid was cut up into small pieces and transferred to a sterile 1.5 mL microcentrifuge tube and immersed in 100 µL molecular grade nuclease-free water overnight at room temperature. Recovered plasmids were stored at -20°C until use.

Plasmids were transformed into MAX Efficiency™ Stbl2™ *E.coli* competent cells (Stbl2™; ThermoFisher Scientific, USA), and transfected into HEK293T cells donated by Dr Iman van den Bout's laboratory (Centre for Neuroendocrinology, Department of Physiology, University of Pretoria). Packaged, infectious virus was harvested from transfected HEK293T cells. Protocols for transformation and transfection were supplied by Mrs Erika Schläpfer (University Hospital Zurich, Switzerland) during a research visit to Zurich, and modified to suit available equipment. Troubleshooting and optimisation of molecular clone production is explained in 4.3.6 *Molecular clone production optimisation*.

4.3.2 Transformation

4.3.2.1 Introduction

Stbl2™ are competent bacterial cells (capable of taking up foreign plasmid DNA), which have been modified to clone unstable genomes containing frequent single-bp or short sequence repeats¹¹, such as lentiviral sequences. Bacteria contain recombinase enzymes which result in homologous recombination of plasmid sequences during replication. Homologous recombination results in repeat sequences of plasmids being joined together, as a consequence of the separating sequences being cut out. This is deleterious to the insert of interest, which is why recombinase modifications such as the *recA* loss-of-function mutation of Stbl2™ are useful for cloning notoriously unstable retroviral genomes¹¹ such as HIV.

Transformed Stbl2™ (containing HIV-1-B-encoding plasmids) were selected by ampicillin resistance. Stbl2™ which did not take up plasmid would not be able to grow in the presence of ampicillin, but successfully transformed Stbl2™ would. Transformation was performed to produce large quantities of HIV-1B encoding plasmid, which were used to produce infectious HIV-1B in transfected HEK293T cells.

4.3.2.2 Medium preparation

Stbl2™ were cultured in both liquid and agar forms of Luria-Bertani (LB) medium. LB medium was prepared by dissolving 10 g tryptone (Neogen, USA), 5 g yeast extract (Neogen, USA), and 10 g NaCl (Sigma-Aldrich, USA) in 1 L distilled water. LB agar was prepared by adding 15 g agar (Thermo Fisher Scientific, USA) per litre LB medium. Both LB medium and LB agar were sterilised by autoclaving, which also activated the polymerisation activity of the agar.

When cool to the touch, sterile LB agar and LB medium used for selecting transformants was supplemented with 100 µg/mL ampicillin (Sigma-Aldrich, USA). LB agar plates were prepared by pouring 12-15 mL LB agar into 15 mm bacterial culture plates (Lasec, South Africa) while still warm enough to pour, and allowed to set overnight. LB agar plates were stored inverted

at 4°C until use. LB plates and medium were used within seven days of antibiotic supplementation.

4.3.2.3 Method

Stbl2™ were provided as frozen competent cell stocks which had to be transformed upon thawing otherwise competence would have been lost. Transformation of Stbl2™ with HIV-1B-encoding plasmids (Table 4.2) was performed according to manufacturer's instructions. Transformation reactions were set up on ice in pre-cooled 1.5 mL microcentrifuge tubes.

Transformation reactions were prepared by dispensing 50 pg of pUC19 control plasmid (transformation control; supplied with Stbl2™), or 10 ng of HIV-1B plasmid, or 5 µL of molecular grade distilled water (untransformed control) to 30 µL aliquots of Stbl2™ competent cells thawed on ice. Transformation reactions were mixed by gently tapping the bottom of the microcentrifuge tubes to avoid mechanical shearing of plasmid DNA which can occur with more vigorous mixing. After mixing, transformation reactions were incubated on ice for 30 min to allow plasmids to associate with Stbl2™ competent cells.

To encourage Stbl2™ uptake of the plasmid in each transformation reaction, transformation reactions were heat-shocked for 25 s in a water bath pre-heated to 42°C. Heat shock facilitates plasmid uptake by competent cells by increasing bacterial membrane fluidity which results in "gaps" between membrane lipids. These gaps reduce the cell membrane potential, allowing plasmid DNA to approach (due to reduced electrostatic repulsion) and cross (due to spaced between lipids) competent cell membranes¹². After heat-shock, transformation reactions were incubated on ice for 2 min to increase the retention of plasmid. Transformation reactions were then transferred to 15 mL centrifuge tubes containing 400 µL super optimal broth with catabolite repression (SOC) medium (supplied with Stbl2™) pre-warmed to 30°C. The addition of SOC medium has been reported to improve transformation efficiency¹³. The transformation reaction cultures were then incubated overnight in a Labtech LSI-3016A shaking incubator (Delta Systech, Romania) at 300 rpm, 30°C, with tube lids loosely screwed on to allow gaseous exchange. Overnight cultures were stored at 4°C until plasmid DNA was successfully extracted.

4.3.2.4 Transformant selection and culture

4.3.2.4.1 Selecting transformants

Transformed Stbl2™ were selected by growing 1:10 and 1:50 dilutions of overnight cultures (prepared in a final volume of 100 µL LB medium) on LB agar. Dilutions were plated on LB agar plates supplemented with ampicillin (prepared as described in 4.3.2.2 *Medium preparation*) by pipetting the 100 µL of overnight culture dilutions onto the centre of the agar and spreading using a flamed glass hockey stick. Glass hockey sticks were sterilised by dipping in 70% ethanol and passing through the flame of a bunsen burner before, between, and after uses, and cooled by pressing into the agar at the edge of the LB plate before spreading bacteria. LB agar transformation cultures were incubated inverted overnight at 30°C.

Success of transformations was determined by (i) the untransformed control (water) failing to grow on ampicillin-supplemented LB agar overnight, and (ii) the transformation control (pUC19) and transformations (HIV-1B-encoding plasmids) producing bacterial colonies on ampicillin-supplemented LB agar overnight. If lawns of growth rather than single colonies were produced by both plated dilutions of overnight transformation culture (1:10 and 1:50), then overnight cultures were further diluted to 1:100 and 1:1000. These dilutions were also prepared in a final volume of 100 µL LB medium, plated on LB agar supplemented with ampicillin, and incubated inverted overnight at 30°C as before.

When single colonies were obtained by dilution and plating on LB agar supplemented with ampicillin, colonies were picked to inoculate starter cultures. At least one plate with good resolution of colonies per transformation was stored inverted at 4°C in the event that sufficient material was not picked for inoculation. Two colonies per plate were picked using sterile pipette tips, and dropped into 10 mL LB medium supplemented with ampicillin in 50 mL centrifuge tubes. Starter cultures were incubated with shaking at 300 rpm, 30°C, with the centrifuge tube lids loosely screwed on to allow gaseous exchange. Turbidity (cloudiness) of overnight starter cultures within 30 hr of inoculation was used as a measure of successful inoculation. Cultures which had not grown by this time were terminated using bleach.

Plasmid DNA was extracted from a small volume of starter cultures (described in 4.3.3.1 *NucleoSpin® Plasmid Miniprep plasmid DNA extraction*) for troubleshooting purposes.

4.3.2.4.2 Transformant culture

Starter cultures were used to inoculate large-volume cultures by adding 1 mL of starter culture to 200-500 mL sterile LB medium supplemented with ampicillin in 500 mL or 1 L glass Erlenmeyer flasks pre-autoclaved with foil strips to seal the mouths. The remaining volume of starter cultures was stored at 4°C until the success of large-volume cultures was confirmed by turbidity (as for starter cultures). Cultures were incubated overnight for a maximum of 30 hr with shaking at 300 rpm, at 30°C prior to plasmid extraction (described in 4.3.3.2 *NucleoBond® Xtra Maxi EF plasmid DNA extraction*).

4.3.2.4.3 Transformed Stbl2™ cryopreservation

Successfully transformed Stbl2™ from large-volume cultures were cryopreserved for future plasmid productions. Glycerol was used as a cryoprotectant for bacterial stocks, as freezing cells in glycerol results in a “softer” frozen product¹⁴ from which small pieces can be easily scraped rather than thawing the whole cryovial. Pure glycerol (Sigma-Aldrich, USA) was diluted to 80% in distilled water, autoclaved to sterilise, and allowed to cool to room temperature before use. Glycerol stocks were prepared by aliquoting 750 µL large-volume cultures into 1.5 mL cryovials, and adding 750 µL 80% glycerol to a final concentration of 40% glycerol. Glycerol stocks of transformed Stbl2™ were stored at -80°C until required. When needed, a small volume of still-frozen glycerol stock of the required transformant was scraped into 5 mL pre-warmed LB broth supplemented with ampicillin using a sterile 1 mL pipette tip.

4.3.3 Plasmid DNA extraction

4.3.3.1 *NucleoSpin® Plasmid Miniprep plasmid DNA extraction*

Plasmid DNA was extracted from starter cultures using the NucleoSpin® Plasmid DNA Miniprep plasmid extraction kit (NucleoSpin®; Macherey-Nagel, USA) according to the manufacturer's instructions.

4.3.3.1.1 **Reagent preparation**

Prior to first use

Wash Buffer A4 was prepared by adding 48 mL absolute ethanol (Sigma-Aldrich, USA) to the concentrated A4 buffer supplied in the kit. RNase A (provided with the kit) was reconstituted in 1 mL Buffer A1, mixed by vortex, and transferred back to the Buffer A1 bottle before mixing thoroughly. Buffer A1 containing RNase A was stored at 4°C until use.

4.3.3.1.2 **NucleoSpin® plasmid DNA extraction procedure**

Bacterial cells were collected by sequential centrifugation from up to 5 mL of starter cultures. This was performed by adding 1 mL bacterial culture to a 1.5 mL microcentrifuge tube and centrifuging at 11 000 x g for 30 s and removing as much supernant as possible, before adding another 1 mL of culture and repeating the centrifugation step. Bacterial cell pellets were resuspended in 250 µL Buffer A1 (containing RNase A) and mixing by vortex until no clumps remained. Cells were then lysed by adding 250 µL Buffer A2, containing sodium dodecyl sulphate (SDS) which disrupts cell membranes, and LyseControl, which measures neutralisation of alkalinity caused by Buffer A2. The lysis mixtures were mixed by gentle inversion and incubated for 5 min at room temperature. To neutralise the alkaline pH caused by Buffer A2 (alkaline lysis), 300 µL Buffer A3 was added. Neutralisation was measured by LyseControl changing from blue (alkaline pH) to colourless (neutral pH), to prevent damage to plasmid DNA.

Following the addition of Buffer A3, cell lysates were mixed by gentle inversion to ensure complete neutralisation. Incomplete neutralisation could result in incomplete protein precipitation, which would contaminate the plasmid DNA extract. Completely neutralised cell lysates were clarified by centrifugation at 11 000 x g for 5 min, which was repeated if the lysate was not completely clear. A maximum of 750 µL of clarified lysate was removed at a time and applied to NucleoSpin® plasmid columns assembled in 2 mL collection tubes. The column-collection tube assembly was centrifuged at 11 000 x g for 1 min and the flow-through discarded before applying the remaining clarified lysate to the column and repeating the centrifugation step.

Plasmid DNA bound to the silica membrane of NucleoSpin® columns was washed by applying 500 µL Buffer AW to the column and centrifuging at 11 000 x g for 1 min. The membrane was then washed with 600 µL Buffer A4, containing ethanol, and centrifuged at 11 000 x g for 1 min. The flow-through was discarded and the columns placed back into empty collection tubes. Residual buffers were removed by centrifuging the column-collection tube assemblies at 11 000 x g for 2 min. Plasmid DNA was eluted into sterile 1.5 mL microcentrifuge tubes by transferring the columns to microcentrifuge tubes before adding 50 µL Buffer AE and incubating at room temperature with the column lid closed for 1 min. Elution was achieved by centrifugation at 11 000 x g for 1 min. Plasmid DNA was quantified by NanoDrop® as described in 3.5.3.4.3 *Nucleic acid quantification by NanoDrop®* (Table 4.3) and stored at -20°C until required.

Table 4.3: NucleoSpin® plasmid DNA extraction concentrations, protein purity (A_{260}/A_{280} ratio), and salt purity (A_{260}/A_{230} ratio).

Sample ID	DNA concentration (ng/ μ L)	A_{260}/A_{280} ratio	A_{260}/A_{230} ratio
pYu2 (1)	282.73	1.85	2.22
pYu2 (2)	287.24	1.85	2.25
pNL4-3 (1)	382.55	1.85	2.25
pNL4-3 (2)	330.44	1.85	2.28
pYK-JRCSF (1)	146.06	1.85	2.19
pYK-JRCSF (2)	125.40	1.84	2.24
p89.6 (1)	93.57	1.82	1.73
p89.6 (2)	94.23	1.83	1.97

*Two plasmid extractions ((1) and (2)) were performed for each transformation reaction to ensure that sufficient plasmid DNA was obtained for storage purposes.

4.3.3.2 *NucleoBond® Xtra Maxi EF plasmid DNA extraction*

Plasmid DNA was extracted from large-volume cultures using the NucleoBond® Xtra Maxi EF Plasmid DNA Miniprep plasmid extraction kit (NucleoBond®; Macherey-Nagel, USA) according to the manufacturer's instructions. This kit was used to isolate and purify large quantities of endotoxin-free (EF) plasmid from large-volume cultures. Endotoxins are produced by bacteria such as *E.coli* and are toxic to mammalian cells used in downstream transfection and infection experiments¹⁵.

4.3.3.2.1 **Reagent preparation**

Prior to first use

Endotoxin-free 70% ethanol was prepared by adding 80 mL absolute ethanol to endotoxin-free water supplied with the kit. RNase A (provided with the kit) was reconstituted in Buffer

RES-EF to a final concentration of 60 µg/mL. Buffer RES-EF containing RNase A was stored at 4°C until use.

Prior to each use

Buffer LYS-EF was examined for SDS precipitation (white precipitate) before each use. If SDS precipitation had occurred, Buffer LYS-EF was warmed to 37°C and stirred until SDS had dissolved.

4.3.3.2.2 NucleoBond® plasmid DNA extraction procedure

Cells from large-volume cultures were pelleted in 50 mL centrifuge tubes by sequential centrifugation at 5000 x g for 10 min at 4°C and the supernatant carefully discarded. Another 50 mL of the large-volume culture was added to the pellet and centrifuged as before. The supernatant was removed and the process was repeated until all the bacteria from the large-volume cultures were pelleted.

Bacterial pellets were thoroughly resuspended in 12 mL Buffer RES-EF (containing RNase A) and vortexed until no clumps remained. Cells were alkaline-lysed by adding 12 mL Buffer LYS-EF (blue, containing LyseControl) and gently mixed by inversion to avoid DNA shearing and resulting contamination of plasmid DNA with genomic DNA. The blue cell lysis suspension was incubated at room temperature for no more than 5 min. During this time, Nucleobond® Xtra Columns were assembled by inserting the filter into the column and placing the column on a waste collection tube, and equilibrated. Equilibration was achieved by applying 35 mL of Buffer EQU-EF in 10-15 mL relays slowly to the funnel-shaped rim of the filter ensuring that the entire filter was wet. The column was allowed to empty by gravity flow.

After the lysis suspension had been incubated for 5 min, 12 mL Buffer NEU-EF was added to each tube and mixed by gentle inversion to neutralise the lysis solution. The suspensions were considered to be neutralised when no traces of blue remained. Crude lysates were then incubated on ice for 5 min to increase protein precipitate. Lysates were homogenised by gentle inversion and clarified by centrifugation at 5000 x g for 10 min. The clear liquid lysate containing plasmid DNA was carefully aspirated and applied to equilibrated NucleoBond®

columns. The filter and column were washed with 10 mL Buffer FIL-EF by applying Buffer FIL-EF to the filter rim (as for equilibration). The filters were removed and discarded, and the silica membrane of the column washed once with 90 mL Buffer ENDO-EF and allowed to empty by gravity. This was followed by washing once with 45 mL Buffer WASH-EF and allowing the column to empty by gravity flow.

Plasmid DNA was eluted into 50 mL centrifuge tubes by applying 15 mL Buffer ELU-EF to the column membranes and allowing them to empty by gravity flow. To precipitate plasmid DNA, 10.5 mL isopropanol (Sigma-Aldrich, USA) at room temperature was added to each tube and vortexed to mix. Precipitated plasmid DNA was collected by centrifugation at 5000 x g for 30 min at 4°C, carefully aspirating the supernatant, and washing each pellet in 5 mL endotoxin-free 70% ethanol. Plasmid DNA was again pelleted by centrifugation at 5000 x g for 30 min at 4°C. Plasmid DNA pellets were dried by removing as much ethanol as possible without disrupting the pellet and allowing the pellets to air-dry at room temperature. Dried plasmid DNA pellets were reconstituted in 1 mL Buffer TE-EF and transferred to 1.5 mL microcentrifuge tubes. Plasmid DNA was quantified by NanoDrop® as described in (3.5.3.4.3 *Nucleic acid quantification by NanoDrop®*) (Table 4.4) and stored at -20°C until required.

Table 4.4: NucleoSpin® plasmid DNA extraction concentrations, protein purity (A_{260}/A_{280} ratio), and salt purity (A_{260}/A_{230} ratio).

Sample ID	DNA concentration (ng/μL)	A_{260}/A_{280} ratio	A_{260}/A_{230} ratio
pYu2	762.36	1.89	2.35
pNL4-3	764.42	1.89	2.34
pYK-JRCSF	59.72	1.91	2.44
p89.6	219.52	1.89	2.36

4.3.4 Transfection

4.3.4.1 Background

Transfection refers to the transfer of plasmid DNA into mammalian cells, which then transcribe and translate proteins from the foreign DNA. This technique is used to produce and package viruses such as HIV from plasmid DNA. This bypasses infection, reverse transcription, and integration in the normal viral lifecycle^{16, 17}, in order to produce infectious virus. This results in a clonal population of viruses (hence the name molecular clones) which are not subject to mutations introduced by the error-prone reverse transcription ultimately contributing to non-infectious virus in infection-driven virus replication¹⁰.

The HEK293T cell line is commonly used for transfection, as it is stably transduced with simian virus 40 (SV40) large tumour antigen (LTag). The transgene is selectable by neomycin or G418 supplementation in culture¹⁸. The presence of the SV40 LTag transgene contributes to increased protein production from plasmids bearing the SV40 origin of replication and improved lentiviral packaging in HEK293T cells compared to the parental (HEK293) line¹⁶. HEK293T cells were donated by Dr Iman van den Bout's laboratory (Centre for Neuroendocrinology, University of Pretoria).

4.3.4.2 HEK293T cell culture and maintenance

4.3.4.2.1 HEK293T cell culture and passaging

Thawing

HEK293T cells were resuscitated from liquid nitrogen as described for GHOST cells in section 3.6.2.1 *GHOST cell thawing*. Briefly, 5×10^6 frozen HEK293T cells were thawed in 30 mL DMEM, and pelleted by centrifugation at 300 x g for 10 min to wash off toxic DMSO used as a cryoprotectant. Cells were resuspended in complete DMEM and seeded at 2.5×10^6 cells per T75 flask in 8 mL complete DMEM supplemented with 500 µg/mL G418.

Culture

HEK293T cells were cultured by incubation at 37°C, 5% CO₂ until confluent. Medium was replaced once with 8 mL complete DMEM supplemented with 500 µg/mL G418 when the medium turned orange. Further medium changes were performed with complete DMEM (without G418). DMEM contains phenol red, a pH indicator which turns orange/yellow when the medium becomes acidic as a result of nutrient depletion. The first few days in culture (from thawing) with G418 served to select HEK293T cells still containing the SV40 LTag transgene, to ensure maximum yield for transfections. Medium was changed by aspirating medium from the flask and replacing with 8 mL pre-warmed complete medium. Typically, confluence was reached within 4 days.

Passaging

HEK293T cells were passaged when confluent by aspirating supernatant and adding 3 mL trypsin per T75 flask, followed by incubation at 37°C for 20-30 seconds or until visibly detached. Trypsin was neutralised with 3 mL complete DMEM and dissociated cells were pelleted by centrifugation at 300 x g for 10 min. Cells were either resuspended in 1 mL complete DMEM per T75 flask for enumeration, or in 4 mL complete DMEM to split the cells for further expansion. In the case of splitting for expansion, 1 mL of the 4 mL cell suspension was added to each of four T75 flasks containing 7 mL complete DMEM (1:4 split). The required

number of HEK293T cells was typically achieved within one passage from thawing, and were enumerated by flow cytometry as described in 4.3.4.2.2 *HEK293T cell enumeration by flow cytometry* prior to seeding for experiments or cryopreservation.

Cryopreservation

Dissociated, enumerated HEK293T cell suspensions remaining after seeding for experiments were pelleted by centrifugation at 300 x g for 10 min. The supernatant was aspirated and cells were resuspended in 1 mL freezing medium (FBS, 10% DMSO) per 5×10^6 HEK293T cells. Aliquots of 1 mL cell suspension were dispensed into 1.5 mL cryovials and stored in liquid nitrogen until further use.

4.3.4.2.2 HEK293T cell enumeration by flow cytometry

Enumeration of viable HEK293T cells was performed on the Gallios™ flow cytometer (Table 3.7) using FL3 (blue laser excitation) to detect Flow-Count™, and FL4 (blue laser excitation) to detect 7-AAD.

Sample preparation

HEK293T cells were enumerated as described in 3.6.3.3 *Enumeration*. Samples were prepared for enumeration by staining 100 µL cell suspension with 3 µL 7-AAD in the dark for 5 min. Before analysing on the Gallios™ flow cytometer, 100 µL Flow-Count™ and 300 µL PBS were added to the sample.

Gating strategy

The sequential gating strategy used for HEK293T cell enumeration is illustrated in Figure 4.2. A two-parameter FS Lin versus SSC Log plot was used to identify intact HEK293T cells. After identifying intact HEK293T cells (HEK293T region), viable HEK293T cells (7-AAD negative; “VIABLE” region) were selected using a 7-AAD Log versus FS Lin plot. The respective sizes of Flow-Count™ beads and HEK293T cells overlap, resulting in both beads and cells being captured in the same “HEK293T cells” region. In order to prevent overestimation of HEK293T

cells, Flow-Count™ were excluded from the HEK293T cells region by applying the “NOT BEADS” Boolean gate to the plot, post-acquisition. Viable HEK293T cells were enumerated by applying Equation 3.1 to the cells in the “Viable” region (Figure 4.2B) and the number of Flow-Count™ bead events in the “Cal” region (Figure 4.2C), as described in 3.6.3.3 *Enumeration*.

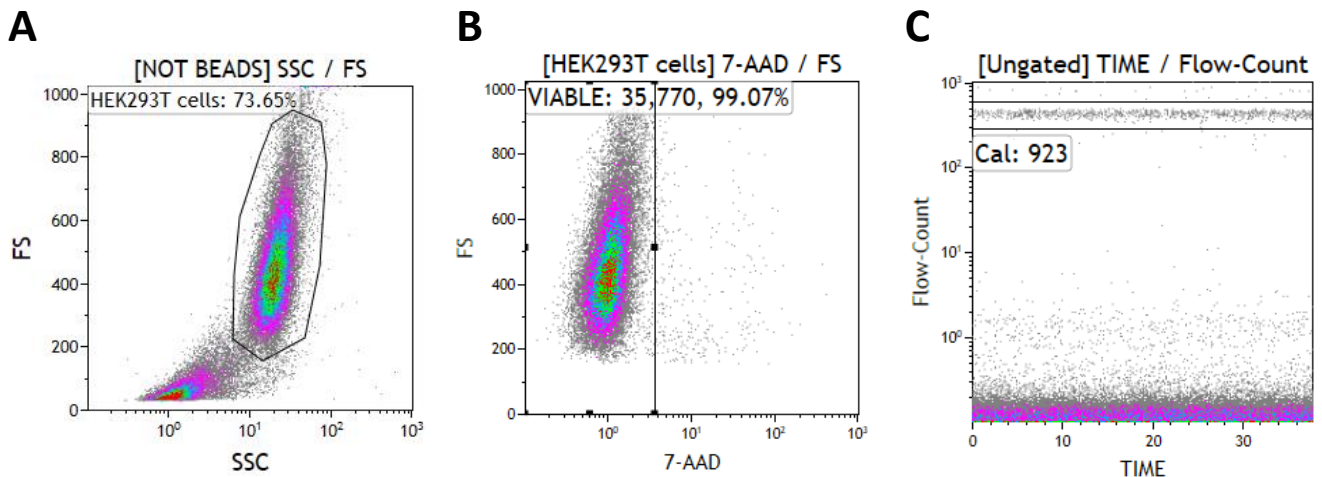


Figure 4.2: Sequential gating strategy for HEK293T cell enumeration. (A) A two-parameter FS Lin versus SSC Log plot was used to identify intact HEK293T cells (“HEK293T cell” region). A “NOT BEADS” Boolean gate was applied to this plot to exclude Flow-Count™ beads from HEK293T cells in the region “HEK293T cells”. **(B)** Viable HEK293T cells were captured in the “VIABLE” region on a two-parameter FS Lin versus 7-AAD plot. **(C)** A two-parameter Flow-Count versus TIME plot was used to enumerate the Flow-Count™ beads analysed (“Cal” region).

4.3.4.3 Transfection - method

4.3.4.3.1 HEK293T cells

HEK293T cells were prepared for transfection by seeding 2.5×10^6 cells per T75 flask, or 5×10^6 cells per T150 flask (Greiner Bio-One, Austria), in 8 mL or 16 mL complete DMEM respectively, and allowed to reach 50-60% confluence by incubating the cells at 37°C, 5% CO₂. Once this level of confluence was reached, the medium on HEK293T cells was aspirated and replaced with 3 mL complete DMEM (T75 flask) or 6 mL complete DMEM (T150 flask) and incubated for 2 hr at 37°C, 5% CO₂. Transfection was commenced after the 2 hr incubation period.

4.3.4.3.2 Preparation of transfection reactions

During the 2 hr HEK293T cell incubation, transfection reactions were prepared as indicated in Table 4.5, mixed by vortex, allowed to stand for 10 min at room temperature, and mixed again by vortex before applying to cells. Transfection was performed in the presence of 1 mg/mL polyethylenimine (PEI; Sigma-Aldrich, USA), which is a stable cationic polymeric transfection reagent which forms positively charged complexes with negatively charged nucleic acids. The net positive charge on PEI-DNA complexes facilitates the endocytosis of DNA following adsorption to the net negative charge on cell membranes¹⁹. Transfection reactions were performed in 15 mL centrifuge tubes, and components were added from left to right as indicated in Table 4.5. Transfection reactions were prepared for each HIV-1B-encoding plasmid from which HIV-1B infectious molecular clones were required.

Table 4.5: Transfection reaction setup for T75 and T150 flasks of HEK293T cells.

	DMEM (μ L)	Plasmid DNA (μ g)	PEI (μ L)
T75 flask	600	32	64
T150 flask	3200	64	128

4.3.4.3.3 Transfection of HEK293T cells

After the 2 hr incubation of HEK293T cells and preparation of transfection reactions, HEK293T cells were transfected. Each HIV-1B-encoding plasmid transfection reaction was added to a separate flask of HEK293T cells, so that each flask produced one isolate of HIV-1B molecular clone. Transfections were performed by pipetting the appropriate transfection reaction into the medium of prepared HEK293T cells, followed by swirling to evenly expose the cells to the transfection reaction. Cells were exposed to transfection reactions for 18 hr in 5 mL (T75 flask) or 10 mL (T150 flask) complete DMEM total volume by incubating at 37°C, 5% CO₂. Transfection reactions were removed after 18 hr by aspirating medium and replacing with 8 mL (T75 flask) or 20 mL (T150 flask) complete DMEM. Transfected cells were incubated at 37°C, 5% CO₂, and virus-containing medium was harvested every three days until confluence

(two harvests). After the first harvest, medium was replaced with 8 mL (T75 flask) or 20 mL (T150 flask) complete DMEM.

4.3.5 Human immunodeficiency virus-1B molecular clone harvest

HIV-1B infectious molecular clones were harvested every three days from transfected HEK293T cells by collecting the virus-containing culture medium. Medium was syringe-filtered through 0.22 µm Millex-HV syringe filter units (Merck, Germany) to remove cells and cell debris. Harvested HIV CFS was then aliquoted into 1.5 mL microcentrifuge tubes and stored at -80°C until use. After two HIV CFS harvests, transfected HEK293T cells were terminated by overnight incubation in sufficient volumes of 1% Virkon™S (prepared as described in 3.2.2 *Safety considerations*) to cover the culture surface.

4.3.6 Molecular clone production optimisation

4.3.6.1 Number of harvests

Molecular clones of HIV-1B were produced by standard protocols (described in 4.3 *Molecular clone production*). Only the number of harvests yielding infectious HIV CFS from transiently transfected HEK293T cells was explored to increase yields. This was achieved by transfecting HEK293T cells (as described in 4.3.4.3.3 *Transfection of HEK293T cells*) using HIV-1B-encoding plasmid DNA (extracted as described in 4.3.3.2 *NucleoBond® Xtra Maxi EF plasmid DNA extraction*) produced by cloning in transformed Stbl2™ *E.coli* (as described in 4.3.2 *Transformation*).

HIV CFS was pooled and harvested every three days (as described in 4.3.5 *Human immunodeficiency virus-1B molecular clone harvest*) from two flasks of HEK293T cells transfected with the same HIV-1B-encoding plasmid. At confluence, transfected HEK293T cells were enzymatically dissociated as described in 4.3.4.2.1 *HEK293T cell culture and passaging* and pelleted by centrifugation at 300 x g for 10 min. Cell pellets were resuspended in 2 mL complete DMEM, and 1 mL was transferred to each of two T75 flasks containing 7 mL

complete DMEM. One further round of HIV CFS harvesting was conducted three days post-split, which yielded non-infectious virus for two of the three molecular clones (Table 4.6). Virus infectivity was determined as described in chapter 3 GHOST GFP assay, and the results are summarised in Table 4.6. Based on these findings, the harvest limit was set at two harvests post-transfection. As molecular clone production is sustained by the presence of HIV-1B-encoding plasmid, declining titres are an indication of plasmid loss. This was expected as transfection of HEK293T cells is transient.

Table 4.6: Functional titrations of three consecutive HIV CFS harvests from HIV-1B molecular clones produced by HEK293T transfection. Non-infectious titres are shown in purple.

Harvest date	Clone NL4-3 (IU/mL)	Clone Yu2 (IU/mL)	Clone 89.6 (IU/mL)
12/10/2018	3.57x10 ⁴	6.09x10 ⁵	6.01x10 ⁴
15/10/2018	4.19x10 ⁴	3.53x10 ⁵	2.66x10 ⁴
18/10/2018	6.16x10 ³	3.54x10 ⁴	5.08x10 ³

4.3.6.2 *Virus-encoding plasmid integrity and infectious yield*

The comparatively low titres of HIV-1B isolate 89.6 were reconciled with the banding pattern observed when undigested plasmid was analysed by gel electrophoresis (Figure 4.4A). Fortunately, empty pUC19, the backbone for the p89.6 plasmid encoding the 89.6 molecular clone, was provided with Stbl2™ and electrophoretic analysis could therefore be performed to postulate the origin of the smaller bands.

4.3.6.2.1 **Agarose gel electrophoresis**

Three plasmid preparations of each of the following plasmids, pYu2, pNL4-3, and p89.6, from different DNA isolations were made by adding 0.5 µL BlueJuice to 100 ng plasmid and making up to a final volume of 5 µL with molecular grade water. Details of plasmid DNA extractions by date are shown in Table 4.7, performed as described in 4.3.3 *Plasmid DNA extraction*.

pUC19 DNA was obtained from the original vial supplied with Stbl2™. All 5 µL of each sample was loaded into separate wells of a 1% agarose gel prepared as described in 3.5.3.6 Agarose gel electrophoresis using TAE. The gel contained EtBr for DNA visualisation. Lanes containing DNA ladders (FastRuler™ HR and FastRuler™ MR) were loaded with 5 µL of the ladder. The band sizes of each ladder are indicated in Figure 4.4B and C. Electrophoresis was performed by applying 90 V for 60 min, and the gel image is shown in Figure 4.4A.

Table 4.7: Plasmid DNA preparations used to evaluate plasmid DNA integrity.

	11/11/2017 extracts	20/11/2017 extracts	03/10/2018 extracts
Plasmid DNA isolation method	NucleoSpin® extraction after the first successful transformation.	NucleoBond® extraction after the first successful large-volume culture.	NucleoBond® extraction from large-volume cultures inoculated from glycerol stocks.

4.3.6.2.2 Results and interpretation

Two sets of three clustered bands were obtained for p89.6, one high up, and one lower down, suggesting the presence of three forms of a large plasmid in the size range of the other molecular clone plasmids, and three forms of a smaller plasmid.

Undigested plasmid is expected to reveal three bands when analysed by gel electrophoresis, which correspond to different forms of plasmid DNA. These plasmid forms are: closed-circular (supercoiled), linear, and open-circular (nicked) forms²⁰ (Figure 4.3). Supercoiled plasmid is tightly coiled in a super-helix, and is therefore more compact than linear DNA, which results in more rapid migration through the agarose gel matrix. Open-circular plasmid is circular, where one strand has been nicked to create a single-strand break. This relaxes tension in the plasmid DNA and prevents super-helix formation. The open-circular form migrates slower than both supercoiled and linear plasmid, as the shape is unweildy in moving through the gel pores²⁰. Although supercoiled is the native form of plasmid DNA and therefore the most prevalent, all three forms of plasmid are expected to appear in the undigested control lanes²⁰ (Figure 4.3).

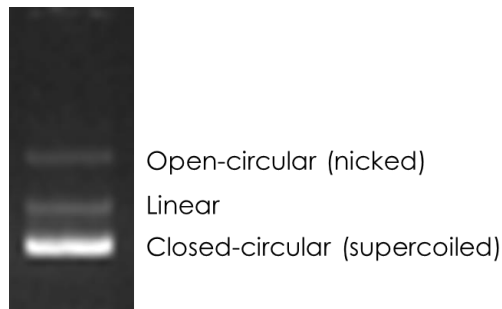


Figure 4.3: Representation of the migration of three plasmid forms of p89.6 to illustrate the migration of the three forms of plasmid DNA. Ladders are not shown as the largest band on available ladders was smaller than p89.6, at 10 000 bp.

Analysis of Figure 4.4A with respect to lanes containing p89.6 (lanes 9-11) reveals 6 bands per lane, the smallest of which were very similar in migration to empty pU19 (lane 12). This suggests that the p89.6 plasmid preparations contained significant proportions (comparing band intensity) of plasmids in which parts of the insert have been lost. The most likely reason is homologous recombination which took place sometime during plasmid cloning, and failure to purify plasmids. This could contribute to the low titres produced by p89.6-transfected HEK293T cells. To rectify this, bands of p89.6 supercoiled plasmids should be excised from agarose gels, and the plasmid DNA present in excised bands should be purified from the gel. Fresh Stbl2™ will then need to be transformed with the purified p89.6 plasmid, from which plasmid DNA can be extracted and used to transfect HEK293T cells. Such transfections would likely yield HIV CFS of greater titres as a greater proportion of the transfected DNA will encode full-length HIV-1B isolate 89.6. Due to time constraints, plasmid purification and transformation using purified plasmid was not performed in this study.

In contrast, low titres of pNL4-3 cannot be explained by plasmid degradation, as the three plasmid forms of a single plasmid appear on the gel (Figure 4.4A, lanes 3-5). Low titres could, however, result from poor uptake of plasmid DNA during transfection. Further investigation is required to determine the cause for low titre achieved using pNL4-3. pYu2 was the best-

performing plasmid in terms of viral titre, and did not indicate degradation when analysed by agarose gel electrophoresis (Figure 4.4A, lanes 6-8).

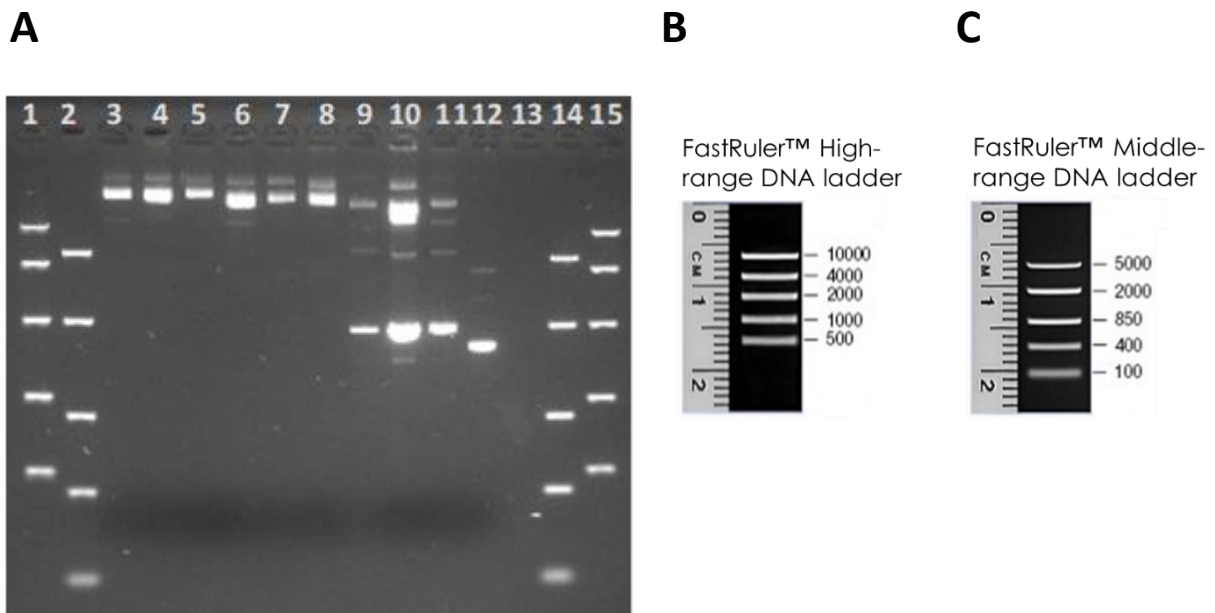


Figure 4.4: Gel image and DNA ladders used for electrophoretic analysis of plasmids from different stocks for comparative purposes. (A) Lanes 1 and 15 were loaded with FastRuler™ HR DNA ladder, and lanes 2 and 14 were loaded with FastRuler™ MR DNA ladder. Lanes 3-5 were loaded with pNL4-3 preparations in the order (left to right) depicted in Table 4.7. Lanes 6-8 were loaded with pYu2 preparations in the same order, and lanes 9-11 contain p89.6 DNA. Lane 12 was loaded with pUC19 DNA. (B) FastRuler™ HR DNA ladder band sizes, loaded in lanes 1 and 15 of (A). (C) FastRuler™ MR DNA ladder band sizes, loaded in lanes 2 and 14 of (A).

4.4 Propagation of HIV in peripheral blood mononuclear cells

4.4.1 Cell stocks

4.4.1.1 Peripheral blood mononuclear cell isolation from peripheral blood

PBMCs were isolated within 2 hrs of peripheral blood donation by density-gradient centrifugation on Histopaque-1077 (histopaque; Sigma-Aldrich, USA). Separation of mononuclear cells (MNCs) from granulocytes, red blood cells, and platelets was achieved by carefully layering 30-35 mL whole blood on 15 mL histopaque in 50 mL centrifuge tubes, followed by centrifugation at 1700 rpm for 30 min with no brake. The plasma layer was aspirated from the top, and the fuzzy, white MNC layer containing PBMCs was collected using a Pasteur pipette. Collected MNC layers were pooled and split into 20-25 mL aliquots between 50 mL centrifuge tubes and washed by topping up the volume to 50 mL with 0.22 µm filter-sterilised TP buffer (PBS (pH7.4) supplemented with 10 µg/mL human albumin (Sigma-Aldrich, USA) and 2 mM EDTA (Sigma-Aldrich, USA)). PBMCs were pelleted by centrifugation at 300 x g for 10 min, and the pellets were pooled and resuspended in 30 mL 0.22 µm filter-sterilised ammonium chloride lysis solution (0.155 M NH₄Cl (Sigma-Aldrich, USA), 0.0119 M NaHCO₃ (Sigma-Aldrich, USA), 0.25 mM EDTA, pH 7.4). Residual red blood cells were lysed by incubation with ammonium chloride lysis solution for no more than 30 min at 4°C. After a maximum of 30 min incubation, ammonium chloride lysis solution was removed by centrifugation at 300 x g for 10 min to pellet the cells.

PBMC pellets were resuspended in 30 mL TP buffer to wash residual ammonium chloride from the cells, and remove platelets. Activated platelets can internalise infectious agents (such as HIV)²¹, which would compromise HIV production in PBMCs. Therefore, platelets were removed by centrifugation at 100 x g for 10 min without brake (platelet spin) and aspiration of the supernatant down to 1 cm from the pellet. Platelets are smaller and lighter than PBMCs, and therefore remain in suspension (supernatant) during slow centrifugation without brake.

The cells were washed once more by topping up the volume to 30 mL TP buffer, and pelleted by centrifugation at 300 x g for 10 min. PBMC pellets were resuspended in 10 mL TP buffer for enumeration by flow cytometry as described in 4.4.1.2 *Peripheral blood mononuclear cell enumeration by flow cytometry* and cryopreserved as described in 4.4.1.3 *Peripheral blood mononuclear cell cryopreservation*.

4.4.1.2 *Peripheral blood mononuclear cell enumeration by flow cytometry*

Phenotyping and enumeration of PBMCs isolated for HIV propagation was performed by flow cytometry using the Gallios™ flow cytometer. The laser and filter configuration is shown in Table 4.8, indicating the channels used to detect fluorochromes relevant to PBMC phenotyping and enumeration (described in 4.4.1.2 *Peripheral blood mononuclear cell enumeration by flow cytometry*).

Table 4.8: Gallios™ laser and filter configuration used for PBMC phenotyping, showing the relevant antibodies or stains and the respective detection channels.

Laser	Filter	Channel	Antibodies + Fluorochromes
488nm, 22mW (BLUE)	525/40	FL1	CD4-FITC
	575/30	FL2	Not used
	620/30	FL3	Flow-Count™
	695/30	FL4	7-AAD
	755 LP	FL5	Not used
638nm, 25mW (RED)	660/20	FL6	Not used
	725/20	FL7	Not used
	755 LP	FL8	Not used
405nm, 40mW (VIOLET)	450/40	FL9	Not used
	550/40	FL10	CD45-KO

4.4.1.2.1 Sample preparation

Two aliquots of 100 μ L were used to phenotype and enumerate PBMCs prior to cryopreservation for HIV production. One aliquot (tube 1) was stained with 3 μ L each of 7-AAD, CD4-FITC (3.6.4.1 *GHOST cell CD4 expression*), mouse anti-human CD45 conjugated to Krome Orange™ (CD45-KO; clone J33; Beckman Coulter, USA) for 10 min in the dark. Before analysis, 100 μ L Flow-Count™ and 300 μ L PBS were added to the flow tube. Phenotyping for CD4 was performed for parallel projects performed by other students using the same samples.

4.4.1.2.2 Gating strategy

The sequential gating strategy used for PBMC phenotype and enumeration is shown in Figure 4.5. Intact PBMCs were identified in a two-parameter FS Lin versus SSC Log plot, in the “PBMCs” region (Figure 4.5A). As explained in 4.3.4.2.2 *HEK293T cell enumeration by flow cytometry*, Flow-Count™ beads were removed from the FS Lin versus SSC Log plot using a “NOT BEADS” Boolean gate. Viable (7-AAD negative) PBMCs were selected in the “VIABLE” region (Figure 4.5B) of a two-parameter SSC Log versus 7-AAD plot gated on PBMCs. Viable PBMCs expressing the panleukocyte marker CD45 were captured in the “Leukocytes” region (Figure 4.5C), which were then used to identify CD45⁺CD4^{dim} monocytes (Figure 4.5D, red population), and CD45⁺CD4⁺ T cells (Figure 4.5D, purple population). Monocytes and T cells were distinguished based on (i) relative CD4 expression, and (i) relative complexity (SSC Log)²². A representative plot for the capture of Flow-Count™ beads is shown in Figure 4.5E.

Cells in the “PBMCs” region (Figure 4.5A) were enumerated by relating the number of cells in the PBMC region and the number of Flow-Count™ beads in the “Cal” region to the calibration factor provided with the Flow-Count™ vial by Equation 3.1.

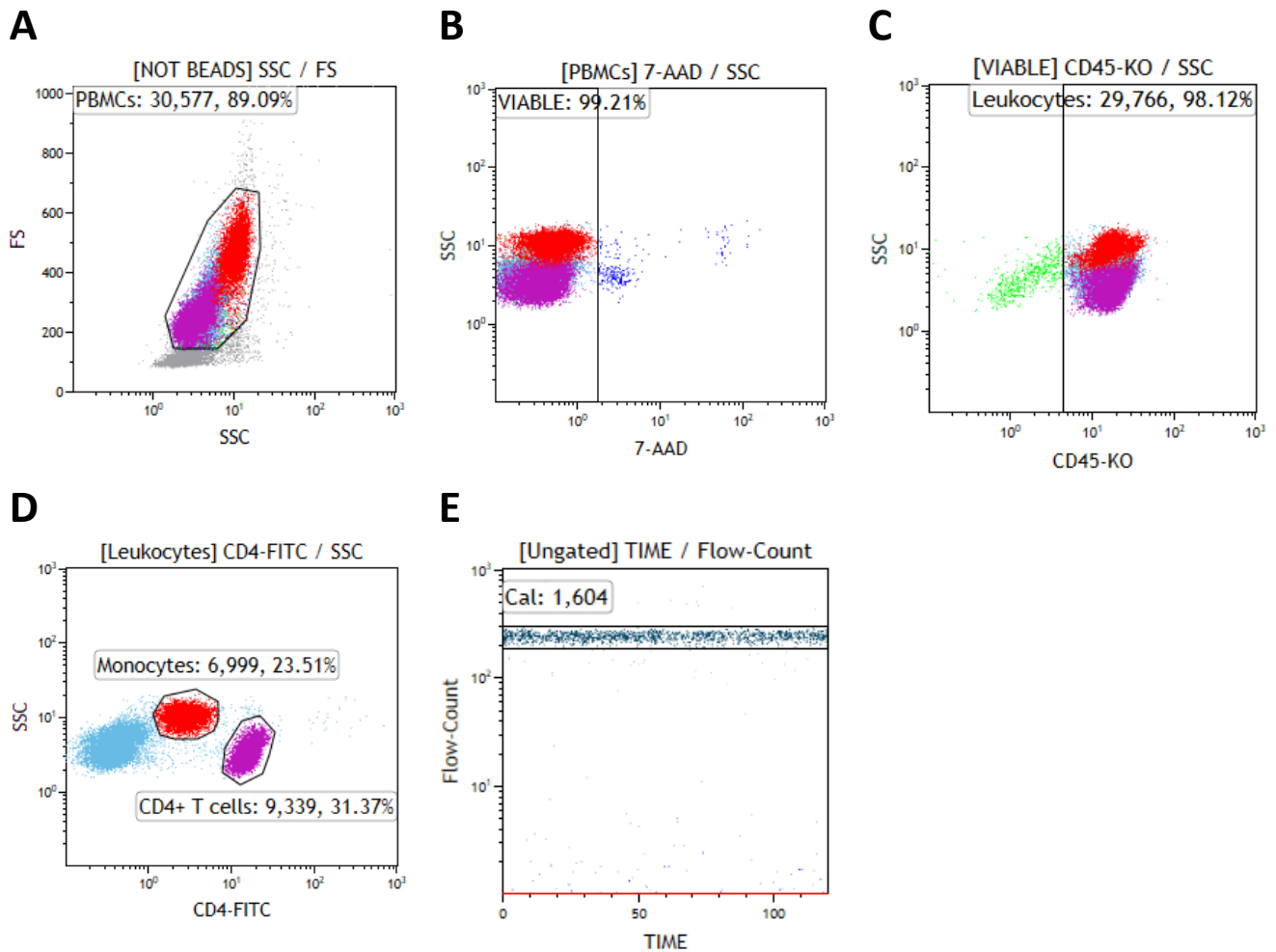


Figure 4.5: Sequential gating strategy used to phenotype and enumerate PBMC stocks for HIV propagation. (A) A two-parameter FS Lin versus SSC Log plot was used to identify intact PBMCs, captured in the “PBMCs” region, gated on the Boolean gate “NOT BEADS” to exclude Flow-Count™ beads from cell analyses. (B) Viable PBMCs were identified using a two-parameter SSC Log versus 7-AAD plot gated on PBMCs based on negative staining for 7-AAD, indicated by the “VIABLE” region. (C) Viable PBMCs expressing the panleukocyte marker CD45 (leukocytes) were identified using a two-parameter SSC Log versus CD45-KO plot gated on viable PBMCs. Leukocytes identified by expression of CD45 were captured in the “Leukocytes” region, which were then used to identify monocytes and T-cells from the remaining leukocytes. (D) A two-parameter plot showing SSC Log versus CD4-FITC (gated on “Leukocytes”) was used to distinguish monocytes ($CD45^+CD4^{dim}$, moderate to high SSC; red population) and $CD4^+$ T-cells ($CD45^+CD4^+$, moderate SSC; purple population). (E) Flow-Count™ bead events were captured in the “Cal” region for enumeration purposes.

4.4.1.3 Peripheral blood mononuclear cell cryopreservation

After enumeration, PBMCs were pelleted once more by centrifugation at 300 x g for 10 min and resuspended in 1 mL freezing medium (described in 4.3.4.2.1 *HEK293T cell culture and*

passaging) per 10×10^6 PBMCs, after which 1 mL aliquots were transferred to 1.5 mL cryovials and stored in liquid nitrogen until required.

4.4.2 Propagation of human immunodeficiency virus in peripheral blood mononuclear cells

4.4.2.1 Overview

Propagation of HIV-1C isolates (Table 4.1) was performed according to an in-house adaptation of the Montefiori method⁴ for HIV production in PBMC cultures (Figure 4.6). This involved culturing HIV CFS or previously cryopreserved HIV-infected PBMCs with PHA-P-activated PBMCs. Details of establishing the adapted method are described in 4.4.3 *Primary virus propagation optimisation*.

4.4.2.2 Human immunodeficiency virus propagation in peripheral blood mononuclear cells – method

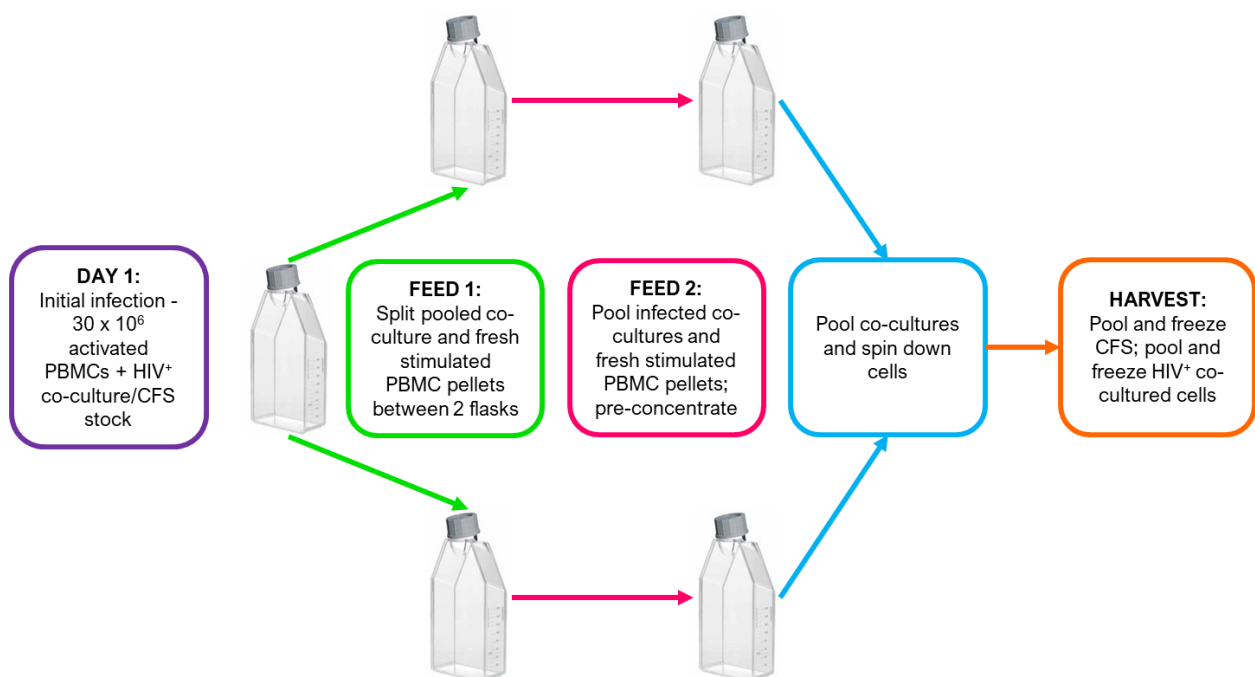


Figure 4.6: In-house modified strategy for HIV propagation in PHA-P/IL-2-stimulated PBMCs.

4.4.2.2.1 Peripheral blood mononuclear cell thawing

PBMCs were resuscitated from liquid nitrogen by diluting cryopreserved cells into pre-warmed RPMI, followed by centrifugation at 300 x g for 10 min. The supernatant (containing DMSO) was aspirated and cells were resuspended in 1 mL activation medium (explained in 4.4.2.2.2 *Peripheral blood mononuclear cell activation*) per 10⁶ thawed PBMCs. Details of the thawing/activation schedule and number of PBMCs thawed during propagation are described in Table 4.9.

4.4.2.2.2 Peripheral blood mononuclear cell activation

Mitogenic stimulation with PHA-P causes mitosis by cross-linking cell surface proteins causing intracellular signalling pathways to trigger cell division and activation²³. T-cell viability during and post-activation was maintained by culture with interleukin-2 (IL-2)²⁴. PBMCs were activated prior to infection for HIV production as transcriptionally active cells more easily support HIV replication²⁵.

Thawed PBMCs were immediately activated using activation medium, called IL-2 growth medium (IL-2GM; RPMI supplemented with 5% recombinant human IL-2 (Roche, Switzerland), 20% FBS, and 2% pen/strep) supplemented with 5 µg/mL PHA-P (Sigma-Aldrich, USA). The number of PBMCs required (Table 4.9) were incubated in 1 mL IL-2GM + PHA-P per 10⁶ thawed PBMCs for 24 hr in an upright T75 flask at 37°C, 5% CO₂.

After 24 hr incubation, the activation medium was removed by centrifugation at 300 x g for 10 min, and replaced with 1 mL IL-2GM per 10⁶ PBMCs. Activated PBMCs were cultured after replacing the medium to allow the cells to replicate before feeding to the HIV/PBMC co-culture. This was performed by incubating the flasks upright at 37°C, 5% CO₂, for 48 hr after replacing IL-2GM + PHA-P with IL-2GM.

Table 4.9: A summary of the schedule of events for the propagation of R5-, R5X4-, and X4-tropic HIV-1C primary isolates. Details of the number of PBMCs required to initiate propagation experiments and for the various feed cycles are included.

Activity	R5- and R5X4-tropic HIV-1C isolates	X4-tropic HIV-1C isolates
Initial activation	<ul style="list-style-type: none"> • Thaw 30x10⁶ PBMCs 	<ul style="list-style-type: none"> • Thaw 30x10⁶ PBMCs
Activations for feeds	<ul style="list-style-type: none"> • Thaw 20x10⁶ PBMCs 	<ul style="list-style-type: none"> • Thaw 40x10⁶ PBMCs
Infection	<p>Day 1</p> <ul style="list-style-type: none"> • 30x10⁶ activated PBMCs • 30 mL RPMI (2% pen/strep) 	<p>Day 1</p> <ul style="list-style-type: none"> • 30x10⁶ activated PBMCs • 30 mL RPMI (2% pen/strep)
Feed 1	<p>Day 4</p> <ul style="list-style-type: none"> • 20x10⁶ activated PBMCs • 15 mL RPMI (2% pen/strep) • Split into two T75 flasks 	<p>Day 3</p> <ul style="list-style-type: none"> • 40x10⁶ activated PBMCs • 20 mL RPMI (2% pen/strep) • Split into two T75 flasks
Feed 2	<p>Day 7</p> <ul style="list-style-type: none"> • 20x10⁶ activated PBMCs • 10-12 mL RPMI (2% pen/strep)/flask 	<p>Day 5</p> <ul style="list-style-type: none"> • 40x10⁶ activated PBMCs • 12-15 mL RPMI (2% pen/strep)/flask
Harvest	<p>Day 10</p> <ul style="list-style-type: none"> • Pool and filter supernatants • Pool HIV⁺ PBMCs • Aliquot and freeze HIV CFS and HIV⁺ PBMCs 	<p>Day 7</p> <ul style="list-style-type: none"> • Pool and filter supernatants • Pool HIV⁺ PBMCs • Aliquot and freeze HIV CFS and HIV⁺ PBMCs

*The differences in feeding schedule and cell numbers for X4-tropic HIV compared to R5- and R5X4-tropic HIV are important to note. These differences result from the optimisation of PBMC-propagation of X4-tropic HIV, explained in detail in 4.4.3 *Primary virus propagation optimisation*.

4.4.2.2.3 Infection

The initial infection (Table 4.9) was performed by pelleting activated PBMCs (24 hr activation and 48 hr culture; see 4.4.2.2.2 *Peripheral blood mononuclear cell activation*) by centrifugation at 300 x g for 10 min and resuspending the cells in 2 mL pre-warmed RPMI (2% pen/strep). The cells were exposed to HIV by incubation with 1 mL HIV⁺ PBMCs from a previous HIV production, or HIV CFS provided by the NICD, for 2 hr at 37°C, 5% CO₂ in 50 mL centrifuge tubes. The initial infections were performed in small volumes to increase the potential for contact between activated PBMCs and virus without the use of a sedimentation agent such as Polybrene®. Polybrene® was not used in PBMC-propagation experiments to encourage the propagation of only the most infectious, efficient virus which did not require the assistance of a sedimentation agent to infect cells.

After incubation, the HIV-exposed PBMCs were topped up to 30 mL total volume with RPMI (2% pen/strep) per 30x10⁶ HIV-exposed PBMCs, and transferred to T75 flasks. These flasks were incubated upright at 37°C, 5% CO₂ until feed days, which differed for HIV-1C viruses depending on tropism (Table 4.9). The optimisation of R5- and R5X4-tropic HIV productions, X4-tropic HIV productions, is discussed in 4.4.3 *Primary virus propagation optimisation*.

4.4.2.2.4 Feeds

The number of PBMCs required for each feed (Table 4.9) were thawed as described in 4.4.2.2.1 *Peripheral blood mononuclear cell thawing*, and activated as described in 4.4.2.2.2 *Peripheral blood mononuclear cell activation*. On each feed day, activated PBMCs were pelleted by centrifugation at 300 x g for 10 min, and resuspended in 2 mL RPMI (2% pen/strep) to prepare for feeding. HIV/PBMC co-cultures of the same HIV-1C isolate were pooled (if necessary) in 50 mL centrifuge tubes, pelleted by centrifugation at 300 x g for 10 min, and resuspended in 2 mL RPMI (2% pen/strep).

Feed 1

The first feed was performed by pooling the activated PBMCs and HIV/PBMC co-culture prepared for feeding, resulting in a total volume of 4 mL RPMI (2% pen/strep). The pooled

freshly-activated PBMC/HIV co-culture was split (2 mL co-culture per flask) between two T75 flasks per 30×10^6 freshly-activated PBMCs used in the initial infection. The volume in each flask was topped up to 15 mL (R5- and R5X4-tropic isolates) or 20 mL (X4-tropic isolates) RPMI (2% pen/strep) per flask, as indicated in Table 4.9. The HIV/PBMC co-cultures were incubated in upright T75 flasks at 37°C, 5% CO₂ until feed 2 (Table 4.9).

Feed 2

The second feed was performed by pooling HIV/PBMC co-cultures and PBMCs activated for feed 2 in a total volume of 2 mL RPMI (2% pen/strep), as described for feed 1. The freshly-activated PBMC/HIV co-culture was split between the same number of flasks as seeded from feed 1, and the volume topped up to 10-12 mL (R5- and R5X4-tropic isolates) or 12-15 mL (X4-tropic isolates) RPMI (2% pen/strep) per T75 flask (Table 4.9). The medium volumes for feed 2 were reduced compared to feed 1 to pre-concentrate HIV CFS before harvesting. The HIV/PBMC co-cultures were incubated in upright T75 flasks at 37°C, 5% CO₂, until harvest (Table 4.9).

4.4.2.2.5 Cell-free supernatant and infected peripheral blood mononuclear cell harvest

HIV CFS, pre-concentrated in feed 2 by adding less medium, was harvested on the day indicated in Table 4.9, by splitting PBMCs and HIV-containing supernatant. This was achieved by transferring the cell suspension to a 50 mL tube and centrifuging at 300 x g for 10 min. Supernatants containing virus of the same isolate were carefully collected and pooled in 50 mL centrifuge tubes. Cells and debris were removed from virus-containing supernatant by filtration through 0.22 µm filters. HIV CFS was then dispensed into 1.5 mL microcentrifuge tubes in 500 µL and 1 mL aliquots, and immediately transferred to -80°C until required. HIV⁺ PBMCs were resuspended in 1 mL freezing medium per T75 flask. Aliquots of 1 mL HIV⁺ PBMCs were dispensed into 1.5 mL cryovials and also transferred to 80°C until required.

4.4.2.2.6 Control medium for experiments

PBMC-conditioned medium (CM) was harvested from activated PBMCs in the same way as PBMC-propagated HIV, without infecting the cells. CM was harvested every three days after the “infection” day, 0.22 µm-filtered, and stored at -80°C in 1.5 mL cryovials until required. This was prepared and stored to control for the effects of PBMC-conditioned medium in HIV CFS to isolate the effects of conditioned medium from the effects of HIV in HIV experiments using HIV CFS.

4.4.3 Primary virus propagation optimisation

Establishment and optimisation of the experimental protocol was performed using HIV-1C R5-tropic primary isolate CM1, and R5X4-tropic primary isolate CM9 (Table 4.1). Initially, propagation was performed by exposing 30×10^6 PBMCs (in 1 mL RPMI) activated using PHA-P/IL-2 (as described in 4.4.2.2.2 *Peripheral blood mononuclear cell activation*) to 1 mL HIV CFS or 1 mL HIV⁺ PBMC co-culture for 2 hr in 2 mL total volume. The cell suspension (2 mL) was then added to 28 mL RPMI (2% pen/strep) in a T75 flask which was incubated upright at 37°C, 5% CO₂ until feeding. Feeding was performed every 3 days with 10×10^6 activated PBMCs, and HIV CFS was harvested every three days from day 10 to day 28 as described in the Montefiori protocol for primary HIV production⁴.

The protocol described above was adjusted to optimise (i) the number of PBMC stocks used per production, (ii) establish the optimal harvest points resulting in peak-production harvests containing the most possible virus, and (iii) attempt to optimise infectious HIV titre. With primary virus produced *in vitro* by infection rather than cloning, the requirement for reverse transcription introduces additional challenges, such as deleterious mutations contributing to the production of significant proportions of non-infectious HIV. Various aspects of the Montefiori protocol were evaluated to improve viral production.

4.4.3.1 Harvest cycles

To begin with, two harvests of HIV CFS were performed per production, at day 10 and day 14. Comparison of p24 ELISA results (performed as described in 3.4 P24) between consecutive harvests showed that day 10 harvests contained more virus than day 14 harvests (Table 4.10). For this reason, HIV CFS was harvested on day 10 only (after 2 feeds) for future productions. Complete RPMI (10% FBS, 2% pen/strep) rather than RPMI without additives was erroneously used as the negative control for the p24 ELISA, possibly contributing to the negative control being out of range for the assay. However, as the 200 pg/mL standards were reproducible between the two wells, the p24 ELISAs were not discarded as invalid.

The limit of linearity of the p24 ELISA could not be established due to the limited quantity of p24 protein standard provided with the kit. The limit of linearity refers to the point at which correlation between OD and p24 concentration ceases to be linear, and begins to plateau out. For this reason, the 1/10 dilutions were considered more reliable when the difference between the neat HIV CFS and the 1/10 dilution of the same harvest was not 10-fold.

Table 4.10: p24 ELISA results comparing day 10 and day 14 HIV CFS harvests for CM1.

Sample ID	Raw OD	Normalised
Negative control (complete RPMI)	0.322	0
12.5 pg/mL p24	0.866	0.544
200 pg/mL p24	1.611	1.289
200 pg/mL p24 (repeat)	1.59	1.268
CM1 (10/10/2016 – 24/10/2016) day 10	3.824	3.502
CM1 (10/10/2016 – 24/10/2016) day 10 (1/10 dilution)	1.271	0.949
CM1 (10/10/2016 – 24/10/2016) day 14	2.514	2.192
CM1 (10/10/2016 – 24/10/2016) day 14 (1/10 dilution)	0.594	0.272

Following the outcome of the p24 ELISA indicating that day 10 harvests contain more virus than day 14 harvests from the same production, a single harvest on day 10 was performed for future harvests. Selecting a single harvest day per production also limited the number of viral replication cycles until viral-containing supernatant was harvested. This was in an attempt to reduce the accumulation of non-infectious HIV moieties arising due to mutation resulting from error-prone reverse transcription during HIV replication^{10, 26}.

4.4.3.2 Feeding cycles

Successful propagation of HIV in PBMCs can be grossly simplified into Equation 4.1. The amount of infectious HIV in generation $n+1$ (HIV_{n+1}) is considered as a function of the availability of susceptible activated host cells, the amount of infectious HIV in generation n (HIV_n), and the probability (Pr) of replication competence of HIV_n ($Pr(\text{replication competence})$). In order to generate sufficient quantities of infectious virus, the probability of generating replication competence should be high (ie. approaching 1), and susceptible host cells should outnumber infectious HIV_n . The chance of replication competence of any given virion of HIV_n is determined by a host of factors including fidelity of reverse transcription, completeness of integration, and evasion of host cell defence mechanisms²⁷⁻³⁰. From Equation 4.1, the only factor which could be manipulated in the laboratory was the availability of host cells.

Equation 4.1: Simplified representation of HIV propagation in PBCMs.

$$HIV_{n+1} = \frac{\text{susceptible host cells}}{HIV_n \times Pr(\text{replication competence})}$$

4.4.3.2.1 Feed 1 co-culture split

Splitting the HIV/PBMC co-culture into two flasks on the first feed was introduced to improve the ratio between PBMCs and HIV, while minimising the volume in the flask separating the cells (which sink to the bottom) and the virus (which remains in suspension). The reduced volume in each flask was a critical point as there should be contact between virus and cells for infection to occur.

Feeding the split flasks the same amount of PBMCs as would be fed to the single flask (from the initial protocol) theoretically reduced the chance of susceptible host cell availability being depleted, and thus being a limiting factor in the production. Cell death during HIV propagation in PBMCs also impacts the availability of host cells, as cell death reduces the number of cells available to be infected in the next infection cycle.

Host cell turnover was particularly high for propagation of the X4-tropic HIV-1C isolate SW7, which induced syncytia in PBMCs. Syncytium formation describes the HIV-induced fusion of many cells into a single, multinucleated structure³¹ which ultimately decreases the number of PBMCs available to be infected in the next round. In the case of SW7 which exhibited this high turnover, three days between feeds proved too long for cell survival and HIV propagation. In order to mitigate the effects of this turnover on HIV production, flasks were fed every two days rather than every three days, with twice the number of activated PBMCs per feed. In order to maintain consistency with R5- and R5X4-tropic productions which were fed twice before harvest, the X4-tropic HIV was also fed twice before harvest, and was consequently harvested on day 7 of HIV production.

4.4.3.2.2 Upscaling virus production

Having adjusted PBMC numbers for feeding, the cycle of feeding, and the harvest time, production was up-scaled by doubling each component. Each aspect of the production protocol was doubled, and co-cultures of the same HIV-1C isolate were pooled before feeding. This resulted in twice the number of HIV CFS on the day of harvest, but more importantly, provided a means to improve propagation despite the loss of infectivity due to replication-driven mutation. This principle is illustrated in Figure 4.7, showing the flask-specific changes that may occur to HIV in each flask (represented by different colour virions) despite starting from the same initial infection. These different viral species (quasispecies) are transmitted to other flasks by pooling during feeding, ensuring that a portion of replication-competent virus is present in each flask which is provided with new activated cells and hence the opportunity to replicate.

The viral quasispecies phenomenon (shown in Figure 4.7) describes the diversity of viral sequences in a population of virus from the same source (production flask, or patient) resulting from mutations accumulated during viral replication³². The quasispecies phenomenon is well-described for HIV^{32, 33}, and was applied to the development of our in-house HIV production protocol to attempt to maximise the production of infectious virus between flasks. Further testing of this hypothesis is recommended, comparing the fitness of virus produced in the Montefiori method with virus produced in the up-scaled in-house method.

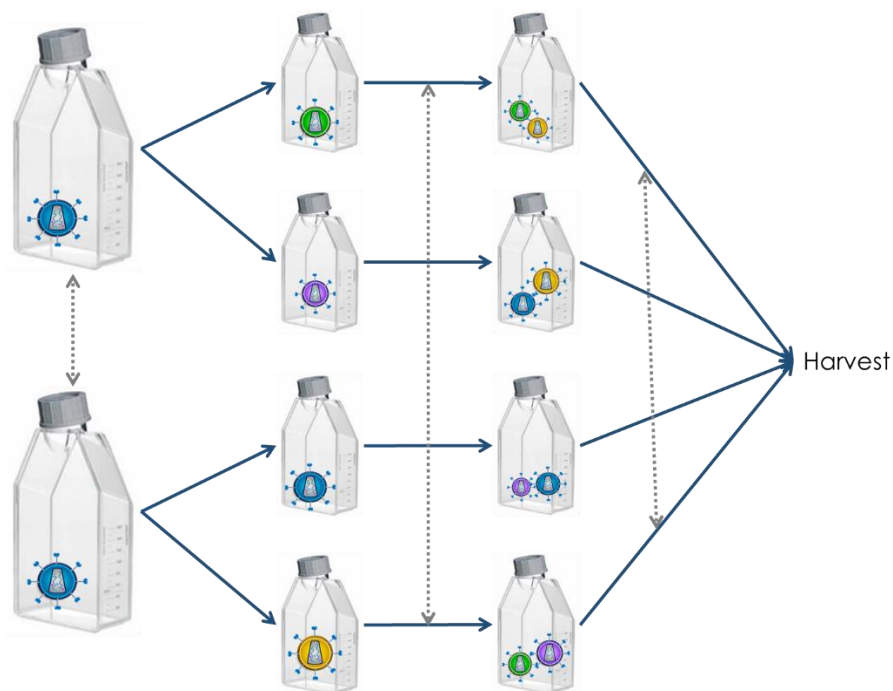


Figure 4.7: Hypothetical illustration of HIV quasispecies formation during HIV propagation. Different coloured virions in each flask represent different populations of HIV which abide in each flask due to mutation resulting from reverse transcription. Each vertical flask series represents a step in HIV production, namely initial infection, feed 1, and feed 2. Grey dotted arrows represent points of pooling, before each feed and before harvesting.

4.4.3.3 Peripheral blood mononuclear cell-propagated virus loses virulence over time

Due to mutations incurred during the error-prone viral replication process, unpredictable loss of virulence in HIV populations is observed with replication (over time), and is well described^{26, 34}. Unfortunately, this unpredictable loss of infectivity with successive productions resulted in the rapid depletion of infectious stocks of virus which could not, despite our efforts, be replenished by further productions. In future, molecular clones of HIV-1C should be considered for experiments requiring infectious virus, as stable, predictable viral production can then be achieved.

Functional titres obtained using the GHOST GFP assay (described in 3.6.6 *GHOST green fluorescent protein* assay – method) for successive productions of representative HIV-1C isolates are shown in Table 4.11. Titres lower than 10^4 IU/mL were considered non-infectious. This was based on the volume of any virus stock which would be required to infect 10^5 cells in a reasonable volume (10 mL or less). Table 4.11 illustrates the loss of virulence over time for PBMC-propagated virus, resulting in insufficient IUs generated to complete experiments with each tropism of HIV for this study.

Table 4.11: Functional titres for successive productions of HIV-1C primary isolates CM9 and SW7 showing a gradual decrease in infectivity over time. Non-infectious harvests (IU/mL $\leq 10^4$) are shown in purple.

Isolate	Harvest date	IU/mL
CM9 (R5X4-tropic)	290118	9.47x10 ⁵
	190218	5.15x10 ⁵
	250918	4.74x10 ³
SW7 (X4-tropic)	240618	3.04x10 ⁵
	010818	4.71x10 ⁵
	220918	7.90x10 ³

4.5 Summary of virus produced

Table 4.12 below summarises the viruses and their infectious titres produced during this study, and their respective functional titres as determined by the GHOST GFP assay (as described in 3.6.6 *GHOST green fluorescent protein assay – method*).

Table 4.12: Representative HIV-1B and HIV-1C HIV CFS stocks and their functional titres generated by the GHOST GFP assay.

HIV-1B stock ID	Functional titre (IU/mL)	Standard deviation	HIV-1C stock ID	Functional titre (IU/mL)	Standard deviation
89.6-041217	5.80×10^4	3.04×10^4	CM1-250217	1.60×10^5	5.18×10^4
89.6-121018	6.01×10^4	1.23×10^4	CM1-110618	1.20×10^5	5.60×10^4
89.6-151018	2.66×10^4	1.28×10^4	CM9-290118	9.47×10^5	2.47×10^5
89.6-181018	5.08×10^3	NA	CM9-280218_P	2.39×10^5	3.20×10^4
NL4-3-041217	3.16×10^4	1.70×10^4	CM9-020518	1.05×10^6	6.28×10^5
NL4-3-121018	3.57×10^4	1.10×10^4	CM9-270618	3.60×10^5	2.25×10^5
NL4-3-151018	4.19×10^4	1.15×10^4	CM9-250918	4.74×10^3	NA
NL4-3-181018	6.16×10^3	2.94×10^3	SW7-240618	7.74×10^4	2.72×10^4
Yu2-041217	5.80×10^5	3.61×10^4	SW7-110718	2.87×10^5	1.26×10^5
Yu2-121018	6.09×10^5	3.27×10^5	SW7-010818	4.71×10^5	4.70×10^4
Yu2-151018	3.53×10^5	2.15×10^5	SW7-220918	7.90×10^3	6.34×10^2
Yu2-181018	3.54×10^4	3.41×10^3	Du422F-240718	2.60×10^4	5.95×10^3

*NA indicates that functional titres were calculated using only the neat virus-infected wells. These isolates were not used in further experiments.

4.6 References

1. German Advisory Committee Blood, S.A.o.P.T.b.B. Human Immunodeficiency Virus (HIV). *Transfusion Medicine and Hemotherapy*. 2016;43(3):203-22.
2. Frankel, A.D., Young, J.A. HIV-1: fifteen proteins and an RNA. *Annual review of biochemistry*. 1998;67:1-25.
3. Freed, E.O. HIV-1 assembly, release and maturation. *Nat Rev Micro*. 2015;13(8):484-96.
4. Protocol for HIV-1 Isolation by PBMC Co-Culture. (January 2014) [Internet]. Montefiori Laboratory, Duke University Medical Center. 2014 [cited September 2016]. Available from: <https://www.hiv.lanl.gov/content/nab-reference-strains/html/home.htm>.
5. Tebit, D.M., Zekeng, L., Kaptué, L., Kräusslich, H.-G., Herchenröder, O. Construction and characterisation of a full-length infectious molecular clone from a fast replicating, X4-tropic HIV-1 CRF02_AG primary isolate. *Virology*. 2003;313(2):645-52.
6. Tiscornia, G., Singer, O., Verma, I.M. Production and purification of lentiviral vectors. *Nature protocols*. 2006;1(1):241-5.
7. Cilliers, T., Nhlapo, J., Coetzer, M., Orlovic, D., Ketas, T., Olson, W.C., et al. The CCR5 and CXCR4 coreceptors are both used by human immunodeficiency virus type 1 primary isolates from subtype C. *J Virol*. 2003;77(7):4449-56.
8. Williamson, C., Morris, L., Maughan, M.F., Ping, L.H., Dryga, S.A., Thomas, R., et al. Characterization and selection of HIV-1 subtype C isolates for use in vaccine development. *AIDS Res Hum Retroviruses*. 2003;19(2):133-44.
9. Choge, I., Cilliers, T., Walker, P., Taylor, N., Phoswa, M., Meyers, T., et al. Genotypic and phenotypic characterization of viral isolates from HIV-1 subtype C-infected children with slow and rapid disease progression. *AIDS Res Hum Retroviruses*. 2006;22(5):458-65.
10. Bebenek, K., Abbotts, J., Wilson, S.H., Kunkel, T.A. Error-prone polymerization by HIV-1 reverse transcriptase. Contribution of template-primer misalignment, miscoding, and termination probability to mutational hot spots. *The Journal of biological chemistry*. 1993;268(14):10324-34.
11. Trinh, T., Jessee, J., R. Bloom, F., Hirsch, V. Stbl2TM: an *Escherichia coli* strain for the stable propagation of retroviral clones and direct repeat sequences. *Focus*. 1994.16(3):78-80.
12. Panja, S., Aich, P., Jana, B., Basu, T. How does plasmid DNA penetrate cell membranes in artificial transformation process of *Escherichia coli*? *Molecular membrane biology*. 2008;25(5):411-22.
13. Sun, Q.Y., Ding, L.W., He, L.L., Sun, Y.B., Shao, J.L., Luo, M., et al. Culture of *Escherichia coli* in SOC medium improves the cloning efficiency of toxic protein genes. *Analytical biochemistry*. 2009;394(1):144-6.
14. Schrader, A.M., Cheng, C.-Y., Israelachvili, J.N., Han, S. Communication: Contrasting effects of glycerol and DMSO on lipid membrane surface hydration dynamics and forces. *The Journal of Chemical Physics*. 2016;145(4):041101.

15. Wicks, I.P., Howell, M.L., Hancock, T., Kohsaka, H., Olee, T., Carson, D.A. Bacterial lipopolysaccharide copurifies with plasmid DNA: implications for animal models and human gene therapy. *Human gene therapy*. 1995;6(3):317-23.
16. Gama-Norton, L., Botezatu, L., Herrmann, S., Schweizer, M., Alves, P.M., Hauser, H., et al. Lentivirus production is influenced by SV40 large T-antigen and chromosomal integration of the vector in HEK293 cells. *Human gene therapy*. 2011;22(10):1269-79.
17. Merten, O.-W., Hebben, M., Bovolenta, C. Production of lentiviral vectors. *Molecular Therapy Methods & Clinical Development*. 2016;3:16017.
18. Mahon, M.J. Vectors bicistronically linking a gene of interest to the SV40 large T antigen in combination with the SV40 origin of replication enhance transient protein expression and luciferase reporter activity. *BioTechniques*. 2011;51(2):119-28.
19. Longo, P.A., Kavran, J.M., Kim, M.-S., Leahy, D.J. Transient mammalian cell transfection with polyethylenimine (PEI). *Methods in enzymology*. 2013;529:227-40.
20. Schmidt, T., Friehs, K., Schleef, M., Voss, C., Flaschel, E. Quantitative analysis of plasmid forms by agarose and capillary gel electrophoresis. *Analytical biochemistry*. 1999;274(2):235-40.
21. Youssefian, T., Drouin, A., Masse, J.M., Guichard, J., Cramer, E.M. Host defense role of platelets: engulfment of HIV and *Staphylococcus aureus* occurs in a specific subcellular compartment and is enhanced by platelet activation. *Blood*. 2002;99(11):4021-9.
22. Janossy, G., Jani, I.V., Bradley, N.J., Bikoue, A., Pitfield, T., Glencross, D.K. Affordable CD4⁺ T-Cell Counting by Flow Cytometry: CD45 Gating for Volumetric Analysis. *Clinical and Diagnostic Laboratory Immunology*. 2002;9(5):1085.
23. Boyman, O., Sprent, J. The role of interleukin-2 during homeostasis and activation of the immune system 2012. 180-90 p.
24. Kelly, E., Won, A., Refaeli, Y., Van Parijs, L. IL-2 and Related Cytokines Can Promote T Cell Survival by Activating AKT. *The Journal of Immunology*. 2002;168(2):597.
25. Alexaki, A., Liu, Y., Wigdahl, B. Cellular reservoirs of HIV-1 and their role in viral persistence. *Current HIV research*. 2008;6(5):388-400.
26. Roberts, J.D., Bebenek, K., Kunkel, T.A. The accuracy of reverse transcriptase from HIV-1. *Science*. 1988;242(4882):1171-3.
27. Gopalakrishnan, S., Montazeri, H., Menz, S., Beerenwinkel, N., Huisinga, W. Estimating HIV-1 Fitness Characteristics from Cross-Sectional Genotype Data. *PLoS Computational Biology*. 2014;10(11).
28. Spira, S., Wainberg, M.A., Loemba, H., Turner, D., Brenner, B.G. Impact of clade diversity on HIV-1 virulence, antiretroviral drug sensitivity and drug resistance. *The Journal of antimicrobial chemotherapy*. 2003;51(2):229-40.
29. Jakobsen, M.R., Ellett, A., Churchill, M.J., Gorry, P.R. Viral tropism, fitness and pathogenicity of HIV-1 subtype C. *Future Virology*. 2010;5(2):219-31.
30. Bar-Magen, T., Sloan, R.D., Faltenbacher, V.H., Donahue, D.A., Kuhl, B.D., Oliveira, M., et al. Comparative biochemical analysis of HIV-1 subtype B and C integrase enzymes. *Retrovirology*. 2009;6(1):103.

31. Bracq, L., Xie, M., Benichou, S., Bouchet, J. Mechanisms for Cell-to-Cell Transmission of HIV-1. *Front Immunol.* 2018;9:260.
32. Sguanci, L., Bagnoli, F., Liò, P. Modeling HIV quasispecies evolutionary dynamics. *BMC Evolutionary Biology.* 2007;7(Suppl 2):S5-S.
33. van Zyl, G., Bale, M.J., Kearney, M.F. HIV evolution and diversity in ART-treated patients. *Retrovirology.* 2018;15(1):14.
34. Cheng, Z., Hoffmann, A. A stochastic spatio-temporal (SST) model to study cell-to-cell variability in HIV-1 infection. *J Theor Biol.* 2016;395:87-96.

Chapter 5 Haematopoietic stem/progenitor cell isolation and purification

5.1 Introduction

Haematopoiesis, the process of reconstituting all blood and immune cells, is achieved by the differentiation of HSPCs in response to a specific cytokine stimulus¹. HSPCs reside in the bone marrow, in specialised niche environments which maintain quiescence or initiate differentiation and mobilisation from the bone marrow as required by the body². The cell surface marker CD34 is used as a proxy for the stem cell population for transplantation purposes, and is widely used to isolate HSPCs in research settings, as the phenotype of the “true” self-renewing HSC remains unknown³⁻⁵. The CD34⁺ HSPC population is heterogenous, including cells which express differentiation markers indicating lineage priming, such as CD38⁶, and markers indicating quiescence, such as CD90 (Figure 5.1)³. However, extensive research has shown that the CD34⁺ population is important for engraftment in HSCT, contains long-term repopulating cells, and can form multilineage colonies *in vitro*⁷⁻¹⁰.

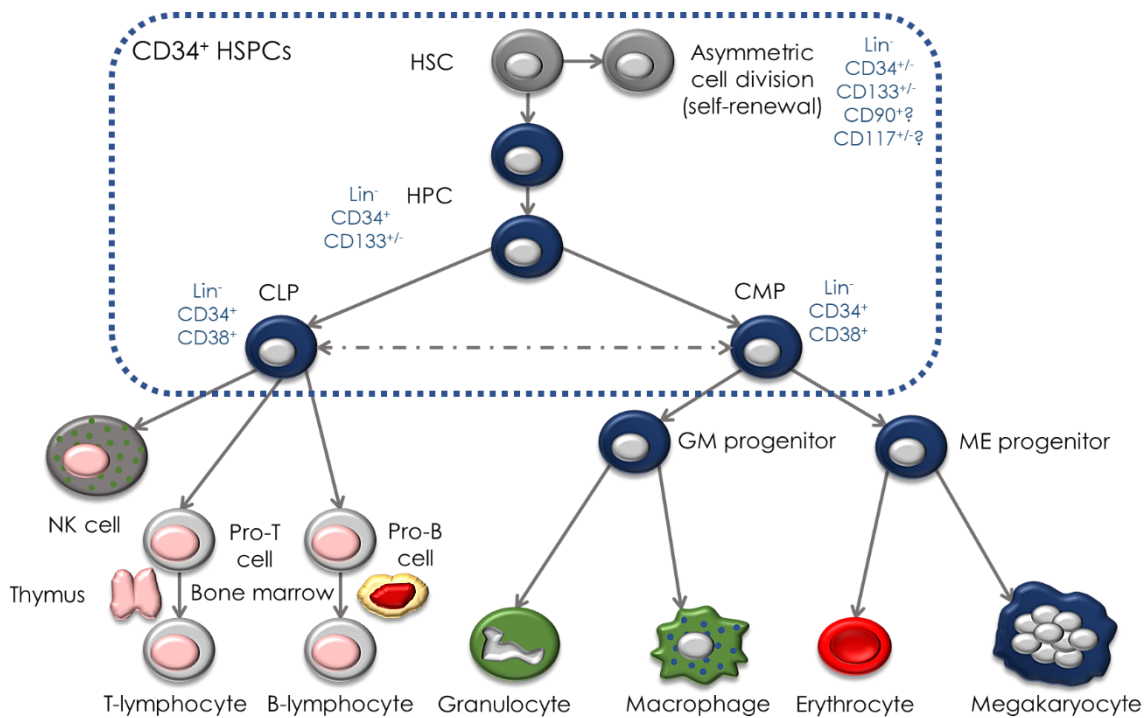


Figure 5.1: Haematopoiesis and the expression of HSPC surface markers^{3, 4, 6, 11}. The self-renewing HSC divides asymmetrically to produce a self-renewing HSC and HPC, which will differentiate as directed by cytokine signalling. The heterogeneous CD34⁺ HSPC population is outlined by the blue dotted line.

For applications which require pure populations of HSPCs, the HSPC population must be teased out of the MNC population, which can be purified from enucleated cells and granulated or multinucleated cells by centrifugation. Purification of HSPCs from MNCs is most often achieved by selection of the CD34⁺ HSPC population, which expresses low to intermediate levels of CD45 (CD45^{dim})¹² depending on the source. Cell surface phenotype can be exploited to remove non-target cells or isolate target cells, using cell surface marker-specific monoclonal antibodies. These antibodies tag target cells (direct selection) or non-target cells (indirect selection) and can be used to separate the population of interest. This is termed cell sorting, and can be achieved using a cell sorting flow cytometer, where selection is based on fluorescent antibody-based tagging¹³, or by magnetic separation, where selection is based on magnetic microbead-based tagging¹⁴.

Bone marrow aspirates, UCB, and mobilised peripheral blood (leukapheresis product) are the sources of CD34⁺ HSPCs most frequently used for research and clinical purposes^{15, 16}. Bone

marrow aspirates are obtained by inserting a needle into bones containing marrow (such as the iliac crest of the hip), and removing small volumes (10-20 mL) of bone marrow. Bone marrow aspiration is invasive and painful and is not performed without clinical indication. Leukapheresis product is obtained by mobilising HSPCs from the bone marrow into circulation by administering a mobilising agent such as G-CSF¹⁷. Mobilised HSPCs are collected with peripheral blood cells by apheresis from a donor, concentrating the cells into an apheresis collection bag, and re-infusing the donor with the remaining plasma in a closed system. This is most often performed to harvest CD34⁺ HSPCs for transplantation purposes¹⁷. UCB is the least invasive source of CD34⁺ HSPCs as blood is collected from the umbilical cord immediately after childbirth, which would otherwise be discarded as medical waste. Bone marrow is reported to be the richest source of CD34⁺ HSPCs, at 5.6% ± 4.6 of harvested cells, compared to leukapheresis product at 1.9% ± 2.6 and UCB at 1.7% ± 2.6 of harvested cells¹⁸. However, leukapheresis product outweighs both UCB and bone marrow with regard to cell number, and is therefore the preferred source of HSPCs in the clinical setting.

5.2 Ethical considerations

5.2.1 Sample collection

Umbilical cord blood (UCB) and leukapheresis products were used as sources of HSPCs in this study. Written informed consent for donation of UCB was obtained from patients scheduled for caesarean section at Netcare Femina Hospital, Pretoria, South Africa. Leukapheresis products were donated by the Alberts Cellular Therapy (ACT) unit at Netcare Pretoria East after consent and approval was obtained to donate products for research purposes. The use of UCB- and leukapheresis-derived HSPCs for the purposes described herein was approved by both the Faculty of Health Sciences Research Ethics Committees (in accordance with the Declaration of Helsinki; protocol number 207/2016) and the Netcare Research Ethics Committee. Samples were anonymised by using a sample ID which identifies the source, and the date on which it was collected/donated/thawed. Donors from the same day were separated by adding an additional numerical epithet. To illustrate, UCB samples harvested in

the afternoon of 02/04/2018 but processed the morning of 03/04/2018 would be labelled CB030418, and leukapheresis samples received on 12/11/2018 would be labelled AP181112.

5.2.2 Human immunodeficiency virus testing

Only HIV-negative samples were included for experimental purposes due to the nature of the experiments. Since HIV testing is routinely performed for pregnancy and transplant purposes, patient files were used to pre-screen potential UCB donors. Leukapheresis donor HIV negative status was provided by ACT staff. UCB sample HIV-status was confirmed by GeneXpert testing (described in 3.3 *Donor testing*) prior to the initiation of experiments. Leukapheresis donor samples could not be reliably tested by GeneXpert, which is not validated for testing samples other than whole blood.

5.3 Sample processing

5.3.1 Umbilical cord blood processing

5.3.1.1 Sample collection and storage

During scheduled caesarian sections, UCB was collected from the umbilical vein into a sterile 250 mL cord blood collection bag (Jiaxing Tianhe Pharmaceutical Co. Ltd, China) containing 20 mL of the anticoagulant CPD. Collection was done by attending obstetricians and/or theatre nurses. Samples were stored at 4°C and used within 24 hr of collection.

5.3.1.2 Isolation of umbilical cord blood-derived mononuclear cells containing haematopoietic stem/progenitor cells

Isolation of MNCs from UCB was performed by layering 30 mL of whole blood on 15 mL histopaque, followed by centrifugation at 1700 rpm for 30 min with no brake. Cells of different size and weight were separated by the density gradient (Figure 5.2). After centrifugation the top plasma layer containing platelets and proteins was aspirated, and the UCB-MNC layer carefully collected using a Pasteur pipette. Collected UCB-MNCs were washed by topping up

the volume to 50 mL with TP buffer, followed by centrifugation at 300 x g for 10 min. Remaining red blood cells were lysed by resuspending the cell pellet in 20 mL 0.22 μm sterile-filtered ammonium chloride lysis solution (pH 7.4) and incubating for 15-20 min at 4°C. The ammonium chloride and red blood cell debris were removed by aspirating the supernatant after centrifugation at 300 x g for 10 min. The MNC pellet was resuspended in 5 mL TP buffer for enumeration of CD34⁺ HSPCs prior to their isolation.

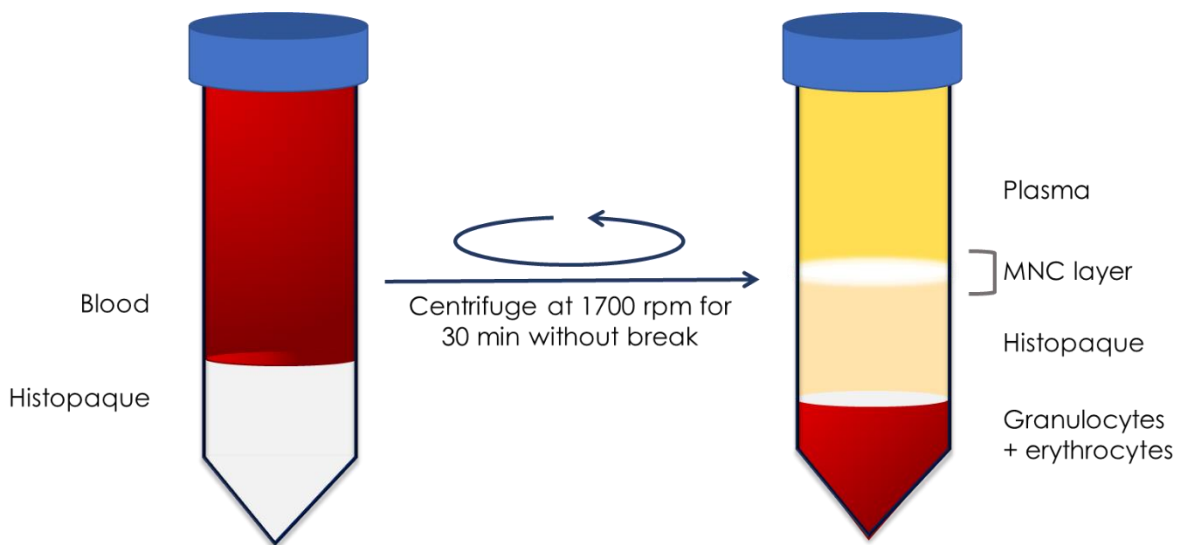


Figure 5.2: Histopaque density-gradient centrifugation facilitates separation of MNCs from granulocytes, erythrocytes, and platelets.

5.3.2 Leukapheresis processing

5.3.2.1 Sample receipt and storage

Leukapheresis products were obtained from storage in liquid nitrogen, in cryobags containing 10% DMSO as a cryoprotectant. Leukapheresis products signed off with informed consent for use in research were collected from the ACT and transferred to the Institute for Cellular and Molecular Medicine (ICMM) between layers of dry ice to prevent thawing during transit. On arrival, products were immediately catalogued and transferred to liquid nitrogen storage.

Leukapheresis products were supplied already de-identified except for HIV-status and whether the samples were intended for autologous or allogeneic HSCT. Sample identifiers were assigned based on date of receipt.

5.3.2.2 Leukapheresis thawing and processing

5.3.2.2.1 Leukapheresis thawing

Leukapheresis products were thawed using a thawing protocol supplied by the ACT with minor modifications. The protocol supplied is routinely used by the ACT during preparation of the cell therapy product for HSPC transplant. Apheresis collection bags were removed from liquid nitrogen and placed on the bench at room temperature for precisely 2 min to prevent the bag from cracking. The sample bag was then transferred to a 2 L glass beaker containing 1.6 L 1% NaCl (Sigma-Aldrich, USA) which was put into a water bath pre-heated to 37°C. The leukapheresis product was thawed for no more than 2 min in by alternately submerging the bag for 10 s and massaging the bag gently for 5 s. The sample was considered thawed when a manageable, icy slush consistency was achieved, typically between 30 s and 1 min of thawing in the water bath.

5.3.2.2.2 Thawed leukapheresis processing

Thawed bags were sprayed with 70% ethanol and wiped down before cutting a small corner of the bag using 70% ethanol-sterilised scissors and aliquoting 10 mL leukapheresis product into pre-cooled 50 mL centrifuge tubes containing 40 mL 4°C (approximately) PBS. Tubes were mixed by inversion as soon as leukapheresis product was aliquoted and centrifuged at 300 x g for 10 min at 4°C to prevent loss of viability due to the presence of DMSO. Cell pellets were resuspended in TP buffer supplemented with 40 µg/mL human albumin (TP₄ buffer) and strained through 70 µm Falcon™ cell strainers (Corning Inc., USA). Additional human albumin was added to TP buffer to reduce clotting¹⁹ caused by aggregation of necrotic cells which form mucous-like clots, trapping a significant number of viable cells. Cells were pelleted once more by centrifugation at 300 x g for 10 min after which up to four pellets were pooled in 50 mL RPMI supplemented with 2% pen/strep for HSPC enumeration. An aliquot of this cell

suspension was used for HSPC enumeration as described in 5.4.2.2 *Leukapheresis product-derived samples*.

The TP₄ buffer wash and strain was performed to save on RPMI and remove necrotic cell clumps sequestering viable cells. However, it was observed that TP₄ buffer resulted in increased non-specific staining with isotype reagent (Figure 5.3B) provided with the Stem-Kit enumeration kit which was not seen in leukapheresis-derived cells stained in RPMI (Figure 5.3A). The suspected increase in non-specific staining observed when staining for the Stem-Kit isotype control in TP₄ buffer was due to non-specific binding of antibodies to human albumin in the buffer. This could compromise the detection of CD34^{dim} HSPCs, leukapheresis product-derived cells were therefore stained and enumerated for CD34⁺ HSPCs in RPMI.

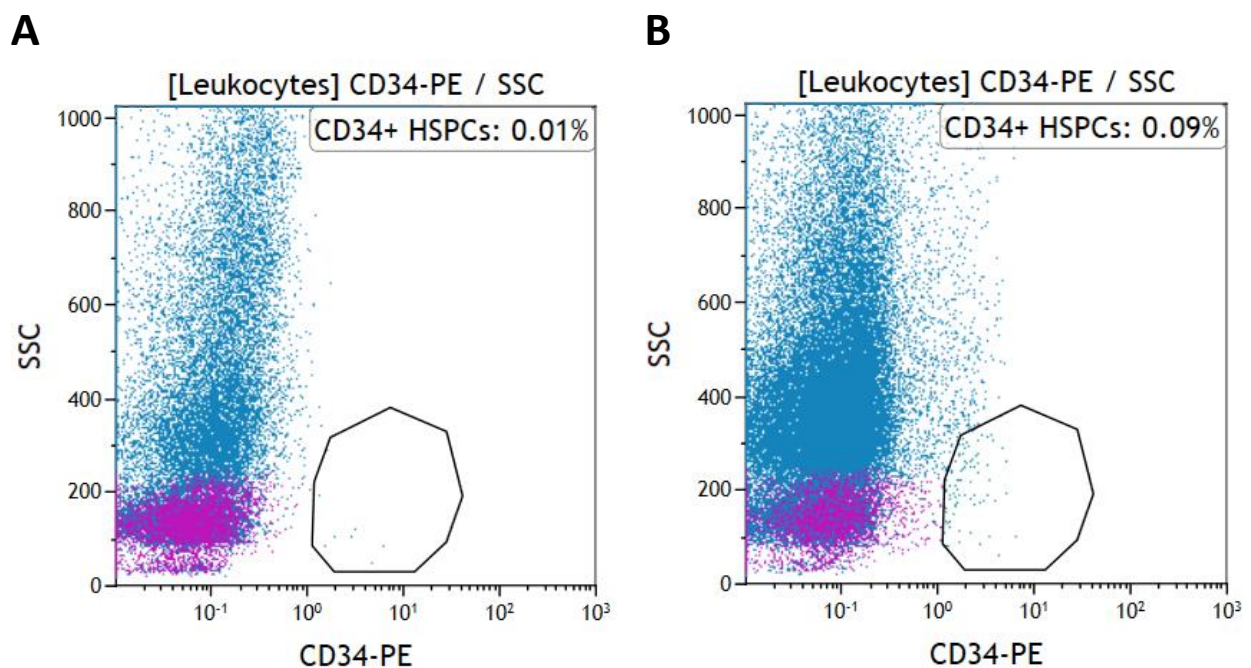


Figure 5.3: Effect of staining medium on isotype control staining (Stem-Kit) during leukapheresis-derived HSPC enumeration. Stemkit iso staining of AP181122-01 cells stained in RPMI (A) versus AP181122-01 cells stained in TP₄ buffer (B).

5.4 Haematopoietic stem/progenitor cell enumeration

5.4.1 Flow cytometer and configuration

Viable CD34⁺ HSPCs were enumerated in processed leukapheresis or UCB samples using the Gallios flow cytometer. This was (i) to determine whether the HSPC content was sufficient to continue with CD34⁺ HSPC isolation, and (ii) to stain with the correct volumes of antibodies for CD34⁺ HSPC isolation. The laser/filter configuration for the Gallios flow cytometer is presented in Table 5.1, with antibodies and their fluorochromes relevant to this chapter indicated next to the appropriate channels.

Table 5.1. Summary of Gallios flow cytometer laser and filter configuration, channel designations and fluorochromes (used in this series of experiments)

Laser	Filter	Channel	Antibodies + Fluorochromes
488nm, 22mW (BLUE)	525/40	FL1	CD45-FITC (Stem-Kit)
	575/30	FL2	CD34-PE (Stem-Kit)
	620/30	FL3	Flow-Count beads
	695/30	FL4	7AAD
	755 LP	FL5	Not used
638nm, 25mW (RED)	660/20	FL6	Not used
	725/20	FL7	Not used
	755 LP	FL8	Not used
405nm, 40mW (VIOLET)	450/40	FL9	Not used
	550/40	FL10	Not used

5.4.2 Sample preparation for enumeration

5.4.2.1 Umbilical cord blood-derived samples

UCB-MNCs isolated from UCB, described in 5.3.1.2 *Isolation of umbilical cord blood-derived mononuclear cells*, were enumerated by staining 50 μ L cell suspension with 3 μ L 7-AAD and 3 μ L of a ready-to-use monoclonal antibody cocktail containing mouse anti-human CD34 conjugated to PE (CD34-PE; clone 581) and mouse anti-human CD45 conjugated to FITC (CD45-FITC; clone J33). The 7-AAD and CD34/CD45 cocktail both form part of the Stem-Kit HSC enumeration kit (Beckman Coulter, USA). Cells were incubated for 10 min in the dark prior to the addition of 50 μ L Flow-Count™ and 300 μ L PBS. Samples were analysed on the Gallios flow cytometer, and absolute counts were calculated as described in 3.6.3.3 *Enumeration*. Isotype control staining was not performed for each UCB-derived sample for the enumeration of CD34⁺ HSPCs as the Stem-Kit reagents are used routinely at the ICMM and previous work has shown that the CD34⁺ HSPC population from UCB was well-defined. When isotype control staining was performed, 50 μ L cell suspension was stained with 3 μ L 7-AAD and 3 μ L of the Stem-Kit isotype control (provided with the Stem-Kit HSC enumeration kit) cocktail containing CD45-FITC and mouse IgG₁ conjugated to PE as the CD34 isotype control. Staining was performed for 10 min in the dark before adding 50 μ L Flow-Count™ and 300 μ L PBS, after which samples were analysed on the Gallios flow cytometer.

5.4.2.2 Leukapheresis product-derived samples

Aliquots of 100 μ L cell suspension (processed as described in 5.3.2.2.2 *Thawed leukapheresis processing*) were stained for enumeration. One aliquot was stained with 5 μ L 7-AAD and 5 μ L Stem-Kit CD34/CD45 cocktail, and the second aliquot was stained with 5 μ L 7-AAD and 5 μ L Stem-Kit CD34 isotype/CD45 cocktail, for 10 min in the dark. Flow-Count™ (100 μ L) was added only to the aliquot stained with the Stem-Kit CD34/CD45 cocktail as the isotype control tube was only used to set the CD34⁺ HSPCs region. Samples were analysed on the Gallios flow cytometer, and absolute counts were calculated as described in 3.6.3.3 *Enumeration*.

5.4.3 Gating strategy

The gating strategy employed for the enumeration of CD34⁺ HSPCs (Figure 5.4) is an adaptation of the ISHAGE CD34⁺ HSPC enumeration protocol suggested by the ISCT¹². The four-parameter gating strategy outlined by ISHAGE is described as four sequentially gated plots¹². Plot 1: ungated SSC Lin versus CD45-FITC two-parameter plot as shown in Figure 5.4B with a defined region indicating CD45⁺ cells. Plot 2: SSC Lin versus CD34-PE two-parameter plot gated on the “Leukocytes” region created in plot 1 as shown in Figure 5.4 with a defined region indicating CD34⁺ cells. Plot 3: CD45-FITC versus SSC Lin two-parameter plot gated on CD34⁺ cells with a region of low to intermediate CD45 expression defined (CD45 dim). Plot 3 was not used in our setup, but colour tracing (purple CD34⁺ HSPCs, Figure 5.4B and D) confirmed that the CD34⁺ HSPCs displayed lower levels of CD45 expression. Plot 4: FS Lin versus SSC Lin two-parameter plot gated on CD45 dim with a region of low to intermediate SSC and FS defined, as HSPCs lack intracellular complexity and are relatively small. This plot was also not used in our setup, as two-parameter plots with SSC Lin on the y-axis were used for leukocyte and CD34⁺ HSPC identification.

Dead cells staining positive for 7-AAD were excluded in the “VIABLE” region (SSC Lin versus 7-AAD Log; Figure 5.4A). Viable cells expressing the panleukocyte marker CD45 were selected in the “Leukocyte” region (SSC Lin versus CD45-FITC Log; Figure 5.4B). Leukocytes expressing CD34 were captured in the region labelled “CD34⁺ HSPCs” (SSC Lin versus CD34-PE Log; Figure 5.4D). Flow-Count™ fluorospheres were enumerated in the Cal region of the Flow count (FL3) versus Time plot and were used to calculate absolute numbers of leukocytes and CD34⁺ HSPCs as described in 3.6.3.3 *Enumeration*.

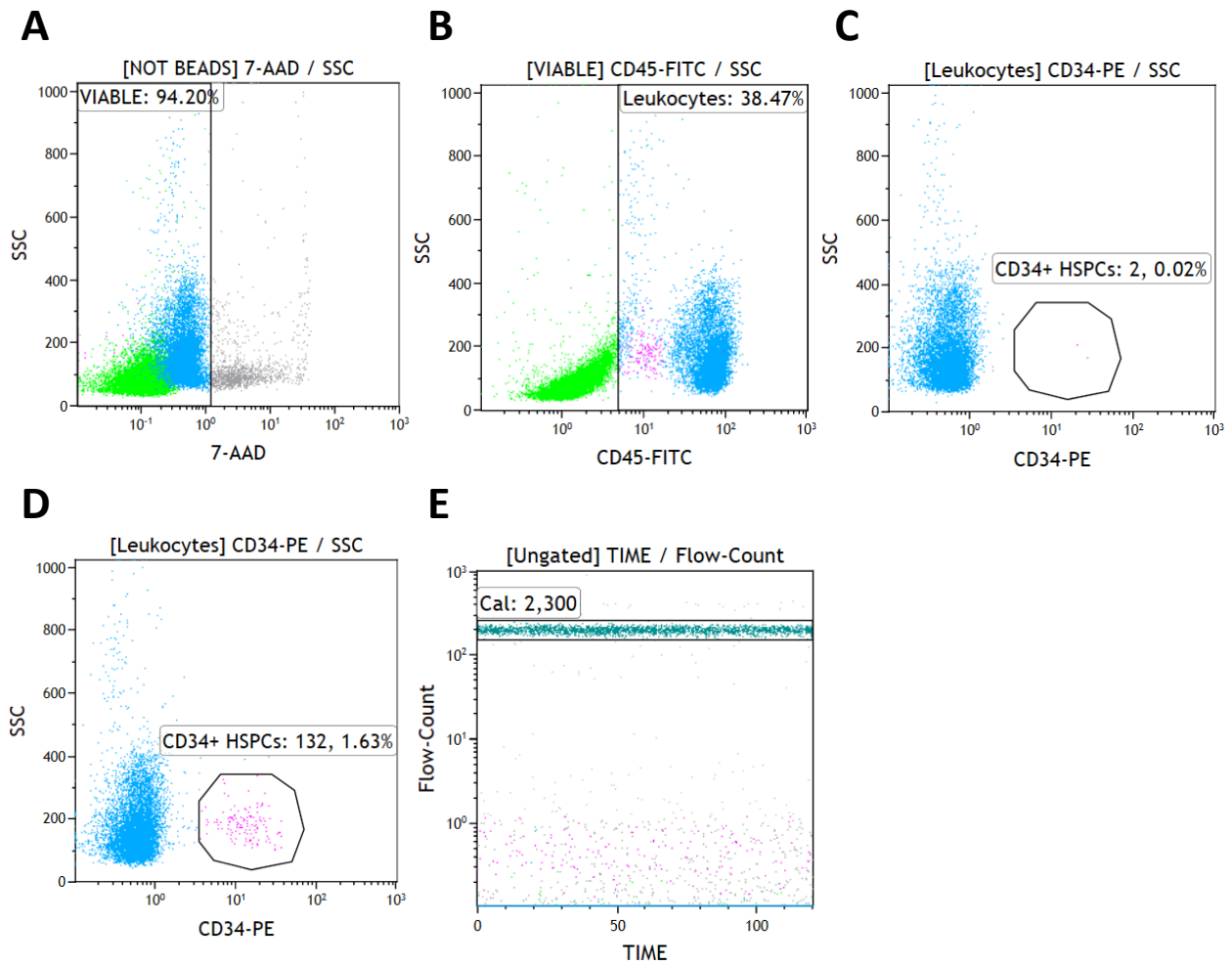


Figure 5.4: ISHAGE-derived gating strategy applied to the enumeration of CD34⁺ HSPCs derived from both UCB and leukapheresis products. Plots represent UCB-MNCs. (A) Viable cells were selected based on negative 7-AAD staining. (B) Viable leukocytes were selected on CD45 expression (“Leukocytes”) in the two-parameter SSC Lin versus CD45-FITC plot gated on the “Viable” region. (C and D) The “CD34+ HSPCs” region was confirmed in random samples using the Stem-Kit isotype control (C), using a SSC Lin versus CD34-PE two-parameter plot. (D) Viable leukocytes expressing CD34 (CD34+ HSPCs) were captured in the “CD34+ HSPC” region. (E) Flow-Count™ beads were identified in the “Cal” region and used to calculate absolute cell numbers.

5.5 Optimisation of leukapheresis processing

Initial attempts to thaw cryopreserved samples yielded low viability, resulting in low CD34⁺ HSPC cell numbers. Isolation of CD34⁺ HPSCs using both magnetic-activated cell sorting (MACS) and FACS are antibody-based, which can bind non-specifically to dead cells. In addition, clotting caused by dead cell aggregation clogs up the sample pick-up line of the FACSAria™ cell sorter as well as the magnetic columns employed in MACS. It was therefore necessary to improve sample viability prior to HSPC isolation. The optimised protocol is described in 5.3.2.2.2 *Thawed leukapheresis processing*. The initial protocol was adjusted systematically in terms of (i) working temperature, (ii) resuspension medium, and (iii) dead cell removal in order to improve post-thaw viability.

5.5.1 Working temperature

Initially, leukapheresis products were thawed in a warming incubator set to 37°C which took anything from five to ten minutes. This was reduced to less than four minutes using the waterbath protocol from the ACT described in 5.3.2.2.1 *Leukapheresis thawing*, already improving post-thaw viability. The initial processing procedure was carried out at room temperature or using solutions pre-heated to 37°C. This encouraged cell metabolism compared to working cold, which increased cytotoxicity from DMSO exposure. Lower working temperatures during sample processing were therefore investigated as an avenue to improve post-thaw viability.

A validation experiment was planned to determine whether processing the leukapheresis product on ice or using cold (4°C) solutions and keeping cells at 4°C between steps, would further improve viability post-thaw.

5.5.1.1 Method

Two leukapheresis products from different donors were independently thawed in a 37°C water bath as described in 5.3.2.2.1 *Leukapheresis thawing*. The first product (AP181010) was diluted on ice into PBS, centrifuged at 300 x g for 10 min at 4°C, and the pellets resuspended

in TP₄ buffer on ice before counting. The second product (AP180823) was diluted into PBS pre-cooled to approximately 4°C, centrifuged at 300 x g for 10 min at 4°C, and the pellets resuspended in cold (~4°C) TP₄ buffer.

Viability was assessed by staining 100 µL cell suspension with 3 µL each of 7-AAD and Stem-Kit CD34/CD45 antibody cocktail. A second 100 µL cell suspension aliquot was stained with 3 µL each of 7-AAD and Stem-Kit isotype control. Aliquots were stained for 10 min in the dark and enumerated by flow cytometry as described in 5.4 *Haematopoietic stem/progenitor cell enumeration*.

5.5.1.2 Results and outcome

Post-thaw viability was significantly improved when working at temperatures around 4°C compared to working on ice (Figure 5.5). It is important to note that working temperature was improved using two independently thawed samples from independent donors rather than a single donor product used to test the two methods concurrently. While this could explain some of the improvement, the trend in increased viability was sustained since switching from working on ice to working at approximately 4°C. A working temperature of approximately 4°C was therefore adopted for leukapheresis sample processing, and yielded sample viability of between 70-80% in subsequent leukapheresis product thaws.

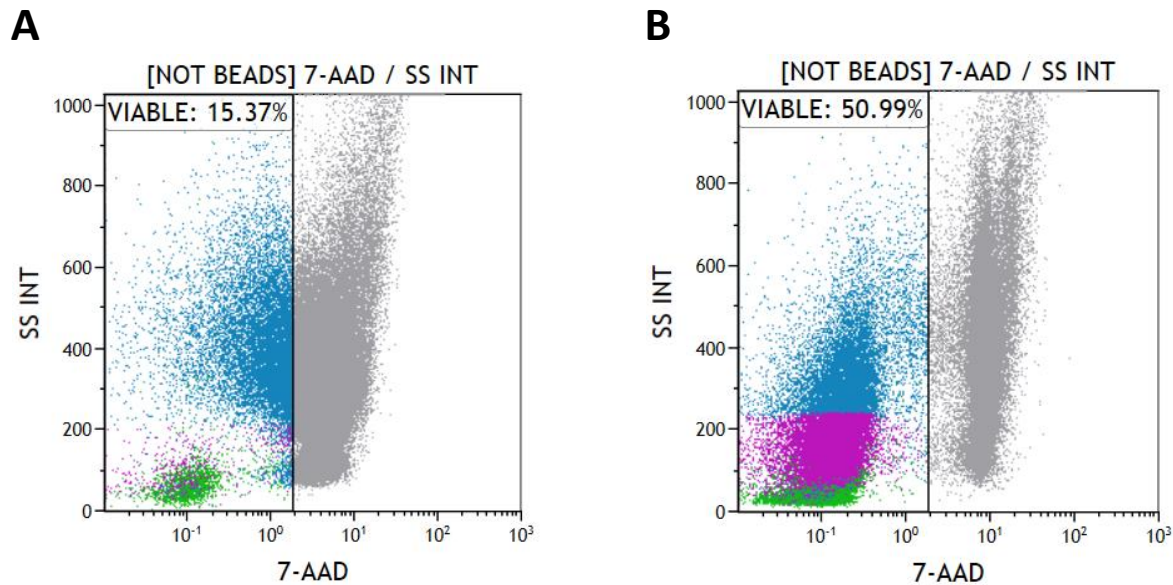


Figure 5.5: Effect of working temperature on post-thaw viability of leukapheresis-derived cells. (A) Viability of cells (AP181010) processed and resuspended on ice contrasted with (B) the viability of cells (AP180823) processed and resuspended using pre-cooled (4°C) solutions.

5.5.2 Post-thaw resuspension medium

Different post-thaw resuspension media were also tested in our quest to improve sample viability. The viability of cells resuspended in RPMI and TP₄ buffer respectively during sample processing was tested. RPMI, formulated for the growth and maintenance of suspended cell cultures, was compared to TP₄ buffer to determine whether nutrient-rich medium would improve viability compared to buffer supplemented only with albumin protein.

5.5.2.1 Method

A single bag of leukapheresis product (AP181122-01) was thawed as described in 5.3.2.2.1 *Leukapheresis thawing*. After the first centrifugation (300 x g, 10 min, 4°C) in cold PBS to wash off DMSO, the supernatant was aspirated from each tube. Cell pellets collected from four tubes were resuspended and pooled in 50 mL cold RPMI, and pellets from the remaining four tubes were resuspended in 50 mL cold TP₄ buffer. Since the measure of viability would be expressed as percentage of total cells rather than absolute count, splitting the number of pellets equally between the two resuspension media was deemed adequate. Each suspension was strained through 70 µm cell strainers and 100 µL aliquots were taken for

flow cytometric analysis. Sample viability was determined as described in 5.4.2.2 *Leukapheresis product-derived samples*. The procedure was repeated using a second biological replicate (AP181211).

5.5.2.2 Results and outcome

Representative results shown in Figure 5.6 and Table 5.2 indicate that there is no significant trend of increased viability (7-AAD negative population) between RPMI and TP₄ buffer. However, a greater spread of the 7-AAD positive population was observed with TP₄ buffer-resuspended cells (Figure 5.6B), which may indicate that cell membranes of neutrophils (more complex and therefore higher on SSC Lin) were more compromised compared to RPMI-resuspended cells (Figure 5.6A). The TP₄ cells were not pelleted and resuspended in RPMI prior to counting (described in 5.3.2.2.2 *Thawed leukapheresis processing*), as cells could be lost by the additional centrifugation. The same gating strategy was employed for both TP₄- and RPMI-resuspended cells. In light of these results, RPMI was used as the resuspension medium in future experiments.

Table 5.2: Percent viabilities for leukapheresis products processed with different post-thaw resuspension media.

Post-thaw resuspension medium	RPMI	TP ₄ buffer
AP181122-01	87.91%	87.04%
AP181211	75.31%	89.17%

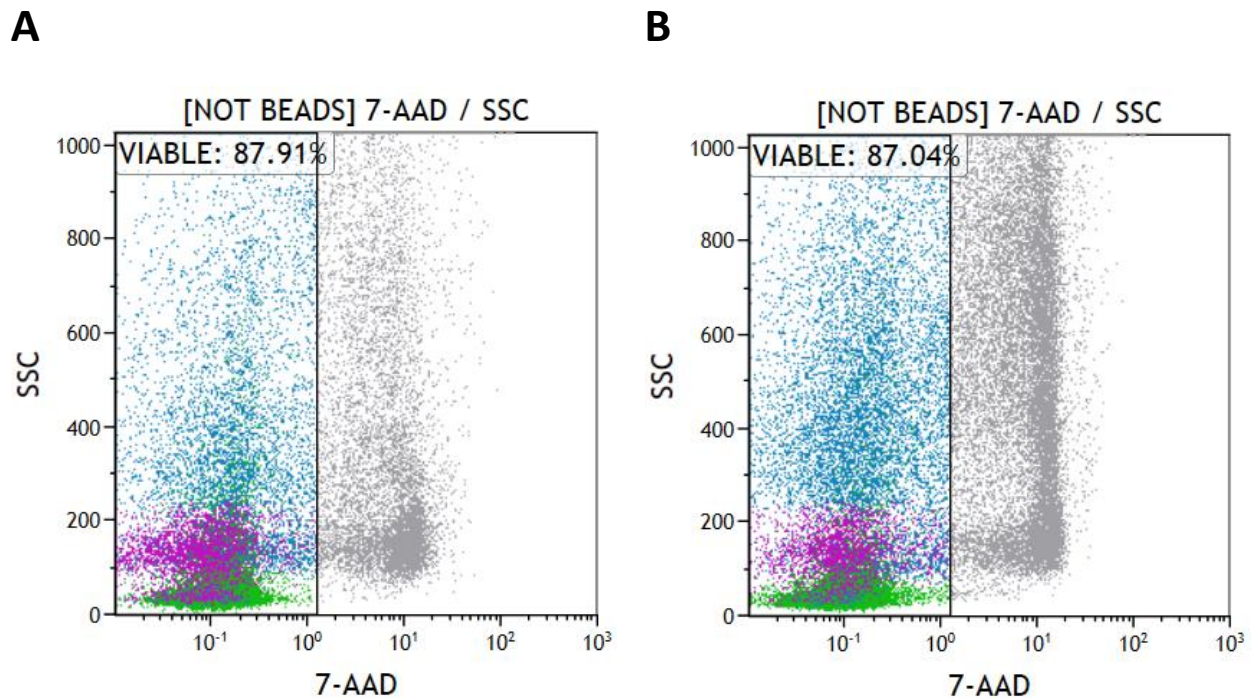


Figure 5.6: Effect of post-thaw resuspension buffer on post-thaw viability. (A) Viability of cells resuspended in RPMI. (B) Viability of cells resuspended in TP₄ buffer.

5.5.3 Dead cell removal

Dead cell removal was explored to improve yield during CD34⁺ HSPC isolation from leukapheresis products. Two methods, namely histopaque and a slow spin akin to the platelet spin described in 4.4.1.1 *Peripheral blood mononuclear cell isolation from peripheral blood*, were compared for removing dead cells. The same leukapheresis products (AP181122-01 and AP181211) thawed and used to test the post-thaw resuspension medium were used directly after testing post-thaw resuspension medium to test dead cell removal strategies.

5.5.3.1 Density-gradient centrifugation

After viability estimation (as described in previous section), cells resuspended in RPMI were pelleted by centrifugation at 300 x g for 10 min at 4°C. Cells were resuspended in 10 mL RPMI and carefully layered on 5 mL histopaque. RPMI was used as the carrier medium as density-gradient centrifugation previously performed with TP₄ buffer did not produce the MNC layer – presumably because the density of the cell suspension was not sufficient to support

separation. Density-gradient separation was performed by centrifugation for 30 min at 1700 rpm without brake. The white, fuzzy MNC layer (Figure 5.7) was collected as described in 5.3.1.2 *Isolation of umbilical cord blood-derived mononuclear cells containing* and diluted to a final volume of 10 mL with RPMI.

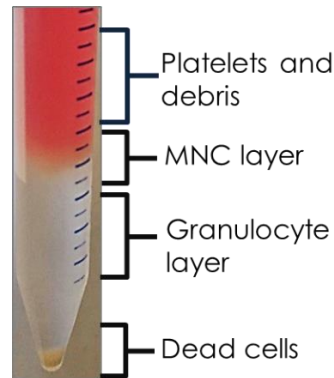


Figure 5.7: Post-centrifugation density gradient of leukapheresis-derived cells in RPMI loaded on histopaque.

5.5.3.2 Slow centrifugation

Cells resuspended in TP₄ buffer (from 5.5.2 Post-thaw resuspension medium) were centrifuged at 300 x g for 10 min without brake in an attempt to separate debris (light, therefore remains in supernatant) and intact cells (heavier, therefore pellet). The supernatant was aspirated and resuspended in 10 mL RPMI for enumeration.

5.5.3.3 Results and outcome

Both sample viability and CD34⁺ HSPC proportion were assessed to ensure that the CD34⁺ HSPCs were not lost in either method. Two aliquots of 100 μ L were taken from each method and stained for enumeration, as described in 5.4.2 Sample preparation for enumeration. Representative results showing the difference between the two dead cell removal methods investigated are shown in Figure 5.8, and results comparing post-thaw proportions to post-histopaque and post-slow centrifugation cells are shown in Table 5.3. Viability was not

improved using either dead cell removal technique, and no significant effect on the respective leukocyte or CD34+ HSPC proportions were observed. Additional biological replicates would be required to establish trends, as it seems that layering cells on histopaque may be useful for CD34+ HSPC enrichment in some cases (Table 5.3; AP181211). Absolute cell counts will be included for future optimisation, to measure absolute cell loss as well as the proportions indicated in Table 5.3. For this study, dead cell removal strategies were not included in the leukapheresis processing protocol.

Table 5.3: Percentage viability, and leukocyte and CD34+ HSPC proportions post-thaw compared to dead cell removal strategies.

Sample ID	Stage	Viability (%)	Leukocytes (%)	CD34+ HSPCs (%)
AP181122-01	Post-thaw (RPMI)	87.91	76.60	0.08
	Post-thaw (TP ₄ buffer)	87.04	69.51	0.03
	Post-histopaque	92.67	89.96	0.08
	Post-slow centrifuge	88.38	78.04	0.02
AP181211	Post-thaw (RPMI)	75.31	91.18	0.05
	Post-thaw (TP ₄ buffer)	89.17	87.50	0.13
	Post-histopaque	76.14	87.22	0.65
	Post-slow centrifuge	72.57	92.42	0.24

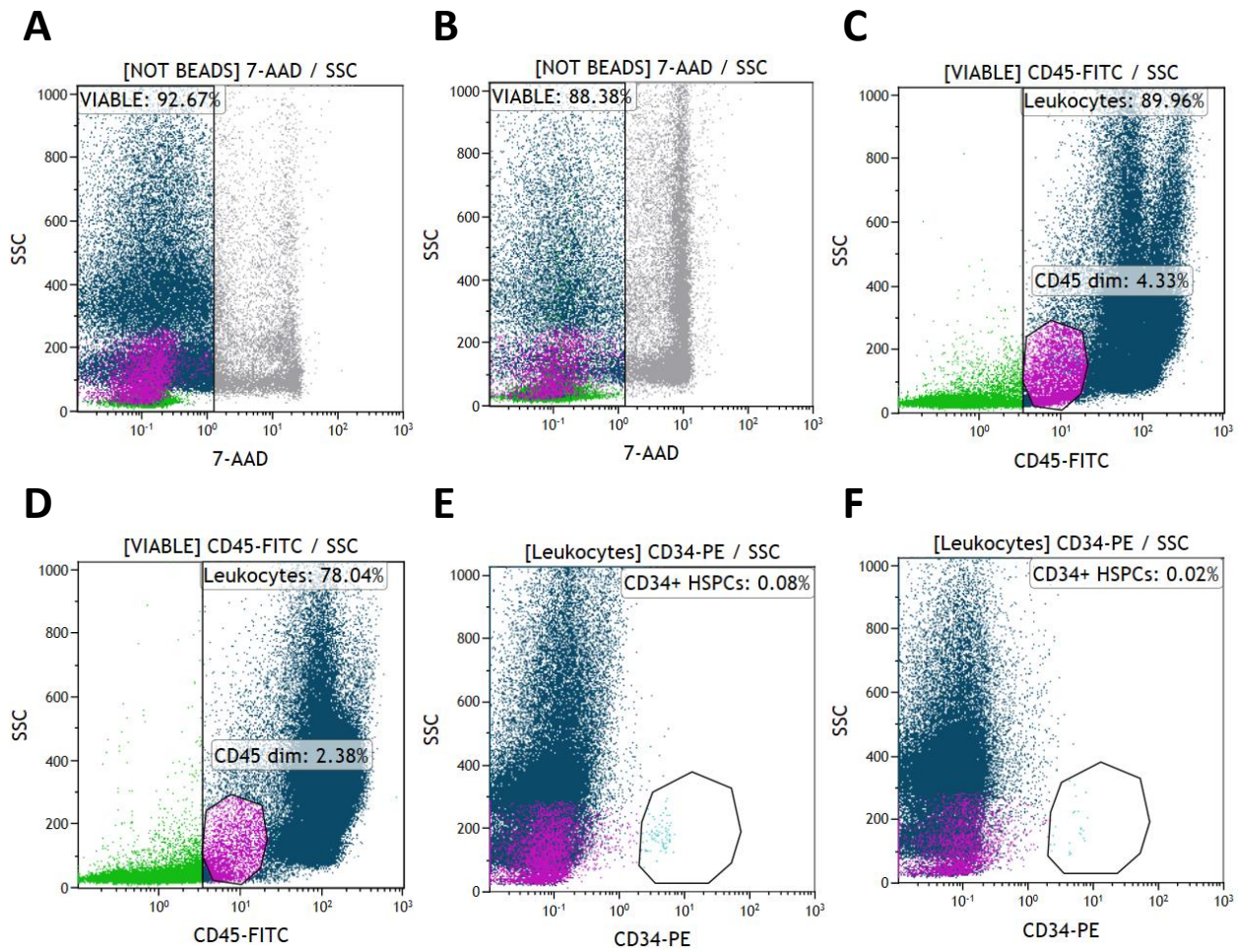


Figure 5.8: Effect of dead cell removal technique on viability and CD34-recovery. (A) The viability of cells subjected to density-gradient centrifugation on histopaque was compared to **(B)** the viability of cells subjected to slow centrifugation. **(C)** The SSC Lin profiles compared to CD45 expression is indicated for post-histopaque, and **(D)** post-slow centrifugation. **(E)** The percentage of CD34⁺ HSPCs after dead cell removal by layering on histopaque was compared to **(F)** slow centrifugation.

5.6 CD34⁺ haematopoietic stem/progenitor isolation

As previously mentioned, the proportion of HSPCs in the MNC fraction of UCB and leukapheresis is small. In order to work with pure populations of HSPCs, immunoselection of cells expressing the HSPC marker CD34 (Figure 5.1) was performed by MACS and/or FACS.

5.6.1 Magnetic-activated cell sorting

5.6.1.1 Introduction

MACS column-based selection is achieved by antibody selection using cell-surface marker-specific antibodies conjugated to magnetic beads¹³. Magnetically-labelled cells are then loaded onto a column inside a magnetic field, where unlabelled cells are washed from the column and labelled cells are retained in the column matrix due to the magnetic field. Labelled cells are released from the column by removing the column from the magnetic field and cells were flushed out of the column using the kit-provided plunger. MACS can be used to purify specific populations by direct selection, where the cells of interest are magnetically labelled and non-target cells are removed in the flow-through, or indirect selection, where non-target cells are magnetically labelled and the cells of interest are collected in the flow-through. An example of direct selection is the isolation of CD34⁺ cells, and an example of indirect selection is the isolation of Lin⁻ cells, where Lin⁺ cells are labelled with a cocktail of lineage-specific magnetic bead-conjugated monoclonal antibodies, resulting in the retention of lineage-committed cells in the column. Basic principles of MACS are illustrated in Figure 5.9.

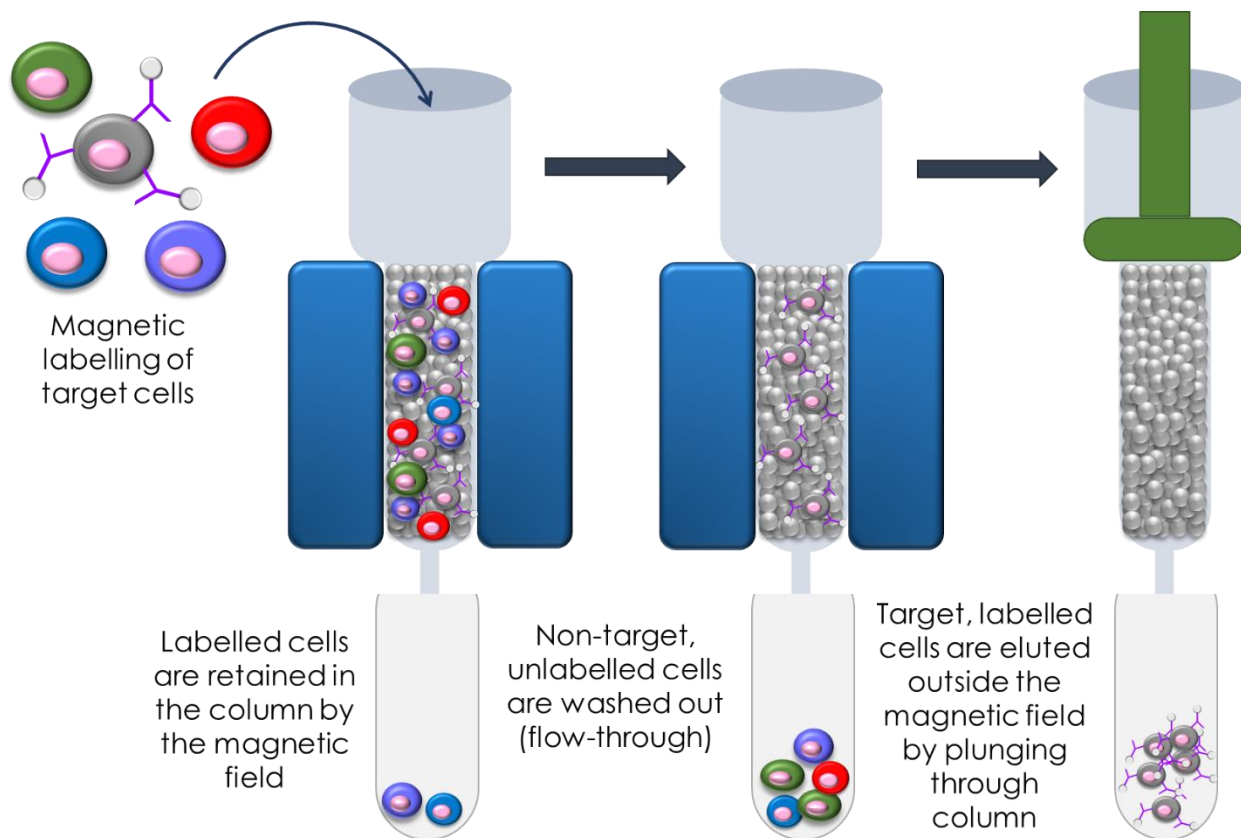


Figure 5.9: Principles of direct selection by MACS.

5.6.1.2 Method

Direct selection of CD34-labelled cells was achieved using the MACS CD34 MicroBead kit (Miltenyi Biotec, Germany) and LS columns (Miltenyi Biotec, Germany), according to manufacturer's instructions. Up to 2×10^9 total cells can be loaded on an LS column. Cell suspensions were prepared as described in 5.3.1 *Umbilical cord* blood processing and 5.3.2 *Leukapheresis processing*, after which cells were enumerated as described in 5.4 *Haematopoietic stem/progenitor cell enumeration*. Total cell counts were estimated by ungating the CD45-FITC plot, and extending the Leukocytes region to include all cells (Figure 5.4B). This was performed to obtain a total cell count, which was used to calculate the volume of magnetic beads required for staining.

5.6.1.2.1 Magnetic labelling

Aliquots of cell suspensions were magnetically labelled in no more than 3 mL TP buffer per 10^9 live leukocytes, as greater volumes resulted in inadequate staining and poor recovery of labelled cells.

First, 100 μ L FcR blocking reagent was added per 10^8 total cells and incubated at 4°C for 10 min to minimise non-specific binding of anti-CD34 microbeads. Cells were then labelled with anti-CD34 microbeads by adding 100 μ L of anti-CD34 microbeads per 10^8 total cells and incubating for 30 min at 4°C. Excess bead-conjugated antibodies were washed off by topping up the volume to 10 mL with TP buffer, followed by centrifugation at 300 x g for 10 min. The supernatant was aspirated and the cells resuspended at a concentration of approximately 2×10^7 cells per 100 μ L in TP buffer.

5.6.1.2.2 Column-based magnetic separation

LS columns were slotted into the indents of a QuadroMACS separator (Miltenyi Biotec, Germany) and primed by passing 3 mL cold TP buffer through the column and allowing it to empty by gravity into a waste collection tube. The labelled cell suspensions were applied to LS columns in the magnetic field of the QuadroMACS separator by passing the cells through a 30 μ m pre-separation filters (Miltenyi Biotec, Germany), moving to a new primed column/filter set up as soon as saturation of the column was suspected. As dead cells and cell debris could clog both the filter and the column, spreading the labelled cell suspension across multiple columns was required for sufficient enrichment and recovery of CD34⁺ cells. Flow-through containing unlabelled cells was collected into waste tubes (Figure 5.9). Each column was washed three times (while in the magnet) with 3 mL cold TP buffer, allowing the column to empty by gravity flow before applying the next wash volume.

5.6.1.2.3 Eluting labelled cells

CD34-labelled cells were eluted from the column by removing LS columns from the QuadroMACS separator and firmly plunging 3 mL and then 2 mL cold TP buffer through the column into a fresh collection tube. Cells were pelleted by centrifugation at 300 x g for 10 min

and pooled and resuspended in 2 mL TP buffer. Cells were enumerated as described in 5.4 *Haematopoietic stem/progenitor cell enumeration*, using 50 µL cell suspension to assess the purity and enumerate CD34⁺ HSPCs in the enriched product.

5.6.1.3 Purity and yield evaluation

5.6.1.3.1 Purity

Representative purity and enrichment results of post-MACS cell suspensions compared to post-processing suspensions (prior to enrichment) are shown in Figure 5.10. Results of magnetic isolations performed on UCB-MNCs and leukapheresis-derived cells are shown in Table 5.4. CD34⁺ HSPCs were enriched in all cases, with purities ranging from 53.27% to 91.65%.

Table 5.4: Paired post-processing and post-MACS viability and purity results for UCB-MNCs and leukapheresis-derived cells.

Sample ID	Viability (%)	Leukocytes (%)	CD34+ HSPCs (%)
CB190418 (post-processing)	96.20	61.83	1.92
CB190418 (post-MACS)	96.13	81.04	78.55
CB100518-02 (post-processing)	95.11	80.66	2.92
CB100518-02 (post-MACS)	89.15	90.06	76.68
CB100518-03 (post-processing)	92.57	80.10	3.14
CB100518-03 (post-MACS)	85.17	60.11	53.27
CB100518-05 (post-processing)	94.45	93.36	4.00
CB100518-05 (post-MACS)	77.59	80.48	62.46
AP180823 (post-processing)	75.81	70.16	1.36
AP180823 (post-MACS)	92.82	87.92	91.65

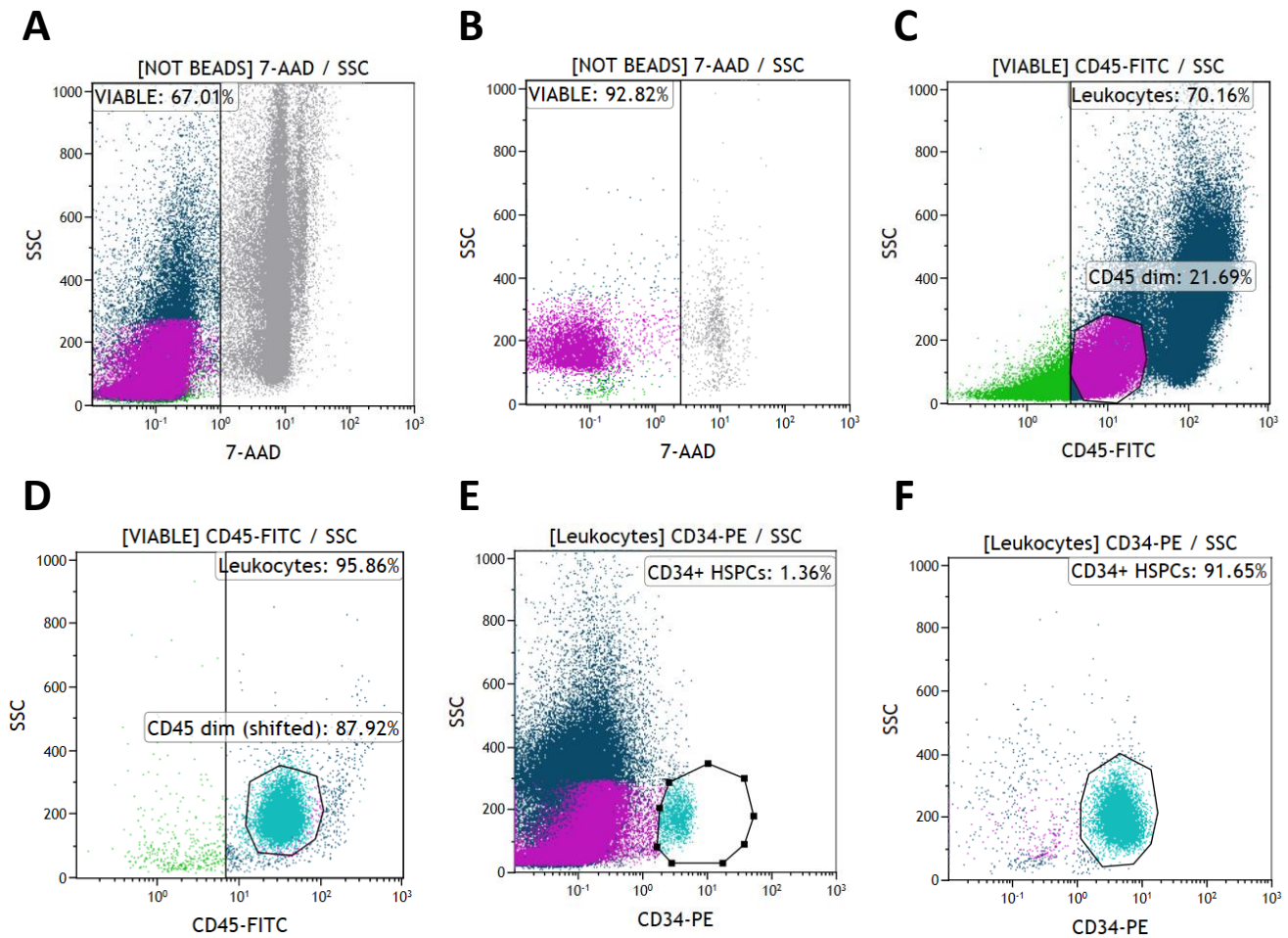


Figure 5.10: Post-thaw (A; C; E) and post-MACS (B; D; F) comparison in terms of viability, leukocyte proportion, and CD34+ HSPC enrichment. (A) The viability of AP180823 post-processing is contrasted with (B) the viability post-MACS indicated by negative staining for 7-AAD. (C) The proportion of leukocytes post-processing compared to (D) post-MACS is indicated by positive staining for CD45. (E) The proportion of CD34+ HSPCs post-processing is compared to (F) the enriched proportion of CD34+ HSPCs post-MACS.

5.6.1.3.2 Yield

Enrichment for the CD34⁺ HSPC population achieved by MACS was sufficient as a pre-enrichment step for FACS, where purities of 97-100% of the CD34⁺ HSPC population were typically achieved. However, the yield of CD34⁺ HSPCs (post-MACS) recovered from the column compared to the CD34⁺ HSPCs (post-processing) applied to the column was not sufficient for experiments when UCB was used as the HSPC source. This was, in part, due to the small volumes of UCB obtained, of which only a small proportion are CD34⁺ HSPCs. Recovery of UCB-derived CD34⁺ HSPCs post-MACS was unpredictable, and ranged between 6-74%.

Leukapheresis product was therefore used as an alternate source of HSPCs, where the cell numbers per bag exponentially outnumber the number of cells per UCB unit collected. Switching sources of HSPCs from UCB to leukapheresis was done in an effort to ensure that a sufficient number of cells were obtained post-MACS.

5.6.2 Fluorescence-activated cell sorting

Depending on the experiments planned, FACS was used to sort viable CD34⁺Lin⁻ HSPCs directly from UCB-MNCs, from pre-enriched post-MACS cells, or from HIV-infected purified HSPC populations.

5.6.2.1 Instrument configuration

Sorting was performed on the FACS Aria™ cell sorter using either a 70 µm or 100 µm nozzle, and an ND1 filter. The 488 nm, 561 nm, 633 nm, and 405 nm lasers were used, and the laser/detector configurations are summarised in Figure 5.11.

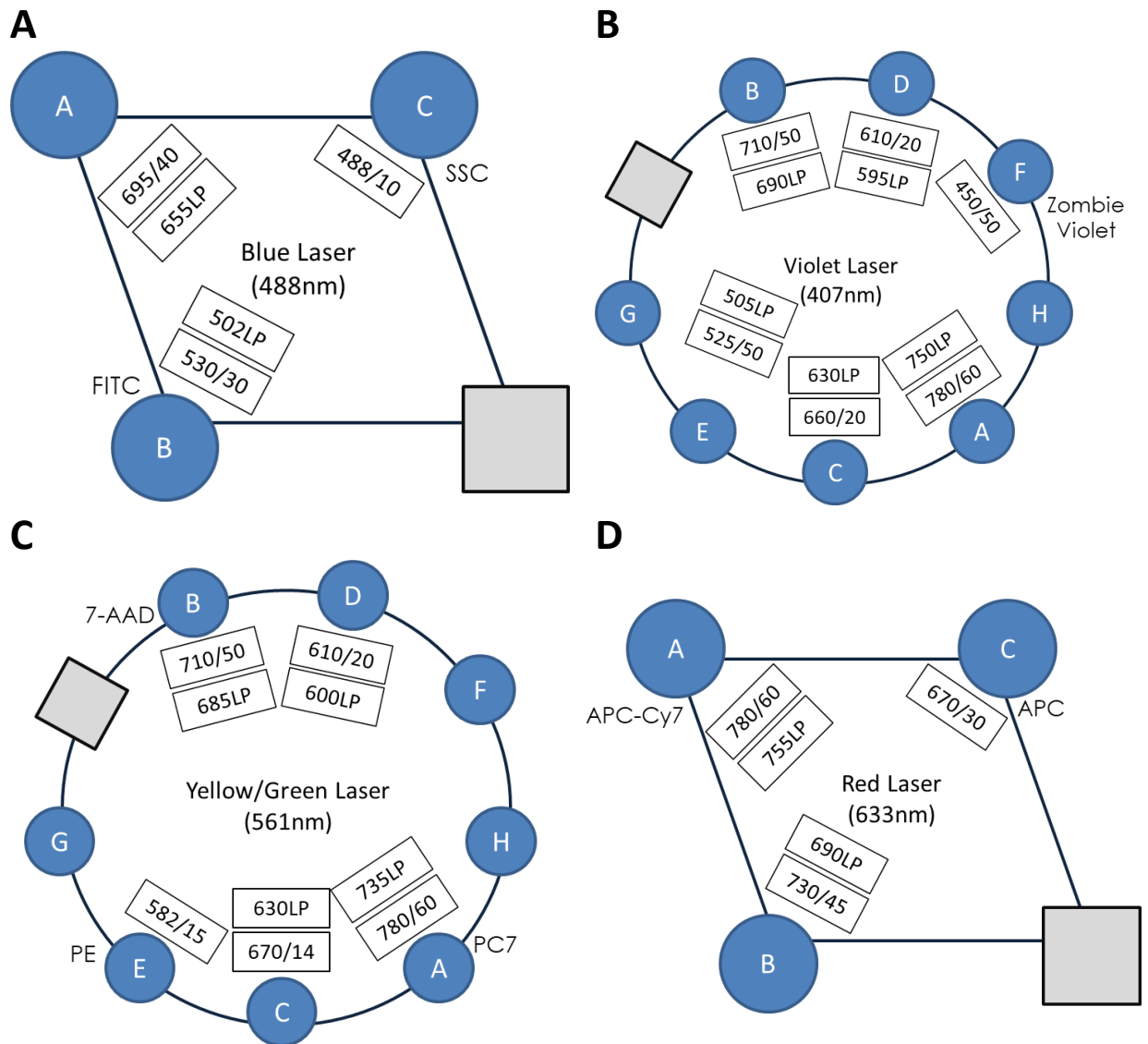


Figure 5.11: FACS Aria Fusion laser/detector configuration for HSPC sorting experiments. (A) The blue laser excited fluorochromes at 488 nm and was used to detect SSC on C and FITC on B. **(B)** The violet laser excites fluorochromes at 407 nm and was used to detect Zombie Violet™ on F. **(C)** The yellow/green laser excites fluorochromes at 561 nm and was used to detect 7-AAD on B, PC7 on A, and PE on E. **(D)** The red laser excites fluorochromes at 633 nm and was used to detect APC-Cy7 on A, and APC on C.

5.6.2.2 *Sample preparation and gating strategies*

5.6.2.2.1 **Haematopoietic stem/progenitor cell sorts from umbilical cord blood-derived mononuclear cells**

Rationale for phenotypic staining

In order to sort more primitive populations of HSPCs from the heterogeneous CD34⁺ HSPC population without selecting particular subpopulations, Lin and CD38 were included for sorting purposes (Figure 5.1). These markers separate primitive from lineage-committed HSPCs without selecting a particular sub-population of primitive CD34⁺ HSPCs, as would be the case if CD90 or CD133 for example were used instead (Figure 5.1).

As mentioned in 2.2.3 *Phenotype and heterogeneity*, CD38 is an HSPC activation marker which is expressed during differentiation¹⁵ from the CD34⁺CD38⁻ primitive progenitor to lineage-committed CD34⁺CD38⁺ CMP and CLPs and beyond^{6, 20}. The lineage cocktail contains mouse anti-human antibodies against CD3 to detect T cells, CD14 to detect monocytes/macrophages, neutrophils, and eosinophils, CD16 to detect natural killer (NK) cells, activated monocytes/macrophages and neutrophils, CD19 and CD20 to detect B cells, and CD56 to detect NK cells.

Sample preparation

Colony forming unit (CFU) assays were optimised by sorting viable, lineage-marker negative, CD34⁺ cells from UCB-MNCs prepared as described in 5.3.1 *Umbilical cord blood processing*. An aliquot of at least 10⁵ CD34⁺ HSPCs (obtained from HSPC enumeration, described in 5.4 *Haematopoietic stem/progenitor cell enumeration*) were stained for sorting. Aliquots were stained with 2 µL antibody or stain per 10⁶ total cells with the following: 7-AAD, Stem-Kit CD34/CD45 cocktail, mouse anti-human CD38 conjugated to a tandem dye consisting of APC and Cy7 (CD38-APC-Cy7; clone HIT2; BioLegend, USA), and a cocktail of anti-human lineage-specific markers conjugated to APC (Lin-APC; BioLegend, USA) for 20 min at 4°C in the dark. After staining, the cell suspension volumes were topped up to 400 µL total volume with TP buffer prior to sorting.

Gating strategy

Viable cells of the following populations were sorted at 100 cells/well into 24-well plates (Greiner Bio-One, Austria) containing semisolid medium: CD45^{dim}CD34⁺; Lin⁻CD45^{dim}CD34⁺; Lin⁻CD45^{dim}CD34⁺CD38⁻; Lin⁻CD45^{dim}CD34⁺CD38⁺; and Lin⁻CD45^{dim}CD34⁺CD38^{dim}. The sequential gating strategy used is shown in Figure 5.12. An example of post-sort purity of the Lin⁻CD45^{dim}CD34⁺ population is shown in Figure 5.12E and F, indicating 100% purity post-sort.

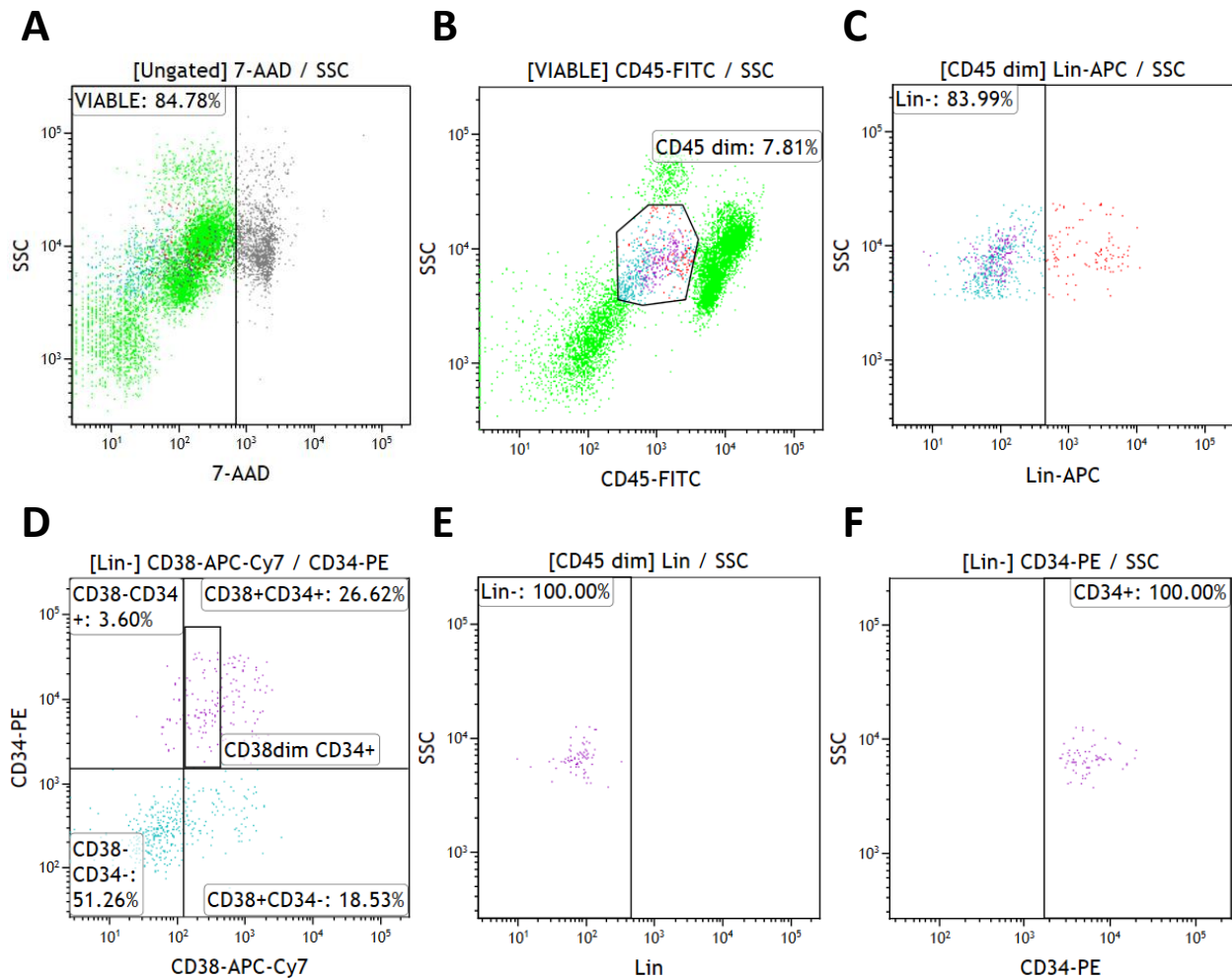


Figure 5.12: Sequential gating strategy for sorting HSPC sub-populations from UCB-MNCs, and resulting post-sort purity of the CD34⁺Lin⁻ HSPC population. (A) Dead cells were excluded by positive staining for 7-AAD. (B) Viable leukocytes expressing low levels of CD45 were selected in the CD45 dim region. (C) Viable, CD45 dim cells already expressing lineage-specific markers were excluded in the Lin⁻ region. (D) The co-expression of CD34 and CD38 on viable, CD45^{dim}Lin⁻ HSPCs is shown, where CD38⁻, CD38^{dim}, and CD38⁺ populations also expressing CD34 are indicated. Post-sort purity of the viable, CD45^{dim}CD34⁺Lin⁻ sorted population (E and F), indicating 100% purity of the sorted population. (E) The viable, CD45^{dim}Lin⁻ population post-sort purity (pre-sort population shown in C). (F) The viable, CD45^{dim}Lin⁻CD34⁺ population post-sort purity (pre-sort population indicated by CD34⁺ populations in D).

5.6.2.2.2 Haematopoietic stem/progenitor cell sorts from leukapheresis

MACS CD34-enriched leukapheresis-derived cells were sorted by FACS for HIV experiments, which were exposed to various conditions and then sorted by FACS again for CFU assays. The

CD45 marker was not included as all CD34⁺ HSPCs dimly expressed CD45, determined during enumeration using the Stem-Kit CD34/CD45 antibody cocktail.

Sample preparation

Cells suspended in TP buffer were stained for sorting with 2 µL of mouse anti-human CD34 conjugated to PC7 (CD34-PC7; clone 581; Beckman Coulter, USA) and 2 µL of 7-AAD per 10⁶ total cells for MACS-enriched cells, or 3 µL of each for cells from HIV experiments. Cells were stained for 15 min in the dark at 4°C, and sample volumes were increased to at least 300 µL total volume with TP buffer (post-MACS cells) or TP₄ buffer (HIV experiment cells) prior to sorting.

Gating strategy

Viable, post-MACS CD34⁺-enriched cells (HSPCs) were sorted into 15 mL centrifuge tubes containing 2 mL pre-warmed StemSpan™-ACF (StemSpan™; STEMCELL Technologies, Canada) medium specifically designed for stem cell culture, supplemented with 2% penstrep. Sorted cells were plated in 2 mL stemspan (2% penstrep) in a 6-well plate (Greiner Bio-One, Austria) and incubated at 37°C, 5% CO₂ overnight. These cells were destined for HIV experiments. Cells from HIV experiments for CFU assays were sorted directly into a 24-well plate containing 500 µL semisolid medium, at 100 viable CD34⁺ cells/well and distributed by vortex before incubation as required for CFU assays. The gating strategy employed for sorting viable CD34⁺ HSPCs for or from HIV experiments is shown in Figure 5.13.

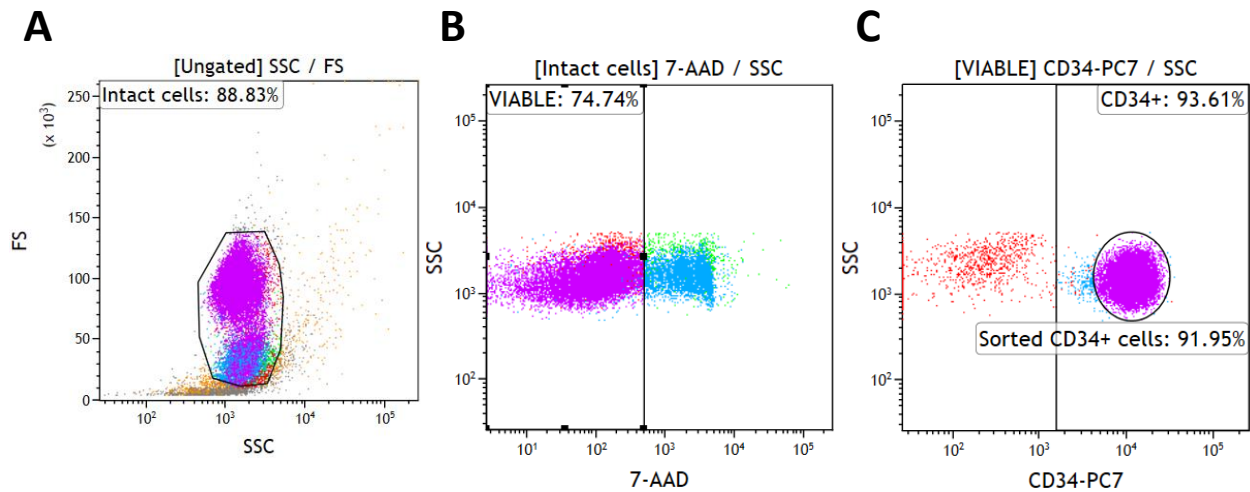


Figure 5.13: Sequential gating strategy for sorting CD34⁺ HSPCs from CD34-enriched populations. Cell debris was excluded by selecting intact cells (A), which were sorted for viability by negative staining for 7-AAD (B). Live cells expressing CD34 are encompassed in the region CD34⁺ (C), and viable, CD34⁺ sorted cells are indicated in the region Sorted CD34⁺ cells.

5.7 Summary

The isolation of CD34⁺ HSPC populations from UCB and leukapheresis product was successfully achieved by MACS, FACS, or a combination of the two sorting techniques. The CD34⁺ HSPC populations obtained by sample processing and sorting were used in the experiments described in Chapter 6 *Haematopoietic stem/progenitor cell colony-forming unit* assays and human immunodeficiency virus infection.

5.8 References

1. Metcalf, D. Hematopoietic cytokines. *Blood*. 2008;111(2):485-91.
2. Mendelson, A., Frenette, P.S. Hematopoietic stem cell niche maintenance during homeostasis and regeneration. *Nature medicine*. 2014;20(8):833-46.
3. Majeti, R., Park, C.Y., Weissman, I.L. Identification of a hierarchy of multipotent hematopoietic progenitors in human cord blood. *Cell Stem Cell*. 2007;1(6):635-45.
4. Takahashi, M., Matsuoka, Y., Sumide, K., Nakatsuka, R., Fujioka, T., Kohno, H., et al. CD133 is a positive marker for a distinct class of primitive human cord blood-derived CD34-negative hematopoietic stem cells. *Leukemia*. 2014;28(6):1308-15.
5. Sumide, K., Matsuoka, Y., Kawamura, H., Nakatsuka, R., Fujioka, T., Asano, H., et al. A revised road map for the commitment of human cord blood CD34-negative hematopoietic stem cells. *Nature Communications*. 2018;9(1):2202.
6. Velten, L., Haas, S.F., Raffel, S., Blaszkiewicz, S., Islam, S., Hennig, B.P., et al. Human haematopoietic stem cell lineage commitment is a continuous process. *Nat Cell Biol*. 2017;19(4):271-81.
7. de Wynter, E.A., Buck, D., Hart, C., Heywood, R., Coutinho, L.H., Clayton, A., et al. CD34+AC133+ cells isolated from cord blood are highly enriched in long-term culture-initiating cells, NOD/SCID-repopulating cells and dendritic cell progenitors. *Stem Cells*. 1998;16(6):387-96.
8. Perez-Simon, J.A., Caballero, M.D., Corral, M., Nieto, M.J., Orfao, A., Vazquez, L., et al. Minimal number of circulating CD34+ cells to ensure successful leukapheresis and engraftment in autologous peripheral blood progenitor cell transplantation. *Transfusion*. 1998;38(4):385-91.
9. Ali, M.A.E., Fuse, K., Tadokoro, Y., Hoshii, T., Ueno, M., Kobayashi, M., et al. Functional dissection of hematopoietic stem cell populations with a stemness-monitoring system based on NS-GFP transgene expression. *Sci Rep*. 2017;7(1):11442.
10. Wilson, N.K., Kent, D.G., Buettner, F., Shehata, M., Macaulay, I.C., Calero-Nieto, F.J., et al. Combined Single-Cell Functional and Gene Expression Analysis Resolves Heterogeneity within Stem Cell Populations. *Cell Stem Cell*. 2015;16(6):712-24.
11. Bryder, D., Rossi, D.J., Weissman, I.L. Hematopoietic stem cells: the paradigmatic tissue-specific stem cell. *The American journal of pathology*. 2006;169(2):338-46.
12. Sutherland, D.R., Anderson, L., Keeney, M., Nayar, R., Chin-Yee, I. The ISHAGE guidelines for CD34+ cell determination by flow cytometry. *International Society of Hematotherapy and Graft Engineering. Journal of hematotherapy*. 1996;5(3):213-26.
13. Tomlinson, M.J., Tomlinson, S., Yang, X.B., Kirkham, J. Cell separation: Terminology and practical considerations. *Journal of tissue engineering*. 2012;4:2041731412472690-.
14. Kekarainen, T., Mannelin, S., Laine, J., Jaatinen, T. Optimization of immunomagnetic separation for cord blood-derived hematopoietic stem cells. *BMC cell biology*. 2006;7:30.

15. Hao, Q.L., Shah, A.J., Thiemann, F.T., Smogorzewska, E.M., Crooks, G.M. A functional comparison of CD34 + CD38- cells in cord blood and bone marrow. *Blood*. 1995;86(10):3745-53.
16. Haspel, R.L., Miller, K.B. Hematopoietic stem cells: source matters. *Current stem cell research & therapy*. 2008;3(4):229-36.
17. Hoggatt, J., Pelus, L.M. Mobilization of hematopoietic stem cells from the bone marrow niche to the blood compartment. *Stem Cell Res Ther*. 2011;2(2):13.
18. Fritsch, G., Stimpfl, M., Kurz, M., Leitner, A., Printz, D., Buchinger, P., et al. Characterization of hematopoietic stem cells. *Annals of the New York Academy of Sciences*. 1995;770:42-52.
19. Paar, M., Rossmann, C., Nussold, C., Wagner, T., Schlagenhaut, A., Leschnik, B., et al. Anticoagulant action of low, physiologic, and high albumin levels in whole blood. *PLOS ONE*. 2017;12(8):e0182997.
20. Seita, J., Weissman, I.L. Hematopoietic Stem Cell: Self-renewal versus Differentiation. *Wiley interdisciplinary reviews Systems biology and medicine*. 2010;2(6):640-53.

Chapter 6 Haematopoietic stem/progenitor cell colony-forming unit assays and human immunodeficiency virus infection

6.1 Introduction

The effect of HIV on the haematopoietic system is well described, resulting in a variety of haematological abnormalities such as cytopenias¹ and haematological cancers², described in detail in 2.3.3 *Human immunodeficiency virus* and haematopoietic stem/progenitor cells. These abnormalities can result from HIV-associated dysregulation of haematopoiesis, or from direct infection of bone marrow niche cells and/or HSPCs. The susceptibility of HSPCs to infection has yet to be conclusively determined, indicated by the summary of research studies shown in Table 2.2.

The question of HSPC susceptibility to HIV infection and determining whether haematological abnormalities are a direct or indirect consequence of HIV infection also has implications for anti-HIV HSPCT-based gene therapy. Proof-of-concept for an HSPCT-based HIV cure was provided by Hütter and colleagues in the Berlin patient, who has been cured of HIV by means of allogeneic HSPCT with donor cells resistant to R5-tropic HIV (CCR5-null)³. Autologous transplant of an HIV⁺ patient's own, CCR5-null engineered HSPCs and T-cells is an expanding field of research, currently showing promising results in murine models⁴⁻⁷. When harvesting HSPCs for autologous transplant, it is important to know whether these cells can potentially be infected with HIV, and what effect HIV has on HSPC function. This is because direct infection of HSPCs would result in the gene editing and infusion of infected cells back into the patient, resulting in proliferation and a resultant spike in viral load⁸. Additionally, if HSPCs harbour HIV, there is the risk that HIV replication may be activated in differentiating HSPCs during patient conditioning and/or post-transplantation.

The effects of HIV infection on HSPC function can be evaluated by CFU assays, which rely on the clonal expansion and differentiation properties of HSPCs to produce identifiable colonies

when seeded in semisolid medium containing cytokines to support differentiation. These colonies give an indication of the capacity of the seeded HSPCs to differentiate into all the lineages assayed (determined by which cytokines are in the medium). Haematopoietic colonies and the cells from which they are derived in a typical multilineage CFU assay are shown in Figure 6.1. The self-renewing HSCs asymmetrically divide to form an HSC and a HPC with the potential to become either a CLP or CMP. The CLP can differentiate into cells of the lymphoid lineage, namely NK cells, T-lymphocytes, and B-lymphocytes. The CMP results in mixed myeloid colonies of granulocytes, macrophages, erythroblasts, and megakaryocytes (GEMM), forming CFU-GEMM. The CMP can differentiate into the granulocyte/macrophage (GM) progenitor, forming CFU-GM colonies, or the megakaryocyte/erythroblast (ME) progenitor. The GM progenitor can differentiate into granulocytes, forming CFU-G, or macrophages, forming CFU-M. The ME progenitor can differentiate into megakaryocytes, forming CFU-Mk, or erythroblasts, forming B/CFU-E.

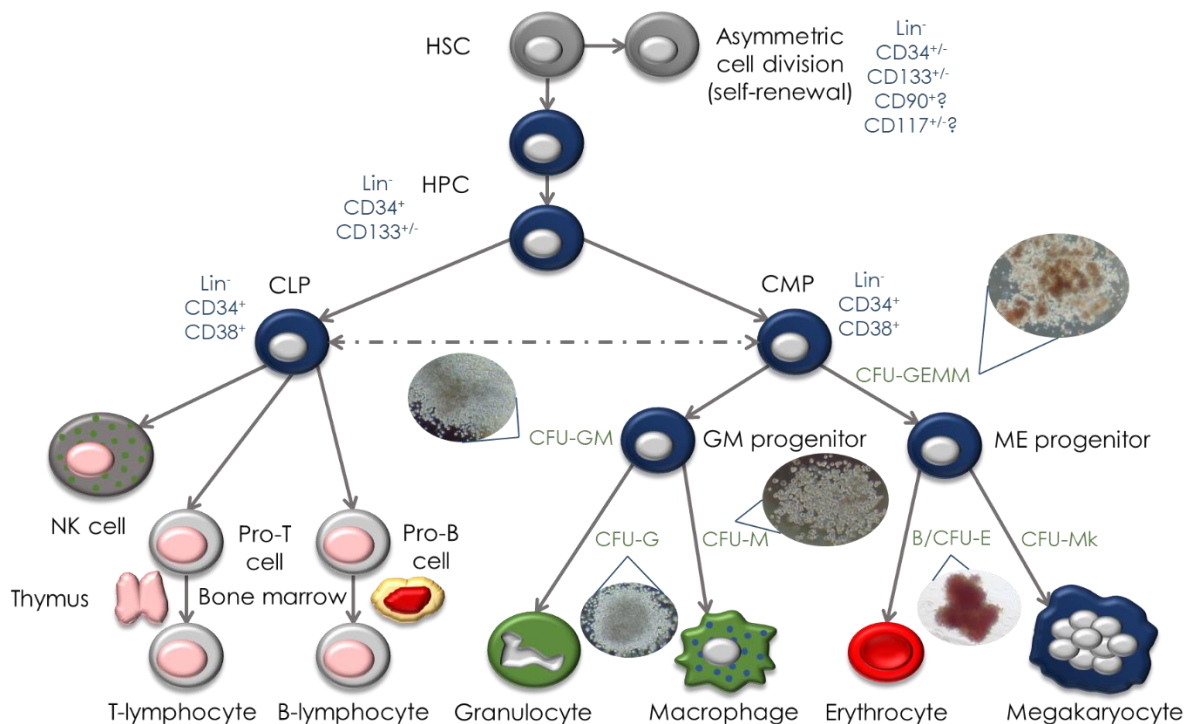


Figure 6.1: Schematic representation of haematopoiesis (adapted from literature⁹⁻¹¹), showing HSC and HSPC phenotype markers (blue), CFUs (green), and colony images relevant to CFU assays. Colony images were obtained from the CFU assay resource “The Human Colony Forming Cell (CFC) Assay Using Methylcellulose-based Media” protocol (R&D Systems) available at <https://www.rndsystems.com/resources/protocols/human-colony-forming-cell-cfc-assay-using-methylcellulose-based-media>.

6.2 Colony-forming unit assay set up and optimisation

6.2.1 Background

The CFU assay, although widely used, is susceptible to subjectivity if standardisation in colony counting is not instituted. It is therefore important to ensure that the researcher performing the CFU assay is trained to recognise and differentiate between the various haematopoietic colonies. To aid in standardisation, a CFU atlas was compiled using colony morphology, colour, cell size, and colony heterogeneity as reference points for colony differentiation. The CFU atlas was used as a reference guide during CFU counting and identification, and was compiled concurrently with CFU assay optimisation to ensure that real data could be applied to the theoretical framework of the atlas.

CFU assays are typically performed in 6-well plates or 35 mm culture dishes by adding a known volume of cell suspension to semisolid medium supplemented with cytokines before plating¹². In this study, HSPCs were sorted by FACS directly into 500 μ L pre-warmed Methocult™ SF H4436 (Methocult™; STEMCELL Technologies, Canada) per well in 24-well plates. Methocult™ SF H4436 is a serum-free semisolid medium supplemented with recombinant human (rh) SCF, rh GM-CSF, rh IL-3, rh IL-6, rh G-CSF, and rh Epo. These cytokines support differentiation into granulocytes, macrophages, erythrocyte progenitors, and megakaryocytes, which can be identified as colonies. Lymphoid colonies were not evaluated by the CFU assay as IL-7, a critical cytokine supporting lymphoid differentiation¹⁰, was not present in the medium (Figure 2.3).

Optimisation of the CFU assay specifically included the non-standard plate size (24-well) and seeding method (sorting directly into medium by FACS). These changes to standard protocols^{12, 13} necessitated the optimisation of (i) seeding cell density, (ii) post-sort distribution of cells, and (iii) scoring and counting conventions.

6.2.2 Method optimisation

6.2.2.1 Colony-forming unit assay method framework

All CFU assays were performed according to the following protocol framework. Outcomes of optimisation experiments were implemented for subsequent experiments.

UCB-derived MNCs were isolated as described in 5.3.1 *Umbilical cord* blood processing and prepared for sorting as described in 5.6.2.2 *Sample preparation and gating strategies*. Samples were sorted as described in 5.6.2.2.1 *Haematopoietic stem/progenitor cell* sorts from umbilical cord blood-derived mononuclear cells into wells of 24-well plates containing 500 μ L pre-warmed Methocult™ per well. Cells seeded in Methocult™ were incubated for 14 days at 37°C, 5% CO₂ for colonies to form as a result of clonal expansion and differentiation of seeded HSPCs. After the 14 day culture period, colonies were counted using light microscopy on a Zeiss Axio Vert A1 (ZEISS, Germany) light microscope.

6.2.2.2 Cell seeding density

Seeding density plays an important role in the success of colony counting, as three dimensional HSPC expansion in semisolid medium may result in colonies overlapping and becoming impossible to count when seeded at high densities. In contrast, too few seeding cells results in a poor representation of differentiation as not all of the seeded HSPCs will necessarily differentiate.

To determine the optimum HSPC seeding density, 100, 150, 200, and 250 viable UCB-derived CD34⁺ HSPCs were sorted into Methocult™ as described in 5.6.2.2.1 *Haematopoietic stem/progenitor cell* sorts from umbilical cord blood-derived mononuclear cells. After 14 days incubation at 37°C, 5% CO₂, colonies were counted and identified by light microscopy. It was determined that 100 cells/well consistently yielded colonies with sufficient resolution to be counted with confidence, while still producing between 15-30 colonies per well.

6.2.2.3 Post-sort distribution

Sorting HSPCs by FACS directly into Methocult™ was problematic as all the sorted cells remain in the zone of the well that the FACS stream strikes during sorting, usually close to the middle of the well. Distribution of cells post-sort therefore required optimisation as Methocult™ is viscous and difficult to work with without losing medium and cells. Pipetting the Methocult™-cell suspension to mix the sorted cells and medium to achieve a more even distribution of cells resulted in a layer of HSPC-containing medium on the inside of the pipette tip which was impossible to recover. Given that any mechanical distribution using an implement to move the medium resulted in similar loss of the viscous medium containing HSPCs, the plates were agitated by vortex. The plates were vortexed by placing the centre of the plate, followed by each corner, on the vortex for 15 seconds directly after sorting. PBS was then added to empty wells to prevent the semisolid medium from drying out during incubation, which would compromise the assay.

Over-mixing by vortex resulted in all the colonies forming on the edges of the wells, making colony counting impossible due to the Methocult™ meniscus resulting in a curved edge which obscured colonies evaluated by light microscopy. Adequate distribution of cells after each vortex cycle was therefore confirmed by microscopy before incubation for the CFU assay.

6.2.2.4 Grid-scoring and counting conventions

6.2.2.4.1 Grid-scoring

In order to prevent counting one colony more than once, a tracking system was required to keep record of which colonies had already been counted. A grid was drawn (using a permanent marker) onto the bottom of the plate or the plate lid, or onto a cover slip which could be moved over each well while counting. None of these inventions were successful, as the lines were out of focus when colonies were in focus. However, a 3x3 grid scored on the bottom of the plate using a scalpel and ruler worked well. This was achieved by turning the empty plate upside down and tracing straight lines dividing the wells into three segments horizontally and vertically so that each well had nine blocks (Figure 6.2).

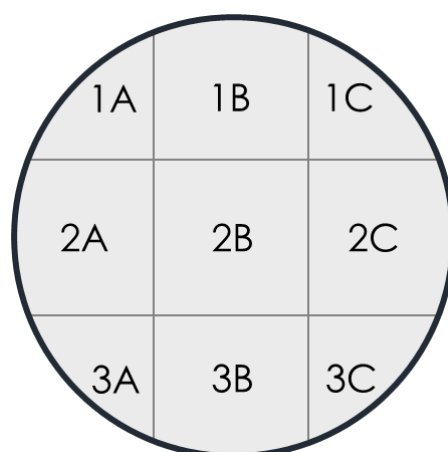


Figure 6.2: Counting grid scored onto the bottom of each well of 24-well plates, showing the grid block positions used for colony counting.

6.2.2.4.2 Colony counting conventions

Colonies which overlapped between blocks were recorded in the block containing the bulk of the colony.

Overlapping colonies were another challenge which required a solution for the purpose of standardising the CFU assay. An excerpt from the CFU atlas is shown in Figure 6.3, which was used as a guideline for counting overlapping colonies and identifying colony boundaries.

Overlapping colonies were either resolved or grouped by evaluating the planes of focus where the colonies were situated. Colonies of the same type, in the same plane of focus, and that had more than 30% overlapping area were grouped as multiple lobes or nodes of one colony. Colonies of the same type in different planes of focus were counted as separate colonies. Planes of focus were defined by focusing on cells as close to the centre of a colony as possible.

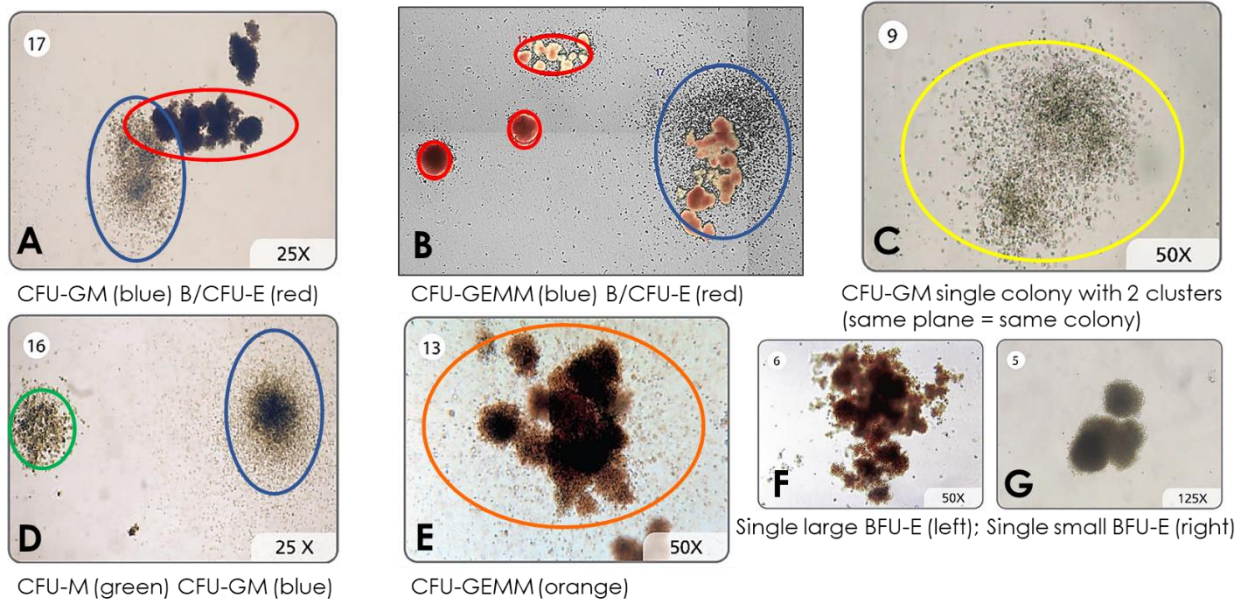


Figure 6.3: Single/multiple colony designation from the CFU atlas for colony counting standardisation. Images above were adapted from the STEMCELL Technologies technical manual (version 4.2.0) for human CFU assays using Methocult¹³, and the STEMVision automated colony counter technical manual. Circles indicate how colonies were counted. (A) Overlapping CFU-GM (blue circle) and B/CFU-E (red circle) were counted as separate colonies. (B) Well-resolved colonies, with a CFU-GEMM encircled in blue and B/CFU-E in red. The granulocyte/macrophage “halo” in the CFU-GEMM is noteworthy as it distinguishes the CFU-GEMM from the B/CFU-E. (C) Two nodes of a single CFU-GM colony are encircled in yellow, indicating that two overlapping nodes of the same colony type in the same plane are counted as one colony. (D) The difference between CFU-M (green circle) and CFU-GM (blue circle) is shown, with good resolution between the colonies. (E) Multiple lobes of a single CFU-GEMM are encircled in orange, distinguishable from a B/CFU-E by the granulocyte/macrophage halo. (F) A single large BFU-E with multiple lobes (and no granulocyte/macrophage halo) is shown in contrast to a single small BFU-E (G), which show the resolution which can be used to count erythroid colonies as a single colony.

6.2.2.5 Establishing the colony-forming unit atlas

6.2.2.5.1 Colony recognition

Haematopoietic colonies were identified by systematic classification as shown in Table 6.1. Cell variety, shape, density, colour, and constituent cell size were considered for each colony, and categorised for easy stratification according to a picture atlas (Figure 6.4). The specific cytokine cocktail present in Methocult™ is optimised for the differentiation of HSPCs into CFU-GEMM, CFU-GM, CFU-G, CFU-M, CFU-E, BFU-E, and CFU-Mk (Figure 6.1). As CFU-E are infrequently formed from UCB-derived HSPCs, CFU-E and BFU-E were counted together as B/CFU-E. Although CFU-Mk are rare and difficult to distinguish from CFU-M without staining, CFU-Mk are comprised of cells which are slightly larger than the cells making up CFU-M, in smaller, sparser colonies than CFU-M¹⁴. Cell size relative to CFU-M and colony size and density were used to identify CFU-Mk.

Table 6.1: Haematopoietic colony classification criteria and categories.

Cell variety	Colony shape	Colony density	Colour	Cell size
Different cell types	Multiple lobes/close clusters	Sparse cluster	Brown/red	Small cells
Uniform cell type	Single cluster	Dense cluster	White/transparent	Large cells

Table 6.1, in conjunction with a picture atlas (Figure 6.4) with key points for quick identification of colonies, was kept on-hand during counting for consistent evaluation of colony types. This atlas was compiled from literature^{12, 15, 16}, online resources¹³, and CFU assays performed for optimisation.

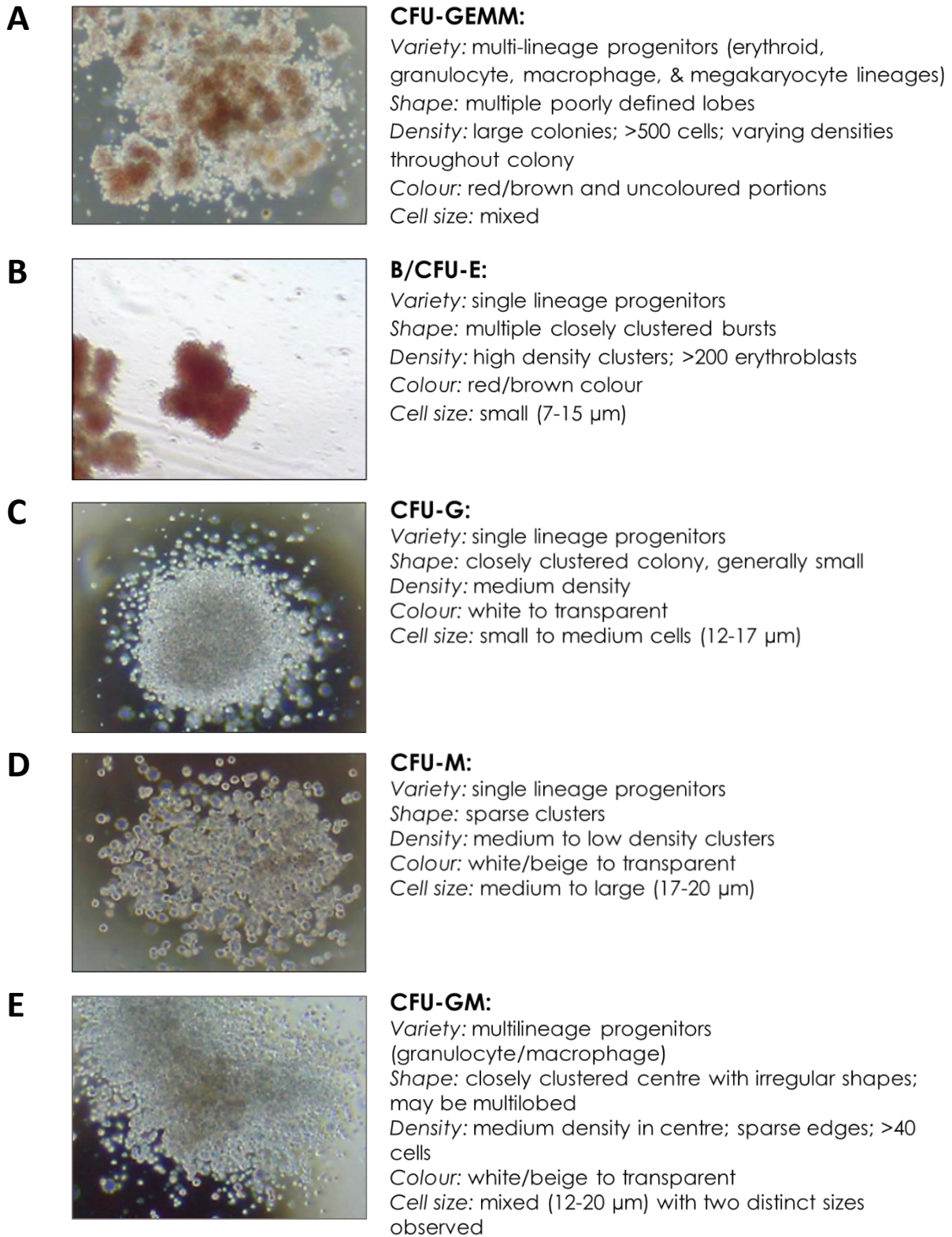


Figure 6.4: Picture atlas for haematopoietic colony recognition with key points for easy identification of colonies characterised (Table 6.1). (A) Characteristics of CFU-GEMM colonies. (B) Characteristics of B/CFU-E colonies. (C) Characteristics of CFU-G colonies. (D) Characteristics of CFU-M colonies. (E) Characteristics of CFU-GM colonies. Colony images were obtained from the CFU assay resource “The Human Colony Forming Cell (CFC) Assay Using Methylcellulose-based Media” protocol (R&D Systems) available from <https://www.rndsystems.com/resources/protocols/human-colony-forming-cell-cfc-assay-using-methylcellulose-based-media>.

6.2.2.5.2 Counting tools

Counting sheets for accurate data tracking and representation were developed to capture data while counting and during processing.

During counting, single wells were counted using a laminated per-well counting sheet (Table 6.2) and an erasable marker. Colonies were tallied by type for each grid block (Figure 6.2). The “total” column was used as a secondary colony scoring control measure. Once the colonies per well had been identified and tallied, the number of total colonies in the well were counted again to confirm that colonies were not missed during counting.

The data captured on the per-well sheet was transferred to the per-plate sheet (Table 6.3), where the totals of each colony type per grid block were tallied. This was recorded as a representation of spread and distribution of colonies in a well and between wells. Data was transferred from the per-well sheet to the final data translation sheet (Table 6.4) as hard copies before electronic transcription. The CFU assay performed using CB240118-02 was used as an example of data capture and transfer.

Table 6.2: Per-well counting sheet laminated for recording colonies of a single well while counting. Colonies of each type were counted per grid block (Figure 6.2). Example values are filled in. The CFU assay for CB240118-02, well A2 was used as an example (green).

Grid block	CFU-GEMM	CFU-GM	CFU-G	CFU-M	B/CFU-E	CFU-Mk	Total
1A							0
1B	1	1		2	2		6
1C							0
2A		2	1		1		4
2B	2	3	2	2			9
2C				1			1
3A	2						2
3B		2			1		3
3C							1

Table 6.3: Per-plate counting sheet used to record colonies in each grid block (blue numbers) of each well (black numbers) of 24-well plates. Well numbers were adjusted according to the plate layout specific to the experiment. The CFU assay for CB240118-02, well A2 are used as an example (green).

A2		1GEMM 1GM 2M 2E		A3	1A	1B	1C	A4	1A	1B	1C	A5	1A	1B	1C
	2GM 1G 1E	2GEMM 3GM 2M 2G	1M		2A	2B	2C		2A	2B	2C		2A	2B	2C
	2GEMM	2GM 1E	1E		3A	3B	3C		3A	3B	3C		3A	3B	3C
B2	1A	1B	1C	B3	1A	1B	1C	B4	1A	1B	1C	B5	1A	1B	1C
	2A	2B	2C		2A	2B	2C		2A	2B	2C		2A	2B	2C
	3A	3B	3C		3A	3B	3C		3A	3B	3C		3A	3B	3C
C2	1A	1B	1C	C3	1A	1B	1C	C4	1A	1B	1C	C5	1A	1B	1C
	2A	2B	2C		2A	2B	2C		2A	2B	2C		2A	2B	2C
	3A	3B	3C		3A	3B	3C		3A	3B	3C		3A	3B	3C
D2	1A	1B	1C	D3	1A	1B	1C	D4	1A	1B	1C	D5	1A	1B	1C
	2A	2B	2C		2A	2B	2C		2A	2B	2C		2A	2B	2C
	3A	3B	3C		3A	3B	3C		3A	3B	3C		3A	3B	3C

Table 6.4: Final consolidation of experimental data for CFU assay data capture. The data captured in this sheet was recorded for each 24-well plate. Wells were adjusted according to the plate layout specific to the experiment. . The CFU assay for CB240118-02, wells A2-A5 are used as an example (green).

Well	CFU-GEMM	CFU-GM	CFU-G	CFU-M	BFU/CFU-E	Total
A2	5 _{0Mk}	8	3	5	5	26
A3	7 _{1Mk}	10	1	1	5	25
A4	9 _{4Mk}	9	0	7	6	35
A5	8 _{2Mk}	5	0	13	6	34
B2						
B3						
B4						
B5						
C2						
C3						
C4						
C5						
D2						
D3						
D4						
D5						

6.3 CD34⁺ haematopoietic stem/progenitor cell colony-forming unit assays

6.3.1 Rationale

The CD34⁺ population is transcriptomically and phenotypically heterogeneous¹⁷⁻¹⁹. In order to evaluate the effects of HIV infection on the function of a heterogeneous population of HSPCs, the seeding population should produce similar, reproducible results between biological replicates. For this reason, additional cell surface markers were included which do not select for a particular subpopulation of HSPCs, but ensure the exclusion of less primitive, lineage-restricted (committed) CD34⁺ progenitors.

CD38 and a cocktail of lineage-specific (Lin) markers were included as additional phenotype selection markers for HSPCs seeded for CFU assays. Cells expressing lineage-specific markers (Lin⁺ cells) were excluded as they already express markers which indicate lineage commitment. CD38 was included as it is an activation marker which increases expression as HSPCs proceed to terminal differentiation. It is well-reported that primitive HSPCs do not express CD38²⁰⁻²², therefore Lin⁻CD38⁻CD34⁺ HSPCs were sorted for CFU assays. The expression of CD34, Lin markers, and CD38 on HSPC populations during clonal expansion and differentiation of self-renewing HSCs to terminally differentiated haematopoietic cells are shown in Figure 6.1 and Figure 6.5.

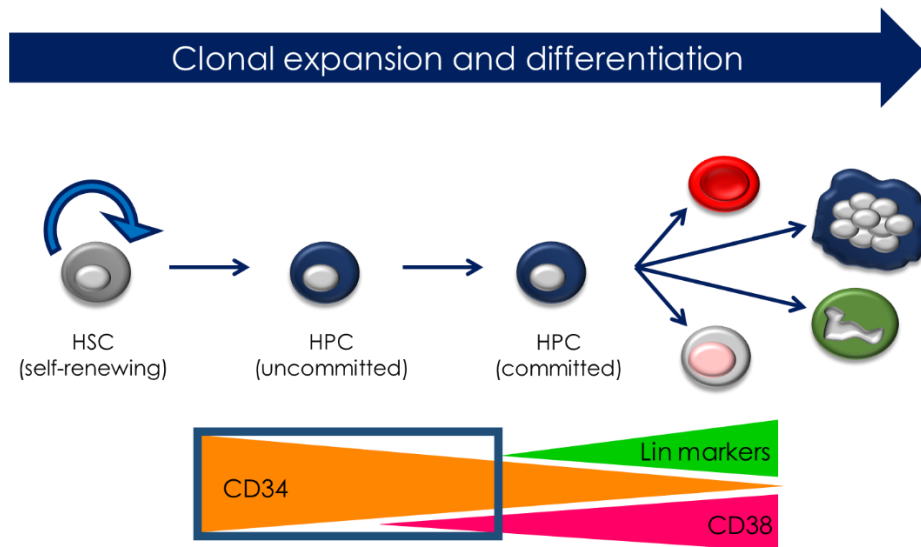


Figure 6.5: Schematic representation of clonal expansion and differentiation of HSPCs into terminally differentiated cells and the expression of key cell surface markers over time. The blue block indicates the range of phenotypes selected for CFU assays performed in this study.

6.3.2 Method

6.3.2.1 Sample preparation

UCB-derived MNCs were isolated from UCB as described in 5.3.1 *Umbilical cord* blood processing, enumerated by flow cytometry (as described in 5.4.2.1 *Umbilical cord* blood-derived samples), and prepared for sorting as described in 5.6.2.2.1 *Haematopoietic stem/progenitor cell* sorts from umbilical cord blood-derived mononuclear cells. Absolute leukocyte and $CD34^+CD45^{dim}$ HSPC counts are shown in Table 6.5.

Table 6.5: Absolute (total cell) counts for UCB-derived MNCs from which CD34⁺ HSPC sub-populations were sorted.

Sample ID	Viability (%)	Leukocytes (absolute count)	CD34 ⁺ CD45 ^{dim} HSPCs (absolute count)
CB300817	94.02	1.08 x 10 ⁷	1.94 x 10 ⁵
CB060917-02	96.81	7.22 x 10 ⁷	3.37 x 10 ⁶
CB041017	95.82	2.81 x 10 ⁷	5.18 x 10 ⁵
CB171117	93.49	2.38 x 10 ⁷	9.62 x 10 ⁵
CB240118-02	96.41	6.46 x 10 ⁷	4.27 x 10 ⁶
CB240118-04	97.31	1.60 x 10 ⁸	9.86 x 10 ⁵
CB070318	99.11	1.74 x 10 ⁸	1.37 x 10 ⁶
CB290318	97.39	7.09 x 10 ⁷	2.39 x 10 ⁶

6.3.2.2 Haematopoietic stem/progenitor cell sorting

CD45^{dim}CD34⁺ (referred to as CD34⁺), CD45^{dim}CD34⁺Lin⁻ (referred to as CD34⁺Lin⁻), CD45^{dim}CD34⁺Lin⁻CD38⁺ (referred to as CD34⁺Lin⁻CD38⁺), CD45^{dim}CD34⁺Lin⁻CD38^{dim} (referred to as CD34⁺Lin⁻CD38^{dim}), and CD45^{dim}CD34⁺Lin⁻CD38⁻ (referred to as CD34⁺Lin⁻CD38⁻) cells were sorted into Methocult™-containing wells as described in 5.6.2.2.1 *Haematopoietic stem/progenitor cell sorts* from umbilical cord blood-derived mononuclear cells. In 24-well plates, no less than triplicate wells were sorted for each population into 500 µL Methocult™, at a density of 100 cells/well. A typical plate layout is shown in Figure 6.6. To prevent dehydration of Methocult™ during culture, 1 mL PBS supplemented with 2% pen/strep was added to empty wells (Figure 6.6 column 1 and 6). Cells were distributed in the semisolid medium by vortex as described in 6.2.2.3 *Post-sort distribution*. Colonies were counted after 14 days using the conventions and tools described in 6.2.2.4 *Grid-scoring and counting conventions* and 6.2.2.5 *Establishing the colony-forming unit atlas*.

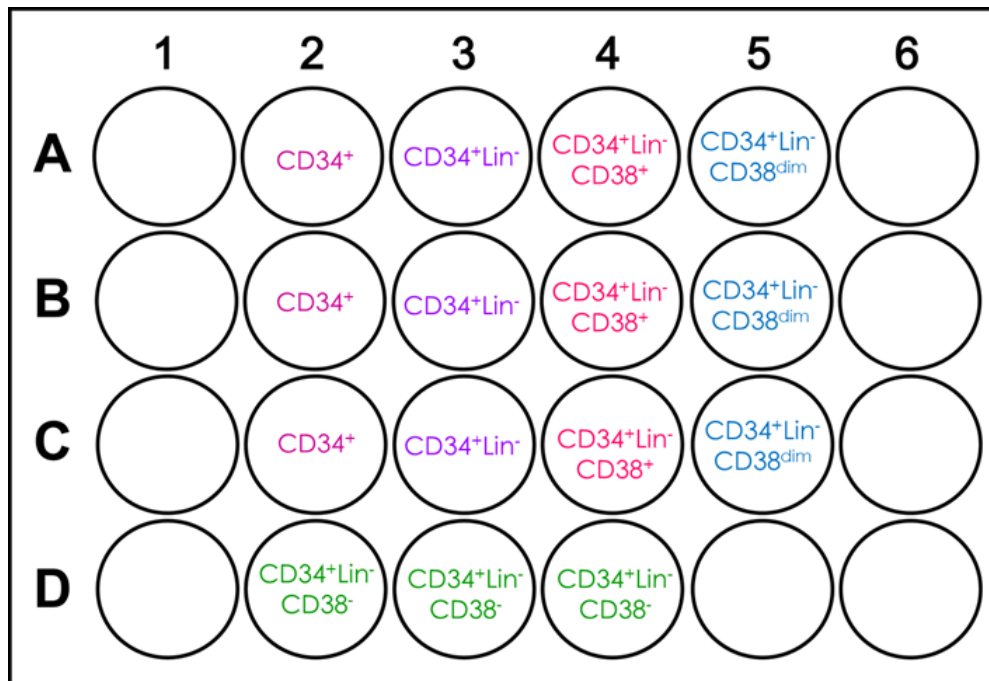


Figure 6.6: Typical HSPC population sort plate layout. The sorted population phenotypes are shown in each well. Unlabelled wells contained 1 mL PBS or PBS supplemented with 2% pen/strep.

6.3.2.3 Data capture and processing

6.3.2.3.1 Data capture

Colonies were identified using the CFU atlas as described in 6.2.2.5.1 *Colony recognition* and counted using the tools described in 6.2.2.5.2 *Counting tools*.

6.3.2.3.2 Data processing

Data was transferred to MS Excel spreadsheets from the final data translation sheet. The data was grouped by sorted population and transferred to GraphPad Prism7 (GraphPad Software Inc., USA) which was used to perform statistical analysis. The variance between biological replicates for each sorted population was investigated by graphing the average of technical repeats and the associated standard deviations (Figure 6.7). The variance between sorted

populations was investigated by combining technical and biological replicates for each sorted population to determine the capacity of the different HSPC subpopulations to form the various colonies (Figure 6.8).

6.3.2.3.3 Statistical analysis

The Shapiro-Wilk test for normality was used to test the normality of the data. Non-parametric statistical analysis was performed, recommended by both the normality test and the sample size of the data.

Variance within sorted populations

For each sorted population, the mean and standard deviation of colony types were calculated using two to four technical repeats of five to eight biological replicates. Data is graphed in Figure 6.7.

Variance between sorted populations

The technical repeats for each of the five biological replicates with data for all five sorted HSPC populations were compiled into a table to compare the variance between colony types and total colonies for each sorted population. A two-way analysis of variance (ANOVA) was performed (Friedman two-way ANOVA) with Tukey correction for multiplicity, applied due to the number of biological replicates used to perform the analysis. Adjusted p -values ≤ 0.05 were reported as statistically significant. Data is shown in Figure 6.8, and Table 6.6.

6.3.3 Results and outcome

6.3.3.1 Variance within sorted populations

Five graphs (Figure 6.7A-E) show the data for within-sorted population variation between (i) technical replicates, and (ii) biological replicates. The mean colony number for each type of colony (CFU-GEMM (GEMM), CFU-GM (GM), CFU-G (G), CFU-M (M), CFU-E (E), CFU-Mk (Mk),

and total colonies (Total)) for each biological replicate is shown. The standard deviation between technical repeats is indicated by the error bars.

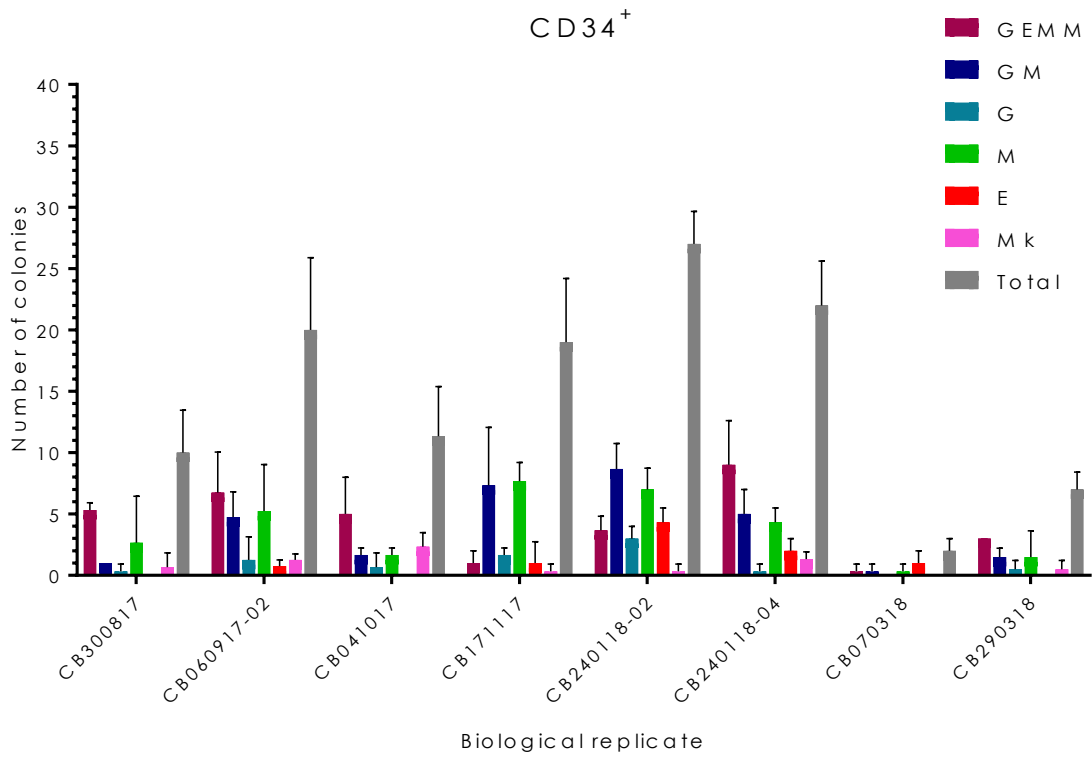
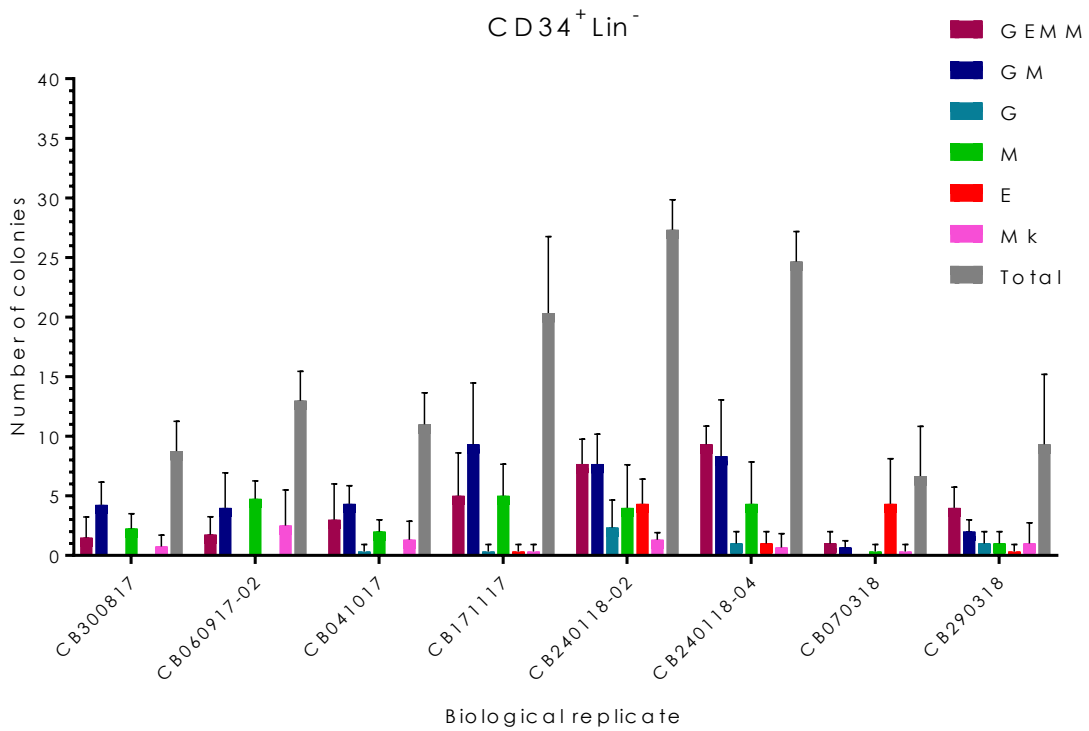
The CD34⁺ sorted population (Figure 6.7A) showed a good distribution of colony types across biological replicates. This means that most colony types were represented in each biological replicate, the notable exceptions being B/CFU-E, and CFU-Mk. Single-lineage B/CFU-E are not commonly formed by UCB-derived HSPCs¹³, therefore the absence of these colonies was not surprising. Erythroid potential can be ascertained using the abundance of CFU-GEMM, which contain haemoglobinised (red) erythroid cells. CFU-Mk are not common using Methocult™ H4436, although it contains the cytokines allowing for the formation of CFU-Mk¹³. The sporadic distribution of CFU-Mk was therefore not concerning. As with erythroid potential, megakaryocytic potential can also be determined using CFU-GEMM as a proxy, even though the presence of megakaryocytes is less identifiable in CFU-GEMM than the red colour produced by erythroid progenitors. As is expected for primitive subsets of HSPCs, multilineage CFU-GEMM and CFU-GM colonies were the most common colony types in general. The standard deviation between technical replicates was low to moderate between wells, which is good for reproducibility of colony distribution in technical repeats. In addition to reproducible colony distribution between technical replicates, the colony distribution between biological replicates was similar. This indicates that in spite of expected biological variance, most colonies are represented between UCB donors for the CD34⁺ HSPC population.

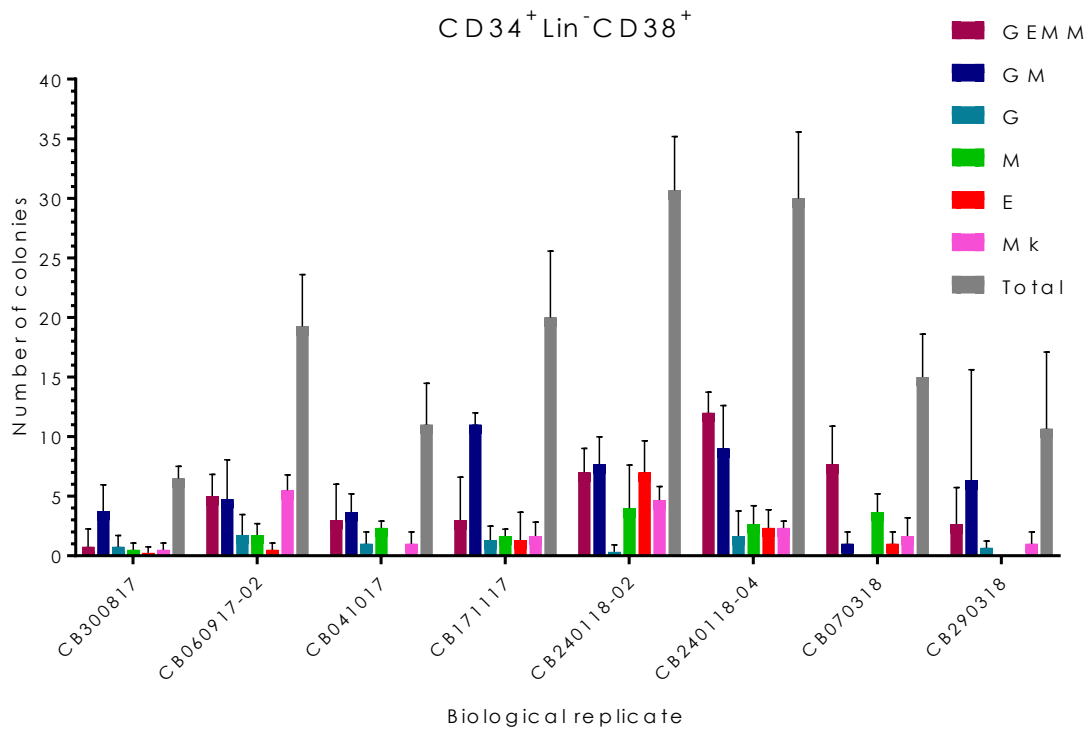
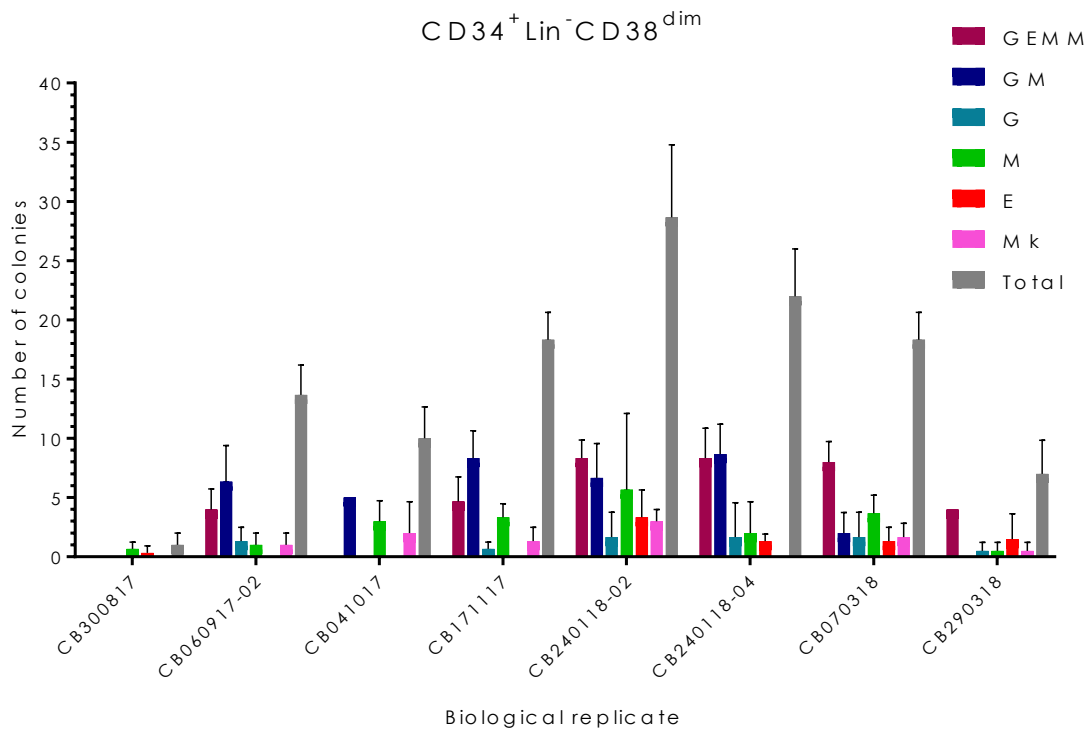
The same trends were true for the CD34⁺Lin⁻ (Figure 6.7B), CD34⁺Lin⁻CD38⁺ (Figure 6.7C), and CD34⁺Lin⁻CD38^{dim} (Figure 6.7D) sorted HSPC populations. Technical repeats were reproducible, indicated by low to moderate standard deviations. The distribution of colony types indicated that each of the above-mentioned sorted populations were capable of multilineage and single-lineage colony formation. Biological replicates showed similar trends in terms of colony distribution between sorted populations, indicating that the four above-mentioned sorted populations were highly similar in colony forming capacity.

In contrast, CD34⁺Lin⁻CD38⁻ sorted HSPCs (Figure 6.7E) rarely formed colonies, and the colony type distribution between biological replicates was not representative of multilineage and single-lineage potential. In addition to low colony forming capacity, a number of CD34⁺Lin⁻

CD38⁻-sorted wells contained round, intact cells after 14 days in culture, which appeared inert or very slowly dividing. This phenomenon was attributed to the primitivity of UCB-derived CD34⁺Lin⁻CD38⁻ HSPCs compared to HSPCs of the same phenotype from adult sources such as bone marrow²⁰. Interestingly, colony formation of CD34⁺Lin⁻CD38⁻ HSPCs could not be predicted by high colony-forming capacity of other sorted HSPC populations within the same biological replicate. This suggests that the colony-forming capacity of CD34⁺Lin⁻CD38⁻ HSPCs is highly donor-dependent.

Considering the reproducibility of colony distribution within and between biological replicates for each sorted HSPC population, and the similarity in colony-forming capacity of CD34⁺Lin⁻ (Figure 6.7B), CD34⁺Lin⁻CD38⁺ (Figure 6.7C), and CD34⁺Lin⁻CD38^{dim} (Figure 6.7D) sorted HSPC populations, the CD34⁺ population was selected for future CFU assays. Important to note is that most UCB-derived CD34⁺ HSPCs are Lin⁻ on the day of isolation (observed during several isolations), therefore the CD34⁺Lin⁻ population and CD34⁺ population are essentially the same population. For HSPCs derived from non-UCB sources, the Lin cocktail would be included for sorting of CFU assays.

A**B**

C**D**

E

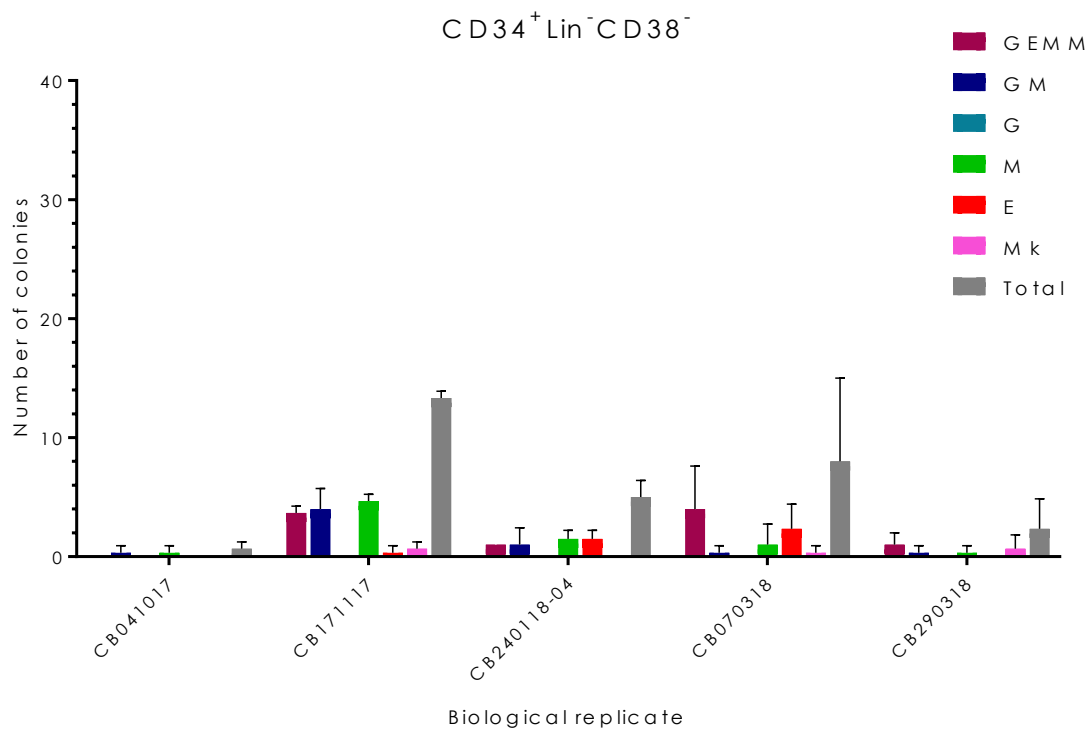


Figure 6.7: Average number of colonies counted for each sorted HSPC population, per biological replicate. Error bars represent the standard deviation of technical repeats. GEMM indicates CFU-GEMM (granulocyte, erythrocyte, megakaryocyte, macrophage) colonies, GM indicates CFU-GM (granulocyte-macrophage) colonies, G indicates CFU-G (granulocyte) colonies, M indicates CFU-M (macrophage) colonies, E indicates B/CFU-E (erythroid) colonies, and Mk indicate CFU-Mk (megakaryocyte) colonies. (A) CD34⁺ HSPC colonies; (B) CD34⁺Lin⁻ HSPC colonies; (C) CD34⁺Lin⁻CD38⁺ HSPCs colonies; (D) CD34⁺Lin⁻CD38^{dim} HSPC colonies; (E) CD34⁺Lin⁻CD38⁻ HSPC colonies.

6.3.3.2 Variance between haematopoietic stem/progenitor cell populations

The variance between sorted HSPC populations in terms of each colony type and total colonies is represented in a box-and-whisker plot (Figure 6.8). The whiskers indicate the highest and lowest colony numbers for each colony type, and the mean is indicated by the box bisector. Significance is indicated by the asterisks. Table 6.6 shows the outcomes of the Friedman two-way ANOVA with Tukey correction for multiplicity in terms of significance (adjusted *p*-values).

Sorted HSPC populations were compared by combining all technical repeats of each biological replicate within sorted populations, and performing an ANOVA. A box-and-whisker plot was

selected to represent the mean and distribution of colony types between sorted populations. From Figure 6.8, CFU-GEMM (GEMM) and CFU-GM (GM) are the most well-represented of all colony types. This was expected as primitive HSPCs were selected by sorting Lin⁻ cells, resulting in multilineage colonies having the highest frequency. Single-lineage CFU-G (G) colonies were the least frequent, although similar distributions of CFU-G were observed between sorted HSPC populations. Single-lineage CFU-M (M) were the most frequent single-lineage colony type.

Comparing sorted populations (Figure 6.7), the variance within colony types between sorted populations (Figure 6.8) was expected. However, the only statistically significant ($p \leq 0.05$) variance between sorted populations was detected in Total colonies. The CD34⁺Lin⁻CD38⁻ sorted population was a clear outlier (although lacking statistical significance) compared to the other sorted populations particularly in multilineage colony forming capacity (GEMM and GM). The CD34⁺, CD34⁺Lin⁻, CD34⁺Lin⁻CD38⁺, and CD34⁺Lin⁻CD38^{dim} populations were not significantly different from each other in their capacity to form multilineage or single-lineage colonies, although the CD34⁺Lin⁻CD38⁺, and CD34⁺Lin⁻CD38^{dim} populations appear to have increased multilineage colony-forming capacity resulting in increased total colonies for these populations.

Each of the CD34⁺, CD34⁺Lin⁻, CD34⁺Lin⁻CD38⁺, and CD34⁺Lin⁻CD38^{dim} populations was significantly different from the CD34⁺Lin⁻CD38⁻ sorted population (indicated by asterisks). The CD34⁺Lin⁻CD38⁺ HSPCs were the most significantly different from the CD34⁺Lin⁻CD38⁻ sorted population in terms of colony-forming capacity. This was not surprising, as CD38 is a well-described activation marker and is associated with HSPC lineage commitment. This serves to further confirm that CD38 would be a good marker to sort more primitive HSPCs from less primitive HSPCs. Unfortunately, due to the relatively low colony-forming capacity of UCB-derived CD34⁺Lin⁻CD38⁻ HSPCs in most biological replicates, sorting CD34⁺Lin⁻CD38⁻ HSPCs for CFU assays may not be useful for evaluating the effects of HIV infection of HIV infection on HSPC colony formation.

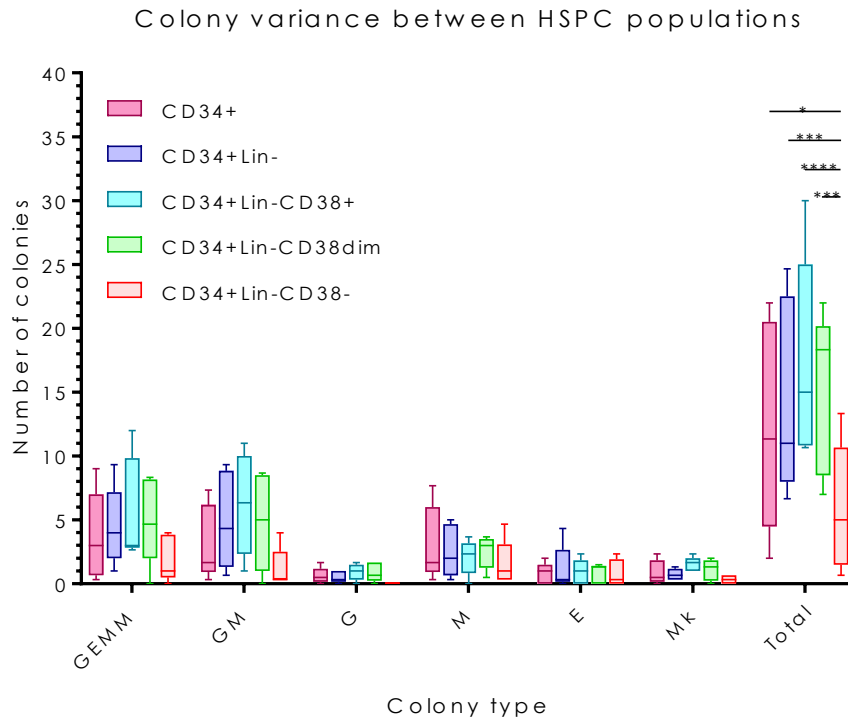


Figure 6.8: Colony variance between HSPC populations, and distribution of colony types for each sorted HSPC population, displayed in a box-and-whisker plot. The data represents five biological replicates. The lowest and highest values are indicated by the whiskers, and the mean number of colonies is indicated by the line bisecting each box. Significance tested by two-way ANOVA with Tukey correction for multiplicity is indicated by asterisks; * $p \leq 0.05$, ** $p \leq 0.01$, * $p \leq 0.001$, **** $p < 0.0001$.**

Due to the lack of significant difference between CD34⁺, CD34⁺Lin⁻, CD34⁺Lin⁻CD38⁺, and CD34⁺Lin⁻CD38^{dim} sorted HSC populations shown in Figure 6.8 and Table 6.6, we recommend using the CD34⁺/CD34⁺Lin⁻ HSPC populations (CD45^{dim}CD34⁺/CD45^{dim}CD34⁺Lin⁻ populations) for CFU assay sorts in future experiments. As most UCB-derived CD34⁺ HSPCs were Lin⁻ on the day of sorting, a distinction between the CD34⁺ and CD34⁺Lin⁻ populations could not be made.

Table 6.6: Comparison of total colonies between sorted HSPC populations using a two-way ANOVA with Tukey correction for multiplicity. Significance indicated by asterisks denotes adjusted p -values as follows: * $p \leq 0.05$, ** $p \leq 0.01$, * $p \leq 0.001$, **** $p < 0.0001$.**

Comparison (total colonies)	Significance	Adjusted p-value
CD34+ vs. CD34+Lin-	ns	0.8542
CD34+ vs. CD34+Lin-CD38+	ns	0.1272
CD34+ vs. CD34+Lin-CD38dim	ns	0.6630
CD34+ vs. CD34+Lin-CD38-	*	0.0258
CD34+Lin- vs. CD34+Lin-CD38+	ns	0.6432
CD34+Lin- vs. CD34+Lin-CD38dim	ns	0.9969
CD34+Lin- vs. CD34+Lin-CD38-	***	0.0009
CD34+Lin-CD38+ vs. CD34+Lin-CD38dim	ns	0.8397
CD34+Lin-CD38+ vs. CD34+Lin-CD38-	****	<0.0001
CD34+Lin-CD38dim vs. CD34+Lin-CD38-	***	0.0002

6.3.3.3 Outcome

CD34⁺Lin⁻CD38⁻ HSPCs infrequently formed colonies and were therefore the only HSPC population which significantly differed from any of the other four sorted populations in colony-forming capacity. The CD34⁺Lin⁻CD38⁻ population was thus to be found unsuitable for determining changes in HSPC function in future experiments. Since the addition of the Lin cocktail and CD38 did not result in HSPC sub-populations with statistically greater or lesser colony-forming capacity compared to the CD34⁺ population, the CD34⁺ population was selected for future experiments. However, phenotypic data showed that the majority of UCB-derived CD34⁺ HSPCs were Lin⁻ on the day of isolation and sorting ($\geq 95\%$; unpublished data). For this reason, the Lin status of non-UCB sources should be evaluated before sorting CD34⁺ HSPCs for CFU assays.

6.4 Effect of human immunodeficiency virus infection on haematopoietic stem/progenitor cell colony formation

6.4.1 Introduction

After establishing and developing competence in performing the CFU assay, experiments to determine the effect of HIV-infection on HSPC colony formation were commenced.

HSPCs were originally sourced from UCB, however, the cell numbers required for HIV experiments (upwards of 5×10^6 CD34⁺ HSPCs) far exceeded what could be isolated from one UCB unit. Three to five UCB units were therefore pooled to determine whether enough CD34⁺ HSPCs could be obtained. The logistical challenges of obtaining multiple UCB units for experiments at any given time and sorting sufficient CD34⁺ HSPCs from pooled units for experiments contributed to the abandonment of UCB as a source of HSPCs for HIV experiments. Leukapheresis products donated for research purposes were therefore adopted as the source of HSPCs for HIV experiments.

Unfortunately, due to time constraints, only a single pilot experiment was performed to evaluate the effects of HIV-infection on HSPC colony formation. A single R5X4-tropic HIV-1C isolate (CM9) was used to perform this experiment, as multiple virus comparisons would have required more HSPCs than we were able to isolate for the experiment. This pilot experiment failed due to massive cell death during the experiment, described in detail in 6.4.3 *Methods and outcomes* and 6.4.4 *Limitations*.

6.4.2 Optimisation of haematopoietic stem/progenitor cell infection strategy

Prior to performing the final pilot experiment, an HIV infection strategy was required. Strategy development and optimisation of HSPC infection with HIV was performed using UCB-derived HSPCs. Multiplicity of infection (MOI), exposure time, and infection medium were all evaluated towards developing a strategy for HSPC infection with HIV. MOI refers to the ratio of infectious virus particles to cells used in experiments.

6.4.2.1 Experimental design

A single experiment was designed to test two MOIs (MOI3 and MOI5), two exposure times (24 hr and 48 hr), and the effect of cytokine stimulation on HSPC susceptibility to infection. Comparing HSPCs infected in medium with or without cytokine supplementation was included because *in vitro* infection of HSPCs has previously been performed both with²³⁻²⁸ and without²⁹⁻³¹ cytokines by different research groups. This inconsistency, and the inconsistency in cytokine cocktails used, could contribute to the lack of consensus regarding the susceptibility of HSPCs to HIV infection (Table 2.2).

For this experiment, viable CD34⁺CD45^{dim} UCB-derived HSPCs were isolated from UCB as described in 5.3.1 *Umbilical cord* blood processing, and purified by FACS as described in 5.6.2.2.1 *Haematopoietic stem/progenitor cell* sorts from umbilical cord blood-derived mononuclear cells. Two hundred thousand (2×10^5) viable CD45^{dim}CD34⁺ UCB-derived HSPCs were sorted per well into 500 μ L RPMI (2% pen/strep, 10% human albumin) in each of 16 wells of a 24-well plate. Eight wells were supplemented with 100 ng/mL of each of the following cytokines: FLT3-L (STEMCELL Technologies, Canada), SCF (STEMCELL Technologies, Canada), and TPO (STEMCELL Technologies, Canada). This cytokine cocktail was derived from previous studies on UCB-derived HSPC expansion performed at the ICMC forming part of Juanita Mellet's PhD study. In a separate plate, a control group of unexposed cells was prepared by sorting 4×10^5 UCB-derived, viable CD34⁺CD45^{dim} HSPCs into 1 mL RPMI (2% pen/strep, 10% human albumin) per well in 8 wells of a 24-well plate. Four of the eight control

wells were also supplemented with the cytokine cocktail as described above. Both plates were incubated overnight at 37°C, 5% CO₂ to recover.

6.4.2.2 Infection

After isolation, sorting, and overnight incubation in medium, cells from each well were transferred to 1.5 mL microcentrifuge tubes and pelleted by centrifugation at 300 x g for 10 min, after which the supernatant was aspirated. Cell pellets were pooled per plate by cytokine condition (CYT+ or CYT-) by resuspending pellets in 1 mL of the appropriate medium as follows. HIV-exposed wells (from plate sorted with 2x10⁵ cells/well) were resuspended in CM9-241016 HIV CFS (5.155x10⁵ IU/mL; produced as described in 4.4 *Propagation of HIV in*), and HIV-unexposed wells were resuspended in CM (produced as described in 4.4.2.2.6 *Control medium for experiments*).

The purpose of the PBMC-conditioned medium (CM) HIV-unexposed control was to control for effect of PBMC-conditioned medium in which HIV CFS was harvested. This resulted in four pooled suspensions each in 1 mL total volume: CYT+ resuspended in HIV CFS, CYT- resuspended in HIV CFS, CYT+ resuspended in CM, and CYT- resuspended in CM. Each suspension was divided in four, by aliquoting 250 µL into labelled, upright T75 flasks. Each flask was topped up to the volume indicated in Table 6.7 with the medium indicated. Once topped up with HIV CFS or CM, the flasks were incubated upright at 37°C, 5% CO₂.

Half the volume of each flask was collected 24 hr post-HIV-exposure after gentle pipetting to ensure a homogenous cell suspension, and the other half was collected in the same way 48 hr post-exposure. Cells collected at each time point were pelleted for DNA extraction by centrifugation at 300 x g for 10 min.

Table 6.7: Final volumes of HIV CFS (HIV-exposed) or CM (HIV-unexposed) for each flask in the HSPC infection optimisation experiment.

HIV-exposed flasks	HIV CFS final volume (µL)	HIV-unexposed flasks	CM final volume (µL)
MOI3 CYT+	4656	HIV- MOI3 CYT+	4656
MOI3 CYT-	4656	HIV- MOI3 CYT-	4656
MOI10 CYT+	15518	HIV- MOI10 CYT+	15518
MOI10 CYT-	15518	HIV- MOI10 CYT-	15518

6.4.2.3 DNA extraction

DNA was extracted from cells using the Zymo Quick-gDNA™ microprep kit (Zymo Research, USA) according to manufacturer’s instructions. At first opening, 250 µL β-mercaptoethanol was added to 50 mL Genomic Lysis buffer to a final concentration of 0.5%.

DNA extraction from 24 hr and 48 hr post-exposure harvests was performed immediately after pelleting post-harvest. The supernatants were aspirated and cells were resuspended in 100 µL PBS before being transferred to 1.5 mL microcentrifuge tubes. To lyse cells, 400 µL Genomic Lysis buffer was added to each tube and mixed by vortex, before incubating at room temperature for 5 min. Cell lysates were transferred to Zymo-Spin™ IC columns assembled in 2 mL collection tubes and centrifuged at 10 000 x g for 1 min. The flow-through was discarded and columns placed in new collection tubes. Salts and protein were washed from the membrane by adding 200 µL DNA Pre-wash buffer and removed by centrifugation at 10 000 x g for 1 min. The flow-through was discarded and membrane-bound DNA was washed a second time with 500 µL gDNA Wash buffer per column followed by centrifugation at 10 000 x g for 1 min. Collection tubes and flow-through were discarded, and the columns were placed in sterile 1.5 mL microcentrifuge tubes for elution. DNA was eluted from column membranes by adding 25 µL nuclease-free water (QIAGEN, Germany), incubating at room

temperature for 5 min, and centrifugation for 30 s at 14 000 x g. DNA concentrations and purity were determined by NanoDrop®, shown in Table 6.8.

Overall, the concentrations seemed to be high for the number of cells from which DNA was extracted. Protein contamination, indicated by A_{260}/A_{280} ratios, were mostly within range, but salt and small molecule contamination, indicated by A_{260}/A_{230} ratios, was significantly higher than is generally acceptable for PCR applications (3.5.3.4.3 *Nucleic acid quantification by NanoDrop®*). In an attempt to overcome this, 10 ng/μL stocks of each DNA isolation were made with molecular grade water, effectively diluting contaminating salts and small molecules. As a further cautionary measure, the amount of DNA per PCR reaction was reduced from 50 ng to 20 ng of 10 ng/μl dilutions, again to reduce the amount of contaminants which could inhibit PCR.

Table 6.8: DNA concentrations and purity ratios for HSPC MOI optimisation experiments.

Sample ID	DNA concentration (ng/μL)	A₂₆₀/A₂₈₀ ratio	A₂₆₀/A₂₃₀ ratio
HIV- MOI3 CYT+ 24 hr	26.38	2.11	0.14
HIV- MOI3 CYT- 24 hr	12.37	1.43	0.23
HIV- MOI10 CYT+ 24 hr	26.37	1.96	0.12
HIV- MOI10 CYT- 24 hr	11.23	1.58	0.17
MOI3 CYT+ 24 hr	30.92	1.70	0.26
MOI3 CYT- 24 hr	34.73	1.72	0.16
MOI10 CYT+ 24 hr	24.45	1.76	0.63
MOI10 CYT- 24 hr	28.24	1.78	0.46
HIV- MOI3 CYT+ 48 hr	17.89	1.88	0.05
HIV- MOI3 CYT- 48 hr	15.44	1.85	0.09
HIV- MOI10 CYT+ 48 hr	21.15	1.98	0.07
HIV- MOI10 CYT- 48 hr	33.24	2.05	0.10
MOI3 CYT+ 48 hr	16.23	2.10	0.05
MOI3 CYT- 48 hr	19.05	1.94	0.08
MOI10 CYT+ 48 hr	23.31	1.80	0.05
MOI10 CYT- 48 hr	27.83	1.98	0.09

6.4.2.4 *Human immunodeficiency virus detection polymerase chain reaction*

HIV detection PCR was performed after diluting the DNA as described above to dilute contaminants. Reactions for HIV detection by PCR were prepared as described in 3.5.3.5 *P* with the amount of DNA modified from 50 ng per reaction to 20 ng per reaction, using the LTR primer pair which generates a 297 bp amplicon. The following controls were included: PCR control (HIV- CYT- MOI10 48 hr DNA with L32 primers), NTC for both L32 and LTR primer pairs, HIV-unexposed PB-01 DNA as an HIV-negative control for LTR primer pair specificity, and CM9-infected PBMC DNA as an HIV-positive control. Thermocycling was performed as described in 3.5.3.5.2 *Thermocycling specifications*. Amplicons were analysed by gel electrophoresis as described in 3.5.3.6 *Agarose gel electrophoresis*, using 1% agarose gels made up with TAE at 100 V for 60 min with EtBr for visualisation. Sample preparation for electrophoresis was performed as previously described in 3.5.3 *Primer validation*, and wells were loaded with 10 μ L of loading dye/PCR product solution.

A compiled gel image showing the complete data set for 24 hr post-infection samples and the respective controls are shown in Figure 6.9. Amplification was observed for MOI3 CYT+, MOI10 CYT+, and MOI10 CYT- DNA using LTR primers. From Figure 6.9, it can be deduced that cytokines are required to achieve infection at low MOI, as MOI3 CYT- (Figure 6.9, lane 8) did not amplify. However, the presence of cytokines is not required for infection using a high MOI, as both CYT- and CYT+ conditions exposed to MOI10 produced LTR-amplicons.

The gel image for 48 hr post-infection is not shown as no amplification was observed. As the DNA extraction concentration and A_{260}/A_{230} and A_{260}/A_{280} ratios were equally variable between 24 hr and 48 hr extractions, the quality of DNA extractions was not likely to explain the lack of amplification. It is possible that HSPCs harbouring HIV proviral genomes died between 24 hr and 48 hr of incubation with virus, as exposure of HSPCs to the HIV-1 or HIV-1 envelope protein gp120 has been shown to reduce DNA content in cells, which is an apoptotic trait³².



Figure 6.9: Compiled gel image of HIV detected in CYT+ and CYT- UCB-derived CD34⁺ sorted HSPCs at MOI3 and MOI10, 24 hr post-infection. (A) Lane 1 was loaded with the FastRuler™ LR DNA ladder (shown in B). Lanes 2 and 4 were loaded with NTC for the L32 (lane 2) and LTR (lane 4) primer pairs. Lane 3 was loaded with the PCR products amplified using the L32 primer pair and HIV- CYT- MOI10 DNA as the positive reaction control. To show LTR primer specificity, a positive control (CM9-infected PBMC DNA, lane 5) and negative control (HIV-unexposed PB-01 DNA, lane 6) were loaded. Lanes 7-10 were loaded with the PCR products for MOI3 CYT+, MOI3 CYT-, MOI10 CYT+, and MOI10 CYT- respectively, amplified using LTR primer pair. Lanes 11-14 were loaded with the PCR products for HIV-MOI3 CYT+, HIV- MOI3 CYT-, HIV- MOI10 CYT+, and HIV- MOI10 CYT- respectively, amplified using the LTR primer pair. The grey block indicates where amplification was observed.

6.4.2.5 Outcome

From these experiments it was determined that exposure of HSPCs to HIV for 24 hr was sufficient for adequate detection of HIV proviral DNA in HSPCs, and was therefore used as the HIV-exposure time for future experiments. It was also determined that HIV DNA could be detected in HSPCs exposed to moderate (MOI3) and high (MOI10) quantities of virus, although cytokine stimulation appeared to play a role in HIV infection at low MOI. For this reason, MOI3 was proposed for use in HSPC infection experiments.

6.4.3 Methods and outcomes

6.4.3.1 CD34⁺ haematopoietic stem/progenitor cell isolation

One leukapheresis product bag (AP181122-03) was thawed and process as described in 5.3.2 *Leukapheresis processing* and enumerated as described in 5.4.2.2 *Leukapheresis product-derived samples*. Post-thaw enumeration indicated that 75.81% of the cells were viable after processing, and the frequency of viable CD45^{dim}CD34⁺ HSPCs in the sample was

1.36%. In total, the sample contained 4.24×10^9 viable leukocytes, and 3.02×10^7 viable CD45^{dim}CD34⁺ HSPCs, resuspended in a final volume of 100 mL RPMI.

CD34⁺ HSPCs were enriched from the processed leukapheresis product by MACS as described in 5.6.1 M. CD34⁺CD45^{dim} HSPCs were enumerated post-MACS as described in 5.4.2.2 *Leukapheresis product-derived samples*, which indicated that 92.82% of the CD34-enriched cells were viable. The proportion of CD34⁺ HSPCs in the sample was enriched to 91.58%. From the enriched product, 3.7×10^6 viable CD34⁺ HSPCs were sorted by FACS as described in 5.6.2.2.2 *Haematopoietic stem/progenitor cell sorts from leukapheresis*. Sorted cells in 2 mL StemSpan™ (2% pen/strep) were incubated overnight at 37°C, 5% CO₂ to recover from the strenuous sorting methods.

6.4.3.2 *Haematopoietic stem/progenitor cell infection*

After overnight recovery (approximately 18 hr), the purified CD34⁺ HSPC population (described in 6.4.3.1 *CD34+ haematopoietic stem/progenitor cell isolation*) was divided into aliquots of 6×10^5 CD34⁺ HSPCs per infection condition, and transferred to 2 mL microcentrifuge tubes.

An adequate number of tubes of frozen CM and HIV CFS of the isolate CM9-020518 (1.05×10^6 IU/mL) were thawed at 37°C. HSPCs were exposed to the relevant infection condition in 2 mL microcentrifuge tubes at an MOI of 2, requiring 1143 µL HIV CFS. Consequently, 1143 µL CM or RPMI was added to the CM-exposed and Control HSPC aliquot, respectively. Due to low volumes of virus available and subsequent propagations resulting in non-infectious virus being produced, the MOI was lowered from 3 (determined in 6.4.2.5 *Outcome*) to 2. Given the level of HIV proviral DNA detected during optimisation using MOI3 (described in 6.4.2 *Optimisation of haematopoietic stem/progenitor cell infection strategy*), this was to be a reasonable choice.

For the initial exposure, all three tubes (HIV CFS, CM, Control) were incubated in a rotating incubator at 37°C in 2 mL microcentrifuge tubes for 2 hr, to ensure adequate contact between cells and virus. After the initial 2 hr incubation, aliquots were split in half and plated into a 6-

well plate (Figure 6.10). Pre-warmed StemSpan™ (2% pen/strep) was added to a final volume of 1.5 mL per well for each well.

To one of the two wells of each infection conditions, 100 ng/mL of each of the following cytokines was added: SCF, TPO, FLT3-L, IL-3 (STEMCELL Technologies, Canada), and G-CSF (STEMCELL Technologies, Canada). The resulting plate layout is shown in Figure 6.10. This cytokine panel contains two additional cytokines (IL-3 and G-CSF) compared to the minimal cytokine panel previously used (6.4.2 *Optimisation of haematopoietic stem/progenitor cell infection strategy*). This was because expansion of HSPCs exposed to the three infection conditions using the above five-cytokine cocktail was to be performed for Juanita Mellet's PhD project (not part of this dissertation). The cells were incubated at 37°C, 5% CO₂ for 24 hr after infection.

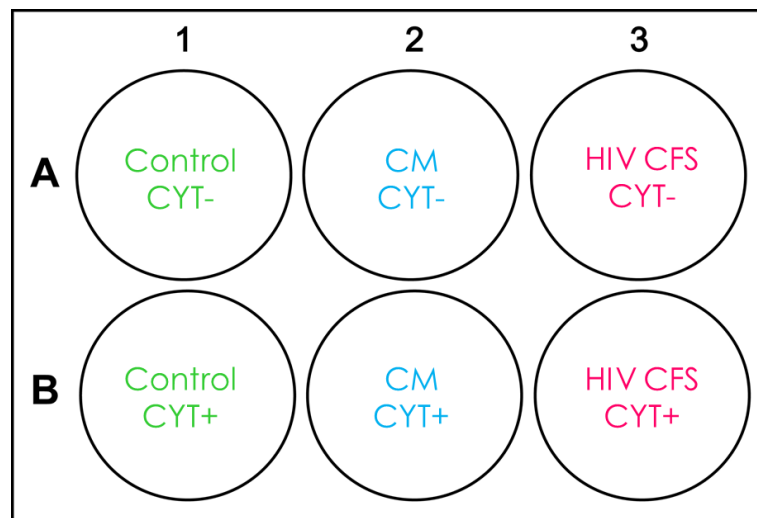


Figure 6.10: Plate layout for CD34⁺ HSPC exposure to three infection conditions, towards evaluating the effects of HIV infection on HSPC colony formation. CFS refers to HIV CFS-exposed cells, control refers to cells mock-infected in RPMI, and CM refers to cells mock-infected with conditioned medium. CYT+ indicates cells incubated overnight with cytokines, and CYT- indicates cells incubated overnight without cytokines.

6.4.3.3 *Colony-forming unit assay and polymerase chain reaction*

6.4.3.3.1 **Colony-forming assay**

Method

After the 24 hr incubation post-infection, the cells from each well (Figure 6.10) were collected into separate 2 mL microcentrifuge tubes. Each well was washed with 400 μ L PBS to collect any remaining cells, and the PBS was transferred to the corresponding tubes. Cells were pelleted by centrifugation at 300 x g for 10 min, the supernatants were discarded, and each pellet was resuspended in 300 μ L TP₄ buffer. Of this volume, 200 μ L was used for Juanita Mellet's experiment, and 100 μ L was stained to sort for CFU assays. Each 100 μ L aliquot was stained for sorting with 3 μ L CD34-PC7 and 3 μ L 7-AAD as described in 5.6.2.2.2 *Haematopoietic stem/progenitor cell sorts from leukapheresis*. The Lin marker was excluded from sorting as 97% of the viable, intact cells in this sample were found to be Lin⁻ based on data generated by Juanita Mellet (PhD student) in an independent study in the group.

Viable CD34⁺ HSPCs were sorted in triplicate into wells of a 24-well plate containing 500 μ L Methocult™ per well, at a density of 100 cells/well as described in 5.6.2.2.2 *Haematopoietic stem/progenitor cell sorts from leukapheresis*. The plate layout of sorted cells is shown in Figure 6.11. The plate was incubated for 14 days as described in 6.2.2.1 *Colony-forming unit assay method* framework.

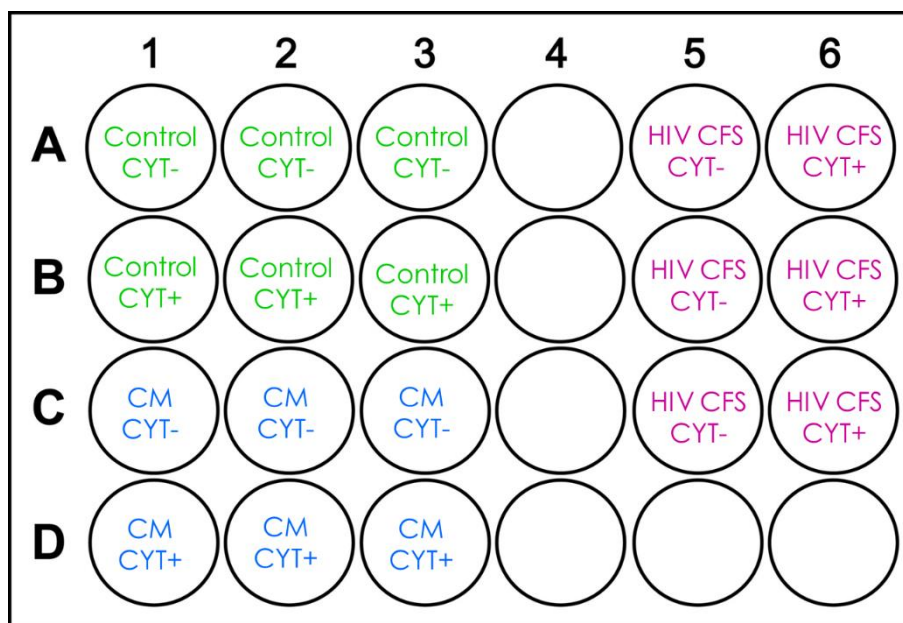


Figure 6.11: Plate layout for CFU assay of pilot experiment, seeded 24 hr post-infection. HIV CFS refers to HIV CFS-exposed cells, control refers to cells mock-infected in RPMI, and CM refers to cells mock-infected with conditioned medium. CYT+ indicates cells incubated overnight with cytokines, and CYT- indicates cells incubated overnight without cytokines. Empty wells contained 1 mL PBS (2% pen/strep).

Results

Unfortunately, the seeded cells did not produce any colonies after 14 days in culture. This could be due to a massive decrease in viability from the day of sorting HSPCs from MACS-enriched cells (74.47%) to the day of infection (7.77%), and viabilities ranging between 2.07% to 10.49% on the day of sorting for CFU assays. As membrane permeability occurs in the later stages of apoptosis³³, it is possible that the apparently viable (7-AAD⁻) cells were undergoing intracellular apoptosis pathways which occur prior to the membrane being compromised. This could explain the cells being impermeable (pre-apoptotic) to 7-AAD on the day of sorting, and permeable (apoptotic) on the day of infection (24 hr after sorting) after being incubated overnight in culture medium. Viable cells were sorted nonetheless in the hope that the cells would recover in culture, which was not the case.

6.4.3.3.2 Polymerase chain reaction

Sample preparation

Cells remaining from CFU sorts were pooled with cells of the same infection condition remaining from phenotyping for DNA extraction. The cells were pelleted in 1.5 mL microcentrifuge tubes by centrifugation at 300 x g for 10 min. The supernatant was aspirated, and the pellets were snap-frozen at -20°C until DNA extraction.

DNA extraction

DNA was extracted from snap-frozen cell pellets by thawing on ice and resuspending in 50 µL PBS. DNA was extracted using the QIAamp DNA Micro kit as per manufacturer's instructions, described in 3.5.3.4.2 DNA extraction procedure. DNA concentration and purity (A_{260}/A_{280} and A_{260}/A_{230}) ratios determined by NanoDrop® are shown in Table 6.9.

Table 6.9: Pilot HIV experiment HSPC DNA concentrations, protein purity (A_{260}/A_{280} ratio), and salt purity (A_{260}/A_{230} ratio).

Sample ID	DNA concentration (ng/µL)	A_{260}/A_{280} ratio	A_{260}/A_{230} ratio
Control CYT -	19.92	3.72	0.72
Control CYT +	21.50	3.32	0.79
CM CYT -	22.38	3.63	0.76
CM CYT +	23.85	3.01	0.87
HIV CFS CYT -	27.86	2.85	0.89
HIV CFS CYT +	22.55	3.09	0.51

The A_{260}/A_{280} ratios were rather high and the A_{260}/A_{230} ratios rather low, but DNA concentrations in general were reasonable given the low number of cells from which DNA was extracted (less than 10^5 cells). High A_{260}/A_{280} ratios indicate high nucleic acid concentrations relative to proteins. This could be attributed to the addition of cRNA during DNA extraction to assist in DNA recovery from the silica membrane. It is not possible to determine the proportion of cRNA in the nucleic acid extracts using the NanoDrop®. Low A_{260}/A_{280} ratios indicate that salt and small molecule contamination of the DNA product is high, which make the DNA extractions unsuitable for PCR. This salt contamination could result from insufficient washing of DNA on the silica membrane during DNA extraction, or from reagent imbalance relative to starting material.

DNA purification

To attempt to purify the extracted DNA, ethanol precipitation was performed to remove contaminants³⁴. Briefly, 3 M sodium acetate (NaAc; pH 5.2; Sigma-Alrich, USA) was added 1:10 volume-by-volume to each sample (2.8 μ L per sample). Ice-cold absolute ethanol (70 μ L; 2.5 x total volume) was added to each tube and gently vortexed to mix without shearing DNA. The solutions were incubated at -20°C for 1 hr. This incubation allowed salts and protein contaminants to dissolve in the NaAc solution, and the DNA to precipitate in the absolute ethanol. The DNA was pelleted by centrifugation at 14 000 rpm for 30 min, after which the supernatant (containing contaminants) was removed. The DNA pellets were washed with 100 μ L 70% ethanol prepared with nuclease-free distilled water, and centrifuged again for 30 min at 14 000 rpm. As much supernatant as possible was removed without disturbing the tube. The remaining ethanol was removed by air-drying in a heating block set to 50°C for 10-15 min. Dried pellets were resuspended in 25 μ L nuclease-free water before quantifying by NanoDrop®. DNA concentrations and purity post-precipitation are shown in Table 6.10.

Table 6.10: Post-precipitation pilot HIV experiment HSPC DNA concentrations, protein purity (A_{260}/A_{280} ratio), and salt purity (A_{260}/A_{230} ratio).

Sample ID	DNA concentration (ng/μL)	A_{260}/A_{280} ratio	A_{260}/A_{230} ratio
Control CYT -	2.71	2.07	0.93
Control CYT +	13.92	2.07	2.05
CM CYT -	1.35	22.09	1.36
CM CYT +	3.46	2.24	1.48
HIV CFS CYT -	13.08	2.31	1.89
HIV CFS CYT +	1.90	1.60	1.12

Ethanol precipitation of DNA to improve quality was partially successful as it resulted in lower A_{260}/A_{280} ratios and increased A_{260}/A_{230} ratios, respectively. Unfortunately, a significant amount of the DNA was lost during precipitation, therefore HIV detection by PCR could not be performed. The low DNA concentrations after purification lends credence to the suggestion that cRNA from the extraction procedure contributed significantly to the DNA concentration measurements post-extraction.

6.4.4 Limitations

Due to time constraints, the failed pilot experiment could not be repeated. Failure of the experiment was likely due to the loss of viable cells. The loss of viability occurred between the day of FACS sorting of MACS-enriched CD34⁺ cells and the day of infection. The reason for the large decrease in cell viability requires further investigation before the pilot experiment is repeated. Avenues to explore include repeating the procedure until MACS-enriched cells have been further purified by FACS, and periodically assessing viability to determine at which point the cells lose viability. Different overnight media could also be tested to determine whether this could ameliorate the overnight cell death phenomenon.

Due to these unforeseeable circumstances, the colony-forming capacity of HSPCs exposed to HIV could not be evaluated.

6.5 References

1. Vishnu, P., Aboulafia, D.M. Haematological manifestations of human immune deficiency virus infection. *British Journal of Haematology*. 2015;171(5):695-709.
2. Rios, A. HIV-related hematological malignancies: a concise review. *Clinical lymphoma, myeloma & leukemia*. 2014;14 Suppl:S96-103.
3. Hütter, G., Nowak, D., Mossner, M., Ganepola, S., Müßig, A., Allers, K., et al. Long-Term Control of HIV by CCR5 Delta32/Delta32 Stem-Cell Transplantation. *New England Journal of Medicine*. 2009;360(7):692-8.
4. Myburgh, R., Ivic, S., Pepper, M.S., Gers-Huber, G., Li, D., Audigé, A., et al. Lentivector Knockdown of CCR5 in Hematopoietic Stem and Progenitor Cells Confers Functional and Persistent HIV-1 Resistance in Humanized Mice. *Journal of Virology*. 2015;89(13):6761-72.
5. Holt, N., Wang, J., Kim, K., Friedman, G., Wang, X., Taupin, V., et al. Human hematopoietic stem/progenitor cells modified by zinc-finger nucleases targeted to CCR5 control HIV-1 in vivo. *Nat Biotechnol*. 2010;28(8):839-47.
6. Khamaikawin, W., Shimizu, S., Kamata, M., Cortado, R., Jung, Y., Lam, J., et al. Modeling Anti-HIV-1 HSPC-Based Gene Therapy in Humanized Mice Previously Infected with HIV-1. *Molecular Therapy - Methods & Clinical Development*. 2018;9:23-32.
7. Hofer, U., Henley, J.E., Exline, C.M., Mulhern, O., Lopez, E., Cannon, P.M. Pre-clinical Modeling of CCR5 Knockout in Human Hematopoietic Stem Cells by Zinc Finger Nucleases Using Humanized Mice. *The Journal of Infectious Diseases*. 2013;208(Suppl 2):S160-S4.
8. Trono, D., Marzetta, F. Profaning the Ultimate Sanctuary: HIV Latency in Hematopoietic Stem Cells. *Cell Host & Microbe*. 2011;9(3):170-2.
9. Bryder, D., Rossi, D.J., Weissman, I.L. Hematopoietic stem cells: the paradigmatic tissue-specific stem cell. *The American journal of pathology*. 2006;169(2):338-46.
10. Metcalf, D. Hematopoietic cytokines. *Blood*. 2008;111(2):485-91.
11. Kode, J., Khattry, N., Bakshi, A., Amrutkar, V., Bagal, B., Karandikar, R., et al. Study of stem cell homing & self-renewal marker gene profile of ex vivo expanded human CD34(+) cells manipulated with a mixture of cytokines & stromal cell-derived factor 1. *The Indian journal of medical research*. 2017;146(1):56-70.
12. Pereira, C., Clarke, E., Damen, J. Hematopoietic colony-forming cell assays. *Methods Mol Biol*. 2007;407:177-208.
13. Technologies, S. Technical manual: Human Colony-forming Unit (CFU) Assays Using Methocult™. 4.2.0 ed. Online: STEMCELL™ Technologies.
14. Kaufman, D.S., Hanson, E.T., Lewis, R.L., Auerbach, R., Thomson, J.A. Hematopoietic colony-forming cells derived from human embryonic stem cells. *Proceedings of the National Academy of Sciences*. 2001;98(19):10716-21.
15. Nissen-Druey, C., Tichelli, A., Meyer-Monard, S. Human hematopoietic colonies in health and disease. *Acta haematologica*. 2005;113(1):5-96.

16. Gordon, M.Y. Human haemopoietic stem cell assays. *Blood reviews*. 1993;7(3):190-7.
17. Velten, L., Haas, S.F., Raffel, S., Blaszkiewicz, S., Islam, S., Hennig, B.P., et al. Human haematopoietic stem cell lineage commitment is a continuous process. *Nat Cell Biol*. 2017;19(4):271-81.
18. Haas, S., Trumpp, A., Milsom, M.D. Causes and Consequences of Hematopoietic Stem Cell Heterogeneity. *Cell Stem Cell*. 2018;22(5):627-38.
19. Pranke, P., Hendriks, J., Debnath, G., Alespeiti, G., Rubinstein, P., Nardi, N., et al. Immunophenotype of hematopoietic stem cells from placental/umbilical cord blood after culture. *Brazilian journal of medical and biological research = Revista brasileira de pesquisas medicas e biologicas*. 2005;38(12):1775-89.
20. Hao, Q.L., Shah, A.J., Thiemann, F.T., Smogorzewska, E.M., Crooks, G.M. A functional comparison of CD34 + CD38- cells in cord blood and bone marrow. *Blood*. 1995;86(10):3745-53.
21. Mehta, K., Shahid, U., Malavasi, F. Human CD38, a cell-surface protein with multiple functions. *FASEB journal: official publication of the Federation of American Societies for Experimental Biology*. 1996;10(12):1408-17.
22. Majeti, R., Park, C.Y., Weissman, I.L. Identification of a hierarchy of multipotent hematopoietic progenitors in human cord blood. *Cell Stem Cell*. 2007;1(6):635-45.
23. Chelucci, C., Hassan, H.J., Locardi, C., Bulgarini, D., Pelosi, E., Mariani, G., et al. In vitro human immunodeficiency virus-1 infection of purified hematopoietic progenitors in single-cell culture. *Blood*. 1995;85(5):1181-7.
24. Weichold, F.F., Zella, D., Barabitskaja, O., Maciejewski, J.P., Dunn, D.E., Sloand, E.M., et al. Neither Human Immunodeficiency Virus-1 (HIV-1) nor HIV-2 Infects Most-Primitive Human Hematopoietic Stem Cells as Assessed in Long-Term Bone Marrow Cultures. *Blood*. 1998;91(3):907-15.
25. Redd, A.D., Avalos, A., Essex, M. Infection of hematopoietic progenitor cells by HIV-1 subtype C, and its association with anemia in southern Africa. *Blood*. 2007;110(9):3143-9.
26. Carter, C.C., Onafuwa-Nuga, A., McNamara, L.A., Riddell, J., Bixby, D., Savona, M.R., et al. HIV-1 Infects Multipotent Progenitor Cells Causing Cell Death and Establishing Latent Cellular Reservoirs. *Nature medicine*. 2010;16(4):446-51.
27. Carter, Christoph C., McNamara, Lucy A., Onafuwa-Nuga, A., Shackleton, M., Riddell Iv, J., Bixby, D., et al. HIV-1 Utilizes the CXCR4 Chemokine Receptor to Infect Multipotent Hematopoietic Stem and Progenitor Cells. *Cell Host & Microbe*. 2011;9(3):223-34.
28. McNamara, L.A., Ganesh, J.A., Collins, K.L. Latent HIV-1 infection occurs in multiple subsets of hematopoietic progenitor cells and is reversed by NF-kappaB activation. *J Virol*. 2012;86(17):9337-50.
29. Shen, H., Cheng, T., Preffer, F.I., Dombkowski, D., Tomasson, M.H., Golan, D.E., et al. Intrinsic human immunodeficiency virus type 1 resistance of hematopoietic stem cells despite coreceptor expression. *J Virol*. 1999;73(1):728-37.

30. Zhang, J., Scadden, D.T., Crumpacker, C.S. Primitive hematopoietic cells resist HIV-1 infection via p21Waf1/Cip1/Sdi1. *The Journal of Clinical Investigation*. 2007;117(2):473-81.
31. Griffin, D.O., Goff, S.P. HIV-1 Is Restricted prior to Integration of Viral DNA in Primary Cord-Derived Human CD34+ Cells. *J Virol*. 2015;89(15):8096-100.
32. Zauli, G., Vitale, M., Gibellini, D., Capitani, S. Inhibition of purified CD34+ hematopoietic progenitor cells by human immunodeficiency virus 1 or gp120 mediated by endogenous transforming growth factor beta 1. *The Journal of experimental medicine*. 1996;183(1):99-108.
33. Olson, E.D., Nelson, J., Griffith, K., Nguyen, T., Streeter, M., Wilson-Ashworth, H.A., et al. Kinetic Evaluation of Cell Membrane Hydrolysis during Apoptosis by Human Isoforms of Secretory Phospholipase A2. *Journal of Biological Chemistry*. 2010;285(14):10993-1002.
34. OpenWetware Contributors. Ethanol precipitation of nucleic acids: OpenWetWare; 2012 [611420:[Available from: https://openwetware.org/mediawiki/index.php?title=Ethanol_precipitation_of_nucleic_acids&oldid=611420.

Chapter 7 Concluding remarks

7.1 Conclusions and limitations

The overall aim of this project, namely to evaluate the effect of HIV-1 (three tropisms of HIV-1B and HIV-1C) infection on HSPC colony formation was not achieved. However, despite this shortcoming, four of the five objectives of the project were met.

Objective 1: Production of three tropisms of HIV-1C primary isolates, and three tropisms of HIV-1B molecular clones for experimental purposes.

HIV-1B molecular clones of three tropisms were successfully produced in HEK293T cells following transformation of Stbl2 *E.coli* and transfection of HIV-1B-encoding plasmids into HEK293T cells. Molecular clone production could be optimised in future by purifying plasmids before transfection, to ensure that only HIV-1B insert-containing plasmids are used for transfection. Although the transfection protocol is standardised and has been optimised for molecular clone production, the plasmid to cell ratio could be evaluated to maximise transfection (and therefore molecular clone production). HIV-1C primary isolates were propagated in activated PBMCs with varying levels of success, due to challenges impossible to overcome under the present circumstances. These challenges included the viral lifecycle which results in unpredictable loss-of-function mutation, resulting in very low levels of infectious virus present after propagation.

Comparing the challenges between molecular clone production by transfection and primary isolate propagation in PBMCs, molecular clone production was more consistent and reliable. This is because molecular clones produced by transfection do not undergo reverse transcription, as the viral genome is encoded by a plasmid. This eliminates the introduction of loss-of-function mutations which were debilitating in primary HIV isolate production.

Objective 2: Detection of HIV and titration of infectious virus for experimental purposes.

Detecting HIV and quantifying infectious virus was essential for successful titration of viral suspensions and for determining the infection status of cells in various experiments. HIV produced in objective 1 was functionally titrated on GHOST cells using the optimised GHOST GFP assay. HIV detection for optimisation purposes was achieved using p24 enzyme-linked immunosorbent assay (ELISA) targetting the HIV capsid protein, p24. For optimisation and experimental purposes, HIV was detected by the PCR using primers from literature as well as *de novo* designed and validated primers.

Objective 3: Isolation of HSPCs obtained from umbilical cord blood and leukapheresis product for experimental purposes.

HSPCs were isolated from UCB and leukapheresis product donated for research purposes and were isolated in the MNC fraction of cells from UCB, and from bulk cells from leukapheresis product. HSPCs were purified from MNCs and bulk cells by MACS and/or FACS for use in further experiments.

Objective 4: Optimisation of the CFU assay and acquisition of skills required to consistently identify, count, and categorise haematopoietic colonies.

UCB-derived HSPCs were used to optimise the CFU assay and establish the CFU atlas which was used during CFU data collection. As a step in the optimisation process, different CD34⁺ subpopulations of HSPCs were evaluated for use in HIV experiments to evaluate the effects of HIV-1 infection on HSPC colony formation. It was found that CD34⁺Lin⁻CD38⁻ cells rarely formed colonies when seeded for CFU assays, and these cells are thus not suitable for downstream CFU assays. All other HSPC sub-populations investigated consistently produced sufficient colonies for analysis.

Objective 5: Exposure of HSPCs to three tropisms of HIV-1C, and three tropisms of HIV-1B, to evaluate the effect of HIV-1 infection on HSPC colony formation.

Due to time constraints, inability to purify enough viable CD34⁺ HSPCs from leukapheresis product, and limited virus stocks, a single pilot experiment was performed. This experiment failed for reasons which will be explored in future research in order to achieve Objective 5.

7.2 Future work

In order to contribute meaningfully to the current literature regarding HSPC susceptibility to HIV infection, the ultimate aim of this project must be achieved. This would require optimisation of viral production, and the generation or procurement of HIV-1C molecular clones, as HIV propagation in PBMCs was unpredictable in terms of infectious viral yield. Using molecular clones of HIV-1C would be more comparable to the currently available HIV-1B molecular clones than using primary isolates. Obtaining enough viable CD34⁺ HSPCs to perform a full experiment comparing R5-, X4-, and R5X4-tropisms of HIV-1B and HIV-1C head-on would also need to be addressed. This study was part of a larger project which required a vast number of cells per infection condition. In order to assess the effect of HIV infection on HSPC colony formation, perhaps CFU assays of HIV-exposed HSPCs should be performed separately. As multiple bags of a single leukapheresis product donor are typically donated, it would be possible to use the same donor's cells and the same virus harvest to perform CFU assays and the remainder of the larger experimental series independently. The data could still be compared, provided that virus stocks and leukapheresis donor were matched between experiments.

Appendix I BSL2+ Operations and Safety Manual

1. Introduction, Purpose, and Policy

1.1. Introduction

Biosafety Level (BSL) assignment refers to standardised practices required to be implemented by laboratories working with hazardous or infectious biological agents of specified classes. BSL2+ designation indicates that work is conducted in a BSL2 facility with additional biosafety practices and procedures in accordance with BSL3 standards. BSL2 classifies work involving agents of moderate potential hazard which requires specialised, facility-specific training.

The BSL2+ facility at the Institute for Cellular and Molecular Medicine, University of Pretoria, operates under BSL2+ stipulations. In the BSL2+ facility, human immunodeficiency virus (HIV) as well as lentiviral vectors are produced and used in controlled experiments. While these agents are non-infectious via inhalation, exposure to mucosal tissue may be dangerous. For this reason, specialised personal protective equipment (PPE) is employed to minimise potential exposure via the nose, mouth, and eyes. Personnel are expected to don PPE appropriate to their purpose in the facility as outlined in this manual upon entry and proceed with said purpose according to protocols outlined in this manual while inside the BSL2+ facility.

1.2. Purpose

The purpose of this manual is to describe all procedures and training to be undertaken by individuals entering the Institute for Cellular and Molecular Medicine BSL2+ facility (HIV lab) at the University of Pretoria for any reason. This manual is to be read and understood by all persons who will be performing experiments in the HIV lab. All standard operating procedures (SOPs) outlined in this manual are to be followed within the HIV lab.

1.3. Policy

The ICMM BSL2+ Operations and Safety Manual details all SOPs pertaining to the HIV lab with respect to operation and safety. Revisions to any parts of this manual are to be disseminated to all authorised and responsible personnel, where upon revisions must be implemented effective immediately.

All persons (staff and students) working in the HIV lab must be trained according to procedures outlined in section **3.2. Training** and comply with all prerequisites for working in the HIV lab. Any maintenance must be performed as outlined in section **3.2 Access and Maintenance**. Only authorised personnel as described in section **2.1.1 Authorised personnel** may enter the HIV lab, supervise maintenance, or train prospective HIV lab personnel. Training of authorised personnel must be documented and filed, as per SOP outlined in this manual.

The HIV lab operates under the authority of the Responsible Investigator, under the supervision of the appointed Health and Safety Officer (see **Appendix 1: Authorised Personnel and Officers**). Breach of policies and protocols outlined in the ICMC BSL2+ Operations and Safety Manual will result in disciplinary steps as outlined in section **3.3 Disciplinary Procedure** which will be signed off by authorised personnel as well as Professor M.S. Pepper (Responsible Investigator) and placed on record. Signage within the BSL2+ facility will be obeyed at all times.

2. Authority and Responsibility

2.1. Authority

The HIV lab is access controlled. Access codes and protocols are only to be made available to authorised and responsible personnel. Only authorised personnel may accompany non-authorised persons (maintenance and cleaning staff, visitors) into the HIV lab under the restriction of section **3.2.2 Unauthorised persons**. Authorised personnel must be trained according to procedures outlined in this manual under section **3.1 Training and Compliance**. Only personnel who have completed training to the satisfaction of Training Officer(s) will be provided with the access code, with the exception of the Responsible Investigator.

2.1.1. Authorised personnel

A current list of authorised personnel will be made available to all responsible and authorised personnel, as well as being documented in **APPENDIX 1**.

Position	Authorised to:	Description
Laboratory Manager	<ul style="list-style-type: none"> • document training, repair, maintenance, and equipment logs • supervise and direct maintenance and repair of equipment and facility • supervise and direct cleaning • direct and document visitation to the HIV lab • stock-take and replenishing of consumables 	The Laboratory Manager facilitates practical and administrative running of the BSL2+ facility. The Laboratory Manager must be kept informed of documentation filed regarding training and incident reports, as well as changes to SOPs and equipment report records.
Health and Safety Officer	<ul style="list-style-type: none"> • supervise and direct health and safety procedures outlined by the University of Pretoria • receive and document incident reports 	The Health and Safety Officer facilitates incident/crisis management with respect to incidents within or involving the BSL2+ facility and authorised

	<ul style="list-style-type: none"> • stock-take and replenishing of consumables • ensure that Health and Safety provisions are within required standards 	<p>personnel. This includes signing off on training, managing disciplinary protocols, as well as documenting incident reports, as outlined in this manual.</p>
<p>Authorised Personnel</p>	<ul style="list-style-type: none"> • perform experiments inside the BSL2+ facility • document incident reports • supervise and sign off on BSL2+ training (as Training Officers) according to the specifications of this manual • monitor equipment regularly • clean the BSL2+ facility (shared rotational duty) • stock-take and replenishing of consumables 	<p>Authorised personnel must have received training as outlined in this manual and may enter and work inside the BSL2+ facility. Authorised personnel facilitate training of new personnel and will adhere to all guidelines outlined in this manual. Authorised personnel are expected to be in regular contact with the Health and Safety Officer, Laboratory Manager, as well as the Responsible Investigator regarding their work in the lab, incidents, and any training taking place in the BSL2+ facility.</p>
<p>Responsible Investigator</p>	<ul style="list-style-type: none"> • managing funding, administration, and operation of the BSL2+ facility • signing off on training documentation as outlined in this manual • signing off on incident reports as outlined in this manual • managing disciplinary processes in training and infringement protocols 	<p>The Responsible Investigator must be kept informed of all activity in and regarding the BSL2+ facility. This includes incident reports, training processes and documentation, disciplinary processes and documentation, as well as equipment report records and Health and Safety administrative matters.</p>

3. Health and Safety

3.1. Training and Compliance

Training of new personnel (trainees) will be facilitated by Authorised Personnel acting as Training Officers (see section **2.2.1 Authorised Personnel**). Training Officers will document training as required per **Appendix 1: Training Documentation**. Regular signing of training

documents by the relevant Training Officer(s), Health and Safety Officer, and Responsible Investigator must be performed as outlined in **Appendix 1: Training Documentation**, for training certification (see **Appendix 1: Training Documentation – Training Certificate**) to be valid. Incomplete training documentation will void the Training Certificate. Training documentation includes the Training Hours Log Sheet, Trainee Agreement, and Vaccination List.

Failure to comply with protocols and procedures outlined in this manual will result in mandatory Retraining (see section **3.1.2 Retraining**). Banned personnel will not be eligible for training for 365 days from commencement of ban. Eligibility for training of banned individuals will be determined on a case-by-case basis by a committee of Training Officers and Authorised Personnel, the Health and Safety Officer, Laboratory Manager, and Responsible Investigator. Failure to comply with evacuation protocols and incident report documentation (see **3.4 Emergency Protocols**) will result in a temporary ban of 3 weeks, and mandatory Retraining.

3.1.1. Training

The HIV lab training program consists of three parts: shadowing, supervised work, and a probation period. This is to ensure that trainees have every opportunity to familiarise themselves with the procedures and protocols in this manual and integrate themselves with the practical aspects of working inside the HIV lab while under the supervision of an authorised Training Officer. At least two Training Officers must sign off on Supervision hours to ensure completeness. Training Officers may at no point, under no circumstance, leave a trainee inside the HIV lab unaccompanied. This rule does not apply for voluntary Retraining (see **3.2.1 Retraining**). If the Training Officer needs to leave the HIV lab at any point during training, the trainee will cease all work, contain all hazardous material appropriately (close all tubes and exit the Biosafety Cabinet, or terminate all work in the Biosafety Cabinet), decontaminate appropriately (see **Appendix 2: SOP – Working in the BSL2+ Biosafety Cabinet**), and exit the lab (see **Appendix 2: SOP – Leaving the HIV lab**). Trainees **must** have read this manual prior to commencement of training.

The **Training Hours Log Sheet** (see **Appendix 1: Training Documentation**) must be completed by Training Officers and signed by the trainee. Information logged includes course components Shadowing, Supervision, or Probation, and Retraining if necessary at a later stage, and hours completed under each Training Officer. Any training notes may also be written in on the **Training Hours Log Sheet** to make fellow Training Officers aware of any repeated deviation from protocols which need to be corrected prior to certification.

PART 1: Shadowing

The trainee will shadow Training Officers into the lab and be practically instructed on proper procedure for entering the HIV lab, working in the HIV lab with and without live virus, and exiting the HIV lab. Emphasis will be placed on personal protective equipment (PPE) appropriate for different circumstances (see **Appendix 2: SOP – PPE**), and decontamination of the Biosafety Cabinet, work areas, and waste management (see **Appendix 2: SOP –**

Working in the BSL2+ Biosafety Cabinet). A mandatory shadowing period of 10 hours is a prerequisite to Part 2 of the program, which may be increased on a case-by-case basis at the discretion of the Training Officer or trainee. Shadowing hours must be documented in the Training Certificate and are compulsory to the training.

PART 2: Supervision

The trainee, after completing 10 hours of shadowing, will be allowed to conduct general experiments in the HIV lab under the close supervision of a Training Officer. General experiments to be conducted under supervision include Viral Quantitation and Infectivity assays, p24 ELISAs, and HIV productions (see **Appendix 3: Protocols**) which will be required as part of rotational duties once the trainee is certified. Individual project-related experiments are not to be performed as part of training. Trainees will be expected to run through entry, working, and exit procedures as outlined by SOPs in **Appendix 2: SOP**. Training Officers must closely observe all work and guide the trainee with regards to laboratory technique and BSL2+-specific practices so that these practices become habit. A mandatory minimum period of 20 hours working under the supervision of a Training Officer is to be completed before a trainee may be considered for Part 3 of the program. Training Officers or trainees may request for this period to be increased in accordance with their confidence in following BSL2+ SOPs. Hours supervised by each Training Officer must be documented and signed off on the Training Certificate. Trainees cannot be cited for written warnings at this stage except in extreme circumstances where the trainee and/or the Training Officer are put at risk of exposure.

PART 3: Probation

The trainee, after completing a minimum of 20 hours of supervised work in the HIV lab, may work without close supervision by a Training Officer for 30 hours prior to certification as Authorised Personnel. During these probationary hours, a Training Officer must be made aware that the trainee will be working in the HIV lab and must be available to perform regular checks for the duration of the Probation period. This is to ensure that proper procedure is being followed, and to support the trainee as these are still trainable hours. Trainees cannot be cited for written warnings at this stage except in extreme circumstances where the trainee and/or the Training Officer are put at risk.

3.1.2. Retraining

Mandatory Retraining will be enforced when an individual who has completed the BSL2+ training fails to comply with HIV lab protocols outlined in this manual and has been reported **three times by written warning**. Formal written warning explaining the transgressions and a call for Mandatory Retraining will be issued via email from fellow Authorised Personnel, with the Health and Safety Officer and Laboratory Manager being copied on the email. Retraining is an opportunity to revise HIV lab procedures practically and under the supervision of a Training Officer to ensure that everyone authorised to operate within the BSL2+ facility is safe at all times.

Retraining requires 20 to 30 hours of supervised work in the HIV lab to be overseen by a Training Officer. Individuals under Retraining will not be allowed to enter the HIV lab without supervision, to ensure that all potentially hazardous actions are corrected according to the initial SOP-directed training outlined in this manual. Mandatory Retraining must be documented on the individual's training certificate.

Voluntary Retraining may be undertaken by individuals who are unsure or uncomfortable with working in the HIV lab without supervision. Between 20 and 30 hours of supervised work in the HIV lab in addition to completing the full training program should be sufficient. Voluntary Retraining **is not** documented on the individual's training certificate.

3.1.3. Banned Personnel

Personnel are banned from the HIV lab following two unsuccessful Mandatory Retraining attempts. A formal written notice of banning will be issued by email from the Responsible Investigator with a complete list of transgressions resulting in the ban. Banned personnel will not be considered for training within 365 days of the ban being imposed; exceptions will be considered on a case-by-case basis. Post-ban retraining will be considered on a case-by-case basis at the discretion of the Responsible Investigator, under advisement from all Authorised Personnel working in the HIV lab. Banned personnel must be listed in **Appendix 1: Banned personnel**, including the date of ban and a list of transgressions resulting in the ban.

3.1.4. HIV-buddy system

Work in the HIV lab must always be conducted with the knowledge of at least one other Authorised Personnel who must be available to attend to you in case of emergency. This is especially important on weekends and public holidays when there is no one in the ICMM main lab/student offices. This becomes your HIV-buddy for your session in the HIV lab. Availability of your HIV-buddy must be confirmed prior to undertaking weekend work as a precaution in case of HIV exposure (see **3.4.1 Emergency protocols**). As an HIV-buddy, you are required to be telephonically available in the hours specified by the person working in the HIV lab. An HIV-buddy may be required to drive to the nearest emergency room, complete experiments, clean up the lab, or assist with experiments, as well as assist in writing up the incident report (see **Appendix 1: Incident Report**). HIV-buddies are to be informed when work in the HIV lab is complete and they are no longer required to be available. As Authorised Personnel, agreeing to be an HIV-buddy for a session in the HIV lab means that HIV-buddy requirements take precedence over all other occurrences until your HIV-buddy is finished working in the HIV lab.

3.2. Access and Maintenance

The BSL2+ Facility is access-controlled. The code-lock on the door ensures that no unauthorised persons have accidental access to the HIV lab. The presence of unauthorised persons in the HIV lab will be considered breach of protocol. Authorised Personnel responsible for the breach will be disciplined according to section **3.3 Disciplinary Procedure**.

3.2.1. Authorised persons

Authorised Persons are ONLY to be afforded access to the HIV lab under strict supervision of the Lab Manager, Health and Safety Officer, or Authorised Personnel.

Authorisation is granted to maintenance staff for equipment maintenance, repair, and validation, and laboratory maintenance and repair. Authorised persons must be informed of the nature of work conducted in the laboratory and must be fitted with appropriate PPE upon entry into the BSL2+ facility.

Equipment scheduled for maintenance, repair, and validation are to be decontaminated according to **Appendix 2: SOP – Equipment decontamination** prior to being worked on regardless of whether the work will be performed on-site or off-site. For off-site work, it is preferable for Authorised Personnel to have removed equipment from the lab. With large equipment such as the Biosafety Cabinet, maintenance staff will have to remove it from the lab.

Authorised person business	Appropriate PPE
Equipment maintenance, repair, and validation (ON-SITE)	<ul style="list-style-type: none"> • Inner gloves • Disposable lab coat • Safety glasses • Outer gloves
Equipment maintenance, repair, and validation (OFF-SITE)	<ul style="list-style-type: none"> • Inner gloves • Disposable lab coat • Outer gloves <p>PPE only required when moving equipment to avoid contact with possibly contaminated surfaces.</p>
Lab maintenance and repair (ON-SITE)	<ul style="list-style-type: none"> • Inner gloves • Disposable lab coat • Safety glasses • Outer gloves
Lab maintenance and repair (OFF-SITE)	<ul style="list-style-type: none"> • Inner gloves • Disposable lab coat

	<ul style="list-style-type: none"> • Outer gloves <p>PPE only required when moving equipment to avoid contact with possibly contaminated surfaces.</p>
--	---

3.2.2. Unauthorised persons

“Unauthorised Persons” describes anyone who has not been trained in BSL2+ laboratory practice in the HIV lab, is unaccompanied by Authorised Personnel, or is not scheduled maintenance staff. This includes visitors to the facility. No Unauthorised Persons are permitted in the HIV lab without accompaniment by Authorised Personnel. Visits must be cleared with Authorised Personnel currently conducting experiments in the HIV lab to avoid possible exposure. Prior to entry of Unauthorised Persons, Authorised Personnel should decontaminate the facility, with the exception of the incubator, should experiments be underway. No visits may be scheduled while bench-top experiments are underway.

In the case of Unauthorised Persons gaining entry without authorised supervision, an investigation by the Laboratory Manager will be conducted. The incident must be documented in an Incident Report (**Appendix 1: Incident Report**). Means of entry, Authorised Personnel involved in gaining unauthorised entry, compromise of passcodes, and possible HIV exposure must be included in the report. In the case of passcode compromise, the passcode must be changed immediately. Where Authorised Personnel are implicated, access to the HIV lab will be suspended until the conclusion of the investigation. Further disciplinary action will be undertaken at the discretion of the Responsible Investigator and will be documented in a Disciplinary Report (**Appendix 1: Disciplinary Report**).

3.3. Disciplinary Procedure

Disciplinary action will be taken against any Authorised Personnel who puts themselves or others working in the HIV lab at risk of exposure due to carelessness or negligence in the BSL2+ facility. Due to the nature of experiments conducted in the HIV lab, this includes all conduct between entering and leaving the facility. Appropriate disciplinary procedures are described below.

3.3.1. Failure to comply with SOPs

Failure to comply, after training and verbal correction, with any SOP (**Appendix 2: SOPs**) outlined in this manual may result in a written citation documenting failure to comply delivered by email from Authorised Personnel, with the Health and Safety Officer and Laboratory Manager being copied on the email. This action is to be undertaken only when recipient has successfully completed training as per **3.1 Training and Compliance**, including completion of 30 hours of probation. At this point, recipient is assumed to have read and

understood all SOPs, as well as have practical experience working in the HIV lab under BSL2+ conditions, with all opportunity for potential transgressions to be corrected. Citations serve as a written warning and are issued at the discretion of fellow Authorised Personnel. Following a written citation, it is the responsibility of the recipient to undertake corrective action to ensure that the action is not repeated. Upon receipt of three written warnings, recipient will undergo mandatory Retraining (**3.1.2 Retraining**) without exception. The Laboratory Manager and Health and Safety Officer carry the responsibility of documenting written warnings and serving a final notice for retraining by email which is effective immediately.

3.3.2. Failure to comply with Training Officer requirements

Failure to comply with Training Officer requirements describes the deviation from expectations of Training Officers outlined in **3.1.1 Training**. This includes leaving a Trainee alone in the HIV lab prior to commencement of Probation hours, failure to document training, or putting the Trainee at risk of exposure to HIV while training in the BSL2+ facility. Notice of failure to comply with Training Officer requirements will be served by email from the Health and Safety Officer or Laboratory Manager. Two written warnings are allowed for transgressions while training a Trainee within the BSL2+ facility. Three written warnings are allowed for failure to complete paperwork regarding training, within the bounds of reason. Upon receipt of the allotted number of written warnings, the Training Officer in question will be served with written meeting summons including the Health and Safety Officer and Laboratory Manager to manage the situation appropriately. Appropriate action will be decided on a case-by-case basis, which may result in relief of Training Officer duties for a certain period for failure to keep up with paperwork owing to project-related activities, or final notice for mandatory retraining in the case of poor training. Failure to comply with Training Officer requirements may be reported by Trainees, fellow Authorised Personnel, the Laboratory Manager, or the Health and Safety Officer, and will be moderated prior to written warning being issued by the Laboratory Manager.

3.3.3. Failure to comply with Emergency Protocol initiation

Failure to comply with initiation of emergency protocols will result in a disciplinary hearing involving the Health and Safety Officer and Responsible Investigator. This includes failure to adhere to University of Pretoria Evacuation protocols upon engagement of alarm systems described in **3.4 Emergency Protocols**. Authorised Persons operating within the BSL2+ facility when building alarms are triggered are expected to contain contaminated work and adhere to University of Pretoria evacuation procedures immediately.

3.4. Emergency Protocols

Emergency protocols describe actions to be taken by Authorised Personnel upon incidence. This includes documenting incidents in the Incident Report file (inside the HIV lab) as well as

reporting to relevant authorities as required by the specific protocol. Specific incident protocols are described in this section.

3.4.1. Stick/Prick Injuries

Stick/prick injuries in the HIV lab are considered medical emergencies! Stick/prick injuries describe situations where the outer glove is compromised, and the inner glove is either compromised or suspected to be compromised while operating in the HIV lab at any point in time. Stick/prick injuries where the inner glove is compromised can be divided into two classes: skin uncompromised, and skin compromised.

In stick/prick injuries where ONLY the outer glove is compromised but the inner glove remains intact, all work must cease immediately. Pipette tips are discarded appropriately (see **Appendix 2: SOP – Working in the BSL2+ Biosafety Cabinet** and **Appendix 2: SOP – Working on the BSL2+ Bench**), all tubes are closed, and all culture plates and flasks are closed. Gloves are sprayed with 10% Bleach, followed by 70% Ethanol, and compromised outer gloves are removed and discarded in the biohazard bin. Inner gloves are inspected rigorously for any tears or weak spots. Intact inner gloves may be replaced for good measure by removing PPE (see **Appendix 2: SOP – PPE**) and redressing. If inner gloves are not replaced, they are to be decontaminated thoroughly with 70% Ethanol by spraying on gloved hands and rubbing dry before applying outer gloves.

In stick/prick injuries where the inner glove is compromised, all work must cease immediately. Only tubes, culture plates, and flasks containing HIV are to be closed before initiating emergency procedure for appropriate skin uncompromised/skin compromised procedure. Remove outer glove as carefully as possible and conduct initial inspection of inner glove to assess whether the skin is compromised. DO NOT SQUEEZE OR RUB ANY SITES OF POTENTIALLY COMPROMISED SKIN. Upon assessment of inner glove damage, remove all PPE according to **Appendix 2: SOP – PPE** avoiding contact with damaged region of inner glove. Carefully remove the inner gloves last. Wash hands thoroughly with F10 hand wash situated on the first shelf next to the gloves and masks, making use of elbows to open and close taps. Make sure any areas of skin compromise (scabs, scratches, cuts, holes) are documented. In the case of stick/prick injury resulting in bleeding, phone the emergency number of the nearest emergency room located on the wall next to the telephone in the HIV lab and inform them of HIV exposure in a research setting. The emergency centre will provide you with post-exposure prophylaxis (PEP) which should be taken immediately. The street address of the emergency room is provided under the telephone number. Immediately proceed to the emergency room. Ensure that the door to the HIV lab is locked behind you. If you are incapable of transporting yourself, phone your HIV-buddy (see **3.1.4 HIV-buddy system**) who will drive you, or phone a friend or family member to drive you. Make sure that the bleeding wound is treated at the emergency room. IT IS IMPERATIVE THAT PEP IS OBTAINED AND TAKEN AS SOON AS POSSIBLE AFTER THE INJURY. Once treatment has been obtained and administered, return to the HIV lab and finish work if possible. If wound dressing prevents

proper PPE application, DO NOT ATTEMPT TO RESUME WORK IN THE HIV LAB. Your HIV-buddy will complete the experiment and clean up on your behalf. Complete an incident report as per the template as soon as possible.

3.4.2. Building alarms

When the building alarm is triggered, Authorised Personnel working in the HIV lab are to cease work immediately and contain experiments containing virus.

In the Biosafety cabinet: tubes, bottles, and the Virkon™S bucket are to be closed with lids. Seeded experiments are to be replaced in the incubator before closing and turning off the Biosafety cabinet. The UV cycle of the cabinet should not be turned on.

On the bench: all bottles and tubes are to be closed, and experiments are to be placed in the fridge, incubator, or the BSL2+ transfer box (from BSL2+). Alternatively, contaminated waste containers are to be closed and all experiments are to be placed in the Biosafety cabinet, which is to be closed properly and left off. PPE is to be removed before exiting the lab. Swiftly proceed with University of Pretoria emergency/evacuation protocols.

When relevant authorities have declared the building safe for re-entry, Authorised Personnel are to return to the HIV lab to terminate experiments which cannot be continued, and complete experiments which can be continued. Working surfaces are to be wiped down with 70% ethanol prior to resuming experiments. An incident report is to be filed as soon as possible after the incident detailing reason for evacuation, which experiments were being performed at the time of alarm, actions taken to contain experiments, and action taken upon returning to the HIV lab.

Appendix 1

Authorised Personnel and Officers

Authorised Personnel and Officers last updated on: 09/09/2017

Position	Occupant
Responsible Investigator	Professor M.S. Pepper (Director, Institute for Cellular and Molecular Medicine)
Laboratory Manager	Candice Murdoch
Health and Safety Officer	Candice Murdoch
Authorised Personnel	Juanita Mellet
	Candice Herd
	Catherine Wickham
Banned personnel	

Training Documentation

Training Hours Log Sheet

Trainee Name: _____ **Training** **commenced:**

Course Component	Training Officer	Hours	Trainee Sign

Trainee Agreement

I, _____ Student no. _____, hereby agree to undertake training in the HIV lab, under strict instruction of the most recent ICMM BSL2+ Operations and Safety Manual. This includes ensuring my vaccination is up to date with the international requirements for working in a BSL2+ facility, as outlined in the ICMM BSL2+ Operations and Safety Manual.

I have been informed of the risks, regulations, and procedures pertinent to proceeding with my project in the HIV lab. I have been informed of the nature of work which must be performed in the HIV lab as outlined in the ICMM BSL2+ Operations and Safety Manual.

I understand and accept that I am equally responsible for my safety and the safety of the Training Officer while in the HIV lab, and I will make the Training Officer aware of any instances of uncertainty regarding protocol or procedure. I will make the Training Officer aware of any hesitation to proceed with the next part of the HIV lab training course regardless of the number of hours I have logged for the course component.

I will make the Training Officer aware of any protocols or procedures I will be performing for my work in the HIV lab which do not appear in the SOPs of the ICMM BSL2+ Operations and Safety Manual.

I have read and understood the ICMM BSL2+ Operations and Safety Manual **prior** to the commencement of my HIV lab training.

Trainee: _____ Date: _____

Health and Safety Officer: _____ Date: _____

Responsible Investigator: _____ Date: _____

Certificate of Competence

Awarded to:

On _____

The recipient of this certificate has successfully completed ICMM BSL2+ training according to the ICMM BSL2+ Operations and Safety Manual and has been deemed competent to conduct experiments in the HIV lab without supervision. The recipient of this certificate will comply with all regulations highlighted in the BSL2+ Operations and Safety Manual while in the HIV lab in accordance with their training or face corrective/disciplinary action as per the BSL2+ Operations and Safety Manual.

Training Officer(s)	1.	Signature(s)	1.
	2.		2.
	3.		3.
Hours supervised	1.	2.	3.
Shadowing hours		Probation hours	
Period of training			
Record of Infringements			
Record of Retraining			

Trainee: _____ Date: _____

Health and Safety Officer: _____ Date: _____

Responsible Investigator: _____ Date: _____

Incident Report

Persons involved (indicate HIV-buddy):	
Description of incident (detailed):	
Description of action taken (detailed):	
PEP required and administered?	
Signatures of persons involved:	

Date of Incident: _____ **Date of Report:** _____ **Report#:** _____

Health and Safety Officer: _____ **Date:** _____

Disciplinary Report

Date of disciplinary action: _____ Disciplinary report #: _____

Persons involved (incl. institutions):		
Incident report #:		
Summary of contraventions:		
Description of disciplinary action:		
	Suspended / Banned	Duration if suspended
Date of discipline commencement:		
Disciplinary Committee:		
Signatures of persons involved:		

Health and Safety Officer: _____

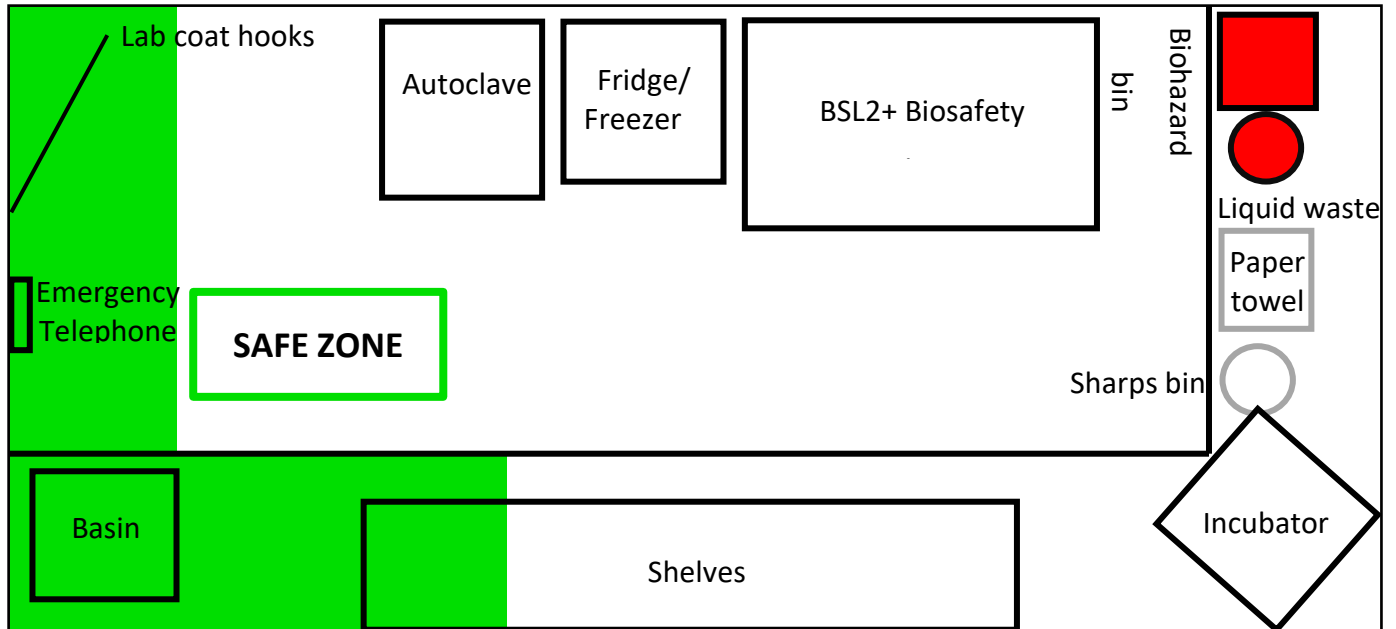
Date: _____

Responsible Investigator: _____

Date: _____

Appendix 2

BSL2+ FACILITY LAYOUT



The purpose of this diagram is to indicate the relative layout of the BSL2+ facility and is therefore not to scale. Important areas to note are the location of the Safe Zone as well as the Biohazard bin. No HIV-contaminated material is permitted in the safe zone unless in the BSL2+ transfer box dedicated for this purpose. The transfer box is safe on the outside and contaminated only on the inside. This means that no outer gloves are ever to be used to touch the transfer box.

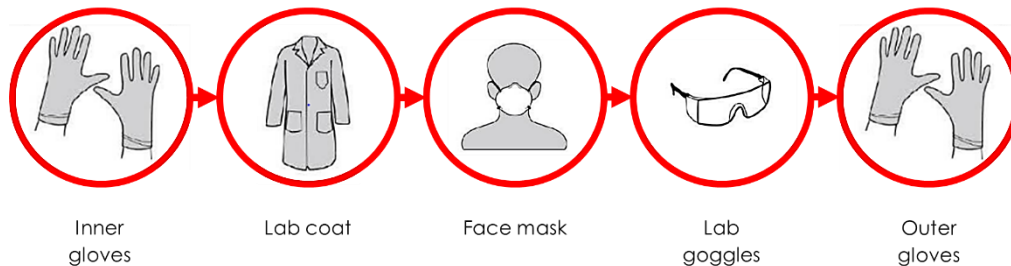
SOP – PPE

SOP NAME	ICMM_VC_SOP001_01_PPE_CLH	VERSION	01
AUTHOR	Candice Herd	LAST UPDATED	08/11/2017
Contributors	Juanita Mellet; Catherine Wickham; Dr Samantha Nicholson		
<p>This SOP describes the correct procedure for donning personal protective equipment (PPE) when entering the ICMM BSL2+ facility. Deviation from this procedure puts the operator at risk of exposure to infectious agents worked with in the BSL2+ facility and may result in disciplinary action. Only Authorised Personnel will be provided with the access code for the door.</p>			
Donning PPE			
1. Prior to entering the BSL2+ facility, operator must be wearing full-length covering on the legs (stockings not acceptable), and fully closed shoes (pumps not acceptable)			
2. All jewellery should be removed prior to entering the BSL2+ facility, and hair should be out of the face as much as possible			
3. Mandatory/Experiment-specific PPE must be donned upon entry to the BSL2+ facility:			
Mandatory PPE	<ul style="list-style-type: none"> • Inner gloves • Disposable lab coat • Outer gloves 		
Experiment-specific PPE	<ul style="list-style-type: none"> • Surgical face mask • Safety glasses • Hair net • Plastic pull-over booties 		
4. Experiment-specific PPE applications:			
Experiments working with HIV	<ul style="list-style-type: none"> • Mandatory PPE • Surgical face mask 		

	<ul style="list-style-type: none"> • Safety glasses (unless wearing prescription glasses)
Preparation for experiments (warming reagents/preparing solutions)	<ul style="list-style-type: none"> • Mandatory PPE
Restocking/packing tips and jars/autoclaving	<ul style="list-style-type: none"> • Mandatory PPE
Decontamination of HIV waste	<ul style="list-style-type: none"> • Mandatory PPE • Surgical face mask • Safety glasses
Decontamination of laboratory/equipment	<ul style="list-style-type: none"> • Mandatory PPE • Surgical face mask

5. PPE appropriate to purpose as outlined in (4.) should be donned upon entry into the BSL2+ facility in the order shown on the following infographic (mounted above the basin)

Order of PPE: BSL2+ Lab



6. Put on inner gloves, located on the first shelf closest to the basin

7. Put on a disposable blue lab coat which can be found on the hooks by the door

- a. Make sure inner glove wrists are under the white sleeves of the lab coat

<ul style="list-style-type: none"> b. If there are not sufficient disposable blue lab coats, retrieve one from the right-most cupboard under the bench labelled “PPE” 	
<ul style="list-style-type: none"> 8. Open the BSL2+ transfer box if work requires HIV-exposed samples or tube racks to be transported between facilities 	
<ul style="list-style-type: none"> 9. Put on a disposable surgical mask and safety glasses, both located on the first shelf closest to the basin <ul style="list-style-type: none"> a. Contour the wire of the surgical mask around your nose to keep it in place b. Position the goggles over the wire contour 	
<ul style="list-style-type: none"> 10. Put on outer gloves, located on the first shelf closest to the basin 	
<ul style="list-style-type: none"> 11. Proceed with decontamination procedure or laboratory work 	
Doffing PPE	
<ul style="list-style-type: none"> 1. PPE is to be doffed in the reverse order to the infographic on the wall above the basin: <ul style="list-style-type: none"> a. outer gloves b. safety glasses c. surgical face mask d. lab coat e. inner gloves 	
<ul style="list-style-type: none"> 2. If leaving the BSL2+ facility temporarily (work not completed), gloves and face mask may be reused: <ul style="list-style-type: none"> a. outer gloves placed to the left of the microscope b. inner gloves, surgical face mask, and safety glasses placed in the safe zone nearest the basin/transfer boxes 	
<ul style="list-style-type: none"> 3. Safety glasses are to be replaced on the shelf in the safe zone, to the left of the gloves upon doffing for the final exit 	
<ul style="list-style-type: none"> 4. Both sets of gloves as well as surgical face mask are to be discarded in the biohazardous waste bin upon doffing for the final exit 	

5. Lab coat and safety glasses are only discarded when damaged or exposed to contaminated material, and are discarded in the biohazardous waste bin	
---	--

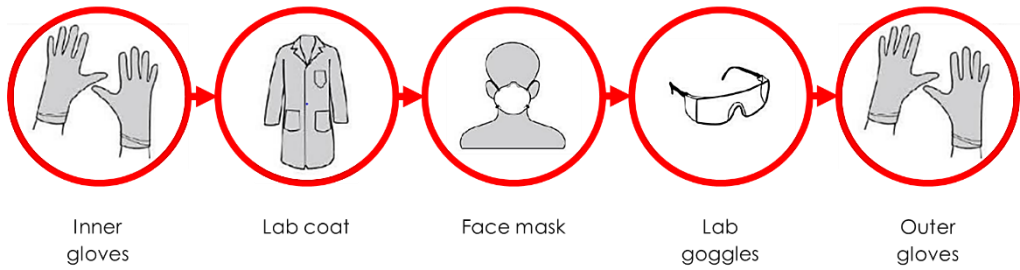
SOP – Entering the BSL2+ Facility

SOP NAME	ICMM_VC_SOP002_01_Enter HIV lab_CLH	VERSION	01
AUTHOR	Candice Herd	LAST UPDATED	08/11/2017
Contributors	Juanita Mellet; Catherine Wickham; Dr Samantha Nicholson		

This SOP describes the correct procedure for entering the ICMM BSL2+ facility. Deviation from this procedure puts the operator at risk of exposure to infectious agents worked with in the BSL2+ facility and may result in disciplinary action. Only Authorised Personnel will be provided with the access code for the door.

1. Enter the access code for the door lock, starting the code with C_ and open the door
2. Step inside the lab and ensure the door closes properly behind you and turn on the light switch next to the door
3. Doff PPE in the order of the infographic on the wall above the basin:
 - a. inner gloves
 - b. lab coat
 - c. surgical face mask
 - d. safety glasses
 - e. outer gloves

Order of PPE: BSL2+ Lab



4. Ensure that the air-conditioning unit is switched on and at a temperature between 18-21°C	
5. Turn the differential pressure unit on by turning the dial by the window to 7	
6. Proceed with decontamination procedure or laboratory work	

SOP – Decontamination and waste disposal

SOP NAME	ICMM_VC_SOP003_01_Decontamination and waste disposal_CLH	VERSION	01
AUTHOR	Candice Herd	LAST UPDATED	08/11/2017
Contributors	Juanita Mellet; Catherine Wickham; Dr Samantha Nicholson		
<p>This SOP describes the correct procedure for decontamination of HIV-exposed waste (Virkon™S-treated waste, and biohazardous and sharps bins) within the BSL2+ facility. Deviation from this procedure puts the operator at risk of exposure to infectious agents worked with in the BSL2+ facility and may result in disciplinary action. Only Authorised Personnel will be provided with the access code for the door.</p>			
Virkon™S-treated waste			
<p>The basin is a dedicated HIV-free zone. When both Virkon™S-treatment and UV-treatment are used to decontaminate waste, cleaning implements are rinsed in the basin after being soaked in diluted bleach. ONLY the colander, funnels, and Virkon buckets are to be treated in this way.</p>			
1. Virkon™S-treated waste in the Biosafety cabinet should have been UV-treated by turning the UV lamp of the Biosafety cabinet on (15 min cycle) prior to commencement of decontamination procedure			
2. Fill the Decontamination Sink located under the bench next to the basin a third full of water – use elbows to open taps			
3. Add approximately 50mL of 3.5% bleach located in the cupboard under the basin			
4. Transfer the Decontamination Sink to the bench left of the incubator (facing the window)			
5. Open the sharps bucket (under the bench) and pull out from under the bench			

6. Remove the Virkon™S bucket from the Biosafety cabinet	
7. Tip the waste in the Virkon™S bucket into the assembled colander so that the liquid waste is caught in the solid plastic container at the bottom and the plastic waste (tips, tubes) remain in the sieve portion at the top.	
8. Transfer the bucket to the Decontamination Sink and ensure bleach-solution makes contact with all sides	
9. Detach the sieve portion carefully from the solid portion and shake gently to avoid liquid spillage	
10. Tip sieve contents (tips, tubes) into the sharps bin	
11. Transfer sieve portion to the Decontamination Sink and ensure bleach-solution makes contact with all sides	
12. Pour contaminated Virkon™S into the red biohazardous liquid waste bucket located next to the biohazard bin	
13. Transfer the solid portion of the colander to the Decontamination Sink and ensure bleach-solution makes contact with all sides	
14. Any spillage should be cleaned immediately with 1% Virkon™S	
15. Transfer the Decontamination Sink carefully to the basin	
16. Remove items one at a time and rinse with water a. use elbows to open taps	
17. Place on the linen saver to the left of the basin to dry	
18. Slowly and carefully discard contents of the Decontamination Sink in the basin – do not let contents splash out of the basin	
19. Rinse the Decontamination Sink, dry with paper towel (discard in biohazard bin), and replace under the bench next to the basin	
20. Rinse the basin with tap water (use elbows to open taps), spray the inside of the basin with bleach and rinse with tap water (use elbows to open taps), and finally spray the inside of the basin with 70% Ethanol and allow to evaporate	
21. When the liquid waste bucket is 3/4 full, the lid is to be sealed properly and the bucket sprayed with 70% ethanol and allowed to air-dry	

22. When dry, the liquid waste bucket should be taped closed with a cross sealing the lid to the bucket	
23. The liquid waste bucket is discarded with the biohazardous waste of the ICMM main lab and should be transferred to the main lab the day before scheduled collection of waste	
Biohazardous waste bin decontamination and discard	
1. The biohazardous waste bin should be full, but not overflowing, prior to commencement of decontamination and discard procedure, OR: <ul style="list-style-type: none"> a. if the lab will not be used for more than 2 weeks b. if Unauthorised Personnel are expected to enter the BSL2+ facility 	
2. If the biohazard bin is replaced following work in the lab, discard outer gloves and face mask and put on a new pair of outer gloves prior to commencement of decontamination and discard procedure	
3. Fold a new biohazardous bin box and lid – located behind the Decontamination Sink – near the basin to limit contamination of new box <ul style="list-style-type: none"> a. use biohazard tape to secure the bottom flaps in a cross-shape 	
4. Remove the lid of the contaminated biohazard bin	
5. Gather and secure the top of the bin bag with biohazard tape	
6. Transfer the contaminated bag into the newly-folded uncontaminated box	
7. Using blunt-end scissors, cut biohazard tape to seal the bag over the rubber band with a cross of tape	
8. Close the biohazard box with the newly-folded uncontaminated lid	
9. Use biohazard tape to secure the lid to the box using a cross of tape	
10. Seal the lid to the box by taping horizontally on the join between lid and box, over the cross of tape securing the lid to the box	
11. Replace a biohazard bin bag in the contaminated box, close the contaminated box lid	
12. Filled, sealed boxes are stored in the BSL2+ facility until collection	

13. The filled, sealed boxes are discarded with the biohazardous waste of the ICMM main lab and should be transferred to the main lab the day before scheduled collection of waste	
--	--

SOP – Equipment decontamination

SOP NAME	ICMM_VC_SOP004_01_Equipment decontamination_CLH	VERSION	01
AUTHOR	Candice Herd	LAST UPDATED	20/04/2018
Contributors	Juanita Mellet; Catherine Wickham; Dr Samantha Nicholson		
<p>This SOP describes the correct procedure for decontaminating equipment in the BSL2+ facility. Deviation from this procedure puts the operator at risk of exposure to infectious agents worked with in the BSL2+ facility and may result in disciplinary action. Only Authorised Personnel will be provided with the access code for the door.</p> <p>IF MAINTENANCE REQUIRES REMOVAL OF EQUIPMENT FROM BSL2+ FACILITY, THE LAB IS TO BE QUARANTINED FOR 7 DAYS PRIOR TO DECONTAMINATION AND REMOVAL OF EQUIPMENT</p>			
Prior to commencement of equipment decontamination			
1. Equipment is to be decontaminated a minimum of 24hrs prior to scheduled maintenance			
2. Ensure that no work in the BSL2+ facility is planned for the duration of the maintenance task			
3. Ensure that equipment is not in use at the time of planned maintenance and decontamination procedure			
4. Clear the area around equipment to be decontaminated			
Decontaminating equipment			
1. Prepare an appropriate volume of 1% Virkon™S in a plastic tub or the plastic bin using Virkon™S powder under the sink, and hot water			
2. Decontaminate outside of equipment with 1% Virkon™S and a sponge where possible			

<ul style="list-style-type: none"> a. Virkon™S should only be used to clean where it can be easily and thoroughly removed as it causes damage to equipment b. Virkon™S should not be used to clean the microscope 	
3. Allow up to 3 mins contact time with non-metal surfaces, and 1 min with metal surfaces	
4. Mop up Virkon™S with paper towel	
5. Decontaminate inside surfaces where possible with 1% Virkon™S, allowing 1 min contact time	
6. Mop up Virkon™S with paper towel	
7. Thoroughly spray both inside and outside surfaces with 70% Ethanol and mop up with paper towel; this should be repeated until there is no pink remaining on the paper towel from the Virkon™S	
8. Mist outside surface with 70% Ethanol and allow to air dry	
9. Clear a suitably sized working area around the equipment	
10. Decontaminate all surfaces in the working area with 1% Virkon™S as in steps 2-4, allowing up to 5 min contact time with non-steel surfaces	
11. Clear up Virkon™S residue as in steps 5-7	
12. Mist area with 70% Ethanol and allow to air dry	
13. If equipment requires moving equipment out of the BSL2+ facility: <ul style="list-style-type: none"> a. ensure that the path from the door is free of obstructions b. sweep and mop the floor with F10® in hot water as described in ICMM_VC_SOP008_01_HIV lab clean_CLH c. ensure that all bench-top items are stowed in cupboards and shelves, or on the back bench furthest from the door d. ensure that the biohazard bin is closed or has been emptied e. ensure that power cords of equipment to be moved has been wiped down with 1% Virkon™S and 70% Ethanol, and that they are suitably packaged to not be damaged in transit 	

<p>14. Equipment is to be decontaminated with F10® and 70% Ethanol after maintenance, prior to use</p> <p>a. if equipment was removed from the BSL2+ facility, decontaminate with 1% Virkon™S, followed by F10®, followed by 70% Ethanol upon return of equipment</p>	
---	--

SOP – Working in the BSL2+ Biosafety cabinet

SOP NAME	ICMM_VC_SOP005_01_Working in the BSL2+ Biosafety Cabinet_CLH	VERSION	01
AUTHOR	Candice Herd	LAST UPDATED	22/01/2018
Contributors	Juanita Mellet; Catherine Wickham; Dr Samantha Nicholson		
<p>This SOP describes the correct procedure for working in the BSL2+ Biosafety cabinet within the BSL2+ facility. Deviation from this procedure puts the operator at risk of exposure to infectious agents worked with in the BSL2+ facility and may result in disciplinary action. Only Authorised Personnel will be provided with the access code for the door.</p>			
Prior to commencement of work in the Biosafety cabinet			
15. Open the Biosafety cabinet glass sash until it is level with the mark on the right-hand side panel			
16. Press the button depicting a fan on the control panel of the Biosafety cabinet			
17. Remove any items in the biosafety cabinet and spray with 10% Bleach; pat dry			
18. Spray items with 70% Ethanol; pat dry and put in their places			
19. Proceed with decontamination of waste procedure if applicable			
20. When the air has been purged and the Biosafety cabinet is ready to be used, the sash alarm will sound, or the light will go on			
21. Adjust the glass sash up or down slightly so that the sash alarm is off			
22. Spray the working surface and walls of the Biosafety cabinet with 70% Ethanol, leave for a minute, and dry with paper towel			

<p>23. When working with multiple viral isolates between cabinet uses, decontaminate the working surface with 1% Virkon™S by:</p> <ul style="list-style-type: none"> a. pouring small amount of Virkon™S onto the working surface b. spread gently with paper towel, avoiding the grates c. mop up with paper towel d. rinse by spraying with distilled water and mopping up with paper towel e. spray working surface with 70% Ethanol, leave for a minute, and dry with paper towel 	
<p>24. Prepare ~200mL 1% Virkon™S in the plastic waste tub for waste disposal in the biosafety cabinet using Virkon™S powder under the sink, and tap water</p> <ul style="list-style-type: none"> a. use elbows to open taps 	
<p>25. Spray the outside of the tub with 70% Ethanol and place in the Biosafety cabinet</p>	
<p>26. Fold a length of paper towel to dry implements on and place in the Biosafety cabinet</p>	
<p>27. Spray down implements to be used in the Biosafety cabinet (pipettes, tip boxes, serological pipettes, tube racks, tubes, lab markers, etc) and place on the paper towel</p> <ul style="list-style-type: none"> a. DO NOT HAVE ANY UNNECESSARY IMPLEMENTS IN THE CABINET! 	
<p>28. Pat implements dry</p> <ul style="list-style-type: none"> a. paper towel can be kept in the Biosafety cabinet to mop up ethanol spots or in the case of spillage, to contain as quickly as possible 	
<p>29. Proceed with work in Biosafety cabinet</p> <ul style="list-style-type: none"> a. Maintain air curtain by limiting side-to-side movement of arms b. Do not remove arms from cabinet unless absolutely necessary c. Keep “clean” and “dirty” workspaces separate 	
<p>Working in the Biosafety cabinet</p>	
<p>1. All tubes, pipette tips, and filters are to be discarded in the Virkon™S tub</p>	

2. Serological pipettes are to be replaced in their packets after being decontaminated by sucking up Virkon™S and aspirating into the waste tub	
3. All liquid waste is to be discarded in the Virkon™S tub a. If the volume of aspirate exceeds 200mL Virkon™S, make a second tub of 1% Virkon™S for discarding waste	
4. Upon termination of experiments, cells are to be bleached (10%), soaked up into paper towel, and discarded in the Biohazardous waste bin a. DO NOT MIX BLEACH WITH Virkon™S UNDER ANY CIRCUMSTANCES	
5. Ensure that all spills are cleaned up immediately a. In the case of virus-contaminated spills, IMMEDIATELY treat the spill with a small volume of 1% Virkon™S (uncontaminated) and then mop up b. Spray area with 70% Ethanol and dry with paper towel	
6. When work has been completed, ensure that the Virkon™S waste solution is still pink a. If not, add more 1% Virkon™S to the waste tub	
After completion of work in the Biosafety cabinet	
1. Ensure that all spills (even droplets) of Virkon™S have been mopped up inside the cabinet a. Virkon™S exposure results in pitting of the cabinet surfaces	
2. Remove all implements from the cabinet except the Pipetboy and contaminated waste tub	
3. Decontaminate all implements removed from the Biosafety cabinet a. Spray with 10% Bleach b. Pat dry with paper towel c. Spray with 70% Ethanol d. Pat dry with paper towel e. Put away f. Discard paper towel in Biohazardous waste bin	

4. Spray the work surface and sides of the cabinet with 70% Ethanol and wipe dry with paper towel a. Repeat if spillage occurred to ensure that no Virkon™S residue remains in the cabinet	
5. Spray down (70% Ethanol) and place any empty tip boxes requiring UV treatment prior to packing in the Biosafety cabinet and open their lids a. Place the tip boxes on one side of the cabinet and the contaminated waste on the other side	
6. Ensure that the surfaces of the cabinet are completely dry before closing the Biosafety cabinet sash and turning off the fan if necessary	
7. Press the UV lamp button on the control panel of the Biosafety cabinet to activate a 15 min UV cycle	

SOP – Working on the BSL2+ Bench

SOP NAME	ICMM_VC_SOP006_01_Working on the BSL2+ bench_CLH	VERSION	01
AUTHOR	Candice Herd	LAST UPDATED	22/01/2018
Contributors	Juanita Mellet; Catherine Wickham		
This SOP describes the correct procedure for working on the BLS2+ bench within the BSL2+ facility. Deviation from this procedure puts the operator at risk of exposure to infectious agents worked with in the BSL2+ facility and may result in disciplinary action. Only Authorised Personnel will be provided with the access code for the door.			
Prior to commencement of work on the bench			
1. Thoroughly spray down the working area with 70% Ethanol and wipe dry with paper towel			
2. Collect all reagents and implements required (pipettes, serological pipettes, Pipetboy, kit components, pipette tips, tubes, tube racks, etc.)			
3. Prepare ~100mL 1% Virkon™S in the plastic waste tub for waste disposal using Virkon™S powder under the sink, and tap water a. use elbows to open taps			

4. Continue with work on the bench	
While working on the bench	
1. Maintain a clean, clutter-free workspace	
2. Put reagents away as soon as possible	
3. Ensure that all spills are cleaned up immediately <ul style="list-style-type: none"> a. In the case of virus-contaminated spills, IMMEDIATELY treat the spill with a small volume of 1% Virkon™S (uncontaminated) and then mop up b. Spray area with 70% Ethanol and dry with paper towel 	
4. Ensure that all contaminated elements are disposed of in 1% Virkon™S while working on the bench	
After completion of work on the bench	
1. Place the Virkon™S bucket in the BSL2+ Biosafety cabinet, close the cabinet, and press the UV lamp button on the control panel of the Biosafety cabinet to activate a 15 min UV cycle	
2. Clear the workspace and ensure all reagents and equipment are appropriately packed away	
3. Wipe the workspace with a small volume of 1% Virkon™S (uncontaminated) and mop up	
4. Spray the bench with 70% Ethanol and dry with paper towel	


SOP – Leaving the BSL2+ Facility

SOP NAME	ICMM_VC_SOP007_01_Leave HIV lab_CLH	VERSION	01
AUTHOR	Candice Herd	LAST UPDATED	16/02/2018
Contributors	Juanita Mellet; Catherine Wickham		

This SOP describes the correct procedure for leaving the BLS2+ facility. Deviation from this procedure puts the operator at risk of exposure to infectious agents worked with in the BSL2+ facility and may result in disciplinary action. Only Authorised Personnel will be provided with the access code for the door.

1. Ensure that equipment and work areas used have been cleaned and closed as appropriate:

Equipment/Work area	Action
Work bench	Cleaned and all items packed away
Biosafety cabinet	Cleaned, with contaminated waste tub exposed to UV lamp Pipette tip boxes for decontamination open and to the side for exposure to UV lamp
Microscope	Off, and covered with dust cover
Incubator	All cell culture experiments replaced in the incubator (uninfected on the top shelf; infected on the bottom shelf) Water bath filled with autoclaved distilled water Inner door and outer door closed properly CO ₂ levels and temperature at 5% and 37°C respectively (unless otherwise noted)
Biohazard and sharps bins	Lid closed
Autoclave	Unless running, the lid is to be slightly opened, and the machine is to be switched off
Basin/basin area	Taps should be in the closed position with no dripping The basin should be clean and dry Decontamination sink should be stowed under the bench to the left of the sink Decontamination plasticware (colanders/funnels/plastic buckets) should be left to dry on a linen saver on the bench to the left of the basin

Transfer boxes	Clean and stored in the Safe Zone to the left of drying plasticware, with lids slightly open ICMM→BSL2+ (HIV-free; green) transfer box should be returned to the ICMM main laboratory	
2. Turn the positive pressure unit off by turning the dial to 0		
<p>3. Doff PPE in the reverse order to the infographic on the wall above the basin:</p> <ol style="list-style-type: none"> outer gloves safety glasses surgical face mask lab coat (to be replaced on the wall hooks) inner gloves <p style="text-align: center;">Order of PPE: BSL2+ Lab</p> <div style="text-align: center;">  </div> <div style="display: flex; justify-content: space-around; text-align: center;"> <div data-bbox="225 1234 411 1290">Inner gloves</div> <div data-bbox="432 1234 619 1261">Lab coat</div> <div data-bbox="639 1234 826 1261">Face mask</div> <div data-bbox="847 1234 1034 1290">Lab goggles</div> <div data-bbox="1054 1234 1241 1290">Outer gloves</div> </div>		
4. Both sets of gloves as well as surgical face mask are to be discarded in the biohazardous waste bin upon doffing for the final exit		
5. Lab coat and safety glasses are only discarded when damaged or exposed to contaminated material, and are discarded in the biohazardous waste bin		

SOP – Laboratory cleaning

SOP NAME	ICMM_VC_SOP008_01_HIV lab clean_CLH	VERSION	01
AUTHOR	Candice Herd	LAST UPDATED	26/02/2018
Contributors	Juanita Mellet; Catherine Wickham		

This SOP describes the correct procedure for cleaning the ICMM BSL2+ facility. Deviation from this procedure puts the operator at risk of exposure to infectious agents worked with in the BSL2+ facility and may result in disciplinary action. Only Authorised Personnel will be provided with the access code for the door.

1. Ensure that the incubator is free of cell cultures and that no experiments are planned during the laboratory clean	
2. Turn the air-conditioning unit and differential pressure unit off (by turning the dial to 0)	
3. All participants are to don PPE as would be appropriate for conducting experiments a. unless there is contaminated waste to be discarded , safety glasses are not required	
4. Surface cleaning is to be performed from high to low surfaces, and from the safe zone to the back bench	
5. Basin linen saver and dry/drying plasticware is to be moved to the back bench for the duration of the laboratory clean	
6. Prepare cleaning equipment: a. 500mL 1% Virkon™S b. 10-15 mL F10® SCXD disinfectant soap per litre warm water (50-60°C) c. pre-soak HIV lab mop in warm water to soften the sponge d. ensure that there are enough cloths and sponges for participants e. 70% Ethanol (everything must be sprayed – ensure there is enough)	
7. Begin at the basin: a. sink is to be cleaned first with 1% Virkon™S, followed by F10® b. counters around basin are to be gently scrubbed with F10® c. cupboard under the basin is to be emptied onto the floor in the safe zone and cleaned with F10® d. basin, cupboards, and counters are to be dried with paper towel prior to ethanol treatment	

<ul style="list-style-type: none"> e. surfaces are to be treated with 70% Ethanol by spraying down, allowing approximately 1 min contact time, drying with paper towel, and lightly sprayed again for the ethanol to evaporate f. before replacing cupboard contents, wipe with lightly damp F10® cloth and drying with paper towel 	
<p>8. Safe zone and safe zone shelves:</p> <ul style="list-style-type: none"> a. decontaminate the safe zone bench before packing the safe zone shelf items onto the bench and cleaning the portion of shelving that is mounted above the safe zone b. ONLY the safe zone shelf items are packed down into the safe zone for cleaning c. all other shelf items are packed onto the back bench to clean the shelves d. safe zone bench is decontaminated before packing shelf items down to remove risk of contamination <ul style="list-style-type: none"> i. wipe bench surface down with 1% Virkon™S ii. mop up with paper towel iii. spray with 70% Ethanol and wipe dry with paper towel e. safe zone shelving is gently scrubbed with 1% Virkon™S, followed by F10®, prior to ethanol treatment from the top of the shelves downwards f. 70% Ethanol is applied to paper towel-dried surfaces, and allowed 1 min contact time before wiping dry with paper towel g. before replacing shelf items, wipe with paper towel lightly soaked with 70% Ethanol and drying with paper towel h. safe zone bench is then cleaned properly by gently scrubbing surface with 1% Virkon™S, followed by F10®, prior to 70% Ethanol treatment i. BSL2+ transfer box is to be wiped with 1% Virkon™S on the inside and the outside (take care not to soak the labels), dried, and sprayed with 70% Ethanol and allowed to air-dry 	
<p>9. The biosafety cabinet and incubator are cleaned next:</p> <ul style="list-style-type: none"> a. turn off alarms if possible b. remove removable parts (to back bench) 	

<ul style="list-style-type: none"> c. non-removable parts are to be gently scrubbed with F10[®], followed by 70% Ethanol which is to be dried with paper towel <ul style="list-style-type: none"> i. work from top to bottom on the inside of the units ii. lightly spray the inside with 70% Ethanol and allow to air-dry prior to replacement of removable parts d. removable parts are to be gently scrubbed on all sides with F10[®], followed by 70% Ethanol which is to be dried with paper towel <ul style="list-style-type: none"> i. lightly spray parts with 70% Ethanol prior to replacement and allow to air-dry in the unit e. turn all alarms back on and close the units properly 	
<p>10. Move all shelf and bench items (not equipment) not in the already-clean safe zone on to the back bench</p> <ul style="list-style-type: none"> a. clean shelves from top to bottom with 1% Virkon[™]S, followed by F10[®], followed by 70% Ethanol (1 min contact time) and then dry with paper towel b. clean bench from the safe zone side towards the back bench with 1% Virkon[™]S, followed by F10[®], followed by 70% Ethanol (1 min contact time) and then dry with paper towel c. wipe all equipment down with paper towel soaked in 70% Ethanol <ul style="list-style-type: none"> i. microscope and dust cover ii. incubator exterior (may need to be cleaned with F10[®] first) iii. vortex and microcentrifuge d. remove all containers/chemicals from cupboards and wipe the insides of the cupboards with F10[®], before drying and spraying with 70% Ethanol and drying with paper towel <ul style="list-style-type: none"> i. wipe all containers with paper towel soaked in 70% Ethanol before replacing in the cupboards ii. leave cupboards open for a short while to allow ethanol to evaporate e. tube racks and plasticware are to be wiped with 1% Virkon[™]S, and then washed in F10[®] with a sponge before being rinsed in clean water <ul style="list-style-type: none"> i. tube racks and plasticware are left to dry on a new linen saver to the left of the basin 	

<p>f. all other items to be replaced on the bench or shelf are to be wiped with a lightly F10[®]-dampened cloth, sprayed lightly with ethanol, and dried with paper towel prior to replacement</p> <ul style="list-style-type: none"> i. any opened pipette tip boxes are to be UV-treated after wiping and placed on the “UV-lamped for packing” shelf for repacking ii. fill microcentrifuge tube jars and pack UV-treated tip boxes for autoclaving 	
<p>11. Place all previously opened pipette tip boxes inside the biosafety cabinet with the lids open for UV-treatment, close the sash, and start the UV-cycle</p>	
<p>12. Gently scrub the back bench with 1% Virkon[™]S, followed by F10[®], followed by 70% Ethanol (1 min contact time) and then dry with paper towel</p>	
<p>13. Sweep the floor with long, gentle motions from the front of the room to the back bench and under all possible fixtures to collect dust and paper towel remnants</p>	
<p>14. Collect sweepings in the dustpan and carefully discard in the biohazardous waste bin</p>	
<p>15. Doff all PPE except inner gloves, and put on plastic surgical booties over shoes</p>	
<p>16. Prepare the mop and bucket:</p> <ul style="list-style-type: none"> a. 10mL F10[®] SCXD disinfectant soap per litre warm water (approximately 3L should be enough) b. squeeze excess water from the mop by pulling the handle towards you and allow to soak in the F10[®] bucket for 30s c. mop the entire floorspace thoroughly <ul style="list-style-type: none"> i. start in the back-left corner where the biohazard bin is, being careful to not soak the cardboard ii. move towards the door, cleaning the safe zone/dressing area last 	
<p>17. Carefully discard the remaining soapy liquid in the basin and rinse both the bucket and the basin clean – use elbows on taps</p>	
<p>18. Fill the bucket half-way with water and stand the mop in the bucket against the wall in front of the autoclave until the floor is dry</p>	

<ul style="list-style-type: none">a. mop is to be rinsed thoroughly in clean water, and bucket is to be rinsed, wiped clean, and dried when the floor is cleanb. mop is to stand in the bucket, behind the door next to the broom until next use	
19. Remove gloves and booties, and discard in the biohazardous waste bin in the ICMM main laboratory	

Appendix 3

PBMC Activation for HIV Propagation

Name: _____ Date: _____

HIV isolate: _____ PBMC stock (s): _____

1. Prepare IL-2GM:
 - a. 500mL RPMI
 - b. Remove 110mL RPMI and store in falcon tubes
 - c. Add 100mL FBS to 400mL RPMI (final - 20% FBS)
 - d. Add 10mL penstrep (final – 2% penstrep)
 - e. Add 25µL IL-2 stock solution to 25mL RPMI+FBS+penstrep (final – 5% IL-2) and replace in 500mL

2. Thaw PBMC stocks (pool) and add cells to 30mL prewarmed IL-2GM – do NOT wait for cells to be completely thawed – dilute DMSO with media ASAP

3. Centrifuge at 300g for 10 mins and aspirate the media

4. Resuspend and plate cells as follows, depending on the purpose:

Procedure	Number of cells required	Volume of IL-2GM	Volume of PHA-P	Flask size	# flasks
Initial HIV infection	30 x 10 ⁶ cells (3 donors)	30mL	150µL (1mg/mL stock; 5µg/mL final concentration)	T75/T80	
HIV feeding	10 x 10 ⁶	15mL	75µL (1mg/mL stock)	T25	
PURPOSE:					

5. Incubate upright at 37°C, 5% CO₂ for 24hrs

6. Change media to IL-2GM (no PHA-P) after 24hrs

- a. Transfer to falcon tube
- b. Spin down at 300g for 10 mins
- c. Aspirate media
- d. Resuspend cells in the correct volume of prewarmed IL-2GM
- e. Replate and incubate at 37°C, 5% CO₂ for 48 hrs prior to HIV exposure

DATE: _____

HIV Propagation in PBMCs

Name: _____ **Date:** _____

HIV isolate: _____ **Harvest date + storage box:** _____

1. Centrifuge activated PBMCs at 300g for 10 mins
2. Resuspend in 2mL prewarmed RPMI
3. Add 1mL coculture stock of HIV-infected PBMCs from a previous production to the cells
4. Infection details:

Co-culture label	# co-cultures used	Supernatant label	# supernatants used
5. Incubate at 37°C for 2 hrs – small volume to maximise cell contact with HIV
6. Add _____mL RPMI and plate in a T80 flask – 30mL per 30×10^6 cells
7. Incubate upright at 37°C, 5% CO₂ until next feed (every 3 days) – infection day is DAY 1
8. DAY ___ FEED + SPLIT: split HIV-infected PBMC co-culture between two T80 flasks per 30×10^6 initial PBMC propagation stock and feed each with 10×10^6 activated PBMCs in 15mL pre-warmed RPMI as described in 8

Initial activation date	# Day ___ split flasks
-------------------------	------------------------

--	--

9. Feeding (day ___ + day ___):
- a. Transfer PBMCs activated for feeding, and HIV-infected co-culture (pooled), into separate, labelled 50mL centrifuge tubes
 - b. Centrifuge at 300g for 10 min – use safety caps on rotor buckets
 - c. Aspirate supernatants and resuspend pellets in 1mL RPMI each
 - d. Pool resuspended pellets (feed step)
 - e. Divide fed cell/HIV suspension equally between flasks generated from day 4 feed + split

10. DAY ___: harvest HIV supernatant
- a. Pool and transfer propagation stocks to 50mL centrifuge tubes
 - b. Centrifuge at 300g for 10 min – use safety caps on rotor buckets
 - c. Harvest supernatant, pool, and filter (0.22µM) to remove cells
 - d. Aliquot into microcentrifuge tubes (1ml and 500µL aliquots)
 - e. Store cell-free supernatants at -80°C
 - f. Pool and resuspend HIV-infected PBMC pellets in 1mL FBS (10% DMSO) per split-day flask
 - g. Store PBMC co-cultures in cryovials at -80°C

STORAGE DATE (day 10): _____

Description + Storage box	# vials/tubes	Description + Storage box	# vials/tubes

PBMC ACTIVATION DETAILS

Feed day	Date	PBMC activation date + # activated
4		
7		

Lentivirus Production (Transfection)

Name: _____ Date: _____

Plasmid IDs: _____

Purpose: _____ Cell line (ID; P): _____

1. Prepare PEI solution (1mg/mL):
 - a. 100mg polyethyleneimine
 - b. Dissolve in 100mL hot dH₂O
 - c. Filter-sterilise (0.22µM); store at 4°C – if solution is cloudy, briefly heat and mix until clear

2. Prepare complete growth medium (293-CGM): for HEK293 T-cells
 - a. DMEM [+] pyruvate [+] glucose [+] glutamine
 - b. 10% FBS
 - c. 2% Pen/Strep
 - d. **5mL 200mM L-Glutamine in 500mL** – optional

3. Seeding density:

Plate/Flask	Seeding density	Volume medium	No. seeded
24-well plate	5×10^4 cells/well	500µL/well	
6-well plate	2×10^5 cells/well	2mL/well	
T _{75/80}	2.5×10^6 cells/flask	15mL 8mL	
T ₁₅₀	5×10^6 cells/flask	30mL 20mL	

4. Allow to attach overnight and grow 50-60% confluent

5. Replace the medium 2-4hrs prior to transfection – just enough medium to cover the surface

6. Prepare transfection reactions as follows: add in order from left to right

Flask size	Transfection type	DMEM (serum-free; µL)	Plasmid type + amount (µg)	PEI (µL)

T ₁₅₀	Lentiviral vector production	3125	Plasmid of interest: 16µg Packaging plasmid: 16µg Envelope plasmid: 8.8µg	250
T ₁₅₀	Molecular clone production	3200	Molecular clone plasmid: 64 µg	128

For smaller flasks, use proportional volumes (T_{75/80} - use half per flask); **add PEI last**

Flask size	No. flasks	DMEM (serum free; µL)	PEI (µL)	Plasmid	Plasmid	Plasmid
T _{75/80}						
T _{75/80}						

7. Vortex the mixture, incubate at room temperature for 10 min, and vortex again
8. Gently add the PEI/plasmid solutions to the relevant flasks by tipping the flask upwards and pipetting the reaction mixtures into the media collected at the bottom of the flask – do not scrape bottom of flask!
9. Swirl gently to expose cells to transfection reagents and incubate at 37°C, 5% CO₂
10. Carefully change medium 3-18hr (_____ hr) after transfection (293-CGM) and incubate at 37°C, 5% CO₂
11. Harvest virus-containing supernatant 72hr after transfection and filter-sterilise (0.22µM) to remove any cells/cell debris
12. Prepare 1mL and 500µL aliquots in screw-cap tubes for freezing at -80°C

HIV ELISA – CloneTech LentiX Rapid Titre p24 ELISA kit

Name: _____ Date: _____

HIV isolate: _____

1. Make up the following:
 - a. 60 mL wash buffer from x20 stock with distilled water
 - b. 200 pg/mL and 12.5 pg/mL standards (as per manufacturers' instructions) and store in blue freezer box (-20°C)
 - c. 1/10 dilutions of viral supernatants (20µL supernatant; 180µL RPMI)

For each kit, use one strip to prepare a standard curve from 12.5 pg/ml to 800 pg/mL p24

2. Add 200µL of the following to one 8-well strip of the ELISA kit:

1	2	3	4	5	6	7	8
RPMI (negative control/ blank)	Positive control (12.5 pg/mL p24)	Positive control (200 pg/mL p24)					

3. Add 20µL lysis buffer to each well and incubate at 37°C for 60 mins – time carefully – steps in assay are time-sensitive

4. Aspirate and wash 4-6 times with wash buffer using a multichannel pipette

5. Add 100µL anti-p24 (Biotin-conjugate) and incubate at 37°C for 60 mins

6. Aspirate and wash 4-6 times with wash buffer using a multichannel pipette

7. Add 100µL Streptavidin-HRP conjugate to each well and incubate at room temperature for 30 mins

8. Aspirate and wash 4-6 times with wash buffer using a multichannel pipette

9. Add 100µL substrate and incubate IN THE DARK for 20 mins – colour change to blue should be observed

10. Add 100µL stop solution – colour change to yellow should be observed

11. Read absorbance by spectrophotometry at 450 nm

12. Report:

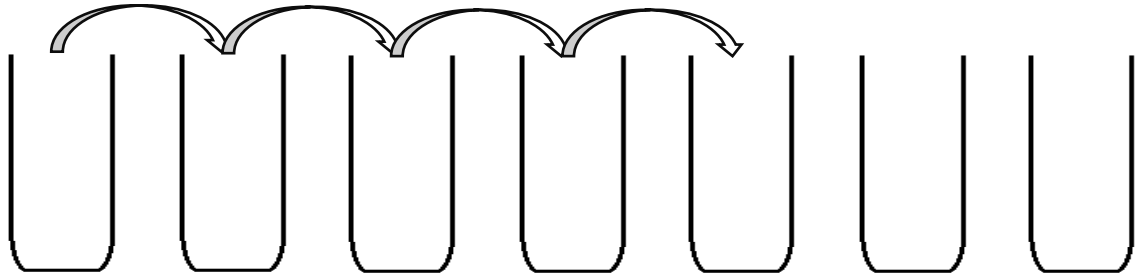
- a. Photo of ELISA strip for qualitative evidence
- b. Spectrophotometry read-out and normalisation to blank (divide each value by blank)
- c. Use standard curve for specific kit to determine p24 concentration in each well

HIV Quantitation and Infectivity (GFP-assay) Protocol

Name: _____ Date: _____

Plate size: _____ HIV isolate: _____

Dilution series:



Dilution factor	Neat (x3)	1/4 (x3)	1/16 (x3)	1/64 (x3)	1/256 (x3)	Negative control (x3)	Count (x3)
Starting volume HIV	2500µL						
Volume HIV transferred	625µL	625µL	625µL	625µL			
Volume medium		1875µL	1875µL	1875µL	1875µL	2500µL	
Final volume	1875µL	1875µL	1875µL	1875µL	2500µL	2500µL	
Polybrene (20mg/mL stock)	1.88 µL	1.88 µL	1.88 µL	1.88 µL	2.5µL	2.5µL	
Volume per well (x3)	500µL	500µL	500µL	500µL	500µL	500µL	

Day 1:

<p>1. Prepare media:</p> <ul style="list-style-type: none"> a. RPMI (no serum) b. DMEM (10% FBS, 2% Pen/Strep) c. Polybrene added must be 10µg/mL final concentration after media top-up (step 5) 	
<p>2. Prepare dilution series as required from frozen HIV CFS stocks (stored at -80°C) – predilute concentrated virus (1:2) and use as “neat” [YES / NO]</p>	
<p>3. Aspirate growth medium from ghost cells and rinse with 1mL room temperature PBS</p>	
<p>4. Aspirate the PBS and add the required volume of each dilution to adherent ghost cells</p>	

5. Swirl the plate gently, and incubate at 37°C, 5% CO ₂ for 2hrs, then add 500µL clean DMEM to each well			
6. Count (Gallios) – to be used in formula:			
a. Aspirate media from Control 1 wells			
b. Wash wells with 1mL room temperature PBS			
c. Add 200µL Trypsin to each Count well and incubate at 37°C for 5min until cells dislodge			
d. Add 200µL DMEM (10% FBS, 2% Penstrep) per well to neutralise Trypsin			
e. Transfer to microfuge tubes and centrifuge at 300g for 10min and aspirate supernatant			
f. Resuspend in 100µL PBS and transfer to flow tube;			
g. Add 3µL 7AAD, 100µL Flow Count, and 600µL PBS; run on Gallios			
	DAY1 COUNT R1	DAY1 COUNT R2	DAY1 COUNT R3
Cells/µL			
Cells/we II			
Day 2:			
7. Change medium after 16-18 hrs: 1mL DMEM (10% FBS, 2% Pen/Strep) per well			
8. Check cells for GFP expression using fluorescence microscopy (blue light) at least every 24hrs			
Day 3:			
1. Aspirate media from each well - tilt the plate towards you – DO NOT SCRAPE BOTTOM			
2. Add 1mL PBS to each well and swirl to wash the adherent ghost cells and aspirate PBS			
3. Add 200µL Trypsin to each well, and incubate at 37°C for 5 mins; tap firmly to dislodge cells			
4. Add 200µL DMEM (10% FBS) to each well to neutralise Trypsin			
5. Transfer well contents into 1.5mL microcentrifuge tubes and centrifuge at 300g for 10min			

6. Add 300µL fixation buffer and incubate for 10min at 4°C and fill up to 1mL with PBS							
7. Centrifuge at 300g for 10min and remove supernatant							
8. Resuspend pellet in 100µL PBS and analyse GFP (FITC channel) expression by flow cytometry							
Dilution	Neat	1/4	1/16	1/64	1/256	Control	
GFP observed							
% GFP detected							
Calculate infectious units (IU)/mL: $\frac{IU}{mL} = Cell\ number \times \left(\frac{\%GFP}{100}\right) \times dilution\ factor \times$ $\frac{1000\mu L}{\mu L\ neat\ virus\ added}$							
Isolate		IU/mL		Standard deviation			

P24 Intracellular Staining (KC57) for HIV Detection

Name: _____ Date: _____

HIV isolate: _____ Target cells used: _____

1. Prepare cell suspensions from HIV-infected and uninfected cells and perform a count

2. Transfer an appropriate volume of each cell suspension to 2 mL microcentrifuge tube

# cells	Vol. infected cells	Cell type(s)	Vol. uninfected cells	Cell type(s)
100 000				
500 000				
1000 000				

3. Centrifuge at 300 x g for 10 min, discard supernatant and resuspend in 100 μ L PBS or medium (do NOT use FBS-containing medium if using Zombie Violet)

4. [Optional] Stain with Zombie Violet fixable viability dye:

- a. Add 1 μ L Zombie Violet (reconstituted in DMSO – interferes with Abs)
- b. Incubate in the dark for 15 min
- c. Wash once with 1 mL PBS
- d. Resuspend in 100 μ L PBS

5. [Optional] Stain with surface antibodies:

- a. Add required volumes of desired Ab:
- b. Incubate in the dark for 15 min
- c. Wash once with 1 mL PBS
- d. Resuspend in 100 μ L PBS

6. Add 100 μ L IC Fixation Buffer (0.22 μ m filtered) to each sample and pulse vortex to mix

7. Incubate at room temperature in the dark for 60 min

8. Prepare 1X Permeabilization buffer (PB) from the 10X stock in sterile dH₂O

9. Wash cells with 1 mL 1X PB, centrifuge at 500 x g for 5 min, discard supernatant

10. Wash cells with 1 mL 1X PB, centrifuge at 500 x g for 5 min, discard supernatant

11. Resuspend pellets in 100 μ L 1X PB and stain as follows:

	HIV Negative Cells		HIV Positive Cells	
Antibody	KC57-PE	Isotypic	KC57-PE	Isotypic
Tube 1 (iso)		5 / 2.5 μ L		5 / 2.5 μ L
Tube 2 (mAb)	5 / 2.5 μ L		5 / 2.5 μ L	

12. Incubate in the dark at room temperature for 60 min or at 4°C overnight

13. Wash cells with 1 mL 1X PB, centrifuge at 500 x g for 5 min, discard supernatant

14. Wash cells with 1 mL 1X PB, centrifuge at 500 x g for 5 min, discard supernatant

15. Resuspend in 300 μ L PBS and analyse on the FACS Aria

Appendix II Ethics approval documentation

The Research Ethics Committee, Faculty Health Sciences, University of Pretoria complies with ICH-GCP guidelines and has US Federal wide Assurance.

- FWA 00002567, Approved dd 22 May 2002 and Expires 20 Oct 2016.
- IRB 0000 2235 IORG0001762 Approved dd 22/04/2014 and Expires 22/04/2017.



UNIVERSITEIT VAN PRETORIA
UNIVERSITY OF PRETORIA
YUNIBESITHI YA PRETORIA

Faculty of Health Sciences Research Ethics Committee

30/06/2016

**Approval Certificate
New Application**

Ethics Reference No.: 207/2016

Title: Evaluating the effects of HIV-1 infection on haematopoietic stem cell colony formation.

Dear Candice Herd

The **New Application** as supported by documents specified in your cover letter dated 24/06/2016 for your research received on the 27/06/2016, was approved by the Faculty of Health Sciences Research Ethics Committee on its quorate meeting of 29/06/2016.

Please note the following about your ethics approval:

- Ethics Approval is valid for 4 years
- Please remember to use your protocol number (**207/2016**) on any documents or correspondence with the Research Ethics Committee regarding your research.
- Please note that the Research Ethics Committee may ask further questions, seek additional information, require further modification, or monitor the conduct of your research.

Ethics approval is subject to the following:

- The ethics approval is conditional on the receipt of 6 monthly written Progress Reports, and
- The ethics approval is conditional on the research being conducted as stipulated by the details of all documents submitted to the Committee. In the event that a further need arises to change who the investigators are, the methods or any other aspect, such changes must be submitted as an Amendment for approval by the Committee.

Additional Conditions:

- Conditional approval, pending permissions from Netcare Femina Clinic.

We wish you the best with your research.

Yours sincerely

*** Kindly collect your original signed approval certificate from our offices, Faculty of Health Sciences, Research Ethics Committee, H W Snyman South Building, Room 2.33 / 2.34.*

Dr R Sommers; MBChB; MMed (Int); MPharMed, PhD

Deputy Chairperson of the Faculty of Health Sciences Research Ethics Committee, University of Pretoria

The Faculty of Health Sciences Research Ethics Committee complies with the SA National Act 61 of 2003 as it pertains to health research and the United States Code of Federal Regulations Title 45 and 46. This committee abides by the ethical norms and principles for research, established by the Declaration of Helsinki, the South African Medical Research Council Guidelines as well as the Guidelines for Ethical Research: Principles Structures and Processes 2004 (Department of Health).

☎ 012 356 3085 ✉ fhsethics@up.ac.za 🌐 <http://www.up.ac.za/healthethics>
✉ Private Bag X323, Arcadia, 0007 - Tswelopele Building, Level 4-5B, Gezina, Pretoria

The Research Ethics Committee, Faculty Health Sciences, University of Pretoria complies with ICH-GCP guidelines and has US Federal wide Assurance.

- FWA 00002567, Approved dd 22 May 2002 and Expires 03/20/2022.
- IRB 0000 2235 IORG0001762 Approved dd 22/04/2014 and Expires 03/14/2020.



UNIVERSITEIT VAN PRETORIA
UNIVERSITY OF PRETORIA
YUNIBESITHI YA PRETORIA

Faculty of Health Sciences Research Ethics Committee

16/11/2018

**Approval Certificate
Amendment**

(to be read in conjunction with the main approval certificate)

Ethics Reference No.: 207/2016

Title: Evaluating the effects of HIV-1 infection on haematopoietic stem cell colony formation.

Dear Ms Candice CL Herd

The **Amendment** as described in your documents specified in your cover letter dated 12/09/2018 received on 13/09/2018 was approved by the Faculty of Health Sciences Research Ethics Committee on its quorate meeting of 24/10/2018.

Please note the following about your ethics amendment:

- Please remember to use your protocol number (207/2016) on any documents or correspondence with the Research Ethics Committee regarding your research.
- Please note that the Research Ethics Committee may ask further questions, seek additional information, require further modification, or monitor the conduct of your research.

Ethics amendment is subject to the following:

- The ethics approval is conditional on the receipt of **6 monthly written Progress Reports**, and
- The ethics approval is conditional on the research being conducted as stipulated by the details of all documents submitted to the Committee. In the event that a further need arises to change who the investigators are, the methods or any other aspect, such changes must be submitted as an Amendment for approval by the Committee.

We wish you the best with your research.

Yours sincerely

Dr R Sommers; MBChB; MMed (Int); MPharMed; PhD
Deputy Chairperson of the Faculty of Health Sciences Research Ethics Committee, University of Pretoria

The Faculty of Health Sciences Research Ethics Committee complies with the SA National Act 61 of 2003 as it pertains to health research and the United States Code of Federal Regulations Title 45 and 46. This committee abides by the ethical norms and principles for research, established by the Declaration of Helsinki, the South African Medical Research Council Guidelines as well as the Guidelines for Ethical Research: Principles Structures and Processes, Second Edition 2015 (Department of Health).

☎ 012 356 3084 ✉ deepeka.behari@up.ac.za / fsethics@up.ac.za 🌐 <http://www.up.ac.za/healthethics>
✉ Private Bag X323, Arcadia, 0007 - Tswelopele Building, Level 4, Room 60 / 61, 31 Bophelo Road, Gezina, Pretoria

*** Kindly collect your original signed approval certificate from our offices, Faculty of Health Sciences, Research Ethics Committee, Tswelopele Building, Level 4-60*



Faculty of Health Sciences

The Research Ethics Committee, Faculty Health Sciences, University of Pretoria complies with ICH-GCP guidelines and has US Federal wide Assurance.

- FWA 00002567, Approved dd 22 May 2002 and Expires 03/20/2022.
- IRB 0000 2235 (ORG0001762 Approved dd 22/04/2014 and Expires 03/14/2020)

28 March 2019

**Approval Certificate
Annual Renewal**

Ethics Reference No.: 207/2016

Title: Evaluating the effects of HIV-1 infection on haematopoietic stem cell colony formation

Dear Ms CL Herd

The **Annual Renewal** as supported by documents received between 2019-03-19 and 2019-03-27 for your research, was approved by the Faculty of Health Sciences Research Ethics Committee on its quorate meeting of 2019-03-27.

Please note the following about your ethics approval:

- Renewal of ethics approval is valid for 1 year, subsequent annual renewal will become due on 2020-03-28.
- Please remember to use your protocol number (207/2016) on any documents or correspondence with the Research Ethics Committee regarding your research.
- Please note that the Research Ethics Committee may ask further questions, seek additional information, require further modification, monitor the conduct of your research, or suspend or withdraw ethics approval.

Ethics approval is subject to the following:

- The ethics approval is conditional on the research being conducted as stipulated by the details of all documents submitted to the Committee. In the event that a further need arises to change who the investigators are, the methods or any other aspect, such changes must be submitted as an Amendment for approval by the Committee.

We wish you the best with your research.

Yours sincerely

Dr R Sommers

MBChB MMed (Int) MPharmMed PhD

Deputy Chairperson of the Faculty of Health Sciences Research Ethics Committee, University of Pretoria

The Faculty of Health Sciences Research Ethics Committee complies with the SA National Act 61 of 2003 as it pertains to health research and the United States Code of Federal Regulations Title 45 and 46. This committee abides by the ethical norms and principles for research, established by the Declaration of Helsinki, the South African Medical Research Council Guidelines as well as the Guidelines for Ethical Research: Principles Structures and Processes, Second Edition 2015 (Department of Health)

Research Ethics Committee
Room 4.00, Level 4, Tswelopele Building
University of Pretoria, Private Bag 3024
Arcadia 0001, South Africa
Tel: +27 (0)12 356 3004
Email: depeka.belem@up.ac.za
www.up.ac.za

Fakulteit Gesondheidswetenskappe
Lefapha la Disaense tša Maphelo